UNIVERSITY OF TURIN

Phd School in Life and Health Sciences
Molecular Medicine

XXIX Cycle
Academic Years: 2014-2017

Identification and Evaluation of Molecular Targets Associated to the Cancer Stem Cell Phenotype in Mammary Tumor

Tutor: Prof. Federica Cavallo
Coordinator: Prof. Francesco Novelli

Candidate: Roberto Ruiu

“Nel mezzo del cammin di nostra vita
mi ritrovai per una selva oscura,
ché la diritta via era smarrita.”

“Midway upon the journey of our life
I found myself within a forest dark,
For the straightforward pathway had been lost.”

Dante Alighieri (1265-1321)

La Divina Commedia - Inferno: C. I, vv. 1-3

These are the words Dante used to describe his entry into hell…and the words that well describe my decision to start a PhD.

TABLE OF CONTENTS

ABSTRACT

Breast cancer is the most common invasive cancer in women and represents a significant cause of morbidity and mortality. Tumor relapse and metastatic spreading act as a major hindrance to achieve complete cure of this disease. Similar to other tumors, breast cancer shows intratumor heterogeneity, as functional distinct cell types compose tumor tissue and differ with respect to proliferation, differentiation, and ability to initiate tumors. Evidence suggests that heterogeneity within tumors results from an intrinsic hierarchy of cells, with a small population of undifferentiated tumorigenic cells at the apex of the hierarchy, the so-called cancer stem cells (CSC). CSC are endowed with the biological properties required for tumor progression and spreading, and can differentiate into non-tumorigenic cancer cells that compose the bulk of the tumor, which has little or no capacity to contribute to cancer progression. Importantly, CSC would function as a reservoir for the local and distant recurrence of the disease, due to their resistance to radio- and chemo-therapies, which likely enrich CSC population by preferentially killing differentiated cancer cells. Therefore, the efficacy of a therapeutic approach may rest on its ability to effectively target and deplete CSC. The identification of appropriate molecular targets expressed by CSC may thus be critical in the development of more effective therapies.

To this aim, we took advantage of the ability of CSC to grow as non-adherent spherical colonies *in vitro* (tumorspheres) to expand the CSC subpopulation within breast cancer cell lines, thus allowing us to compare their transcriptional profile to that of the more differentiated parental cells growing as a monolayer.

Initially, transcriptional analysis was performed on the murine Her2/neu^{+} mammary cancer cell line named TUBO, that was previously established from a BALB/c mouse transgenic for the activated rat Her2/neu oncogene. Focusing on genes strongly upregulated in tumorspheres and coding for proteins expressed on cell surface, more easily targetable, we selected the most promising: xCT and SCARA5.

In the first study, we assessed the usefulness of xCT as a CSC-related target both *in vitro* and *in vivo*. Downregulation of xCT impaired tumorsphere generation and affected CSC intracellular redox balance *in vitro*, suggesting that xCT plays a functional role in CSC biology. Subsequently, we developed a DNA-based vaccination to target xCT *in vivo*. We showed that anti-xCT vaccination delayed primary tumor growth and strongly impaired pulmonary metastasis formation in mice challenged with tumorsphere-derived cells. Despite xCT being a self-antigen, DNA vaccination was able to induce a humoral immune response against the tumor. Finally, anti-xCT vaccination increased CSC chemosensitivity to doxorubicin *in vivo*, suggesting that immunotargeting of xCT may act synergistically to chemotherapy.

In the second study, we observed that tumorspheres displayed an increased uptake of L-Ferritin compared to their monolayer counterparts because of the upregulation of the L-Ferritin receptor SCARA5. We thus exploited L-Ferritin internalization for the simultaneous delivery of Curcumin, a natural molecule with reported anticancer activity, and the MRI contrast agent Gd-HPDO3A, both encaged in the L-Ferritin cavity. Using this delivery system, we were able to impair self-renewal and viability of tumorspheres *in vitro* and to induce the regression of established tumors in mice. Thus, we showed that L-Ferritin has a good therapeutic potential due to its ability to target CSC and to improve Curcumin bioavailability, opening up the possibility of a future use in a clinical setting.

In the last study, our interest moved to triple negative breast cancer (TNBC), that currently lacks targeted therapies and thus its management relies exclusively on surgery and chemo/radiotherapy. We established tumorsphere cultures from TNBC cell lines 4T1 (murine) and HCC1806 (human) and performed RNA-Seq analysis to identify differences in gene expression between tumorspheres and their monolayer counterparts. Enrichment analysis of biological processes showed an upregulation in genes involved in negative regulation of apoptosis in tumorspheres, and a down-regulation in genes involved in lipid metabolism and cell cycle regulation. By focusing on upregulated genes coding for cell membrane-associated proteins, we selected Teneurin-4 (TENM4) as a candidate target for further studies. Silencing of TENM4 was reflected by a partial impairment of tumorsphere-forming ability. TENM4 silencing also led to a small but significant decrease in Focal Adhesion Kinase (FAK) phosphorylation, which has been previously linked to CSC biology, thus strengthening the possible link between TENM4 and a CSC-like phenotype.

In conclusion, our approach based on the use of tumorspheres allowed us to identify novel CSC-related targets and to develop preclinical therapeutic approaches adapted to the role of the molecular target and able to impact on CSC biology and tumor growth. Furthermore, analysis of high throughput data allowed us to identify apoptosis, lipid metabolism and cell cycle as key processes specifically involved in CSC biology.

LIST OF PAPERS

List of papers discussed in the thesis.

Paper I

- Lanzardo S*, Conti L*, Rooke R, **Ruiu R**, Accart N, Bolli E, Arigoni M, Macagno M, Barrera G, Pizzimenti S, Aurisicchio L, Calogero RA, Cavallo F. *Immunotargeting of antigen xCT attenuates stem-like cell behavior and metastatic progression in breast cancer.* Cancer Research. 76, 1 :62-72 (2016)

Paper II

- Conti L*, Lanzardo S*, **Ruiu R**, Cadenazzi M, Cavallo F, Aime S, Geninatti Crich S. *L-Ferritin targets breast cancer stem cells and delivers therapeutic and imaging agents.* Oncotarget. 7, 41: 66713-66727 (2016)

Paper III

- **Ruiu R***, Arigoni M*, Riccardo F, Conti L, Lanzardo S, Calogero RA, Cavallo F, Quaglino E. *Comparative Transcriptomics of Triple Negative Breast Cancer Stem Cells and Differentiated Tumor Cells Identifies TENM4 as a Potential Therapeutic Target.* [Manuscript]

List of the other papers authored during the Ph.D. course.

- Bandini S, Macagno M, Hysi A, Lanzardo S, Conti L, Bello A, Riccardo F, **Ruiu R**, Merighi IF, Forni G, Iezzi M, Quaglino E, Cavallo F. *The non-inflammatory role of C1q during Her2/neu-driven mammary carcinogenesis.* Oncoimmunology. 5, 12: e1253653 (2016)

- Geninatti Crich S, Cadenazzi M, Lanzardo S, Conti L, **Ruiu R**, Alberti D, Cavallo F, Cutrin JC, Aime S., *Targeting ferritin receptors for the selective delivery of imaging and therapeutic agents to breast cancer cells.* Nanoscale. 7, 15: 6527-33 (2015)

- Conti L, **Ruiu R**, Barutello G, Macagno M, Bandini S, Cavallo F, Lanzardo S., *Microenvironment, oncoantigens, and antitumor vaccination: lessons learned from BALB-neuT mice.* Biomed Res Int. 534969 (2014)

* Equal contribution

INTRODUCTION

1. Breast cancer

Currently, breast cancer affects approximately 12% of women worldwide, is the most commonly diagnosed cancer and the leading cause of cancer deaths in women, accounting for 23% of total cancer cases and 14% of all cancer-related deaths [1].

Histological analysis allows distinguishing between carcinoma *in situ*, where cancer cells proliferate without invading the surrounding tissue, and invasive carcinoma, where cancer cells infiltrate the surrounding tissue. The ductal and lobular subtypes, termed according to the site of insurgence that can be within the ducts or the lobules of the mammary gland, respectively, constitute the majority of all breast cancers with the ductal subtype representing 70-80% of all invasive lesions [2]. The current model of human breast cancer progression proposes a linear multistep process. For the ductal subtype, the proposed model describes flat epithelial atypia (FEA), atypical ductal hyperplasia (ADH) and ductal carcinoma in situ (DCIS) as the non-obligate precursors of invasive and metastatic ductal carcinoma [3]. For the lobular subtype, atypical lobular hyperplasia (ALH) and lobular carcinoma in situ (LCIS) are described as the non-obligate precursor lesions to invasive lobular carcinoma [3]. Nevertheless, recent evidences challenge this model, suggesting that tumor cells can invade and disseminate from the earliest preneoplastic lesions, even before the formation of overt primary tumors [4].

Breast cancer should not be considered as a homogeneous disease, but a rather complex pathology that can be classified in different subtypes according to histopathological features, stage, grade, molecular classification and receptor status [2]. The latter defines the positivity by immunohistochemical analysis for Estrogen Receptor (ER), Progesterone Receptor (PR) and Epidermal Growth Factor Receptor 2 (EGFR2, ErbB2, Her2, neu). The amplification of the Her2 locus can also be assessed through fluorescent in situ hybridization (FISH). Breast cancers that are negative for the aforementioned markers are consequently defined as triple negative breast cancer (TNBC). Recent studies have further classified breast cancer into six intrinsic molecular subtypes, according to their gene expression profiles: Luminal A, Luminal B, Her2-enriched, basal-like, normal breast-like and claudin low cancer [5].

Thus, numerous factors such as the subtype of breast cancer, the stage, sensitivity to hormones, the patient's age, menopausal state, diabetes and the overall health influence the response to therapy. So far, the primary treatments include surgery, radiation therapy, hormone therapy, chemotherapy and monoclonal antibody therapy [6]. Drugs can be administered following surgery (adjuvant therapy) or before surgery (neoadjuvant therapy). In the adjuvant setting, hormone blocking therapy involves the administration of drugs that block estrogen receptors or of aromatase inhibitors, thus blocking ER-mediated proliferation. Chemotherapy is another predominantly employed medication:

cyclophosphamide, doxorubicin and docetaxel are some of the chemotherapeutic drugs used [6], which work by destroying fast-proliferating cancer cells mainly by inducing DNA damage upon replication. Radiation therapy involves the use of controlled doses of radiation to remove the remaining cancer cells. In targeted therapies, monoclonal antibodies against Her2 are currently employed for Her2-positive tumors, while others are under investigation in several clinical trials [6].

Despite the outcomes associated with breast cancer have been dramatically improved by the advances in diagnosis, understanding and management of the disease, many patients still do not respond to treatments, resulting in the progression or relapse of the disease, finally leading to reduced survival expectations [7]. The reduced efficacy of the therapy is often attributable to the inner complexity of the tumor. In fact, current therapies treat cancer as a homogenous disease, while it is now clear that tumors can be represented as complex ecosystems that contain different populations of non-tumor cells (endothelial, hematopoietic, stromal) that infiltrate the tumor and that contribute to create the tumor microenvironment, which provides nutrients and stimuli for the growth of tumor cells [8]. The latter display many differences from the genetic, phenotypic and functional point of view [9]. These differences determine an overall intratumor heterogeneity, with the presence of regions characterized by different degrees of differentiation, proliferation, vascularization, inflammation and invasion within the same tumor. Thus, it is not surprising that drug resistance occurs extensively in all types of cancer.

2. The origin of intratumor heterogeneity: clonal evolution model and hierarchical model

Two separate models have been historically used to explain tumor progression and heterogeneity [10]: one attributes intratumor heterogeneity to genetic causes (clonal evolution, or stochastic, model), the other one to non-genetic causes (hierarchical, or CSC, model). The clonal evolution model of cancer, developed by Nowell in 1976 [11], proposes that the tumor arises from a single cell upon the appearance of multiple driver mutations, and that maintenance and progression of the tumor depends on acquired genetic variability within the original clone. This variability allows progressive selection of more aggressive subclones following the rules of Darwinian evolution [12]. Thus, distinct stochastic mutations characterizing distinct clones (all deriving from the same cell of origin) can provide a selective advantage to a clone with respect to another, thus allowing a continuous alternation of dominant clones that expand and permit the tumor perpetuation. An important assumption of the clonal evolution model is that every cell belonging to the same genetic clone displays the same tumorigenic potential.

In the CSC model, also named hierarchical model, phenotypic heterogeneity is explained as a reflection of non-genetic diversification that exists in normal tissues. As all the normal cells in an

individual share the same genotype (with the exception of adaptive immune cells), the phenotypic diversity of normal cells depends on developmental pathways which are required for the maintenance of the hierarchy of normal tissues, with the stem cells at the apex and differentiated cells at the base. In a similar manner, these non-genetic features contribute to a hierarchical organization of the tumors, where a population of CSC is responsible for the long-term maintenance of the tumor, while more differentiated tumor cells representing the bulk of the tumor lose their tumorigenic potential [13]. In this model, only tumor cells displaying stem cell-features are able to generate a new tumor, independently from their genetic background [14]. Thus, cancer cells sharing a common genetic background can exist in a CSC and a non-CSC state [15].

These two models have been long considered as mutually exclusive. However, each view in isolation in insufficient to fully explain the heterogeneity seen within cancers. The clonal evolution model focuses on genetic heterogeneity without considering that individual cells within a genetically homogeneous subclone could exhibit functional diversity due to non-genetic determinants. Similarly, a major limitation of the hierarchical model is that it considers the tumor as being genetically homogeneous and static, without accounting for the existence of genetically distinct subclones during tumor evolution [16].

In more recent years, there is the tendency to harmonize these models and to consider their contribution to the intratumor heterogeneity and tumor maintenance as complementary. Integrating these two models could more accurately describe tumor progression. CSC may in fact be subjected to clonal selection, with a dominant CSC clone emerging upon the appearance of advantageous mutations [14]. In this "*integrated model*", the acquisition of genetic mutations could produce genetically different lineages of CSC that are heterogeneous in dominancy and malignancy (**Figure 1**).

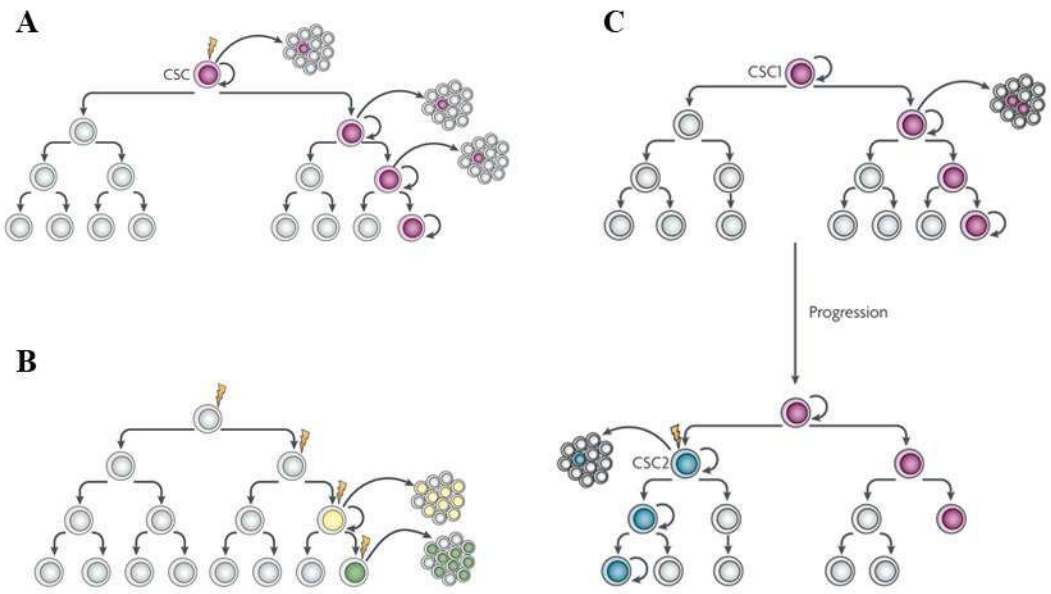

Figure 1. Models for tumor heterogeneity and propagation. A) Cancer stem cell model. Tumor heterogeneity results from existence of phenotypically diverse populations of different stages of cell maturation. In this model, only the CSC can generate a tumor, based on its self-renewal properties and unlimited proliferative potential. **B)** Clonal evolution model. Accumulation of genetic mutations results in a large number of cells differing in genotype and thus phenotype. The best fitted cells are selected by Darwinian processes to generate clonal variants of the tumor. In this model, all cells in the dominant clones have similar tumorigenic capacity. **C)** Integrated model. The acquisition of genetic alterations in separate subclones of CSC may lead to functionally diverse lineages. Thus, a distinct CSC (CSC2) may arise due to clonal evolution of CSC1. This more aggressive CSC2 becomes dominant over CSC1 and drives tumor formation. Adapted from *Visvader JE and Lindeman GJ, Nat Rev Cancer. 8, 2008* [14].

3. Historical perspective of the cancer stem cell model

The notion that cancer cells have properties reminiscent of stem cells has its roots in the nineteenth century. This idea was first postulated by Rudolph Virchow, which noted the similarities between teratocarcinomas and embryonic tissues regarding their ability to proliferate and differentiate. His "embryonal rest hypothesis" postulated that cancers are caused by cells with properties similar to those of the early embryo [17]. Subsequently, Julius Cohnheim extended this concept by hypothesizing that embryonal remnants persist in mature organs, and that these residual embryonic cells could later re-activate to form cancer [17].

The modern idea that the same developmental programs that are at the basis of normal tissue organization are retained in cancer, began with seminal studies on teratocarcinomas in the '60s. In 1960, Pierce and colleagues suggested that the majority of the cells within a teratocarcinoma are differentiated, and that the appearance of such differentiated cells occurs after an initial phase of proliferation, a phenomenon similar to that observed in normal embryo development (reviewed in ref. [18]). Later, in 1964, Pierce proved the clonal origin of mouse teratocarcinomas from single transplanted multipotent tumorigenic cells [19]. Thus, Pierce and colleagues formulated a general view in which tumors can be considered as a caricature of normal development in embryogenesis, where

multipotent malignant cells propagate the cancer and give rise to more differentiated, benign populations of cells [13,20]. Early studies on blood tumors as well contributed to pave the way of cancer stem cell research. Studies in the '60s and '70s showed the existence of a rare population of slow-cycling leukemia cells that were not susceptible to anti-proliferative therapies and were therefore responsible for recurrence. These slow-cycling leukemia cells were also responsible for the continued generation of the proliferative fraction that eventually leads to post-mitotic leukemia cells, which represent the majority of leukemia blasts (reviewed in ref. [16]). In the same years, the heterogeneous potential of tumor cells to self-renew both *in vivo* and *in vitro* was reported. These studies showed that an extremely low percentage of cells had clonogenic potential, and proposed a view of hierarchical organization of leukemia, as established for normal hematopoiesis (reviewed in ref. [21]).

However, it was not until the development of fluorescence-activated cell sorting techniques coupled with refined techniques of xenografting in immune-compromised mice, that the hierarchical organization of leukemia was demonstrated. In the '90s, Dick and colleagues prospectively isolated human Leukemia-Initiating Cells (L-IC) by sorting acute myeloid leukemia (AML) cells using the cell surface markers CD34 and CD38. It was shown that leukemia cells able to engraft in an immunocompromised mouse were exclusively in the $CD34^+/CD38^-$ fraction [22]. Further studies established that AML is organized as a hierarchy with $CD34^+/CD38^-$ cells at the apex [23], thus proving that AML is composed by heterogeneous populations in which only rare cells have tumorigenic potentials.

The initial studies on AML paved the way for the subsequent studies on CSC in solid tumors. The first prospective isolation of CSC in solid tumors was performed in human breast cancer over a decade ago by Al-Hajj and colleagues [24]. They showed that as few as 100 cells with $CD44^+/CD24^-$ phenotype were able to generate tumors in mice, while thousands of cells with alternative phenotypes were not able to generate tumors. This tumorigenic subpopulation could be serially passaged, each time generating new tumors containing both $CD44^+/CD24^-$ tumorigenic cells as well as the phenotypically heterogeneous populations of non-tumorigenic cells present in the initial tumor. Since then, CSC have been identified in many solid tumors.

4. What is a cancer stem cell? Concepts and definitions

Stem cells in normal tissues are generally defined as undifferentiated cells that have the capacity to produce the specialized cells of that tissue (differentiation), as well as undifferentiated daughter stem cells with tissue-maintaining potential (self-renewal) [25]. A self-renewing cell division results in one or both daughter cells that have essentially the same ability to replicate and generate differentiated cell lineages as the parental cells. Similarly, the consensus definition of CSC (as established at the

AACR Workshop on Cancer Stem Cells [26]) is a cell within a tumor that possesses the capacity to self-renew and to generate the heterogeneous lineages of cancer cells that compose the tumor (**Figure 2**). CSC can thus only be defined experimentally by their ability to recapitulate the generation of a continuously growing tumor. For this reason, putative CSC are operatively referred to as "tumor-initiating cells" or "tumorigenic cells".

It should be noted that the term "cancer stem cell" has led to some confusion over the years [25]. Some proposed that CSC arise through mutations acquired in normal tissue stem cells, while others suggest that CSC originate from differentiated or progenitor cells that have reverted to a stem-like state, which refers to a complex interaction of intrinsic molecular pathways, epigenetic modifications and transcription factors that regulate and maintain the stem cell form [10]. However, the CSC concept does not imply any specific hypothesis in this regard. CSC may indeed arise from normal stem cells by oncogenic mutations, but it is also conceivable that progenitors or more differentiated cells can acquire the self-renewal capacity that characterizes CSC through multiple mutagenic events [26]. In conclusion, any cell that acquires mutations restoring the capacity for self-renewal, whilst suppressing the terminal differentiation program, could potentially act as CSC of a particular cancer [27,28]. The same confusion is caused by the term "tumor-initiating cell" [25]. A tumor-initiating cell is not necessarily the cell that received the first oncogenic hits in the patient (the cell of origin of cancer), but simply refers to the cell that has the ability to initiate a new tumor when transplanted into a host [26]. As stated in the previous section (see "*integrated model*"), the stem-like status can be acquired by a cell at any given moment in the tumor development due to accumulation of advantageous mutations.

5. Biological features of the cancer stem cells

5.1 Signaling pathways in cancer stem cells

Despite having in common the self-renewal and tumor-initiating capacity, not all CSC necessarily share the same mechanisms that regulate these fundamental features. In fact, the intra- and inter-tumor heterogeneity characterizing different tumor types represents one of the major challenges in specifically define CSC from the phenotypic, genetic, functional and molecular points of view [29]. Nonetheless, it has been observed that gene expression profile derived from normal mammary SC can stratify breast cancers according to their biological and molecular features, and that high grade breast cancers show enrichment in normal mammary SC profile due to a higher CSC content [30]. Furthermore, it has been observed that the activation of specific signaling pathways occurs frequently across different tumor types, and that these pathways can contribute to the acquiring and maintenance of stemness features in CSC. In fact, the same pathways that are conserved in regulating normal stem

cell self-renewal and tissue homeostasis, such as Notch, Wingless-related integration site (Wnt) and Hedgehog (Hh) signaling pathways, appear to contribute to neoplastic progression when deregulated [31]. Other stem cell-related genes, such as Bmi1, Nanog, SOX2 and OCT4 have been frequently linked to the CSC phenotype [29].

Wnt plays a critical role in highly proliferative tissues, such as the hematopoietic system, skin and intestine [32]. Two pathways are activated downstream of Wnt. The canonical pathway acts through β-Catenin and is involved in cell fate determination, while the non-canonical pathway is independent of β-Catenin and is involved in cell movement and polarity [29]. In the canonical Wnt pathway, the Wnt ligands bind to their transmembrane receptor Frizzled (Fzd), leading to stabilization of β-Catenin. β-Catenin then translocates to the nucleus, resulting in the transcription of Wnt target genes such as Myc and Cyclin D1, which drive cell proliferation and expansion. Wnt1 was first identified as an oncogene involved in breast cancer in mice infected by the mouse mammary tumor virus (MMTV), which integrated into the Wnt1 gene resulting in its ectopic activation. Activation of Wnt1, as well as constitutively activated β-catenin, have been shown to induce mammary tumor formation[33,34]. MMTV-Wnt-induced tumors are dependent on continuous Wnt signaling, which leads to progenitor-like signatures in tumor cells[35]. In humans, Wnt signaling results to be activated in over 50% of breast cancer patients and is linked to reduced overall survival, with canonical Wnt ligands and receptors often upregulated in breast cancers despite the lack of somatic mutations [35].

The Hedgehog (Hh) signaling pathway was initially described in Drosophila as a mediator of segmental patterning during embryonic development. The most studied vertebrate homolog of the Drosophila Hh gene is Sonic Hedgehog (Shh). Shh regulates proliferation, migration, and differentiation [29]. Shh is an extracellular ligand of the transmembrane receptor Patched (Ptch). In absence of Shh ligand, Ptch represses the G protein receptor and signal transducer Smoothened (Smo), thus preventing Gli zinc finger transcription factor modulation. In absence of Shh activation, Gli acts as transcriptional repressor. Binding of Shh to Ptch releases its repression on Smo, which in turn exerts post-transcriptional modification on Gli proteins, turning them into transcriptional activators. Excessive Shh signaling has been implicated in a range of cancers and significantly contributes to the long term self-renewal of breast CSC [36]. Members of the Shh pathway are expressed during all stages of mouse mammary gland development, with $Ptch1^{+/-}$ mice showing an expansion of the mammary regenerative compartment [29]. A strong evidence for Shh involvement in breast carcinogenesis comes from a study in which conditional over-expression of GLI1 alone in the mouse mammary gland was sufficient to induce tumor formation [37]. GLI1 over-expression was accompanied by expansion of mammary progenitors and upregulation of genes involved in proliferation, cell

survival and metastasis, indicating that the Shh signaling pathway is fundamental for initiation and propagation of breast CSC [29].

The Notch signaling pathway plays a role in controlling cell fate, proliferation and self-renewal during the development of most tissues, including breast [38]. Notch is a transmembrane receptor, and its ligands Delta-like (DLL) and Jagged are transmembrane proteins as well, thus ligand-receptor interactions occurs through cell-cell contact. Binding of the ligand to Notch receptor triggers two consecutive proteolytic cleavages by ADAM and γ-secretase, leading to release of an active intracellular domain (NCID). NCID translocates to the nucleus and binds to CSL/RBPJ transcription factor, inducing the expression of target genes including HES, PI3K, AKT, NF-kB, PPAR, CyclinD1, p21 and p27 [29]. The role of Notch in breast cancers was first identified in mouse models. Frequent integration of MMTV into the Notch4 or Notch1 genes results in constitutively activated forms of these receptors [29]. Activation of Notch4 is sufficient to induce mammary adenocarcinomas, while Notch1 activation is sufficient to transform mouse mammary epithelial cells *in vitro* and accelerates tumor growth in cooperation with Her2/neu *in vivo*, indicating an oncogenic role for Notch receptors in mammary tumor development [29]. Expression of components belonging to the Notch signaling is common in breast cancer patients, where it relates to poor prognosis [29].

5.2 Epithelial-to-mesenchymal transition and stem-like state

One of the most important processes associated with cancer stemness is the epithelial-to-mesenchymal transition (EMT) [39]. EMT is a multi-step process manifested by the loss of cell junctions and the reorganization of the cytoskeletal network, resulting in the loss of epithelial polarity and acquisition of a mesenchymal-like phenotype. During embryogenesis, EMT enables embryonic epithelial cells to become mesenchymal-like and travel to distant sites where new tissues and organs form. Similarly, during tumor progression, this EMT process is thought to be reactivated and ultimately facilitates tumor cell migration through the basement membrane, invasion into adjacent tissues, and penetration into the circulation. EMT is induced by humoral factors such as TGF-β, EGF, FGF and Wnt and is mediated by transcription factors such as Snail, Slug, Twist1/2 and Zeb1/2 [4], which suppress the expression of E-cadherin and promote the loss of epithelial and adhesive characteristics and the acquisition of invasive and migratory properties [40]. The expression of EMT-related transcription factors in primary tumors has been linked to tumor invasion, metastasis, and poor prognosis [41]. Besides these pro-invasive and metastatic functions, EMT has been linked to the promotion of stemness in cancer cells, particularly in breast cancer. The activation of EMT by multiple means, including TGF-β treatment and the expression of various EMT-inducing transcription factors, generates cells that express breast CSC markers and functional features,

including tumor initiation in immunodeficient mice [39,42]. Furthermore, cellular changes induced by EMT have direct impact on stem cell signaling pathways. The loss of E-cadherin induced by EMT transcription factors releases β-catenin from cell membrane sequestration and facilitates its nuclear translocation to activate canonical Wnt signaling [43]. Moreover, the disruption of epithelial polarity leads to activation of the Hippo pathway effectors YAP/TAZ, which favor the acquisition of CSC traits by increasing the chemoresistance, tumorigenicity and metastatic capacity of breast cancer cells [44,45].

5.3 Cancer stem cells and metastasis.

A feature linked to EMT, and often attributed to CSC, is that of being responsible of distant metastasis (**Figure 2**). Investigations on clinical relevance of CSC markers expression in human tumors have suggested that prevalence of CD44+/CD24-/low cells in breast cancer may favor distant metastasis [46], similarly to what has been shown for ALDH expression [47]. Cells isolated via stem cell marker expression from primary tumor samples or blood of breast cancer patients can generate metastasis when inoculated in immunocompromised mice [48], and a study on disseminating tumor cells in 50 bone marrow specimens of breast cancer patients showed that an average of 72% of the cells displayed a CSC marker positivity, while the percentage in the primary tumors is reported to be less than 10% [49]. Although EMT favors the migration of cancer cells from the primary tumor, it inhibits cell proliferation and interferes with the initiation of metastatic outgrowth [48]. Cancer cells that have undergone an EMT must revert to an epithelial phenotype in order to initiate growth at the metastatic site, a process known as mesenchymal-to-epithelial transition (MET). Of note, it has been reported that breast CSC can exist in both epithelial and mesenchymal state [50]. The two populations of CSC appear to coexist in the same tumor, with mesenchymal-like breast CSC being primarily quiescent and localized at the tumor invasive front, whereas epithelial-like breast CSC being proliferative and located more centrally[50]. It is thus proposed that the plasticity of CSC allows them to actuate transition between EMT- and MET-like states and endows these cells with the capacity for tissue invasion, dissemination, and growth at metastatic sites.

5.4 Resistance to conventional therapies

Chemotherapy and radiotherapy have represented the treatments of choice for cancer patients for the past decades, often affording reduction in the tumor burden. The efficacy of these therapies is indeed assessed by efficient reduction in tumor mass. However, a minority of cells non-responding to therapies may still survive, representing the minimal residual disease that leads to local and distant recurrence [51]. In many circumstances, including breast cancer, CSC have been shown to be more

resistant to cytotoxic drugs compared to non-CSC of the same tumor [52]. Along with chemoresistance, CSC of various histotypes exhibit greater resistance to radiation therapy compared to non-CSC [52] (**Figure 2**).

In general, CSC resistance to therapy can be ascribed to multiple mechanisms. Increased expression of multidrug efflux pumps from the ATP-binding cassette (ABC) transporter superfamily has been reported in CSC [53]. This family includes several proteins, but three of them have been extensively studied as regulators of multidrug resistance in tumors. These are P-glycoprotein (P-gp, MDR1, ABCB1), multidrug resistance protein 1 (MRP1, ABCC1) and breast cancer resistance protein (BCRP, ABCG2) [54]. Enhanced expression of such proteins results in ATP-dependent efflux of a broad spectrum of cytotoxic drugs, including taxanes, anthracyclines, antimetabolites, as well as several tyrosine kinase inhibitors [54].

Radiation therapy and many chemotherapeutic drugs such as DNA cross-linkers (Platinum-based drugs) and topoisomerase inhibitors (anthracyclines) act by inducing DNA damage, which is lethal to cells if not repaired. CSC can defend from DNA damaging treatments through multiple mechanisms, including regulation of the cell cycle, enhancement of DNA-repair and prevention of DNA damage by ROS-scavenging [54].

As quiescent cells do not go through the cell cycle, they are not susceptible to conventional therapies that target the mitotic mechanisms of rapidly-dividing cells. As for normal adult stem cells, quiescence has been observed also for CSC [55]. Besides passive resistance to therapy, also active DNA Damage Response (DDR) mechanisms have been shown to be highly upregulated by CSC. These include Nucleotide Excision Repair (NER), which is involved in intra-strand crosslinks repair, and Homologous Recombination (HR) pathway for the repair of double-strand breaks [53].

Detoxification from chemo- and radiotherapy-induced reactive oxygen species (ROS) is also an important mechanism of resistance activated by CSC. Most CSC upregulate aldehyde dehydrogenase (ALDH), which confers survival to therapy since ALDH proteins are able to directly scavenge radiation or drug-induced free radicals generated by oxidative stress by producing the antioxidant NADPH [56]. This suggests that ALDH activity could be an important regulator of sensitivity to both chemotherapy and radiotherapy. Pharmacological inhibition of ALDH activity in therapy-resistant CSC leads to accumulation of toxic levels of ROS, which causes irreversible DNA damage and apoptosis [57]. Furthermore, ALDH activity has been correlated to the activation of pro-survival signaling pathways, including PI3K/Akt, as well as stem cell-associated pathways such as Notch [54].

Anti-apoptosis mechanisms contribute to therapy-resistance directly by blocking cell death and indirectly by providing time for enhanced DDR mechanisms to repair therapy-induced DNA damage. Increased resistance to apoptosis has been linked to downregulation of death receptors by CSC, thus

providing resistance to the extrinsic pathway, as well as to upregulation of the members of the BCL2 family involved in negative regulation of the intrinsic pathway of apoptosis [53].

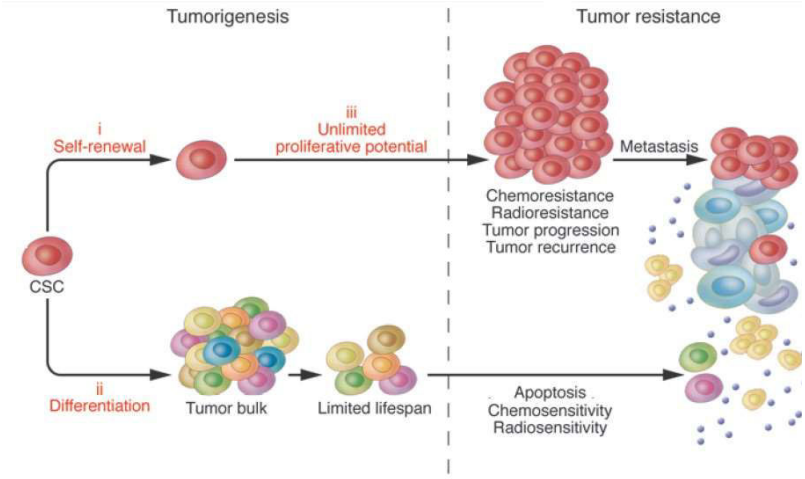

Figure 2. Features of cancer stem cells. CSC are thought to be exclusively capable of driving tumorigenesis through 3 defining features: (i) their ability for long-term self-renewal, (ii) their capacity to differentiate into tumor bulk populations devoid of CSC characteristics, and (iii) their unlimited potential for proliferation and tumorigenic growth. CSC can exhibit increased resistance to chemotherapeutic agents and/or ionizing radiation. If CSC indeed represent the pool of resistant cells in human cancer patients, they likely also drive neoplastic progression, tumor recurrence, and metastasis. Adapted from *Frank NY et al. J Clin Invest. 120, 2010* [65].

6. Clinical implications of the cancer stem cell concept

From a clinical perspective, the CSC concept has significant implications. Conventional anticancer approaches are in fact predominantly directed against the bulk population of the tumor. As CSC are endowed with features that make them resistant to chemo- and radiotherapy, these therapeutic strategies may fail in eradicating them, thus allowing this self-renewing tumor population to cause relapse. In breast cancer patients, it was shown that the cells composing tumor tissue remaining after either endocrine therapy or chemotherapy, displayed a more pronounced CSC-related expression signature compared to pretreatment [51]. Using *in vivo* tracing of a tumor cell subpopulation in a genetically engineered mouse model of glioblastoma, it was shown that not all tumor cells but a restricted and relatively quiescent cell population with CSC features was responsible for the tumor re-growth following treatment with Temozolomide [58]. Re-growth from these surviving cells was shown to occur through the production of highly proliferative transiently amplifying tumor cells derived from quiescent CSC [58]. Similarly, experiments based on tracing a subpopulation of human breast cancer cells with CSC features through an *in vivo* fluorescent imaging system in xenograft models showed that fluorescent CSC are not proliferating. Cancer cells were engineered to express a fluorescent protein that is a target of the 26S protesome, a multiprotein complex which appeared to have reduced proteolytic activity in CSC. The pool of fluorescent CSC expanded through increased proliferation following radiotherapy, thus repopulating the tumor [59]. In these works, the activation of a suicide gene in the tracked population led to ablation of the tumor, thus proving that the observed cells were effectively those leading to relapse. Besides enrichment of intrinsically resistant CSC following therapy, evidence exists of chemo- and radiotherapy-induced conversion of non-stem cancer cells into a stem-like status [60–64]. This reprogramming was shown to occur upon

stress-induced re-expression of stemness transcription factors, including Sox2, Oct4 and Nanog, and the activation of CSC-related signaling pathways such NF-kB and Notch, finally resulting in the restoration of tumorigenic capacity in these induced CSC.

If it is true that CSC are responsible for therapy failure and tumor relapse and progression, then approaches targeting CSC could potentially increase the long-term efficacy of currently available treatments (**Figure 3**). Despite all the resistance mechanisms activated by CSC make appear the task of destroying them discouraging, the same features on which CSC rely for their survival could represent the Achille's heel to be exploited [65].

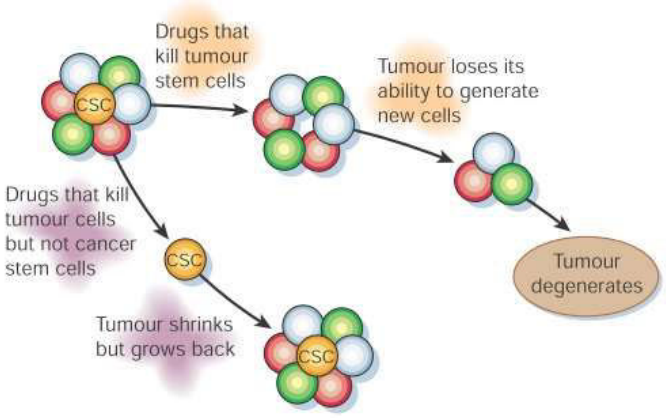

Figure 3. Therapeutic implications of the CSC model. Conventional therapies may shrink tumor by killing mainly differentiated cells with limited proliferative potential. If CSC are less sensitive to these therapies, then they will remain viable after treatment and re-establish the tumor. By contrast, if therapies can be directed against CSC, then they may render the tumor unable to maintain itself or grow. Thus, even if CSC-targeted therapies do not shrink tumor initially, they may eventually lead to cures. Adapted from *Reya T et al. Nature. 414, 2001* [31].

To date, most efforts have focused either on searches for targets expressed in CSC but not in normal stem cells, or on screens for compounds able to selectively kill CSC while not damaging normal stem cells. However, studies aiming at targeting CSC with therapeutics have to face many caveats associated with the intrinsic characteristics of CSC, such as the current lack of univocal CSC markers [66]. Moreover, CSC populations within the same tumor appear to be heterogeneous [50] and this can be reflected in heterogeneous sensitivity to therapies. Even if some CSC are responsive, the target may not be expressed in other CSC. This would allow the malignant cell population to escape a particular targeted therapy and produce a relapse. A possible solution would be to target a molecule that is not a simple marker, but that has a fundamental biological role in the CSC biology. Thus, targeting the mechanisms that are responsible for the biological features of CSC would render the escape from targeted therapies by CSC more difficult. However, interactions between CSC and their niche may contribute to a lack of treatment response *in vivo* even when sensitivity is observed *in vitro* [25].

Furthermore, a major hindrance to achieve efficacious anti-CSC treatments relies on the plasticity of the CSC phenotype. This concept has started to emerge relatively recently, with studies suggesting that the differentiation of CSC into non-tumorigenic cells may be reversible [67], and at least in some cases appears to be induced by chemotherapy and radiotherapy [60–64]. It has been further suggested that this chemoresistant stem-like state is transient, occurring as a reversible adaptation to treatment

[68]. In this case, finding the driver of the acquired CSC phenotype would allow the targeting of *de novo* induced CSC following chemotherapy, leading to their depletion [68].

The plasticity and instability of the CSC state thus suggests that, compared to anti-CSC treatment alone, combinatorial treatments could be favorable. If standard therapy can only deplete bulk tumor cells while favoring the expansion of CSC or their *de novo* appearance in response to stress, approaches targeting the resistance mechanisms could sensitize CSC to standard treatments.

7. Methods for the identification, isolation and characterization of cancer stem cells

As previously stated, the possibility of prospectively isolate CSC allowed researchers to characterize specific molecular and cellular features preferentially associated to CSC. Such features can contribute to tumor initiation, growth and progression. Since normal stem cells and CSC have some characteristics in common, it is possible to exploit some of them – such as expression of specific surface markers, increased activity of ABC transporters and ALDH, self-renewal and multipotency – to identify and isolate CSC (**Figure 4**). Therefore, methods commonly employed for the isolation and enrichment of CSC include: i) sorting on the basis of cell surface markers expression; ii) sorting of a side population (SP) based on Hoechst dye efflux; iii) sorting on the basis of ALDH activity (Aldefluor assay); iv) generation of floating tridimensional cell clones (tumorspheres).

i) *Cell surface markers.* CSC in solid tumors can be identified and isolated through an extensive set of markers that are found to be expressed non-uniformly throughout the tumor and are often reflective of the markers related to developmental programs of the tissue of origin. The original studies on leukemia stem cells rested heavily on the well understood stem-progenitor hierarchy in the hematopoietic compartment. Thus, normal hematopoietic stem cell markers CD34 and CD38 were chosen for the definition of leukemia stem cells [22,23]. In other cases, such as the CD44 and CD24 combination used for human breast CSC isolation, markers were selected on the basis of their heterogeneous expression in breast tumor and not because they defined normal breast stem cells [24]. Nonetheless, the combination of CD44 and CD24 is the most extensively employed in breast CSC research. The pioneering study by Al-Hajj and colleagues [24] showed that an extremely low number of human breast cancer cells with the $CD44^+/CD24^-$ phenotype were able to generate a tumor in immunocompromised mice, whereas breast cancer cells with alternative phenotype did not have tumor-initiating ability, even when injected at higher numbers. Since then, many studies investigated the reliability of this marker combination, some of them confirming the association with the CSC phenotype, some others obtaining ambiguous results [69]. In particular, it has been proposed that the $CD44^+/CD24^-$ CSC phenotype could be associated to the basal-like breast cancer subtype [66], and the finding that $CD44^+/CD24^-$

phenotype shows very little overlap with the $ALDH^+$ phenotype (that will be discussed later in this section) suggests that multiple CSC phenotypes could co-exist within the same tumor [50,70]. Furthermore, CD44 exists in several splice variants, with some of these CD44 variants (CD44v) better identifying breast CSC compared to the standard isoform (CD44s) [71] . Thus, studies using pan-CD44 antibodies may overestimate the CSC content of a tumor cell population. Other breast CSC markers include the integrins CD29 (β1) and CD49f (α6) [66], as well as Stem cell antigen 1 (Sca-1) for murine mammary CSC [72].

ii) *ALDH activity*. As described previously in this chapter, aldehyde dehydrogenase 1 (ALDH1) is broadly used as a functional marker in various types of cancer. ALDH1 is a detoxifying enzyme responsible for the oxidation of intracellular aldehydes whose activity was initially found to be increased in hematopoietic and neural stem and progenitor cells. The first report of increased ALDH activity in breast cancer stem cells was reported by Ginestier and colleagues [73], which showed that $ALDH^+$ breast cancer cells had increased tumor-initiating ability in immunocompromised mice compared to $ALDH^-$ cells. ALDH activity can be detected in live cells through an enzymatic assay that was first developed by Jones and colleagues to isolate viable hematopoietic stem cells [74]. This assay, frequently named Aldefluor assay, is based on the use of the ALDH fluorescent substrate BODIPY-aminoacetaldehyde (BAAA), which freely diffuses into intact and viable cells. In the presence of ALDH, BAAA is converted into BODIPY-aminoacetate (BAA), which is retained inside the cells. The amount of fluorescent reaction product is proportional to the ALDH activity in the cells and can be measured using a flow cytometer, thus allowing the sorting of viable $ALDH^+$ cells, an operation that would be impossible with the use of antibodies since ALDH is an intracellular protein.

iii) *Side Population*. The observation that a small population of murine cells from bone marrow aspirate did not accumulate the vital dye Hoechst 33343 was first described by Goodell and colleagues [75]. The population capable of excluding this dye was named side population (SP), which was shown to be enriched in hematopoietic stem cells. Using flow cytometry, SP has been isolated from a variety of tumors, including breast, and was associated to CSC features such as increased tumorigenicity and self-renewal [76]. SP results from the extrusion of the dye from the cell through ABC transporters including MDR1, MRP1-5 and BRCP1 [76], whose function was described previously in this section. Although SP is clearly enriched in stem cells, SP is not a common feature of stem cells through different tissues. Moreover, SP can represent differentiated cells with specialized function within organs, where ABC transporters play a role in protection against cytotoxic effects of toxins and xenobiotics [76]. Similarly, not all cancers contain SP cells, and SP could include cancer cells that are not CSC.

iv) *Generation of floating tridimensional cell clones (tumorspheres).* The 2000s saw the emergence of spherical anchorage-independent clones as a means for propagating and analyzing stem cell populations. Such floating tridimensional clones have been termed "sphere" or "spheroids", and can be referred to both normal and CSC. Originally, the quantification and characterization of these floating spheroids was developed for normal neural stem cells, in which a single cell is able to give rise to a sphere by clonal expansion [77,78]. In the following years, spheres were developed from a wide range of solid tumors, including breast cancer [79], under the same assumption that sphere generation ability allows measuring self-renewal ability. Spheres from brain and breast (either normal or cancerous) stem cell culture are termed "neurospheres" [77,80] and "mammospheres" [79,81], respectively, in relation to their tissue of origin. "Tumorsphere" generically refers to spheres derived from cancer tissues or cell lines [82]. Methods for CSC isolation and expansion as spheres do not differ much from one cancer type to another [82]. The first step consists in mechanical and enzymatic dissociation of the tumor in single-cell suspensions. CSC culture can also be obtained from cancer cell lines. Subsequently, the cell suspension is plated at low density in a specific medium in low-adherent conditions to promote cell expansion as non-adherent spherical clones. The medium used is serum-free and supplemented with factors that favor stem cell growth, including basic fibroblast growth factor (bFGF), epidermal growth factor (EGF) and insulin [82]. In breast cancer, use of serum-containing medium promotes cell differentiation from an undifferentiated state [79]. Moreover, inhibition of adhesion induces death through *anoikis* in nonmalignant and differentiated cells, while CSC survive and grow in serum-free suspension [83]. Given the exclusive ability of CSC to survive and grow under these conditions, tumorsphere generation gained popularity as an in vitro surrogate assay substituting the more time and money consuming tumor-initiation assay (that will be described in the next section). Readout of the "sphere-generation assay" involves the evaluation of the number and size of the spheres. However, it should be noted that recent works highlighted the high degree of phenotypical heterogeneity in tumorspheres from different cell lines [84,85], while others reported that the tumorsphere assay enriches CSC population in a cell line–dependent manner and that the conventional monolayer culture might maintain tumor-initiating phenotype more effectively than the tumorspheres depending on the cancer cell line [86,87]. Thus, as I will describe soon, the usage of tumorsphere model should be complemented by *in vivo* assays.

Despite the isolation methodology, establishing that a subpopulation of cells is a *bona fide* CSC population relies on the validation of the biological characteristics of CSC, including tumor-initiating ability, self-renewal and the ability to histologically recapitulate the tumor of origin (**Figure 4**).

- *Tumor-initiating ability.* As stated previously in this chapter, the operative definition of CSC is that of tumor-initiating cell. Theoretically, implantation of a single CSC should be able to generate an entire tumor in a mouse model. Therefore, as mentioned earlier, an important test for a prospectively isolated CSC population is the ability to recapitulate a tumor at low cell densities, and limiting dilution assays are useful to estimate the frequency of CSC within a cell population [17]. As stated previously, *in vitro* surrogate of tumor formation is considered the ability to form a sphere (sphere-generation assay) or a colony in soft agar.
- *Self-renewal.* As a property of stem cells is that of generating at least one cell with the same biological properties upon mitotic division, thus self-renewing itself, a CSC must have the ability to sustain itself by continuously generating cells with the same potential of tumorigenicity. Self-renewal in CSC can be experimentally demonstrated *in vivo* by serial transplantation of tumors. This assay represents the gold-standard for CSC assessment [17]. Following prospective isolation of CSC from a bulk population, the putative CSC are injected in a mouse to initiate a tumor. The tumor is subsequently removed and dissociated to re-isolate cells with prospective CSC phenotype, which are then re-injected into a new mouse to test again its tumor-initiating potential. If the isolated cells are *bona fide* CSC, they should be able to maintain their tumor-initiating potential across subsequent passages of transplantation, while cells with alternative phenotypes should not display this ability. As for the tumor-initiating assay, also the serial transplantation assay has its *in vitro* surrogate, which is represented by the assessment of the capability of the cells to form spheres or colonies in soft agar through multiple generations.
- *Recapitulating tumor heterogeneity*. Besides the ability of self-renewing, normal stem cells have the ability to generate a daughter cell that can differentiate into a more specialized, non-stem cell. Stem cells are thus defined as totipotent, pluripotent, multipotent or unipotent according to their potency of generate few or several differentiated cell types. Normal stem cells of adult tissues (e.g. hematopoietic stem cells and epithelial stem cells) are usually multipotent, being able to regenerate multiple cell types composing the specific tissue they belong. In the same way, CSC should be able to differentiate and recapitulate the heterogeneity seen in the tumor of origin. This can be assessed *in vivo* by examining the intra-tumor heterogeneity in CSC-derived tumors in mice, or by determining the ability of the CSC to differentiate *in vitro.* For instance, al-Hajj and colleagues showed that injection of

$CD44^+/CD24^-$ cells from breast cancer biopsies into host mice led to development of tumors with a heterogeneous surface phenotype reminiscent of the original tumor, with only a minority of cells retaining the CSC phenotype [24]. Differentiation in culture has been shown to occur in the presence of serum both with and without other factors known to induce differentiation in the specific tissue type being studied. The in vitro differentiated cells not only lose markers of CSCs, but also lose tumorigenic potential [17].

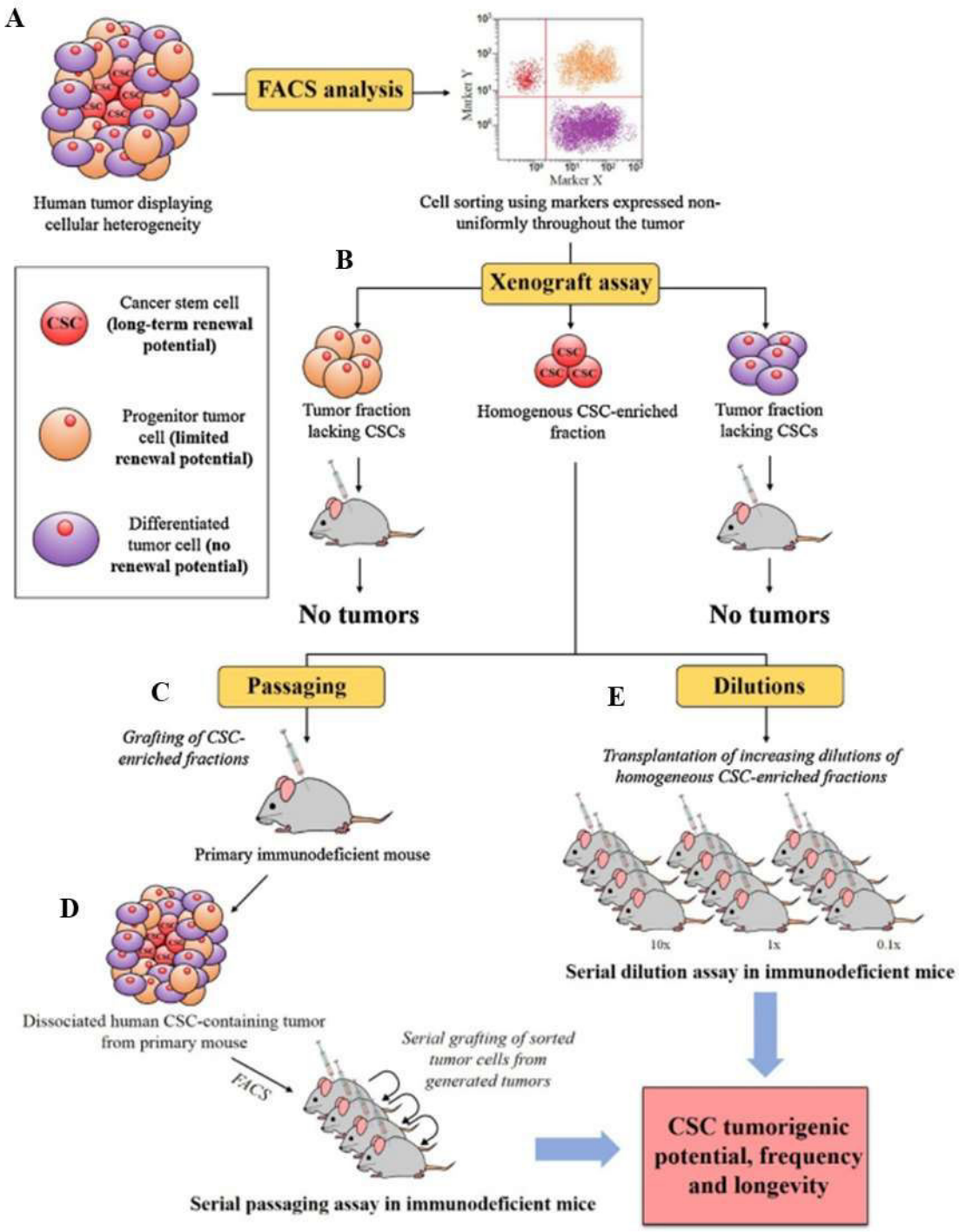

Figure 4. Validation of the biological characteristics of CSC. A) To identify bona fide CSC, markers found to be expressed non-uniformly within the tumor can be used to isolate different subpopulations via FACS. **B)** Following isolation of putative CSC, the xenotransplantation assay indicates the ability of the isolated CSC to give rise to a new tumor. **C)** Long-term self-renewal capacity is determined by serially transplanting the putative CSC subpopulation, indicating that the selected population retains the tumor-initiating potential across multiple generations **D)** The tumors grown in mice should recapitulate the heterogeneity of the initial tumor, in which both CSC and non-CSC populations are present. **E)** Tumorigenic potential and frequency of CSC can be quantified by performing a serial dilution assay, which involves administering increasing dilutions of putative CSC into mice. Adapted from *Koren E and Fuchs Y. Drug Resistance Updates. 28, 2016* [52].

BACKGROUND & AIMS OF THE THESIS

Breast cancer immunotherapy has always been the focus of our research group, under the guidance of Professor Federica Cavallo. In particular, our group produced a large number of studies regarding DNA-based vaccination against the oncogenic protein Her2/neu in the BALB-neuT mouse model, derived from inbred BALB/c mice overexpressing the activated rat Her2/neu oncogene under the transcriptional control of the MMTV-LTR promoter. These transgenic mice recapitulate human breast cancer progression finally leading to the development of tumors in all 10 mammary glands with 100% incidence and eventually of distant metastases [88]. A Her2/neu$^+$ cell line was derived from the mammary cancers of BALB-neuT mice. This cell line, named TUBO, is able to grow when injected in syngeneic BALB/c mice, thus allowing the testing of anti-rat Her2/neu vaccines in mice with no central tolerance towards this mutated oncogene, as well as the study of biological properties of this tumor *in vitro*. Furthermore, Professor Cavallo and colleagues contributed to coin the term "oncoantigens", which refers to tumor-associated molecules that have a causal role in the promotion of carcinogenesis and cannot be easily down-modulated or negatively selected by cancer cells under the pressure of a specific immune attack [89]. When expressed on the cell membrane they can be the target of both cell-mediated and antibody-mediated immune responses.

The interest of our research group in the CSC field came along with a collaboration with the group of Professor Benedetta Bussolati, whose focus was on the use of stem cells in the regenerative disease.

The aim of this joint effort was to evaluate the presence and characteristics of tumor – initiating cells in the BALB-neuT model. Tumorspheres derived from BALB-neuT tumors could be passaged several times without losing their clonogenic potential, that on the contrary increased compared to the primary tumor population. Furthermore, when cultured in differentiation conditions, sphere-derived cells displayed the ability to differentiate in epithelial/myoepithelial cells of the mammary gland expressing basal and luminal cytokeratins and α-smooth muscle actin. In addition, tumor spheres were more resistant to doxorubicin compared with parental tumor cells. Furthermore, tumorspheres had a superior tumor-initiating ability compared to cells grown as monolayers. It was found that Stem cell antigen (Sca)-1$^+$ population derived from mammary BALB-neuT tumors is responsible for sphere generation *in vitro* and for initiating tumors *in vivo* [72].

By that time, our group was on the look for fresh oncoantigens other than Her2/neu to be used as targets for immunotherapy. Thus, a pipeline to identify and characterize genes differentially activated during cancer progression was developed to help in this task [90]. High-throughput transcription analysis can be used to highlight the gene signatures that differentiate successive stages of tumor progression in transgenic mice. Of the transcripts upregulated going from pre-neoplasia to overt cancer, only those that have an orthologue in humans, low expression in normal human tissues, and

a high and homogeneous expression in human cancers are selected as "putative" oncoantigens. They are then validated by immunizing tumor-bearing mice with DNA vaccines targeting them.

Following that first experience with CSC, came the idea that greater efficacy could be achieved by targeting oncoantigens expressed by CSC [91] by virtue of their role in the progression, metastasis, resistance to therapy, and recurrence of tumors.

Thus, to identify oncoantigens expressed by CSC of mammary cancer, our group performed a comparative transcriptomic analysis between TUBO cells cultured as monolayer and serial sphere passages of the same tumor cells. Serial passages of spheres displayed increasing clonogenic potential, as well as a higher tumor-initiating ability, even at very low numbers, compared to TUBO cells grown as monolayer. Furthermore, spheres showed stronger positivity to several CSC markers including Sca-1, Nanog, Oct-4 and ALDH activity [92]. All these data strongly suggested that tumorspheres of the TUBO cell lines were enriched in CSC. Despite CSC are likely contained also in the monolayer culture, they are so few compared to tumorspheres that they do not affect the result of the transcriptomic analysis. The investigation I performed throughout my doctoral studies starts from these premises.

The general aim of my thesis was in fact that of identifying suitable targets expressed by CSC, validating their role in CSC biology and testing targeted approaches against CSC in the preclinical setting.

Since this main topic includes three lines of research, which led to three independent papers, this thesis will be structured in three chapters:

- *Chapter 1*: here, I will provide general notions regarding cancer immunology and immunotherapy, with a particular focus on DNA-based vaccination. This will allow the reader to fully understand the rationale and the context of the study reported in ***Paper I***. In this paper, we selected xCT as one of the candidate targets whose expression is upregulated in tumorspheres, and it is known to be involved in the detoxification of ROS. xCT is highly expressed by a variety of malignant tumors and plays an important role in cancer growth, progression, metastatic dissemination and drug resistance. All these features make xCT an interesting target for DNA-based vaccination. The aim of this project was therefore to explore the link between xCT and CSC biology and to evaluate the effects of anti-xCT DNA-based vaccination on tumor growth and metastasis formation.

- *Chapter 2:* In this chapter, I will provide notions regarding the use of nanoparticles loaded with contrast agents and drugs in therapy and diagnosis of cancer. In particular, I will focus

on the use of L-Ferritin based nanoparticles and of the natural compound Curcumin as anticancer drug. This will introduce the research carried out in ***Paper II*** in collaboration with Professor Silvio Aime and his research group of molecular imaging. Here, we observed that the only known L-ferritin receptor, Scavenger Receptor Class A, Member 5 (SCARA5), is upregulated in TUBO-derived tumorspheres compared to epithelial TUBO cells. Hence, the aim of this project was to explore the possibility that loading curcumin into ferritin cavity can represent a feasible way for targeted drug delivery to breast CSC.

- *Chapter 3:* In this chapter, I will provide a brief introduction on triple negative breast cancer (TNBC), one of the most aggressive types of human breast cancer. Since women with TNBC have the highest rates of early cancer recurrences as compared to other breast cancer subtypes, we hypothesized that CSC could play a central role in TNBC. Thus, by taking advantage of our workflow developed for the identification of oncoantigens expressed by CSC on TUBO cells, in ***Paper III*** (unpublished) we performed a transcriptome analysis of cells grown as monolayer and tumorspheres derived from human (HCC1806) and mouse (4T1) TNBC cell lines, with the aim of identifying common pathways regulated in CSC and novel potential therapeutic targets.

CHAPTER I

Fighting breast cancer stem cells through the immune targeting of the xCT cystine/glutamate antiporter

I.1 Cancer immunology: an overview

During cancer arising and progression, tumor cells interact with and are shaped by a huge variety of accessory cells, which can either positively or negatively affect their evolution. Among them, cells belonging to the immune system are major players in this interaction. The concept that a physiological function of the immune system is to recognize and eliminate continuously arising transformed cells was postulated by Burnet and Thomas in the '50s with the name of *immunosurveillance* [93]. Since then, many others tried to experimentally validate this hypothesis, but with contrasting results. In recent years, better techniques and models contributed to establish the physiological relevance of cancer immunosurveillance in both mice and humans, giving new impetus to the research field of cancer immunology [94].

The first experimental demonstration that tumors can induce protective immune responses came from studies on transplantable tumors performed in the '50s and reviewed in [93]. In inbred mice, sarcoma was induced by painting the skin with the chemical carcinogen methylcholanthrene (MCA). When the tumor was resected and transplanted into other syngeneic mice, the tumor was able to grow. However, if the tumor was transplanted back into the original mouse, tumor rejection occurred. Furthermore, T cells from the tumor-bearing mouse transferred to a tumor-free mouse could confer protection against tumor challenge. These observations indicate that the tumors express antigenic peptides that can become targets of a tumor-specific T-cell response that rejects the tumor. These tumor rejection antigens expressed by experimentally induced murine tumors are usually specific for an individual tumor. In fact, transferring T cells from a tumor-bearing mouse protects a syngeneic mouse from challenge with cells from that same tumor, but not from challenge with a different syngeneic tumor.

I.1.1 Tumor antigens

Earlier classification of tumor antigens distinguished between tumor-associated antigens (TAA) and tumor specific antigens (TSA): the formers are expressed by both normal and cancer cells and are usually represented by molecular components of normal cells whose expression is deregulated in tumors; the latter are expressed exclusively by cancer cells and are usually the product of mutated genes. However, this classification is often replaced by a more modern one, which takes into account the molecular structure and the source of the tumor antigens.

The most common tumor antigens are those represented by products of mutated genes, and thus defined as neo-antigens [95]. The transformation of normal cells towards malignant cells in fact requires one or more mutations in oncogenes or oncosuppressors. If protein-coding, such genes can produce mutated proteins which can enter the class I antigen processing pathway, with subsequent

presentation of their derived peptides on the cell surface by Major Histocompatibility Complex Class I (MHC-I). These proteins can also enter the class II antigen processing pathway if tumor cell debris are phagocyted by APC, and their derived peptides can then be presented on the cell surface by MHC class II (MHC-II). Since normal cells do not express these mutated antigens, they are recognized as non-self and can elicit both $CD4^+$ and $CD8^+$ T cell activation. Besides oncogenes and oncosuppressors, mutations can involve also non-tumor related genes that, if protein-coding, can anyway produce mutated antigens recognized by the immune system. Since a high number of mutations is often associated to mutagen-induced cancers [96], tumors such as UV rays-induced melanomas and cigarette smoke-induced lung cancers are often highly immunogenic [97]. As a consequence, patients with tumors carrying an high mutational burden are responsive to checkpoint inhibitors (that will be described in *Section 2.2* of this chapter) thanks to the presence of tumor-antigen specific T cells [98–100].

Other antigens recognized as non-self by the immune system are represented by products of oncogenic viruses, such as B cell lymphoma-associated Epstein - Barr virus (EBV) or cervical carcinoma-associated Human Papilloma Virus (HPV). Oncogenic viruses enter normal cells in the host organism and start producing viral proteins. Such proteins can be processed in the class I antigen processing pathway and thus recognized by $CD8^+$ T cells or can be recognized by antibodies if expressed on the cell surface. Unlike products of mutated genes, which are specific for each patient since they are often the result of random mutations, antigens of oncogenic viruses are shared by many patients and can thus represent an ideal target for antitumor vaccines. HPV-induced cervical cancers, whose incidence has been strongly reduced by preventive vaccination programs [101], represent a significant case and therapeutic anti-HPV-related cancer vaccines are under study in patients [102].

Proteins that are not mutated but that are abnormally expressed by tumor cells can also represent tumor antigens. This is for example the case of the melanocyte differentiation antigen tyrosinase, which has been found to induce cellular and humoral responses in melanoma-bearing patients. This likely happens because tyrosinase is expressed in normal melanocytes at such low levels that it is not able to induce tolerance of the immune system. As its expression levels in melanoma increases, this elicits an immune response [103]. A similar phenomenon occurs for the so-called cancer/testis antigens, which are expressed in gametes and trophoblast but not by normal somatic cells. Such antigens, such as NY-ESO-1 and those belonging to the MAGE family, are re-expressed by many tumors. As such, non-mutated antigens such as differentiation and cancer/testis antigens have been explored by several pre-clinical and clinical studies as targets for anticancer vaccination [104,105].

Additionally, antigenicity of cancer can derive from altered glycosylation pattern of surface glycoproteins and glycolipids. This can result in the presence of novel tumor-specific carbohydrate

or peptide epitopes that can elicit a humoral immune response. An example of such altered glycoproteins is represented by MUC-1, a member of the mucin glycoprotein family whose expression is deregulated in breast cancer. As for other non-patient specific antigens, studies aimed at targeting MUC-1 with vaccines are ongoing [106].

In the next section, I will briefly describe the mechanisms through which the immune system attacks the tumor. As we will see, despite T-cell response being the main mediator of tumor rejection, other cell populations belonging to both innate and adaptive immune response play their roles in the fight against cancer. Of particular relevance is the antibody response that can be mounted against antigens expressed on the cell surface. Regarding breast cancer, I have already mentioned MUC-1, but another remarkable example is represented by Her2, which is overexpressed by about 20% of primary breast carcinomas compared to normal tissue [107]. A strong correlation between antibodies against Her2 and Her2 overexpression in breast cancer is observed [108], indicating that, at least in the early stages of cancer progression, the organism is able to mount an humoral response against cancer antigens. Although no benefits in terms of survival have been reported, these auto-antibodies modulate the transforming properties of Her2/neu signaling toward an anti-proliferative state, similar to what has been demonstrated for the therapeutic Her2 antibody [109].

I.1.2 Immune evasion of tumors

Despite the pivotal role of immunosurveillance, it is now clear that the immune system's action is not limited to protection against tumor development, but can select for lowly immunogenic clones of tumor cells thus indirectly promoting tumor growth [110]. This property is named cancer immunoediting, and it results from three subsequent phases described as the 3 Es [111]: i) **E**limination, which corresponds to the immunosurveillance, where innate and adaptive immune cells recognize arising transformed cells, destroying them before they can outgrow in an overt tumor; ii) **E**quilibrium, where the immune system shapes the tumor through a Darwinian selection, iteratively deleting more immunogenic tumor cells and selecting for tumor cells which are able to survive the immune attack; iii) **E**scape, where the immunologically shaped tumor expands in an uncontrolled manner and the immune system of the host is no longer able to restrain it (**Figure 5**).

Several tumor cell-autonomous and non-tumor cell-autonomous mechanisms are involved in the process of immunoediting [112], and more broadly in the tumor-microenvironment interaction [113].

Mechanisms through which tumor cells can escape immune attack can be divided into two broad categories: i) intrinsic mechanisms, which are activated by the tumor cells themselves, and ii) extrinsic mechanisms, which are mediated by non-tumor cells.

The most common intrinsic mechanism of tumor escape is the loss of immunogenic antigens because of the selective pressure exerted by CTL or anti-tumor antibodies, resulting in the generation of antigen loss variants of the tumor [114]. In addition, tumor cells can downregulate the expression or produce non-functional forms of the antigen-processing machinery (APM) and the MHC-I molecules themselves, thus avoiding recognition by T cells [115]. Another phenomenon often occurring is the engagement of inhibitory molecules on the T cells by tumor cells. This is the case, for example, of the checkpoint molecule programmed cell death 1 (PDCD1, or PD-1) expressed by activated T cells [116]. Its ligand PD-L1 is expressed by many tumors, thus when an activated T cell reaches the tumor microenvironment the PD-1/PD-L1 interaction leads to T cell inactivation. Finally, tumor cells can produce immunosuppressive molecules [117], such as transforming growth factor (TGF)-β, which can inhibit the function of lymphocytes and macrophages.

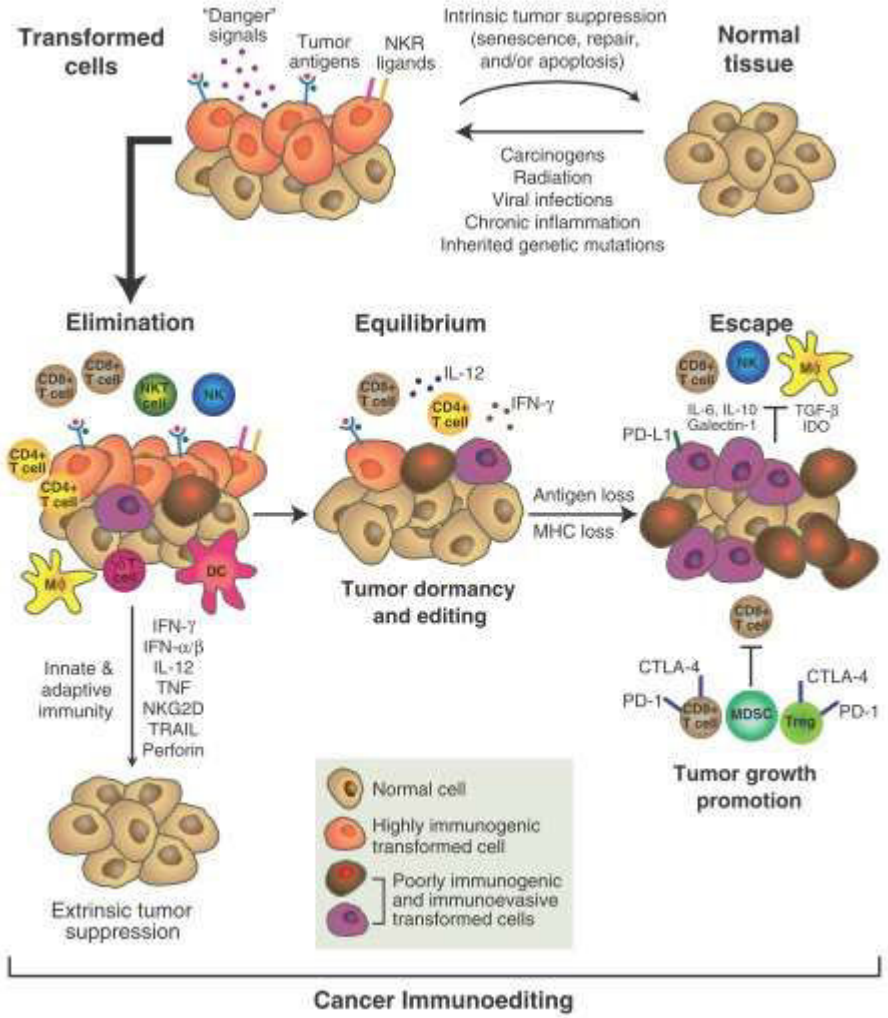

Figure 5. The cancer immunoediting process. Cancer immunoediting consists of three sequential phases: elimination, equilibrium, and escape. In the ***elimination*** phase, innate and adaptive immunity work together to destroy developing tumors before they become clinically apparent (immunosurveillance). If a cancer cell variant is not destroyed in the elimination phase, it may then enter the ***equilibrium*** phase, in which its outgrowth is balanced by immunologic mechanisms. Editing of tumor immunogenicity occurs in the equilibrium phase. As a consequence of constant immune selection pressure exerted on genetically unstable tumor cells, tumor cell variants may emerge that (i) are no longer recognized by adaptive immunity (antigen loss variants or tumors cells that develop defects in antigen processing or presentation), (ii) become insensitive to immune effector mechanisms, or (iii) induce an immunosuppressive state within the tumor microenvironment. These tumor cells may then enter the ***escape*** phase, in which their outgrowth is no longer blocked by immunity. These tumor cells emerge to cause clinically apparent disease. From *Schreiber RD et al. Science. 331, 2011* [110].

As opposite to intrinsic mechanisms, the extrinsic ones involve non-transformed cell populations, which modulate the tumor microenvironment towards immunosuppression [118]. Immuno-suppressive and tumor-promoting cell populations include regulatory T cells (T reg). Physiological T reg have an important function in shutting down immune response after the elimination of the pathogen and to prevent autoimmunity. In the cancer setting, they prevent effector T cell activation by competing with them in the interaction with APC and in the Interleukin (IL)-2 uptake. Moreover, they secrete the immunosuppressive molecules TGF-β and IL-10 [119]. Another tumor-promoting cell population is represented by alternatively-activated macrophages (M2) that, contrarily to M1, behave as if they were trying to heal a wound and not to kill a pathogen. Consequently, they secrete factors that promote tumor neo-angiogenesis, such as vascular endothelial growth factor (VEGF), and that impair T cell function, such as IL-10, prostaglandin E_2 (PGE_2), arginase and TGF-β [120]. Other major players include another population of myeloid cells, the so-called myeloid-derived suppressor cells (MDSC). Deriving from diverse ranges of myeloid precursors, MDSC are recruited to inflammation sites, including the tumor microenvironment. Here, MDSC directly suppress T cell proliferation and function by secreting several molecules including IL-10 and PGE_2, and produce arginase and indolamine 2,3-dioxygenase which metabolize arginine and tryptophan, thus starving T cells. Furthermore, they induce the generation of T reg, which support an immunosuppressive microenvironment [121].

I.1.3 Immune response to tumors

Regarding the adaptive immunity branch, tumors elicit both T cell-mediated and humoral responses. $CD8^+$ Cytotoxic T lymphocytes (CTL) perform a surveillance function by recognizing and killing malignant cells that express tumor antigen-derived peptides associated to the MHC-I molecules through their T cell receptor (TCR). Since most tumor cells lack the expression of the co-stimulatory molecules required to activate a T cell response, tumor cells and their antigens need to be

captured by Antigen Presenting Cells (APC), in particular Dendritic Cells (DC), which process the internalized tumor antigens and present them on both MHC-I and MHC-II molecules. Tumor antigens presented on MHC-II molecules are then recognized by $CD4^+$ T helper lymphocytes (Th), and APC provide the co-stimulatory signals required for their activation, namely B7.1/2-CD28 interaction, followed by CD40-CD40L interaction. By secreting immune-stimulatory cytokines, activated Th cells can provide stimulatory signals to both CTL and B cells. Tumor antigens ingested by DC can also enter the proteolytic pathway, required for antigen presentation on MHC-I molecules. In this way, DC present tumor antigens to and activate CTL, a process called *cross-presentation* [122]. Once tumor-specific CTL clones are activated, they propagate and seek to kill tumor cells with only the MHC-I-TCR interaction being required. When CTL represent a high proportion of the tumor infiltrating lymphocytes (TIL) in patients, there is a higher chance of better prognosis [123]. In addition, tumor-specific antibodies can be generated in tumor-bearing patients [124]: B cells expressing tumor antigen-specific B cell receptors (BCR) can act as APC, internalizing the antigen and presenting the deriving peptides on MHC-II molecules. When interacting with an activated Th specific for that tumor antigen, the B cell undergoes activation and is prompted to produce tumor antigen-specific antibodies, thanks to the activation signals provided by the Th cell.

Like the adaptive immune system, also innate immune cells can recognize and kill tumor cells. NK cells recognize cells that express low or no MHC-I molecules since the engagement of the KIR receptor by MHC-I molecules delivers inhibitory signals to the NK. As a result of negative selection by CTLs, many tumors express low levels of MHC-I, thus making them a good target for NK [125]. In addition, NK cells can be activated by ligands directly expressed by tumor cells or by recognizing anti-tumor IgG bound to tumor cells, which trigger antibody-dependent cell-mediated cytotoxicity (ADCC) with subsequent release of cytolytic granules. In addition to NK cells, classically Interferon (IFN)-γ-activated macrophages (M1) can fight tumor growth as they would fight a microorganism infection [120]. M1 macrophages secrete cytotoxic compounds including lysosomal enzymes, reactive oxygen species (ROS) and nitric oxide (NO), as well as tumor necrosis factor (TNF), which then lead to tumor cell death.

I.2 Immunotherapeutic approaches to fight cancer

Advances in understanding of the immune system and in defining antigens on tumor cells have encouraged many new strategies to fight cancer. Anticancer immunotherapy can be defined as the induction or enhancement of an immune response to treat cancer. Anticancer immunotherapies are generally classified as “active” or “passive”, depending on the ability to stimulate the active host immune response against the tumors or to directly act as anti-tumor agents, respectively.

I.2.1 Passive immunotherapy

Passive immunotherapy involves the transfer of immune effectors endowed with intrinsic antineoplastic activity, including tumor-specific T cells and antibodies, into patients. Passive immunization against tumors is rapid but does not lead to long-lived immunity.

Tumor-specific monoclonal antibodies (mAb) are the best-characterized form of anticancer immunotherapy, and perhaps the most widely employed in the clinic [126]. Anti-tumor mAb specifically recognize molecules expressed on the surface of tumor cells and lead to their destruction by the same effector mechanisms working for microbes elimination, including opsonization and phagocytosis, activation of the complement system, and ADCC [127]. In addition, some antibodies may interfere with signaling pathways required for the progression and survival of tumor cells or may trigger death signals by binding to surface receptors [127]. Finally, anti-tumor mAb can be conjugated to toxins or radionuclides and promote the delivery of these cytotoxic agents specifically to the tumor [127]. Amongst the many available, two examples of mAb approved for clinical use are Cetuximab and Trastuzumab, which respectively target EGFR and Her2 on the tumor cell surface. A particular case is provided by Bevacizumab, which targets and neutralizes the soluble growth factor VEGF, thus preventing tumor angiogenesis.

Adoptive cellular immunotherapy, also named adoptive cell transfer (ACT), is the transfer of cultured immune cells that have anti-tumor reactivity into a tumor-bearing host. In ACT, usually blood or tumor-infiltrating lymphocytes of a patient are isolated and expanded *ex vivo* by culture in immunostimulatory cytokines such as IL-2 and are infused back into the patient. This treatment, often combined with systemic IL-2 administration, leads to tumor regression in some patients [128]. Another approach for adoptive therapy is T cell receptor (TCR) gene therapy in which tumor patient's T cells are transduced *in vitro* with genes encoding a TCR specific for a tumor antigen, expanded, and then infused back into the patient [129]. The patient's T cell can be also engineered to produce a chimeric antigen receptor (CAR), in which the tumor antigen-binding domain of an immunoglobulin is linked to one or more immunostimulatory signal transduction domains, thus making T cells capable of recognizing tumor antigen-expressing cells in an MHC-independent fashion [130]. Very recently, a CAR-T cell therapeutic named tisagenlecleucel has been approved by FDA for certain pediatric and young adult patients with a form of acute lymphoblastic leukemia (ALL)

(https://www.fda.gov/biologicsbloodvaccines/cellulargenetherapyproducts/approvedproducts/ucm573706.htm).

I.2.2 Active immunotherapy

Unlike passive immunotherapy, active immunotherapy exerts anticancer effects only upon the engagement of the host immune system.

The earliest attempts to boost anti-tumor immunity relied on nonspecific immune stimulation, such as local administration of inflammatory molecules. These include pattern recognition receptors (PRR) agonists such as exogenous pathogen-associated molecular patterns (PAMP) and endogenous damage-associated molecular patterns (DAMP). By binding PRR expressed on the surface of immune cells, PAMP and DAMP activate pro-inflammatory cascades in different populations of immune cells, contributing either to their activation and maturation or to the secretion of effector molecules such as immunostimulatory cytokines. PRR agonists can be provided as drugs or can be released by dying cancer cells in a process called "immunogenic cell death" (ICD) [131]. ICD can be induced by some commonly used chemotherapeutic drugs such as anthracyclines and by radiation therapy, whose activity has been shown to rely not only on their intrinsic cytotoxic effects, but also on a properly functioning immune system [132].

Immunostimulatory cytokine therapies represent another method of enhancing the immune response in a nonspecific manner, mainly acting as polyclonal activators of T-cell responses. Cytokines may be administered locally or systemically for the treatment of various human tumors, even though the use of cytokines as standalone therapeutic interventions is generally associated with poor results in cancer patients [126]. Hence, immunostimulatory cytokines are generally used as adjuvants for other anticancer approaches, as is the case for granulocyte colony-stimulating factor (G-CSF), granulocyte-macrophage (GM-)CSF and tumor necrosis factor (TNF)-α. The largest clinical experience is with IL-2, which induces the secretion of other inflammatory cytokines by T-cells such as TNF and IFN-γ, and is FDA-approved for the therapy of melanoma and renal carcinoma [126]. IFN-α is another immunostimulatory cytokine which acts by inhibiting tumor cell proliferation and increasing cytotoxic activity of NK cells, as well as increasing susceptibility of cancer cells to killing by CTL through upregulation of MHC-I. IFN-α is approved for the use against malignant melanoma, carcinoid tumors, and certain types of lymphomas and leukemias [126]. Notably, as cytokines exert pleiotropic functions in the organism, their use is often associated with diverse degrees of toxicity [133].

Another way of non-specifically activating novel or restoring a pre-existing host immune response against tumors is by means of immunomodulatory mAb. Immunomodulatory mAb act by binding to - thus modulating the activity of - molecular components of the immune system. This can be achieved through the inhibition of immunosuppressive axis acting on T lymphocytes, such as cytotoxic T lymphocyte-associated protein 4 (CTLA4)/CD28 and PD-1/PD-L1 and PD-L2 [134]. By interacting

with their ligands expressed on APC or tumor and stromal cells, respectively, these axes prevent the activation or the uncontrolled activity of T cells. Commonly referred to as "checkpoint inhibitors", these mAb have been shown to induce robust and durable responses in cohorts of patients with a variety of solid tumors [135]. Checkpoint inhibitors currently approved in the clinics include the anti-CTLA4 mAb Ipilimumab, the anti-PD-1 mAb Pembrolizumab and Nivolumab, and the anti-PD-L1 mAb Atezolizumab. Despite their impressive results in the clinical setting, the use of checkpoint inhibitors are often associated with toxic autoimmune responses [135]. This is conceivable since the physiological role of checkpoint axis is to prevent unwanted or uncontrolled immune-responses against self-antigens.

Having briefly described nonspecific immune stimulators, I will now focus on the most tumor-targeted form of active immunotherapy in cancer treatment: the anti-tumor vaccines.

I.3 Cancer Vaccines

Generally speaking, cancer vaccines can be either prophylactic or therapeutic. Prophylactic vaccines are designed to prevent the appearance of a given disease, while therapeutic vaccines are aimed to cure an existing disease. In the context of cancer, prophylactic vaccines have proven their efficacy in the case of virus-related cancers, as Human Papillomavirus (HPV)-induced cervical cancer and Hepatitis B Virus (HBV)-induced hepatocarcinoma. These vaccines are meant to generate neutralizing antibodies that prevent the oncogenic virus to infect the target cells. This is defined as primary cancer prevention, i.e. prevention of tumor onset through the elimination of carcinogenic risk factors [89]. However, it should be pointed out that in these cases the etiological agent is known. In most cases, tumors are not caused by a viral infection and their appearance, the type and the antigen burden cannot be foreseen, exception made for hereditary cancer syndromes which represent only 5% of clinical cases [136]. Despite this, the development of prophylactic cancer vaccines is an expanding field, mainly focused on pre-cancerous lesions in which a full immune-suppressive microenvironment has not been established yet and the proliferation rate of the lesion is not that much to develop immune-resistant clones [137]. This is defined as secondary cancer prevention [89]. Of course, targeting of pre-malignant lesions requires the identification of one or more appropriate target antigens, and the efficacy of prophylactic cancer vaccines has been demonstrated in genetically engineered mice in which the tumor-triggering oncogene is known [89]. Translation of secondary cancer prevention in a clinical setting would require an early diagnosis, while usually cancer is diagnosed when a symptomatic lesion has already arisen and an immune-suppressive tumor microenvironment has been already established. Nonetheless, few pioneering clinical trials showed the feasibility of this approach in the context of advanced colonic adenomas [138] and DCIS [139]. A more realistic clinical application

of preventive tumor vaccine is referred to as tertiary cancer prevention or adjuvant therapy, i.e. the prevention of local and distant tumor recurrence after conventional treatment. In this case, even though the immune system is weakened by previous treatments, potential target antigens could be more easily identified on the basis of the primary lesion [89].

Compared to prophylactic vaccination, therapeutic vaccination against established cancer has proven much more challenging, because the vaccine must face an immune system that has been restrained by tolerizing or polarizing mechanisms that sustain the disease in a misguided attempt of self-tolerance [140]. As mentioned before, several immunosuppressive activities contribute to make tumor cells less susceptible of immune attack. Tumor cells can in fact secrete immune-suppressive cytokines such as IL-10 and TGF-β and induce the expansion of T regulatory and myeloid derived suppressor cells. Moreover, immunoediting contributes to the depletion of clones of tumor cells expressing antigens recognized by the immune system, thus selecting tumor cell that are "invisible" to the immune system and are thus allowed to expand [141]. Despite these hurdles, recent advances in cancer immunology have achieved clinical proof-of-concept of therapeutic cancer vaccine. Sipuleucel-T, an immune cell based vaccine, for the first time resulted in increased overall survival in hormone-refractory prostate cancer patients. This led to FDA approval of this vaccine with the brand name Provenge (Dendreon) in 2010 [142].

In conclusion, cancer vaccines have generally reached clinical success when used for the prevention of recurrence after treatment for the primary tumor, when a functional immune system able to benefit from vaccination is re-established [141]. Since CSC have been implicated in metastatic progression and local recurrence of the disease (see *Introduction*), patients would benefit of anti-CSC vaccines in this context. Furthermore, since CSC adopt chemo- and radiotherapy resistance mechanisms (e.g. increased drug efflux and detoxification), vaccination could be and advantageous approach able to overcome resistance since its action relies on different mechanisms. Finally, anti-CSC vaccination would be able to target quiescent cells, which are not otherwise sensitive to therapies targeting fast-proliferating cells.

I.3.1 Classes of cancer vaccines

*Tumor-based strategies***.** Early cancer vaccine studies found that mice could be immunized with irradiated tumor cells, which were not able to give rise to neoplastic lesions but could act as antigen source. These tumor cells can be co-injected with immune stimulatory cytokines such as GM-CSF or can be engineered to produce and secrete these factors themselves to obtain the so-called G-VAX [143]. The tumor cells employed in these studies can be syngeneic (for pre-clinical studies) or allogeneic (for clinical tests) cell lines, as well as autologous (patient-derived) cancer cells. An alternative

approach is to use proteins or mRNAs derived from tumor lysates to load APC *ex vivo*, which are then re-injected in the patient (see "APC-based strategies" section).

*Peptide-based strategies***.** One of the most common approaches for cancer vaccination is the delivery of MHC-I restricted peptide epitopes derived from tumor antigens with the aim of activating specific $CD8^+$ T cell clones that react against these antigens. Peptide based vaccines take advantage of the ability of computer algorithms to screen amino acids sequences for candidate MHC I-restricted epitopes derived from tumor antigens. Candidate epitopes are then screened for their ability to bind MHC-I molecules and for their immunogenicity. They can be administered in different adjuvant formulations to promote in vivo presentation by endogenous APC. Preclinical data support the therapeutic effect of such vaccines, especially when the epitopes include mutated amino acid sequences and the antigen is thus recognized as non-self [144]. Peptide vaccines against cancer have been tested in clinical trials as well [145]. The advantage of peptide-based approaches is that the peptides consist of a short sequence of amino acids, thus they are relatively simple to manufacture. However, because of HLA restriction, people who do not express common HLA types cannot beneficiate of this type of vaccines. In addition, the MHC I-binding short peptides usually do not bind MHC II and thus are unable to activate $CD4^+$ helper T cells, which are important for the full activation of $CD8^+$ cytotoxic T cells [146]. This limitation can be bypassed by adding non-tumor specific help (e.g. MHC II-binding peptides derived from tetanus toxin [146]) or using long peptides which include both MHC I- and MHC II-binding sequences, which have proven to elicit superior T cell activation [147].

*APC-based strategies***.** APC-based vaccines consist on ex vivo loading of professional antigen-presenting cells, in particular Dendritic Cells (DC), with tumor antigens. DC vaccines can be developed starting from peripheral blood mononuclear cells (PBMC) isolated from patients. DC are then cultured in presence of TLR agonists, immunostimulatory cytokines and growth factors required for their maturation. DC are then pulsed with specific tumor antigens or tumor lysates and then reinfused in the patient [148]. Activated DC then process and present these antigens to T cells, eventually activating a tumor-specific immune response. The nature of the antigen (peptide, full protein or mRNA) can affect the resulting immune response, with full protein able to activate both $CD8^+$ and $CD4^+$ and mRNA coding the antigen able to enter only the MHC I-processing pathway and thus being limited to a $CD8^+$ response. APC-based vaccines have been extensively tested in clinical trials and have proven to be safe and able to promote clinically significant tumor regression in some patients [144]. Notably, the only FDA-approved anti-cancer vaccine for human application is a DC-based vaccine, namely Sipuleucel-T, consisting of autologous DC pulsed with prostatic acid phosphatase (PAP), which is present in 95% of prostate cancers, fused with GM-CSF. However, a major hurdle

of the use of DC-based vaccines is their cost: the cost of the treatment with Sipuleucel-T is in the order of 100.000 $ per patient.

*Genetic Vaccines***.** Genetic vaccines use viral or plasmid DNA vectors, or in alternative RNA-based vectors, to deliver *in vivo* the antigen-coding sequence [149]. These vectors can be administered to the subject to be vaccinated through many different routes (e.g. intradermally or intramuscularly). The resident cells take up the vectors and the coding sequence is then translated in the antigen of interest using the cell machinery. Genetic vaccines thus allow the endogenous production of the antigen of interest. For they consist in nucleic acid sequences, genetic vaccines are naturally endowed with the ability of simulating microbe infection, which contribute to induce inflammation at the injection site and to license DC for antigen presentation to T cells. Moreover, the sequence coding for the antigen can be manipulated to deliver multiple antigens or to produce antigens fused with immunostimulatory sequences, making genetic vectors a versatile tool for vaccination [146].

Our laboratory staff has a long-lasting experience with plasmid DNA-based vaccines that started in the late ’90 with the production of a vaccine targeting the Her2 protein [150] and continues nowadays with the exploration of other tumor antigens as a target, including CSC-associated antigens. Plasmid DNA vectors consist in bacterial plasmidic DNA double-strains in which the antigen-coding sequence is inserted through enzymatic digestion and subsequent ligation. DNA vaccines will be discussed in detail in the next section. An alternative to the use of DNA-based vectors is the use of mRNA-based vectors, a vehicle for the delivery of antigens that has been extensively explored [151–153].

For what concerns viral vectors, several viruses can be used as delivery vehicles for the antigen-coding sequence [149]. This sequence is inserted in the viral genome in place of essential viral genes. The virus is then assembled within host cell lines transfected with the viral genome and with plasmidic vectors coding for the missing genes required for the virion assembly. These virions, which are unable to replicate, are then used to infect the cells of the subject to be vaccinated, where they allow the expression of the antigen of interest. Concerns regarding the use of viral vectors include the possible intrinsic immunogenicity which can impede multiple administration and the possibility of integration of viral sequences into the genome host. A recent attractive approach for antigen delivery is the use of oncolytic viruses as vaccine vectors. Oncolytic viruses are intrinsically endowed with the ability to replicate in tumor cells and selectively kill them, while being harmless for normal cells [154]. Notably, in our laboratory it was documented the successful use of a Bovine Herpes Virus-4 (BoHV-4)-based vector to deliver a hybrid rat/human Her2 antigen able to protect BALB-neuT mice from autochthonous $Her2^{+}$ mammary tumor growth [155]. In mice, BoHV-4 behaves as a replication-incompetent virus, with no evidence of malignant transformation or virus-associated pathologies

reported, and displays enhanced oncolytic properties when armed with Herpes Simplex virus-1 thymidine kinase (HSV-1-TK) gene [156].

I.3.2 DNA vaccines

The origin of DNA vaccines dates back to 1992, when Tang, De Vit and Johnston first reported the possibility of eliciting a humoral immune response by directly delivering a protein-coding gene in the skin of mice through DNA-coated beads [157]. In the following years, other exploratory studies contributed to lay the foundation of DNA vaccines as an effective immunization technique, able to confer protection to viral infections through the induction of both antigen-specific antibodies and cytotoxic T lymphocytes in rodents [158–160].

Structure. DNA vaccines share some common structural features: they consist of a plasmid DNA backbone including a multi-cloning site that allows the incorporation of specific sequences, i.e. those coding for the antigen of interest. The antigen-coding sequence is preceded by a strong promoter, e.g. the cytomegalovirus (CMV) early promoter, which ensures high transcriptional efficiency, and is followed by a poly-A signal and a transcription termination signal. As plasmid DNA-based vaccines are expanded in bacterial hosts, an antibiotic-resistance gene and prokaryotic origin of replication are also required (**Figure 6**).

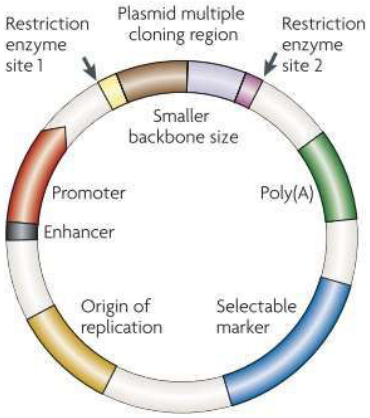

Figure 6. Structure of a DNA vaccine. From *Kutzler MA and Weiner DB. Nat Rev Genetics. 9, 2008* [161].

Mechanism of action. The proposed mechanism of action of DNA vaccines is the following [161] (**Figure 7**). Once delivered in the inoculation site (usually derma, subcutaneoum or muscle), the plasmid enters the local cells, such as myocytes or keratinocytes depending on the injection route, and the resident APC. Using the host cellular machinery, the plasmid enters the nucleus and the coding sequence starts to be transcribed and subsequently translated into a protein or a peptide string. These sequences are then processed by the cells and enter the MHC-I – processing pathway. Furthermore, depending on the encoded protein, the antigen can be either directly displayed on the cell surface as a transmembrane protein or secreted in the extracellular milieu. APC have a fundamental role in the induction of immunity of DNA vaccines by presenting peptides on MHC-I. This is consequent of either a direct transfection of APC with the plasmid, or the uptake of secreted proteins or engulfment of apoptotic cells or debris containing the antigen, and subsequent cross-presentation on MHC-I. The endocytosis of the antigen also allows the APCs to display the peptides on MHC-II molecules. The antigen-loaded APC then migrate to lymph nodes where they interact

with and activate antigen-specific T cells. Depending on the nature of the antigen encoded (full protein, MHC-I or MHC-II-binding peptide) the antigen-loaded APC can trigger a cytotoxic T cell response, a T helper response, or both. T helper response is required to prompt the production of antibodies.

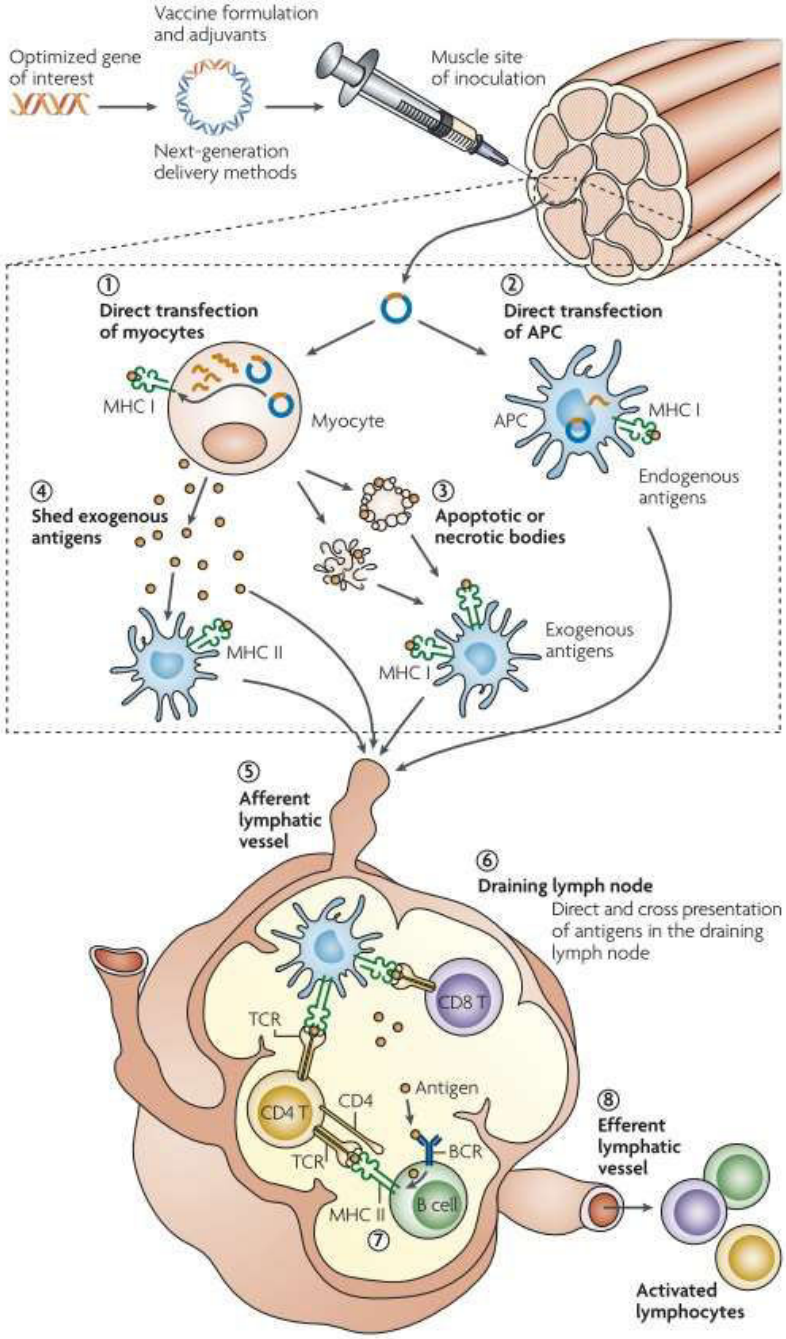

Figure 7. Induction of cellular and humoral immunity by DNA vaccines. The antigen-coding sequence is inserted into a plasmid backbone and delivered to the inoculation site. Using the host cellular machinery, the plasmid enters the nucleus of transfected myocytes (1) and of resident antigen presenting cells (APC) (2). Here, antigen-coding sequence in transcribed and subsequently translated into the foreign antigen. Presentation of vaccine-derived endogenous peptides on MHC I molecules by APC can follow either direct transfection by the plasmid vaccine (2) or cross-presentation of cell-associated exogenous antigens, following APC engulfment of apoptotic transfected cells (3). In addition, APC mediate the display of peptides on MHC II molecules after protein antigens that have been shed from transfected cells are captured and processed within the endocytic pathway (4). Antigen-loaded APC travel to the draining lymph node (DLN) via the afferent lymphatic vessel (5) where they present peptide antigens to naive T cells via MHC-T cell receptor (TCR) interaction in combination with co-stimulatory molecules, providing the necessary secondary signals to initiate an immune response and expansion of T cells (6). Activated CD4 T helper cells secrete cytokines during cell-to-cell interaction with antigen-specific B cells that present processed antigen to CD4 T helper cells and bind to co-stimulatory molecules that are required for B cell activation in the DLN (7). Activated T and B cells can now travel through the efferent lymphatic system (8) and provide a surveillance system. Adapted From *Kutzler MA and Weiner DB. Nat Rev Genetics. 9, 2008* [161].

Of note, DNA vaccines not only trigger an adaptive immune response against the encoded antigen, but they are also capable of stimulating the innate immune system thanks to their bacterial DNA backbone. Exogenous DNA is in fact recognized as a PAMP by toll-like receptors (TLR) expressed by immune cells. In particular, plasmid DNA contains hypometilated CpG dinucleotide-containing motifs that are rare in mammals and are recognized by TLR9 expressed by DC and B cells [146]. Moreover, DNA can stimulate cytoplasmic DNA sensors that lead to the production of IFN-γ and other pro-inflammatory cytokines [162]. Thus, the intrinsic nature of DNA vaccines acts as an auto-adjuvant, leading to the development of inflammatory microenvironments that facilitates the occurrence of an adaptive immune response.

Advantages and concerns of DNA vaccines. Compared to other vaccine platforms, plasmid DNA-based vaccines display high flexibility in their design as they can carry several types of genes. They are more temperature-stable than conventional vaccines and are thus easier to store and transport [161]. Furthermore, they can be rapidly manufactured on a large scale with high reproducibility due to the use of large bacterial cultures and high-yield isolation methods. Compared to viral vectors, there is no risk that DNA vaccines are cleared from the organism by pre-existing antibodies or that they induce anti-vector immunity following repeated vaccinations. In the face of their ability to induce antigen-specific humoral and cellular responses in a similar level to those elicited by other vaccine formulations, DNA vaccines display remarkable safety advantages: unlike live vaccines, they are unable to revert into virulent forms since they are unable to replicate and spread in eukaryotic organisms [161]. Moreover, as DNA vaccines are not produced in mammalian cell cultures, they bypass the risk that unknown pathogens present in the cell lines used to produce the vaccine are transferred to the vaccinated individual. One safety concern relates to the possibility of DNA vaccine to integrate in the host genome, possibly causing insertional mutagenesis and chromosomal breaks or rearrangements. However, plasmid integration in the host genome has been shown to be extremely infrequent, and preclinical and clinical evaluation of DNA vaccines have not highlighted the concreteness of this risk so far [161].

In vivo electroporation. DNA vaccines can be easily administered by simple injection, but this usually results in a weak performance [146]. This is because plasmid DNA entry in eukaryotic cells is normally very poor and simple injection fails to induce the inflammatory milieu required for a proper licensing of resident APC and the subsequent expression of co-stimulatory molecules required to activate naïve T cells. When the DNA vaccine is simply injected into the muscle, the volume of injection has shown to play a major role in the efficacy of the vaccine, with small volumes unable to produce enough hydrostatic pressure to increase transfection efficiency and to cause local damage-induced inflammation [146]. This in part explains why in the past DNA vaccines have been shown to

induce strong and protective response in small animals but were not as effective in larger animals, including humans. Since scaling up to humans would require unacceptable volumes, the study of other delivery methods able to bypass this requirement has been a compelling need. Various strategy have been explored so far, including the use of gene guns, i.e. metal beads coated with DNA plasmid and literally shot in the inoculation site [163]. Although some have shown promising, electroporation (EP) has emerged as the preferential path to bring DNA vaccines to the clinic [164].

EP consists in the delivery of short electric pulses in the inoculation site through plate- or needle-shaped electrodes. EP immediately follows the injection of the DNA vaccine in the muscle or in the skin. On one hand, the electric stimulation induces temporary permeabilization of the cell membrane through the formation of pores that facilitate the entry of the plasmid DNA inside the cells. On the other hand, EP induces cell damage, thus causing secretion of inflammatory chemokines and the subsequent recruitment of inflammatory cells at the injection site. In the case of intramuscular administration, damaged myofibers first become infiltrated by granulocytes and by monocytes. This is followed by a prominent infiltration by differentiated macrophages and DC in the necrotic myofibers. When myofibers start to heal in the following days, they also start to express the DNA vaccine-encoded gene, and B and T cells infiltrate the site. This massive recruitment of both innate and adaptive immune cells facilitates the uptake and presentation of antigens by APC and the contacts between APC and T helper cells, thus amplifying the immune response [91].

EP thus overcomes the failures of low-volume injections, increasing immune responses not only in small rodents but also in larger mammals as well as human patients [164], thus easing the translatability of DNA vaccines to the clinic.

I.3.3 Vaccination against cancer stem cells

The potential of immunotherapy against CSC has recently become an intriguing field of research. Immune effectors may succeed in overcoming some main chemoresistance mechanisms adopted by CSC, like their proliferative quiescence or efflux pumps [165]. Crucial issues under investigation are the expression and modulation by CSC of MHC and APM molecules, as well as the expression of both MHC-restricted and unrestricted antigens and the expression of immunosuppressive or immunostimulatory molecules.

A number of investigators described low immunogenicity of CSC in glioblastoma, colorectal cancer and melanoma, with reduced expression of MHC-I, deficient APM and even inhibitory activity towards specific immune response [166–169]. Similar results were observed also in melanoma, where $ABCB5^{+}$ malignant melanoma initiating cells (MMIC) displayed lower levels of MHC-I, aberrant positivity for MHC-II, and lower expression levels of melanoma-associated antigens (MART-1, ML-

IAP, NY-ESO-1, and MAGE-A) [170]. MMIC displayed immunesuppressive activity, inhibiting lymphocyte proliferation and IL-2 production more efficiently than $ABCB5^-$ melanoma cell populations. Moreover, co-culture with $ABCB5^+$ MMICs increased the abundance of T reg along with IL-10 production by peripheral bloom mononuclear cells (PBMC).

In contrast with the aforementioned reports, some evidence on the superiority of CSC as antigen source compared to non-CSC has been provided in recent years. In one of the first studies aiming to target CSC with a vaccine, neurospheres enriched in CSC were exploited to load DC to be used as a vaccine in a preclinical setting. The vaccination showed a striking curative effect in the vaccinated animals, and this effect was associated with infiltration by $CD4^+$ and $CD8^+$ T cells [171]. *Ex vivo* culturing of neurospheres seemed to increase the membrane expression of MHC-II and costimulatory molecules (B7.1, B7.2) on CSC. These achievements were obtained within murine models, but it was subsequently demonstrated that human brain CSC were capable of antigen processing and presentation, expressed functional MHC-I molecules and were susceptible to CTL-mediated lysis *in vitro* and *in vivo* [172], being a valuable source of TAA capable of triggering effective CTL-mediated immune responses upon DC vaccination [173]. The ability of eliciting a protective immune response by loading DC with irradiated CSC or lysates was also demonstrated for other types of cancer, as prostate cancer [174], ovarian cancer [175,176], melanoma and squamous cell carcinoma (SCC) [177–179]. In particular, the studies on melanoma and SCC showed that CSC, selected for their high ALDH activity, were a better source of antigens compared to non-CSC, since CSC-loaded DC had a better protective effect compared to non-CSC-loaded DC, and CSC-based vaccine was able to induce both cellular and humoral responses. These encouraging pre-clinical results prompted for the translation of CSC-loaded DC vaccines into the clinical setting. The first clinical trial was performed on glioblastoma patients [180]. Seven patients, following standard chemotherapy, received intradermal injections of DC loaded with RNA extracted from autologous neurospheres. The vaccination induced in vitro detectable immune responses in all seven patients, which had prolonged progression-free survival compared to a historical group of matched controls. Other clinical trials followed in lung [181] and pancreatic [182] cancer settings, showing that anti-CSC DC vaccine was able to induce both CSC-specific and CSC-nonspecific immune responses, and proving the vaccine was safe.

All the reported discrepancies in CSC susceptibility to immune response could be due to the tumor type or to the different techniques employed for the selection or enrichment of CSC. They express the complexity of the issue and difficulties in finding representative and reliable pre-clinical models for the investigation of CSC. This also indicates that the study of CSC immunology is still in its infancy and no general rules are defined, and there currently is a large room for further exploration in the field. Moreover, it should be noted that in none of reported anti-CSC vaccination approaches

specific CSC-antigens were identified, as DC were loaded with whole protein or mRNA derived from tumor cells.

I.3.4. Oncoantigens

As stated in *Section I.1.2*, tumors can be "shaped" by the immune system: the selective pressure of immune attack can destroy more immunogenic cells, leading to the expansion of less immunogenic clones. This is a problem faced also by anti-tumor vaccines, which may be able to eliminate the target antigen-expressing cells, but leaving other sub-populations untouched. For this reason, targeting a protein that is required for the survival of tumor cells could be the most effective strategy, as this protein is likely expressed by a high proportion of cells and cannot be easily downregulated due to its non-dispensable role [91]. This made necessary to elaborate a new definition for some tumor antigens, that of *oncoantigens* [89]. Oncoantigens are defined as tumor-associated molecules able to be recognized by the immune system and with a causal role in cancer. According to their cellular localization, oncoantigens can be further subdivided in Class I, II and III [91]. Class I oncoantigens are expressed on the cell surface, and besides T cell-mediated immune response, they can be targeted by antibodies, thus circumventing the immune escape caused by MHC-I downregulation. A clear example of class I oncoantigen is the Her2 receptor, which can be targeted by monoclonal antibodies (e.g. Trastuzumab and Pertuzumab) in $Her2^+$ breast cancers. Class II oncoantigens are soluble factors or molecules composing the extracellular matrix, and thus contribute to the creation of a permissive tumor microenvironment. Because of their localization, they can only be targeted by antibodies. Lastly, Class III oncoantigens are intracellular proteins which cannot be targeted by antibodies but can be processed by the MHC-I machinery and thus be targeted by T cells.

In the light of the encouraging results showing that CSC could be a better source of antigens compared to non-CSC (*Section I.3.3*), oncoantigens expressed by CSC may represent a better target for anti-cancer vaccination. Despite the lack of studies depicting the whole antigenic profile of CSC of different types of tumors, it is known that CSC can display different groups of tumor antigens that can be recognized by T cells, and these antigens belong to the different functional groups described for tumors in general (*Section I.1.1*), such as differentiation antigens, Cancer/Testis antigens and mutated antigens [183]. However, as postulated in the beginning of this section, an ideal antigen should be derived from a non-dispensable protein, in this case a protein required for the survival, self-renewal and tumor-initiating ability of the CSC. Currently, no consensus exists on the expression of specific tumor antigens by CSC. As CSC express various markers (see ***Introduction***) that have proven useful for identifying and isolating CSC from the bulk tumor population, these markers have been suggested as specific targets for CSC immunotherapies [184]. However, several of these markers are expressed

also by normal stem cells and are widespread in a variety of healthy tissues. The identification of novel CSC targets should rely on the following principles: i) restricted expression on healthy tissues ii) shared expression between non-CSC and CSC, to avoid the escape phenomenon and because of plasticity of the CSC phenotype (see Introduction). Of course, identification of candidate targets will be possible by evaluating a differential expression between CSC and non-CSC, since molecules upregulated in CSC are more likely to have a functional role in CSC biology.

For this reason, in ***Paper I*** we performed a high-throughput analysis to identify transcripts upregulated in the CSC-enriched tumorspheres compared to the monolayer parental cells in the murine $Her2^+$ breast cancer cell line TUBO [150]. Among the transcripts coding for surface proteins, we selected xCT as an optimal oncoantigen for anti CSC-vaccination.

I.4 The cystine/glutamate antiporter protein xCT: physiological and pathological roles

xCT is a multipass transmembrane protein of ~500 amino-acids, encoded by the gene *Solute Carrier Family 7, Member 11* (SLC7A11). It consists of 12 transmembrane, 7 intracellular and 6 extracellular domains, with both the N- and C- termini located inside the cell. xCT represents the light subunit of the heterodimeric amino-acid transport system xC- and is coupled through a disulfide bond to the heavy subunit 4F2hc, also termed CD98 [185]. While CD98 is responsible for the trafficking of the heterodimer to the plasma membrane and acts as a subunit also for other amino acid transporters, xCT is responsible for substrate specificity and transport, but requires CD98 co-expression for its activity [186]. System xC- in an obligate, Na^+-independent antiporter which exports intracellular glutamate in exchange for extracellular cysteine, the oxidized form of cysteine, in a gradient-dependent manner and 1:1 ratio [185]. Once inside the cell, cystine is then rapidly reduced to cysteine, the rate-limiting precursor in the biosynthesis of glutathione (GSH). GSH is a tripeptide thiol consisting of glutamate, cysteine, and glycine, and plays a critical role in cellular defenses against oxidative stress, acting as a free radical scavenger and detoxifying agent (**Figure 8**). GSH can reduce, both enzymatically and non-enzymatically, diverse ROS. Albeit ROS are essential for biological functions – they regulate many signaling pathways – an imbalance of ROS content within the cell can lead to harmful effects. ROS are in fact highly reactive with biological molecules, including DNA, proteins and lipids, and this reaction can result in an oxidative modification of these molecules and their functions. This may result in transient cellular alterations, up to irreversible oxidative damage and eventually cell death [187].

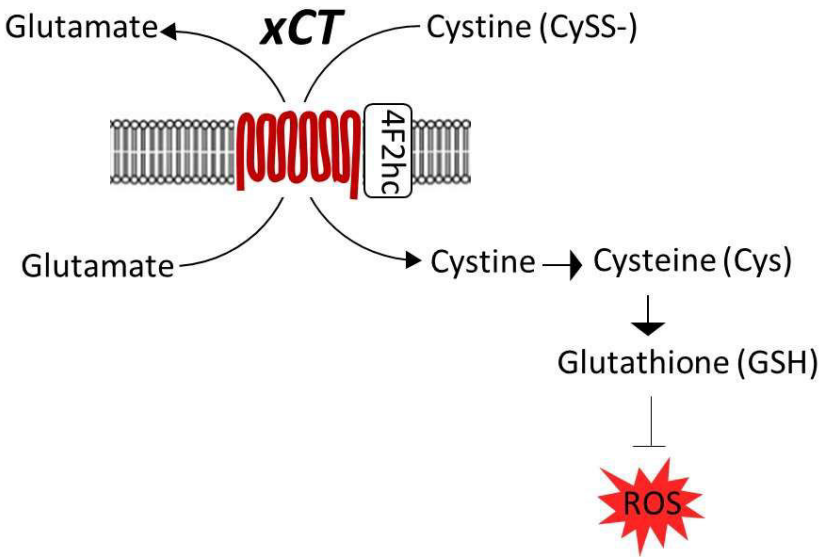

Figure 8. Structure and function of the xC- transport system. xC- is composed by two subunits, with the 4F2 heavy chain stabilizing the xCT light chain (in red) on the cell membrane. xC- imports cystine in exchange for glutamate. Within the cell, cystine is reduced to cysteine, the precursor of GSH. GSH has a pivotal role in scavenging harmful ROS that may induce cell damage.

In scavenging ROS, GSH is oxidized to GSH disulfide (GSSG). GSSG is then recycled to GSH or exported in the extracellular space. In general, the GSH/GSSG redox couple determines cell's redox state: reducing environment is associated with cell proliferation, while oxidizing environment is associated with differentiation [185].

xCT expression can be induced by a plethora of stimuli, including oxidative stress and electrophilic agents, amino acid starvation, and inflammatory stimuli such as bacterial lipopolysaccharides (LPS) and the cytokine TNFα. The major transcription factor that regulates xCT expression is the ubiquitous NF-E2-related factor 2 (Nrf2), which also orchestrates stress-inducible GSH metabolism [185,188]. Under basal conditions, Nrf2 is rapidly ubiquitinated and subsequently degraded by proteasome. Upon exposure to stimuli such as oxidative stress and endoplasmic reticulum (ER) stress, Nrf2 ubiquitination and degradation are blocked and Nrf2 accumulates in the nucleus, where it induces electrophile response element (EpRE, also known as antioxidant response element ARE)-dependent gene expression to restore intracellular redox homeostasis. As stated above, xCT induction occurs when cells are deprived of several amino acids, including cystine [185]. Amino acid starvation leads to *a*ctivating *t*ranscription *f*actor 4 (ATF4) binding to the *a*mino *a*cid *r*esponse *e*lements (AARE) contained in the proximal promoter of xCT, with subsequent xCT upregulation upon amino acid starvation. This mechanism seems to be strongly dependent on the phosphorylation status of translation initiation factor eIF2α [189]. For what concerns xCT induction by inflammatory stimuli, this seems to occur in part as a consequence of NF-κB activation [185], although the exact mechanisms still have to be elucidated.

xCT activity can be pharmacologically inhibited by alternative substrates, which as such can induce glutamate release thus causing neurotoxicity *in vivo*, or by non-substrate inhibitors, such as

sulfasalazine (SASP) and erastin. SASP is an FDA-approved drug commonly used to treat chronic inflammatory diseases such as rheumatoid arthritis; it is also a potent inhibitor of NF-κB activation. Furthermore, it is insoluble in aqueous solutions and not optimized for the fortuitous interaction with xCT [190]. Moreover, significant side effects associated to the use of SASP occur in about 25% of treated patients, and interruption of a clinical trial due to adverse events on glioma patients has been reported [191]. Erastin is a voltage-dependent anion channels-binding small molecule that, compared to SASP, exerts a stronger inhibitory effect on xCT [192]. In addition, erastin is able to inhibit the activity of some GSH-related enzymes, resulting in more lethal oxidative damage to cells [193]. In general, no specific xCT inhibitor has been discovered yet, since all the studied compounds have shown off-target effects [185].

Albeit expressed almost ubiquitously by mammalian cells cultured *in vitro*, xCT shows a restricted expression pattern *in vivo* under physiological conditions. xCT expression has been detected mainly in the brain and ocular tissues, where it contributes to the maintenance of intracellular GSH levels and thus defends cells from oxidative insults and maintains them healthy [185].

Furthermore, xCT has been shown to play a role in both the innate and the adaptive immune system. Activated neutrophils express high levels of xCT to balance their accelerated GSH consumption [194]. Macrophages upregulate xCT upon activation by inflammatory stimuli as an auto-protective response towards the ROS they release to kill pathogens. APC such as macrophages and DC import cystine through xCT and convert it to cysteine, which is subsequently released to the extracellular milieu and taken up by T cells. In fact, naïve T cells do not express cystine transporters, so they rely on import of APC-derived cysteine via the alanine-serine-cysteine (ASC) transporter for GSH synthesis, which is required for their activation [195]. On the other hand, xCT is highly expressed by myeloid derived suppressor cells (MDSC), a population of cells present in most cancer patients and which act as potent inhibitor of T-cell-mediated antitumor immunity. MDSC compete with APC for extracellular cystine, consume it but do not return cysteine to the microenvironment, thus depriving T cells of the cysteine they require for activation [195].

It is worth noting that $xCT^{-/-}$ mice show no obvious phenotype, even in the brain where xCT is constitutively expressed, indicating that physiological functions of xCT are compensated by still unknown mechanisms *in vivo* [185]. On the contrary, abnormally increased expression of xCT is linked to many CNS pathologies, including Alzheimer's disease, Parkinson's disease, multiple sclerosis, epilepsy, and xCT deficiency is protective in animal models of such diseases [185]. This happens in part by means of increased glutamate release, which can lead to an excessive stimulation of neurons finally causing cell damage or death, a phenomenon named excitotoxicity.

xCT thus plays a role in both the physiology and the pathology of cells and tissues, and its upregulation represents a double-edged sword. As I will describe in the next paragraph, a vast body of research has proven that xCT plays an important role in various aspects of cancer, including: (i) growth, progression and metastatization, (ii) GSH-based drug resistance, (iii) excitotoxicity due to excessive release of glutamate, and (iv) uptake of herpesvirus 8, a causative agent of Kaposi's sarcoma.

I.4.1 Role of xCT in cancer growth, progression and metastatization.

xCT upregulation has been demonstrated in several types of tumors, including lymphoma, glioma [196–200], as well as breast [190,201], gastric [202], colorectal [203], hepatocellular [204,205], renal [206], pancreatic [207] and esophageal carcinoma [208], where it often correlates with poor prognosis. As a result, xCT substrate and PET tracer (4S)-4-(3-[^{18}F]fluoropropyl)-L-glutamate has been used to visualize tumors in preclinical [209] and clinical [210] studies. Consequently, xCT role in cancer biology has been widely investigated in the very recent years.

xCT activity in cancer has been often linked to the expression of CD44 variant (CD44v), an adhesion molecule expressed by CSC [211]. It has been shown that expression of xCT at the cell surface of cancer cell lines relates to that of CD44, and that xCT preferentially interacts with CD44v rather than standard (CD44s) [212,213]. By interacting with CD44v, xCT is stabilized on the plasma membrane and thus mediates the enhanced capacity for GSH synthesis and defense against ROS displayed by CSC [212,213]. CSC are thus facilitated in driving tumor growth, chemoresistance and metastasis [211,213,214]. The CD44v/xCT axis has been shown to play a role also in preneoplastic lesions: CD44v was found to be expressed *de novo* in spasmolytic polypeptide-expressing metaplasia (SPEM) in a mouse model of gastric cancer, and CD44v-positive metaplastic cells manifested upregulation of xCT expression compared with CD44v-negative cells. Genetic ablation of CD44 or treatment with SASP suppressed the development of SPEM and subsequent gastric tumor growth [215].

Another interactor of xCT on the cell membrane is MUC1-C, an oncoprotein aberrantly expressed on the cell surface of many solid tumors, including TNBC [216]. MUC1-C forms a complex with xCT and CD44v and protects TNBC cells against treatment with erastin [217].

It was shown that also the epidermal growth factor receptor (EGFR) interacts with xCT and thereby promotes its cell surface expression and function in human glioma cells, resulting in an enhanced antioxidant capacity. Conversely, targeted inhibition of xCT suppressed the EGFR-dependent enhancement of antioxidant capacity in glioma cells, as well as tumor growth and invasiveness [218]. However, this is in contrast to what reported by Yoshikawa et al [214], showing that xCT inhibition selectively induces apoptosis in CD44v-expressing tumor cells without affecting CD44v-negative

differentiated cells, which in contrast manifest EGFR activation and rely on EGFR activity for their survival and are SASP-resistant. It is thus possible that interactors of xCT at the plasma membrane change depending on the tumor type.

Given its detoxifying role, xCT dysfunction in cancer models has been linked to the induction of ROS-dependent cell death, including apoptosis, autophagy and ferroptosis. Ferroptosis is a recently recognized form of iron- and ROS-dependent regulated cell death [219] that is fostered by p53. p53 has been shown to repress xCT expression, thus inhibiting cystine uptake and sensitizing cells to ferroptosis, while xCT overexpression inhibits ROS-induced ferroptosis and abrogates p53-mediated tumour growth suppression in xenograft models [220]. This study was the first to uncover xCT suppression as a mode by which p53 induces tumor suppression, and was subsequently confirmed by others [221–223]. xCT dysfunction has also been shown to suppress hepatocellular carcinoma cell growth *in vitro* and *in vivo* by triggering ROS-dependent autophagic cell death [204].

Besides being involved in protection from ROS-induced cell death, xCT has been shown to influence and be influenced by several molecular pathways. xCT disruption by SASP has been shown to trigger activation of p38 MAPK as a consequence of oxidative stress. In turn, p38 upregulates Caveolin-1, which recruits β-catenin to the plasma membrane, thus inhibiting β-catenin transcriptional activity which is required for tumor metastatization. This eventually leads to inhibition of both cell invasion *in vitro* and experimental metastasis *in vivo* [224].

xCT expression has been shown to be modulated by STAT3 and STAT5 [225], which bind a region flanking the xCT promoter [226]. STAT5 emerges as a negative regulator of xCT at the transcriptional level, while STAT3 activation is coupled with increased system xC- activity in a cell line-dependent manner [227].

In ER^+ breast cancer cells xCT function was shown to be regulated by insulin growth factor (IGF)-I via activation of the signal transducer insulin receptor substrate (IRS)-1. Breast cancer cell proliferation mediated by IGF-I was suppressed by blocking xCT activity with RNAi or SASP, which conversely sensitized cancer cells to inhibitors of the type I IGF receptor (IGF-IR) [201].

Hypoxia has also been shown to regulate xCT expression in cancer. In hypoxic conditions, glioma growth is sustained by an increased GSH utilization accompanied by upregulation of xCT [228]. In breast cancer cells, chemotherapy has been shown to induce xCT expression in a HIF-1-dependent manner, leading to increased intracellular glutathione levels, which inhibit MEK activity. Loss of MEK-ERK signaling causes the transcriptional activation of the gene encoding the pluripotency factor Nanog, which is required for enrichment of breast CSC. Inhibition of xCT or Nanog blocks chemotherapy-induced enrichment of breast CSC and impairs tumor initiation [229]. HIF-1 and xCT thus cooperate to regulate cancer stemness and tumor initiating ability [230].

xCT has been identified as a target of some microRNAs (miRNAs). miR-26b is down-regulated in human breast cancer specimens and cell lines, and impairs viability and triggers apoptosis when expressed in breast cancer cell lines by targeting xCT [231]. miRNA-27a negatively regulates xCT and its expression is downregulated in cisplatin-resistant bladder cancer. Conversely, cisplatin-resistant cell lines were resensitized by restoring miRNA-27a expression or reducing xCT activity with siRNA or with sulfasalazine [232].

A particular role is played by xCT in brain tumors, especially in gliomas. Although their growth is limited by the bony cavity of the skull and spinal canal, they are able to overcome this physical limitation by killing nearby neurons, thus creating space. The destruction of neuronal tissue apparently occurs by release of excessive amounts of glutamate [233], a process called excitotoxic necrosis. It was found that xCT plays a pivotal role in excitotoxicity, since intracranially implanted xCT-expressing gliomas grew faster, produced pronounced peritumoral glutamate excitotoxicity, induced seizures, and shortened overall survival in mice compared to glioma cells lacking this transporter [198].

Finally, xCT functionally contributes to the pathogenesis of Kaposi's sarcoma herpes virus (KSHV), the causative agent of a connective tissue cancer and of lymphoproliferative diseases commonly found in HIV/AIDS patients. xCT was found to be the predominant receptor in host cells mediating the fusion and entry of KSHV in a cell-context dependent way. xCT has been found to be upregulated in advanced KS lesions, where KSHV-encodes multiple microRNAs that target a negative transcriptional regulator of xCT. xCT upregulation in turn facilitates viral dissemination and enhanced survival of virus-infected cells through a positive feed-back loop (for a review, see [234]).

I.4.2 xCT role in drug resistance in cancer

Chemotherapy is one of the most applied approaches to treat cancer, but drug resistance limits its effectiveness. Tumor cells may be intrinsically drug-resistant or can acquire resistance to chemotherapy during treatment. A broad range of molecular mechanisms has been implicated in drug resistance including, but not limited to: (i) increased rates of drug efflux due to altered expression of drug pumps, (ii) reduced uptake of drugs, or (iii) activation of detoxifying pathways [235].

Radiation and many conventional cytotoxic anticancer drugs can directly or indirectly increase ROS levels in cancer cells. As the intrinsic levels of ROS are high in cancer cells, a further increase of ROS stress in cancer cells using exogenous ROS-inducing agents is likely to cause elevation of ROS above the threshold level, leading to cell death. However some cancer cells, especially those in advanced disease stages, become highly adapted to intrinsic oxidative stress by up regulating antioxidant capacity [236]. This redox adaptation not only enables the cancer cells to survive under

increased endogenous ROS stress, but also provides a mechanism of resistance to many anticancer agents, owing to increased tolerance of exogenous stress.

As GSH-mediated detoxification has been broadly implicated in resistance to chemotherapy [237], xCT-driven redox adaptation might be crucial not only in cancer development, but also in resistance to agents that induce intracellular ROS production. Indeed, several studies explored the contribution of system xC- to drug resistance. A pharmacogenomic approach, using correlations between drug potency and transporters gene expression in the National Cancer Institute's 60 cell lines, showed that xCT expression negatively correlates with drug potency of compounds susceptible to GSH-mediated chemoresistance [238–240]. The number of significant SLC7A11 - drug correlations was much greater than those of other genes tested, such as the known chemoresistance genes ABCB1 (MDR1) and ABCC1 (MRP1), suggesting that xCT plays a critical role in drug resistance [239]. In cell lines strongly expressing xCT, the potency of compounds with predicted GSH-reactivity was enhanced by xCT inhibition, while administration of GSH boosters impaired drug efficacy. These and other studies indicate GSH-mediated ROS scavenging activity as the mechanism through which xCT expression induces chemoresistance [202,203,239,241–247]. Specifically, xCT expression has been associated with resistance to different chemotherapeutic drugs used in clinics, and xCT inhibition has been shown to sensitize otherwise chemoresistant cancer cells in particular to cisplatin [202,203,232,243–245], but also to temozolomide [246,247], doxorubicin [248], gemcitabine [207] and bortezomib [249].

I.5 Paper I. Results and discussion

(*For detailed results and materials & methods, please refer to Attachment A - Paper I*)

In ***paper I***, we explored the link between xCT and CSC biology and evaluated the effects of anti-xCT DNA-based vaccination on tumor growth and metastasis formation.

Briefly, we validated xCT upregulation in tumorspheres through flow cytometry analysis. xCT expression increased progressively from TUBO cells grown in monolayer to first passage (P1), second passage (P2) and third passage (P3) tumorspheres. Tumorspheres were essentially composed by putative CSC, as revealed by widespread positivity for the CSC markers Sca-1, Oct4 and Thy1.1 in immunofluorescence microscopy. Interestingly, most tumorsphere-derived cells that express the stem cell marker Sca-1 were also xCT^{+}. xCT upregulation is not restricted to TUBO-derived CSC as it was also observed in tumorspheres derived from mouse (4T1) and human (HCC-1806 and MDA-MB-231) breast cancer cell lines. Strong positivity for xCT staining in the small $CD44^{high}/CD24^{low}$ population present in monolayer TUBO cells further suggest that xCT expression is not due to the particular growth condition of tumorspheres, but is rather a general feature of CSC, of which tumorspheres are enriched. We further evaluated xCT expression in the tissue microarrays of normal

and neoplastic samples to address its distribution in human cancers: xCT expression was low in normal tissues while high in many neoplastic tissues, including invasive ductal breast carcinomas (IDC) of different histological subtypes.

Next, we evaluated the functional role of xCT in CSC biology. Inhibition of xCT through SASP or with a specific siRNA led to a decreased cell viability and to impairment of tumorsphere generation. FACS analyses performed 24 hours after siRNA transfection showed that the reduction in xCT^+ cells is accompanied by a reduction in $Sca1^+$ and $CD44^{high/}CD24^{low}$ cells. In accordance to the known role of xCT in redox balance, GSH amount was significantly higher in tumorspheres compared to monolayer TUBO cells, whereas ROS levels were lower, suggesting that CSC have a higher ROS defense capability than more differentiated tumor cells. xCT downregulation caused a significant decrease in GSH and an increase in ROS levels, indicating that ROS defense capability relies on xCT expression.

To evaluate whether xCT is a potential target for cancer immunotherapy, we vaccinated BALB/c mice with either empty vector pVAX1, used as control, or pVAX1 in which we inserted the coding sequence of murine xCT (pVAX1-xCT). We stained tumorsphere-derived cells with the sera of vaccinated mice to evaluate their humoral response by FACS: pVAX1-xCT vaccination induced the production of CSC-binding antibodies, which were not detectable in sera of mice vaccinated with empty pVAX1. These results were confirmed in immunofluorescence, where we verified the ability of purified IgG from pVAX1-xCT vaccinated mouse sera to stain tumorspheres. Notably, TUBO cells incubated with IgG purified from pVAX1-xCT vaccinated mice displayed reduced sphere-generation ability, a lower percentage of cells expressing CSC markers, but increased ROS content as compared to control IgG. These results suggest that anti-xCT vaccination induces antibodies targeting xCT, thus affecting ROS production and self-renewal in CSC.

To verify the efficacy of our vaccine to counteract tumor growth *in vivo*, TUBO-derived tumorspheres were s.c. implanted into BALB/c mice that were vaccinated when tumors reached 2 mm mean diameter. Tumors grew progressively in the pVAX1 control group, while tumors regressed in 23.8% of pVAX1-xCT vaccinated mice. Tumor growth kinetics were slower in the latter group than in the pVAX1 group, as proven by the significantly shorter time required for tumors to reach 4 or 6 mm mean diameter. We then evaluated the efficacy of anti-xCT vaccination in BALB/c mice bearing 2 or 4 mm subcutaneous tumors derived from 4T1 tumorspheres. Tumors grew rapidly in the pVAX1 group, while tumor growth kinetics were generally slower in the pVAX1-xCT vaccinated group, indicating that xCT immunotherapy may be beneficial in various breast cancer subtypes.

To evaluate the effects of anti-xCT vaccination on lung metastasis formation, we vaccinated BALB/c mice with pVAX1 or pVAX1-xCT plasmids. Following vaccination, we performed an intravenous

cell injection of TUBO tumorsphere-derived cells. Metastasis number was significantly reduced after pVAX1-xCT vaccination. Anti-xCT vaccination was also able to reduce the number of spontaneous metastases generated from the subcutaneous injection of 4T1 tumorsphere-derived cells, when applied to tumor-bearing mice. Altogether, these findings suggest that anti-xCT vaccination interferes with CSC metastatic properties both in a preventive and therapeutic setting.

In accordance with the notion that CSC are resistant to chemotherapy, monolayer TUBO cells displayed a higher sensitivity to doxorubicin than tumorspheres. Since xCT is involved in maintaining the intracellular redox balance, thus counteracting the effects of ROS-generating cytotoxic drugs, it is likely that targeting xCT could increase CSC chemosensitivity. In order to explore this hypothesis *in vivo*, we injected TUBO tumorsphere-derived cells intravenously in unvaccinated mice as well as in pVAX1-xCT- and pVAX1-vaccinated mice. Following vaccination, we treated mice with doxorubicin, while control groups were left untreated. pVAX1-xCT determined a decrease in the number of lung metastases compared to mice treated with pVAX1 vaccination plus doxorubicin, and the combination of pVAX1-xCT vaccination and doxorubicin significantly improved the activity of individual treatments. We observed similar results in mice challenged with a subcutaneous injection of TUBO tumorsphere-derived cells and subjected to vaccination and chemotherapy when tumors reached 2 mm mean diameter. The tumor regressed in 25% of mice treated with doxorubicin alone or in combination with pVAX1 plasmid, while the combination of doxorubicin and anti-xCT vaccination halted tumor progression in 60% of mice. All together, these data suggest that vaccination against xCT elicits a humoral response able to impair primary tumor growth and metastatization. The underlying mechanism likely involved an antibody-mediated blocking of xCT, which subsequently leads to an increase of harmful ROS within the cell. This is reflected by an impairment of CSC functions. Furthermore, blocking of xCT sensitizes CSC to doxorubicin treatment, making anti-xCT vaccination an efficient adjuvant treatment for chemotherapy both in a preventive and in a therapeutic setting.

CHAPTER II

Exploting SCARA5 for the delivery of L-Ferritin based theranostic agents to cancer stem cells

Another target molecule we decided to focus on is the L-ferritin receptor SCARA5 (**Sca**venger **R**eceptor Class **A** Member **5**), which resulted to be upregulated in tumorspheres compared to cells grown as monolayer from the same microarray analysis that gave also xCT as output (***Paper I***). Our decision to investigate SCARA5 amongst all the possible targets identified came with the fact that our collaborators (Prof. Silvio Aime and colleagues, Molecular Imaging Center, Turin, Italy) were studying the same protein in the context of hepatocellular carcinoma in a transgenic mouse model [250]. Their strategy consisted in the use of magnetic resonance imaging (MRI)-contrast agents loaded into L-ferritin nanocages in order to discriminate hepatocellular carcinoma lesions from healthy liver, which displayed a differential expression of SCARA5. At the same time, they were investigating the use of curcumin-loaded ferritin as therapeutic agent to prevent hepatocellular damage in toxic induced acute hepatitis [251]. Since we observed an increase of SCARA5 expression in CSC, and since curcumin has been reported as an anti-tumor agent with pleiotropic activity [252], our collaborators and us sought to join our expertise to develop a therapeutic strategy based on the SCARA5-mediated targeting of CSC through L-Ferritin nanocages containing both a therapeutic (curcumin) and a diagnostic (Gadolinium-based contrast agent) compound.

II.1 Nanomedicines for targeted therapy of tumors

Despite the considerable efforts directed towards the development of potent anti-cancer agents, conventional chemotherapeutics still display limited efficacy and safety. These anti-cancer agents show a narrow therapeutic window since they are randomly distributed in the body following systemic administration. This may lead to cytotoxicity to normal cells, causing severe side effects to achieve sufficient anti-cancer efficacy. The non-specific toxicity of chemotherapeutic drugs also limits the administrable dose and thus negatively affects the therapeutic efficacy [253]. In addition to this, a large number of barriers such as hepatic and enzymatic degradation, high interstitial fluid pressure, cellular and nuclear membranes, and presence of drug efflux pumps, need to be overcome before systemically administered anticancer agent can elicit antitumor efficacy [254]. To overcome these major hurdles in the treatment of cancer, a large number of nanomedicine formulations have been designed and evaluated over the years.

Nanomedicines are submicrometer-sized carrier materials that are meant to improve the biodistribution of systemically administered drugs [254]. By delivering drugs selectively to target sites and by guiding them away from healthy tissues, nanomedicine formulations aim to improve the balance between the efficacy and the toxicity of systemic chemotherapeutic interventions [254]. Nanomedicine can consist of different formulations, such as liposomes, polymers, micelles, nanoparticles and antibodies [255], and can target tumors via passive accumulation or via active

targeting. Passive accumulation refers to the fact that, due to abnormally leaky vasculature and lack of an effective lymphatic drainage system in tumor tissues, nanomedicines can passively accumulate into the tumor tissue. This phenomenon is referred to as enhanced permeation and retention (EPR) effect [253]. On the contrary, active targeting approaches rely on the use of targeting ligands, like antibodies and peptides, which specifically bind to receptors expressed at the target site [254].

Besides drug targeting to pathological sites for therapeutic purposes, nanomedicine formulations have also been used for imaging purposes. Benefiting from development of the imaging equipment and software, various imaging techniques have rapidly advanced and have been used for detection and diagnosis in different diseases, including cancer. Such imaging techniques include optical imaging (OI), positron emission tomography (PET), single photon emission computed tomography (SPECT), magnetic resonance imaging (MRI), computer tomography (CT), and ultrasound (US) imaging. Many of these imaging modalities use imaging probes, such as iodine and barium for CT, gadolinium or iron oxide nanoparticles for MRI, 18 F-fluorodeoxyglucose (FDG) for PET, and In-111 and Tc-99m for SPECT, whose aim is to enhance the imaging resolution and disease detection sensitivity [256].

In recent years, a major effort has been made on integrating imaging probes and therapeutic agents into one nanoparticle for simultaneous disease imaging and targeted drug delivery or imaging-guided drug delivery. These nanoparticles have thus been described as nanotheranostics, since they combine therapeutic and diagnostic purposes. Besides combining diagnosis and therapy, nanotheranostics provide further advantages compared to a simply additive effect: they in fact allow imaging drug delivery, release and efficacy, depending on the type of platform used [255]. Co-localization of the drug and the imaging agent can thus provide real-time information on the circulation time and organ accumulation of the nanomedicine, and is accomplished mainly through the use of radionuclides as imaging agents. Besides accumulating at the tumor site, the drug also needs to be efficiently released. In this case, MRI contrast agents provide a signal that depends on the surrounding water molecules: this interaction varies substantially when these agents are present within versus outside of water-impermeable vesicles, such as liposomes; thus MRI probes are highly useful materials for monitoring drug release. Finally, theranostic nanomedicines can predict and monitor the efficacy of the therapy, allowing tailoring the approaches to the single patients [255].

Among the different platforms that can be used for the delivery of theranostic agents, naturally occurring biological nanoparticles are of particular interest by virtue of their uniform structure, low toxicity and ability to evade the immune system [257]. Biological nanoparticles are assembled from molecules synthesized in a biological system, with sizes inferior to 100 nm. They include magnetosomes, lipoproteins, viruses, exosomes and ferritins [258]. In the next sections, I will focus on

L-ferritin used as a tumor-targeted delivery system and on SCARA5, the L-ferritin receptor that we found to be upregulated in breast CSC.

II.2 SCARA5

Scavenger **R**eceptor Class **A** Member **5** (SCARA5) is a gene encoding the homonymous ferritin receptor that mediates non-transferrin-dependent uptake of iron within the cells [259]. SCARA5 belongs to the family of scavenger receptors, a type of pattern-recognition receptors (PRR). As stated in *Chapter I*, PRR are host sensors detecting molecules typical of pathogens, and are thus fundamental for the proper functioning of the innate immune system. Scavenger receptors in particular are named after their main function of scavenging foreign substances and waste material within the body. Scavenger receptors are categorized into different classes, each comprising proteins with different structure and binding specificity. Like other members of the Class A scavenger receptor family, SCARA5 is expressed on the cell membrane as a trimer, whose chains are type II transmembrane proteins . Each chain is composed by a short intracellular N-terminus domain, a single-pass transmembrane domain followed by a spacer region and a collagenous domain, ending with a scavenger receptor cysteine-rich (SRCR) domain at the C-terminus [260] (**Figure 9**). In general, Class A scavenger receptors preferentially bind modified low density lipoprotein (LDL), but their ligands include bacterial lipopolysaccharide and lipotechoic acid as well, thus contributing to the innate host defense. Unlike other members of this class, SCARA5 is not able to bind oxidized or acetylated LDL, but is able to bind bioparticles from microbes [260]. Most interestingly, SCARA5 has been found to mediate the transferrin (Tf) independent uptake of extracellular iron by the cells [259].

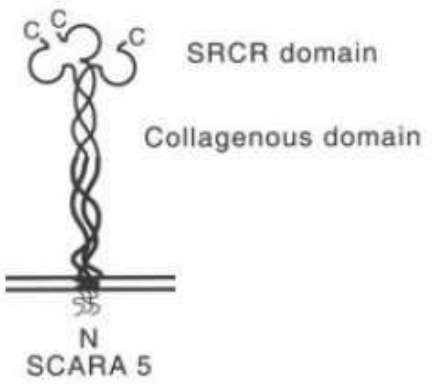

Figure 9. Structure of the trimeric SCARA5 receptor. Adapted from *Jiang Y. et al. The Journal of Biological Chemistry. 281, 2006* [260].

Iron represents an important cofactor for enzymes involved in a wide range of redox reactions. Most cells take up iron through the iron-containing serum protein Tf by binding to Tf-receptors (TfR) on the cell surface. However, some cells express low levels of TfR and high levels of SCARA5 instead. SCARA5 binds to extracellular ferritin, a protein that assembles in multimeric structures to form iron-containing nanocages [258]. Intracellular ferritin works as an iron storage system, but in particular conditions, such as inflammation, it can be found in the serum at high levels. Ferritin monomers in the serum can be of two types, the light (L) and heavy (H) chains, which can assemble in different proportions to form nanocages. SCARA5 preferentially binds to L-Ferritin, whereas another ferritin receptor, Tim-2, preferentially binds to H-Ferritin [259].

In mice, expression of SCARA5 does not overlap with that of the other Class A scavenger receptors and is particularly marked in adult testis and ovary [260], as well as in various embryonic mouse tissues such as brain, eye, head, heart, neural arch, and cartilage primordium [261]. While other members of the family, such as SCARA1 and SCARA2, are mainly expressed by immune cells, SCARA5 appears to be expressed by fibroblasts in various tissues and by epithelial cells of choroid plexus and seminiferous tubes of the testis in mice, although its expression appears to be variable according to the mouse strain used [262]. Expression pattern of SCARA5 in humans has not been studied in details, and its physiological role is unclear. It has been shown that SCARA5 expression is required for proper kidney morphogenesis in the mouse embryo [259], and that SCARA5 deficiency leads to symptoms similar to those of autoimmune disease, characterized by reactive lymphoid proliferations in the interstitial connective tissue of multiple organs and development of anti-nuclear antibodies. This suggests that SCARA5 may be involved in fibroblast-dependent homeostasis of the interstitial connective tissue [262].

Concerning cancer, SCARA5 has been mostly suggested as an oncosuppressor gene in different cancer types. Its promoter results to be frequently hypermetilated in hepatocellular (HCC) and colorectal (CRC) carcinoma cell lines and its expression is low in mouse and human HCC and CRC specimens compared to healthy liver and colon [250,263,264]. Furthermore, SCARA5 appeared to negatively affect cell proliferation, colony formation and tumorigenicity of HCC cell lines [263]. In addition, SCARA5 is reported to be negatively regulated by ROCK2 through the β-Catenin pathway [265] and by Snail1 [266]. Proposed mechanisms of action of SCARA5 as oncosuppressor include inhibition of FAK signaling pathway [263,267] and downregulation of STAT3, Akt, MMP-9, VEGF and cyclins [268,269]. However, others reported that in different contexts a high SCARA5 expression favors cell proliferation and migration by increasing platelet derived growth factor receptor (PDGFR), Akt and Erk1/2 signaling pathways [270]. Furthermore, we have shown that SCARA5 expression increases in breast cancer tumorspheres from TUBO and MDA-MB-231 ***(Paper II)***, and from 4T1 and HCC1806 (***Paper III***) cell lines, and that targeting of cells expressing SCARA5 leads to tumor rejection (***Paper II***). Thus, SCARA5 role and mechanisms of action may vary in a tissue- or even cell line-dependent manner.

II.3 Ferritin structure and role in physiopathology

Iron is a transition metal essential for life, being required as co-factor for many enzymatic processes within the cells. At the same time, iron is potentially toxic due to its involvement in the generation of damaging ROS [271]. For this reason, the presence of free iron within the cells has to be strictly controlled. The control of iron availability within the cells is largely dependent on ferritins,

ubiquitous proteins with storage and detoxifying capacity [272]. Thus, ferritin prevents unwanted toxic effects of iron excess, while at the same time providing a controlled release of the metal when required for enzymatic reactions.

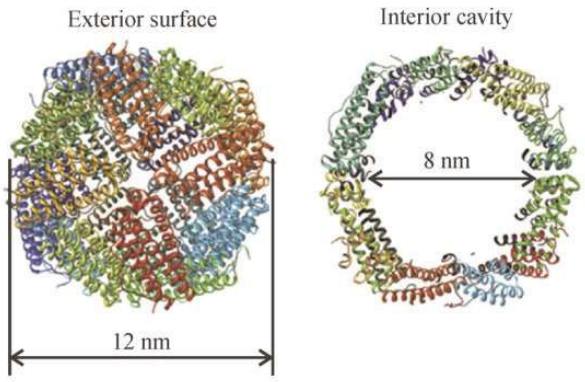

Figure 10. Structure of ferritin. From *Wang Z. et al. Front Chem Sci Eng. 2017* [273]

Mammalian ferritin is composed of 24 subunits, which assemble to form a hollow symmetrical multimeric protein, with an outer diameter of 12 nm and an inner cavity of 8 nm-diameter (**Figure 10**) that can accommodate up to 4500 iron atoms [273]. This structure is designed for a dynamic storage: despite the helix-helix interactions provide great stability, the structure is enough flexible to allow the influx and efflux of iron. Three types of monomers are produced in mammalian cells: the H and L chains, that can be found inside the cells but also in the serum, and the Mitochondrial (M) chain, only present in mitochondria. Despite the high homology of the three chains, only H and M ferritins possess enzymatic activity: they have an amino acidic sequence required for the formation of ferroxidase centers that catalyzes the oxidation from soluble ferrous to insoluble ferric iron and its subsequent deposition into the ferritin cavity. On the contrary, L ferritins have no enzymatic activity, but facilitate iron nucleation and core formation [271]. L- and H- chains can assemble in different proportions to form the 24-mer cage depending of the tissue in which they are produced and on the physiopathological conditions. L-ferritins, with a higher storage ability, are more abundant in the liver, while H-ferritins, with increased detoxifying capacity, are more abundant in heart and brain. Ferritin can be found not only inside the cells, but also in extracellular fluids and in the blood. The prevalent form of extracellular ferritin is represented by L-chains [274]. Serum ferritin is an indicator of the body's iron stores, with lower levers in individuals suffering of anemia and higher levels in patients with iron-overload disease. Furthermore, serum ferritin is elevated during chronic and acute inflammation [274].

Ferritin is overexpressed in tissues from multiple malignancies, with different ratios of H- and L-chains. In breast cancer, the increase is primarily related to L-ferritin and correlates with proliferation, histological dedifferentiation and poor prognosis [275]. Furthermore, serum ferritin level in $Her2^+$ breast cancer patients appears to be a predictor of response to trastuzumab [276]. The predominant presence of L-ferritin compared to H-ferritin in the serum of breast cancer patients could have a biological significance, since the two forms have unique receptors (TfR1 and murine TIM-2 for H-ferritin, SCARA5 for L-ferritin). The increase of serum ferritin appears not to be associated to liver damage,

but rather to local release at the tumor site [275]. The ferritin-rich cell population in breast cancer is represented by tumor associated macrophages (TAM) [277], which may use ferritin as a form of protection from oxidative damage. Since macrophages are one of the few cell types capable of ferritin secretion, it has been hypothesized that TAM locally secreted ferritin may support tumorigenesis at multiple levels, such as increased proliferation of cancer cells and angiogenesis [275]. It was also noted that breast cancer cells display increased expression of iron importers and decreased expression of iron exporters [278], suggesting that cancer cells have a high rate of iron utilization with little export.

II.4 Use of Ferritin Nanocages in Cancer

Ferritin structural features have been extensively studied by researchers and recombinant ferritin nanocages have been exploited as biological nanoparticles for medical applications. As natural ferritin, recombinant ferritin is very stable and biocompatible, and assembles to form tridimensional hollow structures whose cavity can be loaded with drugs or imaging agents. Iron-deprived ferritin, called apoferritin, provides several advantages as a delivery system: its uniform cage hallows the precise control of the amount of molecules loaded and thus drug dosage, and the recombinant ferritin proteins can be functionalized either genetically or chemically to improve the targeting ability [258]. Despite being highly stable under physiological conditions, ferritin nanocages can be disassembled in highly acidic or alkaline conditions, and then reassembled in a shape memory fashion when the pH is brought back to neutrality. Thus, molecules can be encapsulated in solution within the ferritin cavity simply by disassembling and reassembling the multimer [279].

Multiple studies have explored the use of ferritin nanocages, mainly of the H-chains, as imaging and drug delivery systems for the diagnosis and treatment of tumors. Both naïve and functionalized apoferritin cages have been used for the delivery of chemotherapeutic drugs such as cisplatin and doxorubicin, with good results both *in vitro* [280,281] and *in vivo* [282]. For instance, cisplatin-loaded ferritin functionalized with an antibody targeting CSPG4 has been used for the delivery of the drug to melanoma cells [283]. Despite functionalization potentially provides higher target specificity, the use of naïve ferritin seems to be advantageous for many reasons, including higher purification yield and maintenance of the physiological behavior [281]. Furthermore, in the case of H-ferritin, functionalization is not required thanks to the increased expression of H-ferritin receptor TfR1 by cancer cells: Liang and colleagues [282] showed that naïve H-ferritin nanocages loaded with doxorubicin specifically bound to TfR1-overexpressing cells, with subsequent release of the drug in the lysosomes. When administered to tumor-bearing mice, intratumoral doxorubicin concentration was 10-fold higher than free doxorubicin, thus increasing the drug therapeutic efficacy while at the same time preventing exposure of healthy organs to the drug [282].

The ability of ferritin to host heavy atoms and complexes in its inner cavity has led over time to its use in MRI. Iron oxides and hydroxides, which are found in the ferritin core, are efficient contrast agents due to their superparamagnetic properties and the dark contrast they provide in MRI images [284]. However, other strategies use compound that provide a higher contrast than iron, such as gadolinium (Gd) [284].

In conclusion, ferritin nanocages are emerging as a powerful tool for both therapeutic and imaging purposes, and the combination of drugs and imaging agents within the ferritin cavity appears as a promising strategy in the field of cancer theranostics. Specific targeting of cancer cells by means of both ferritin functionalization or natural expression of ferritin receptors on the surface of the tumor cells enhances anti-cancer activity of the drugs, while at the same time preserves healthy tissues from off-target effects. However, the use of ferritin nanocages has not reached the clinical practice yet, since some questions still have to be addressed, such as the fate of systemically injected ferritin, its clearance, biodistribution, toxicity, and the possible immunogenicity of functionalized ferritin particles [258].

So far, the most extensively studied approach is represented by unfuctionalized H-ferritin loaded with doxorubicin, which has proven to be successful in preclinical studies. However, as previously stated, a common feature of CSC is chemo-resistance, thus other drugs able to efficaciously affect this subpopulation deserve attention and investigation. We thus opted for curcumin, a natural compound that has been extensively described as an anti-tumor agent nontoxic to healthy cells, and that - most importantly - has been shown to interfere with the signaling pathways involved in CSC self-renewal. However, curcumin is poorly soluble in water, so its loading into ferritin nanocages appears as a solution for the delivery to cancer cells *in vivo*.

II.5 Targeting cancer stem cells with curcumin

Curcumin is a dietary polyphenol derived from the rhizomes of turmeric (*Curcuma longa*), a yellow-color spice usually used in the preparation of curry. Curcumin has been commonly described to possess anti-inflammatory, antioxidant and antimicrobial activities [285]. The therapeutic role of curcumin has been extensively studied in clinical trials for a wide range of pathologies including, but not limited to, inflammatory bowel disease, Alzheimer's disease, arthritis, atherosclerosis, and cancer [286].

Curcumin interacts with many molecular targets involved in cancer development, as revealed by extensive *in vitro* and *in vivo* studies. These molecular targets include transcription factors, growth factors, receptors, cytokines, enzymes, and genes regulating cell proliferation and apoptosis. The molecular targets and pathways affected by curcumin are reviewed in deep in [252]. As could be

expected, this plethora of pathways affected by curcumin includes those involved in the CSC biology [285]. Hence, a number of studies suggested that curcumin might have the potential to target CSC.

In vitro, curcumin was shown to reduce or completely ablate the sphere-forming potential of breast CSC in a dose-dependent manner, and to lead to a decrease in $ALDH^+$ cells [287]. Other properties of CSC, such as migration ability and chemoresistance, appear to be affected by curcumin. Curcumin in fact inhibits β-catenin nuclear translocation, thus impeding trans-activation of Slug and restoring E-cadherin expression. This finally leads to suppression of EMT and subsequent inhibition of migration ability in breast CSC [288]. Curcumin also interferes with the formation of microtentacles, a type of tubulin-based protrusion of the plasma cell membrane that form on detached or suspended cells and aid in cell reattachment, and that can help metastatic breast CSC to attach to distant tissues [289]. Furthermore, a study showed that curcumin sensitizes breast cancer cells to chemotherapeutic drugs by reducing the CSC population mainly through a reduction in the expression of ABCG (see *Introduction*) [290].

A large number of studies led to similar results for other types of tumor, including colon, brain and pancreatic cancers [285]. Interestingly, curcumin does not seem to have the same deleterious effects on normal stem cells as it does on CSC. Possible explanations provided so far include the increased uptake ability of curcumin by cancer cells compared to normal cells, the shift of a pro-tumor to anti-tumor microenvironment induced by curcumin, and most importantly the effect of curcumin on signaling pathways dysregulated in CSC [291]. For instance, most tumor cells, but not normal cells, express a constitutively activated NF-κB, which is one of the targets of curcumin [252]. Furthermore, curcumin has been shown to suppress abnormalities in the Wnt/β-Catenin pathway, while at the same time stimulating it in normal stem cells [291]. Thus, curcumin appears to selectively impair the biology of cancer cells while not affecting normal cells [252]. Furthermore, since curcumin exerts its effect through multiple cell signaling pathways, there is a reduced likelihood of developing resistance to it. All these features make curcumin an ideal candidate for cancer treatment.

Therefore, several clinical trials have been conducted to address the pharmacokinetics, safety, and efficacy of curcumin in different types of cancer. The published studies generally have reported no toxicity, with up to 8000 mg/day oral intake for 3 months being well tolerated [292]. Besides great tolerability, minor to moderate effects against cancer were sometimes observed. In a cohort of 25 patients with various pre-malignant lesions, 7 patients showed histological improvement [292]. Other studies described stable disease for some of the treated patients [285], even though a major limitation to the response is thought to be the commonly reported low bioavailability of curcumin.

Curcumin is in fact characterized by poor water solubility and short biological half-life, resulting in low bioavailability in both plasma and tissues. The stability of curcumin in aqueous solution is pH-

dependent, being most stable at pH 1–6, but with tendency to crystallize and precipitate in these conditions. Curcumin becomes unstable at pH > 7 and, as such, 90% of curcumin is degraded within 30 min in *in vitro* preparations under physiological pH conditions [293]. Generally, the bioavailability of orally administered curcumin is low due to a relatively low intestinal absorption and rapid metabolism in the liver. Curcumin is mainly eliminated by fecal excretion with minimal elimination in the urine [293]. The highest concentrations of curcumin are found in the intestine. However, curcumin levels are very low and can fall below detection limits in the plasma and other tissues: the plasma levels of curcumin in many bioavailability studies are often below 1 μM [293]. Various methods have been proposed to improve the solubility of hydrophobic curcumin in aqueous solutions to enhance its bioavailability, and these include the formation of complexes with metal ions, alteration of curcumin analogues structure, inhibitors of phase II metabolism, and encapsulation in nanoparticles [294].

An approach explored by us and our collaborators at the Molecular Imaging Center consists in the use of ferritin as a carrier (**Figure 11**). It was shown in fact that encapsulating curcumin into ferritin nanocages prevents its degradation in aqueous solution at neutral pH, with 85% curcumin preserved for at least 48 hours, and greatly improves curcumin bioavailability *in vivo* [251]. A similar study showed that encapsulation of curcumin into ferritin nanocages dramatically increased its solubility [295], since free curcumin is basically insoluble in water or gets degraded, according to pH conditions [293].

II.6 MRI for tumor imaging

A detailed description of imaging modalities, probes ad physics goes beyond the scope of this thesis, as the research I will describe is mainly focused on the targeted therapy against CSC, rather than on the targeted imaging. Nevertheless, a brief description of the methodology used by our collaborators from the Molecular Imaging Center, is important for the full understanding of the work done. As previously stated, a Gd-based contrast agent was co-loaded with curcumin within ferritin nanocages to image the delivery of the nanocages to CSC and to estimate the amount of curcumin inside the cells (**Figure 11**). Therefore, here I will briefly introduce MRI and Gd-based contrast agents, altogether with their advantages and limitations for *in vivo* imaging purposes.

Molecular imaging refers to the characterization and measurement of biological processes at the cellular and/or molecular level [296]. Molecular imaging modalities include optical bioluminescence, optical fluorescence, targeted ultrasound, molecular magnetic resonance imaging (MRI), magnetic resonance spectroscopy (MRS), single-photon-emission computed tomography (SPECT), and positron emission tomography (PET).

MRI is a noninvasive diagnostic technique based on the interaction of certain particles of the nuclei (typically protons) with each other and with surrounding molecules in a tissue of interest [297].

Basically, MRI records the relaxation process of protons after they have been perturbed by a radio frequency pulse from their aligned state within an external magnetic field. Measurement of the longitudinal and transversal relaxation times can thus be used to generate the MRI image.

Different tissues have different relaxation times depending on variations in water concentrations and local environments, which can result in endogenous contrast. Contrast agents (CA) in magnetic resonance work by shortening either the T1 (longitudinal) or T2 (transverse) relaxation time in the target tissue. The contrast enhancement is obtained when one tissue has either higher affinity for the contrast agent or higher vascularity than another one. Diseased tissues, such as tumors, are metabolically different from healthy tissues and have a much higher uptake of the CA, resulting in a higher contrast in MRI images [298]. The MRI image can be weighted to detect differences in either T1 or T2. T1-weighted images give positive image contrast, as the intensity of the image signal increases at the tissue site where the CA concentrates due to T1 shortening. T2 -weighted images give negative contrast, due to the predominant effect of T2 shortening [298]. The major advantages of MRI over radionuclide-based imaging are the absence of radiation and higher spatial resolution (usually sub-millimeter level). The disadvantage of MRI is its inherent low sensitivity, which can only be partially compensated by working at higher magnetic fields (4.7–14 Tesla), acquiring data for much longer periods during imaging, and using exogenous contrast agents [296].

Traditionally, Gd ion complexes (chelates) have been used to increase the T1 contrast. Paramagnetic metal ions, like Gd^{3+}, cannot be used as CA in their ionic form due to their undesirable biodistribution (accumulating in bones, liver or spleen) and relatively high toxicity [298]. Gd^{3+} undergoes a rapid hydrolysis at physiological pH, producing insoluble $Gd(OH)_3$. Thus, chelates with a high thermodynamic and kinetic stability are required for the use of these paramagnetic metal ions *in vivo*, giving appropriate biodistribution and safety profiles [298]. The most important class of MRI CA commercially available are represented by Gd^{3+} chelates of linear or macrocyclic polyaminocarboxylate ligands. They are divided into two groups, the ionic and the neutral agents: the latter having no charge, and thus perturbing to a lower extent the osmolarity of blood. The contrast agent used in our study, Gd- (HP-DO3A) (Gadoteridol, ProHance®, Bracco Spa), is a neutral agent. Gd^{3+}-based agents are usually safe when used in clinically recommended doses, and adverse reactions and side effects, such as allergy, are very rare [298].

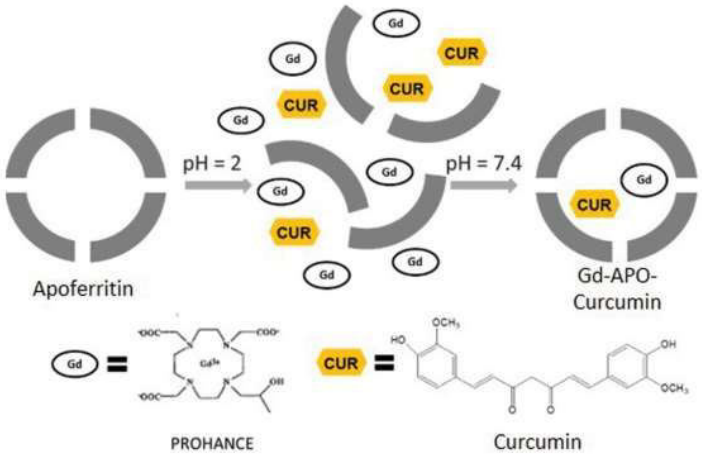

Figure 11. Representation of encapsulation of Gd and Curcumin within L-Ferritin nanocages. L-apoferritin is dissociated by lowering the pH to 2 using HCl. Afterwards, Curcumin is solved in DMSO. Gd-HPDO3A (Prohance) are added to the L-apoferritin solution. The pH is then adjusted to 7.4 to reconstitute the L-apoferritin nanoparticle. Adapted from ***Paper II***.

II.7 Paper II. Results and discussion

(*For detailed results and materials & methods, please refer to Attachment A - Paper II*)

Through transcriptome analysis, we observed that the only known L-ferritin receptor, SCARA5, is upregulated in TUBO-derived tumorspheres compared to epithelial TUBO cells. Hence, loading curcumin into ferritin cavity can represent a solution for targeted drug delivery to breast CSC.

Since SCARA5 mediates L-ferritin uptake, we assessed the enhanced ability of TUBO-derived tumorspheres to take up iron-containing L-ferritin from the incubation media, when compared to the corresponding cells grown as monolayers. MDA-MB-231 cells and their tumorspheres were included in the study to proof that our observations are valid also for a human breast cancer cell line. We measured the amount of iron internalized in cells upon incubation in L-ferritin-containing medium, extrapolated by the ICP-MS (inductively coupled plasma mass spectrometry) determination of the intracellular iron content and by MRI. The amount of iron internalized by tumorspheres was significantly higher than in monolayer cells in both TUBO and MDA-MB-231 cells. We assessed the specificity of the uptake by carrying out a competition study in which we incubated cells in the presence of an excess of native apoferritin in order to saturate the specific receptors. In tumorspheres generated by both MDA-MB-231 and TUBO cells the uptake decreased by about 60% and 66%, respectively, confirming that iron uptake was mediated by ferritin specific receptors. To ensure that the uptake of L-Ferritin is mediated by SCARA5, we incubated TUBO-derived tumorspheres with a siRNA specific to SCARA5 or a Negative Control siRNA. After 48 hours, cells were incubated with L-ferritin. The amount of iron internalized by cells treated with siRNA was significantly lower than the iron internalized by control cells, to a level comparable to the decrease of the protein as assessed by western blot. In order to further confirm that breast tumorspheres take up more ferritin than their monolayer counterpart, we loaded apoferritin with FITC (hereafter referred to as Apo-FITC), and incubated TUBO or MDA-MB-231 cells and their derived tumorspheres for 24 hours in the presence

of Apo-FITC. Flow cytometry analysis revealed that Apo-FITC was internalized by both monolayer cells and tumorspheres, but its intake in tumorspheres was significantly higher, as demonstrated by their enhanced mean fluorescence intensity (MFI). Of note, Apo-FITC MFI was higher in cells positive for the CSC marker Sca-1, that were only present in tumorspheres, suggesting that ferritin uptake is higher in CSC than in more differentiated cells.

We then loaded the natural drug Curcumin and the Gd-based MRI contrast agent Gd-HPDO3A within apoferritin cages (Gd-APO-Curcumin; **Figure 11**) to monitor the release of Curcumin within the cells. Tumorspheres gave a higher MR signal compared to monolayer cells upon incubation with Gd-APO-Curcumin, indicating once again an increased uptake of the nanoparticles. Furthermore, since the ratio between the contrast agent and Curcumin molecules is estimated to be constant within the apoferritin cavity, by measuring the amount of Gd moles per mg of protein, we were able to estimate the amount of curcumin released within the cells, that was higher in tumorspheres compared to monolayer cells.

In order to analyze whether Apo-Curcumin is able to exert inhibitory effects on CSC survival and self-renewal, we incubated TUBO cells and their derived tumorspheres in the presence or absence of Apo-Curcumin for different time points, and then we evaluated apoptosis. Apo-Curcumin did not induce cell death in TUBO epithelial cells, while it progressively increased over time the presence of dead cells in tumorspheres when compared to untreated cells. Of note, Apo-Curcumin was more efficient than free curcumin in inducing apoptosis in tumorspheres. This enhanced effect was not due to any toxicity of ferritin, since treatment with apoferritin did not induce apoptosis in either TUBO or tumorspheres, but probably to the ability of Apo-Curcumin to induce curcumin uptake in CSC. The inhibitory activity played by Apo-Curcumin and curcumin on tumorspheres was due to their ability to target CSC and decrease their self-renewal capacity, which on the contrary was not hindered by treatment with apoferritin alone. None of these compounds altered TUBO cell morphology, while tumorspheres cultured in presence of curcumin and Apo-Curcumin were smaller than those cultured in medium or with apoferritin. The ability of Apo-Curcumin to target CSC and decrease tumorsphere survival and self-renewal is not restricted to the TUBO model, since similar results were obtained with MDA-MB-231 cells.

To assess the therapeutic efficacy of Apo-Curcumin treatment *in vivo*, we challenged female BALB/c mice with a subcutaneous injection of TUBO tumorsphere-derived cells. When tumors reached 2 mm mean diameter, we started to treat mice with intravenous injections of Apo-Curcumin or empty apoferritin as a control, twice per week. We observed that 5/8 (62.5%) mice treated with Apo-Curcumin, following an initial tumor progression, showed a regression of the tumor burden, while in 3/8 (37.5%) tumor progressed to 10 mm mean diameter (size we set as upper threshold). On

the other hand, only 1/9 (11.1%) of control mice experienced tumor regression, while in 8/9 (88.9%) of them the tumor progressed to 10 mm mean diameter. Such differences between the two groups were significant, as revealed by Fisher's test ($p= 0.026895$, significant at $p<0.05$). These results show that breast CSC display an increased L-Ferritin uptake capability, supposedly by virtue of the upregulation of SCARA5, the only L-ferritin receptor identified up to now. The increased L-Ferritin uptake can be exploited to target curcumin to CSC when loaded into L-apoferritin nanoparticles. Of note, loading curcumin into apoferritin not only enables specific targeting to SCARA5-expressing cells, and thus to breast CSC, favoring the uptake of curcumin, but also improves curcumin bioavailability, opening up the possibility of *in vivo* treatments. Our *in vivo* results highlight the therapeutic potential of Apo-curcumin. Further analysis on intracellular pathways and on histopathological features of treated mice will give insights on the mechanism of action of Apo-Curcumin on CSC and on established tumors, as well as insights on the effects of Apo-Curcumin on healthy tissues.

CHAPTER III

On the way of finding new targets for triple negative breast cancer treatment

III.1 Targeted therapy for Triple Negative Breast Cancer: an unmet medical need

I have already described, at the beginning of this thesis, the clinical and molecular heterogeneity of breast cancer. The advancement and now common application of genomics, epigenomics, transcriptomics or proteomics has provided unprecedented insights and understanding of the molecular complexity of this disease [299]. Despite this molecular complexity, clinical decisions still rely primarily on the assessment of the expression of the endocrine receptors ER and PR and the overexpression of Her2 [300]. Since these markers are molecular targets for therapeutic agents, patients with tumors expressing one of these could potentially benefit from endocrine therapy and/or Her2-targeted drugs. However, the lack of any of these three targets in some breast cancers, hence named triple negative breast cancer (TNBC), renders chemotherapy the standard therapeutic approach for TNBC at all stages [300].

TNBC affects between 12-24% of breast cancer patients [301]. Compared with non-TNBCs, a larger proportion of TNBCs occurs in younger women, particularly of African American or West African ancestry [301]. Compared with other breast cancer patients, those with triple-negative breast cancer have an increased likelihood of distant recurrence and death within 5 years of diagnosis, with the risk of distant recurrence peaking at 1-3 years, while in the non-TNBC patients the risk is costant over the period of follow up [302]. However, patients with TNBC appear to be more sensitive to anthracycline-based neoadjuvant chemotherapy than other subtypes of breast cancers, reaching higher percentages of complete pathologic response (22% vs 11%) [303]. Higher sensitivity to neoadjuvant anthracycline in a breast cancer subtype known to have a poor prognosis (a phenomenon described as TNBC paradox [304]) is explained by higher relapse among patients with TNBC that did not achieve complete pathologic response [303]. These observations suggest that there is a sub-group of women with TNBC whose tumors are extremely sensitive to chemotherapy, but there are many women for whom chemotherapy is of uncertain benefit [305]. Moreover, patients with TNBC have a higher probability of developing visceral metastasis (brain and lungs) compared to patients with other subtypes [305].

Ninety-five percent of TNBC are classified histologically as invasive ductal carcinomas, but other different subtypes can be observed [300]. However, TNBC are much more heterogeneous from a molecular point of view. In the introduction of this thesis, I stated that different intrinsic molecular subtypes within the breast cancer family have been decribed according to their gene expression profiles: Luminal A, Luminal B, Her2-enriched, Normal breast-like, Claaudin-Low and Basal-like. The Basal-like subtype is the most frequent subtype of TNBC (55–81%), and 90% of Basal-like breast cancers are TNBC [300]. The basal-like subtype is defined by a gene expression profile characteristic of normal basal/myoepithelial cells, including genes such as those for cytokeratins 5, 14 and 17 and EGFR [305]. Another frequent intrinsic subtype found in TNBC is the claudin-low subtype (that

represents 25-39% on TNBC), and the majority of claudin-low tumors are TNBC (61-71%) [5]. Interstingly, this subtype is characterized by high enrichment for EMT markers, immune response genes and cancer stem cell-like features, as well as low to absent expression of luminal differentiation markers.

However, TNBC itself can be further divided in 6 molecular subtypes on the basis of gene expression profiles: two basal-like (BL)-related subgroups (BL1 and BL2), two mesenchymal-related sub-groups (mesenchymal (M) and mesenchymal stem-like (MSL)), one immuno modulatory subgroup (IM) and one luminal androgen receptor group (LAR) [306]. Moreover, vast majority of tumors classified as claudin-low are composed of M and MSL TNBC subtypes, consistent with the elevated levels of EMT-associated genes [307]. This subtyping also showed to be predictive of response to neoadjuvant chemotherapy, with patients with the BL1 subtype achieving the highest pathologic response rate (52%) and patients with the BL2 subtype the lowest (0%) [308]

It is thus clear that TNBC represents a highly heterogeneous disease, being negativity for Her2, ER and PR the major point in common, even though in literature the terms TNBC and Basal-like breast cancer are used almost interchangeably.

As previously stated, chemotherapeutic drugs – and in particular anthracyclines and taxanes – are currently the basic treatment for TNBC [300]. Nevertheless, other compounds are currently being tested in clinical trials in an attempt to improve the outcome for TNBC patients [300]. Among these, platinum-based agents have received particular attention. Platinum salts act by leading to crosslinks formation in DNA strands, thus leading to breaks that finally cause apoptosis in cells lacking efficient repair mechanisms. In fact, the use of platinum-based agents has shown benefit for TNBC patients with mutation in BRCA1/2 genes, which are critical for maintaining DNA integrity and genome stability. BRCA1 mutations are rare in sporadic tumors, but germline mutations in this gene occur in 10% of patients with TNBC [300].

Despite this, 60-70% of TNBC patients still do not fully respond to chemotherapy, making the development of targeted therapies an urgency. Poly-ADP polymerase (PARP) inhibitors result in double-strand breaks in replicating cells, by blocking the repair mechanism mediated by the nuclear enzyme PARP. Thus, PARP inhibitors have been proved to cause synthetic lethality in cells carrying the BRCA1 mutations, since these cells are unable to repair DNA damage. Other actionable genomic alterations are rare in TNBC, but affect more frequently the PI3K/mTOR or the RAS/RAF/MEK pathways, thus PI3K and MEK inhibitors are currently being tested in clinical trials [300].

On the other hand, some studies suggest that TNBC/Basal-like cancer could be particularly enriched in CSC compared to other breast cancer subtypes, which could explain the aggressiveness and high rate of early recurrence of this breast cancer. A study by Neve and colleagues [309] revealed

the presence of two basal subgroups in a wide cohort of breast cancer cell lines, and linked the Basal B subgroup to a stem cell-like expression profile with $CD44^+/CD24^{low}$ phenotype. The authors further suggested that the Basal B subgroup may reflect the TNBC clinical subtype by the authors [309]. Other authors reported that the $CD44^+/CD24^-$ phenotype was most common in the TNBC basal-like subgroup [70,310–312]. However, these studies failed to demonstrate any difference in frequency of $CD44^+/CD24^-$ in metastasis relative to primary cancer [310] or correlation between $CD44^+/CD24^-$ phenotype and metastasis-free survival in their overall cohort of patients [311], but a trend of association with a worse DFS and OS was detected within the basal-like subtype [70]. Furthermore, it was found that basal-like breast cancer is the intrinsic molecular subtype harbouring the higher percentage of tumor cells positive for ALDH [70,312,313]. However, the $CD44^+/CD24^-$ and the $ALDH^+$ populations usually show very low merge, suggesting that they may represent distinct populations of CSC [50,70].

Despite the lack of definitive proof for an enrichment in CSC within the TNBC subtype, these studies suggest that basal-like/TNBC are indeed enriched in CSC markers, indicating that TNBC patients may indeed benefit from CSC-targeted therapies.

III.2 Paper III. Results and discussion

(*For detailed results and materials & methods, please refer to Attachment A - Paper III*)

Given these premises, we directed our interest on genes differentially expressed between CSC and non-CSC of TNBC cell lines to find possible therapeutic targets. We established tumorsphere cultures from TNBC mammary cancer cell lines 4T1 (murine) and HCC1806 (human) to enrich the CSC population, and performed flow-cytometry analysis to determine changes in CSC markers. 4T1 tumorspheres displayed an increased expression of the CSC markers Sca-1 and CD49f compared to their monolayer counterparts, while HCC1806 showed a trend of increase in $ALDH^+$ cells.

We then performed RNA-Sequencing to identify differences in gene expression between tumorspheres and their monolayer counterparts. Among the up-regulated and down-regulated transcripts, a minor proportion was shared between 4T1 and HCC1806 cell lines with variable distribution among different cell compartments. This allowed us to narrow the field of analysis to find CSC-associated targets in common between murine and human TNBC. In summary, 74 transcripts were upregulated in the tumorspheres of both HCC1806 and 4T1, while 42 transcripts were down-regulated. Enrichment analysis of gene ontology (GO) biological processes, performed through PANTHER over-representation test, indicated an enrichment in genes involved in negative regulation of apoptosis in the gene set up-regulated in tumorspheres, and an enrichment in genes involved in lipid metabolism and cell cycle regulation in the gene set down-regulated in tumorspheres. These results suggest that cells composing tumorspheres are more resistant to apoptotic cell death

while are likely more quiescent or slow-cycling compared to monolayer cells. Quiescence is a key tract of normal stem cells and could be potentially retained in their transformed counterparts. Quiescence has in fact been proposed to have a pivotal role in the resistance to conventional radio- and chemotherapy, with subsequent re-activation of surviving CSC leading to relapse. For what concerns the role of lipid metabolism in CSC biology, it could be linked to the relative quiescence of CSC, thus requiring less "building blocks" compared to highly proliferating cells.

By focusing on up-regulated transcripts coding for transmembrane proteins, which represent the ideal target for antibody-based therapies, we selected Teneurin-4 (TENM4) as a candidate target. TENM4 is a type II transmembrane protein of ~300 kDa, whose expression in healthy tissues is restricted to CNS and developing limbs. Its misregulated expression has been linked to neurological and behavioral disorders, but its link to cancer has not been clarified yet. Since literature reporting a role of this gene/protein in cancer is scarce, we explored the usefulness of targeting TENM4 by investigating its expression level and its prognostic role in breast cancer patients. By investigating TCGA dataset, TENM4 mRNA resulted to be expressed at higher levels in both Invasive Ductal Carcinoma (IDC) and Invasive Lobular Carcinoma (ILC) compared to normal breast. Furthermore, high expression of TENM4 is related to shorter relapse-free survival (RFS) in a cohort of TNBC patients. Given these premises, we decided to further investigate the role of TENM4 in our TNBC model.

We observed TENM4 mRNA upregulation in tumorspheres of different breast cancer cell lines compared to monolayer cells through RT-PCR. Furthermore, we validated TENM4 upregulation at protein level in 4T1 and HCC1806. 4T1 tumorspheres treated with a siRNA specific to TENM4 showed a partial but significant decrease in TENM4 mRNA and protein levels, which was reflected by a partial impairment of tumorsphere-forming ability. This suggests a role of TENM4 in the maintenance of self-renewal. Since TENM4 has been shown to be functionally linked to FAK in non-transformed cells, we investigated whether TENM4 and FAK interact in a cancer cell setting. 4T1 tumorspheres display an increase in FAK protein and phosphorylation level, which has been reported in literature to be an important feature of stem-like phenotype. TENM4 silencing through siRNA leads to a small but significant decrease in FAK phosphorylation, thus strengthening the possible link between TENM4 and a CSC-like phenotype.

Overall, our results seem to indicate that the stem-like status of TNBC cells is accompanied by altered regulation of apoptosis, cell cycle and lipid metabolism pathways. According to these findings, CSC appear to be quiescent and resistant to apoptosis. Poor literature information regarding TENM4 exists, and to the best our knowledge this is the first time that a link between TENM4 and CSC is established. In addition, TENM4 seems to interact with FAK, a protein with a role in cancer

cell-stemness. We observed that a decreased level of TENM4 partially impairs the tumorsphere forming ability of 4T1 cells and leads to a decrease of FAK phosphorylation at Y925 site. However, we cannot exclude that TENM4 could influence others of the many phosphorylation sites in the FAK proteins, as well as other signaling pathways. Further *in vitro* and *in vivo* investigations will help us to better define the role of TENM4 in TNBC cell stemness.

BIBLIOGRAPHY

1. Jemal, A., Bray, F. & Ferlay, J. Global Cancer Statistics: 2011. *CA Cancer J Clin* **49,** 69–90 (2011).

2. Malhotra, G. K., Zhao, X., Band, H. & Band, V. Histological, molecular and functional subtypes of breast cancers. *Cancer Biol. Ther.* **10,** 955–960 (2010).

3. Bombonati, A. & Sgroi, D. C. The Molecular Pathology of Breast Cancer Progression. *J Pathol* **223,** 307–317 (2011).

4. Kang, Y. & Pantel, K. Tumor Cell Dissemination: Emerging Biological Insights from Animal Models and Cancer Patients. *Cancer Cell* **23,** 573–581 (2013).

5. Prat, A. & Perou, C. M. Deconstructing the molecular portraits of breast cancer. *Mol. Oncol.* **5,** 5–23 (2011).

6. McDonald, E. S., Clark, A. S., Tchou, J., Zhang, P. & Freedman, G. M. Clinical Diagnosis and Management of Breast Cancer. *J. Nucl. Med.* **57,** 9S–16S (2016).

7. Gonzalez-Angulo, A., Morales-Vasquez, F. & Hortobagyi, G. Overview of resistance to systemic therapy in patients with Breast Cancer. *Adv. Exp. Med. Biol.* **608,** 1–22 (2007).

8. Hanahan, D. & Weinberg, R. A. Hallmarks of cancer: The next generation. *Cell* **144,** 646–674 (2011).

9. Marusyk, A., Almendro, V. & Polyak, K. Intra-tumour heterogeneity: A looking glass for cancer? *Nat. Rev. Cancer* **12,** 323–334 (2012).

10. Shackleton, M., Quintana, E., Fearon, E. R. & Morrison, S. J. Heterogeneity in Cancer: Cancer Stem Cells versus Clonal Evolution. *Cell* **138,** 822–829 (2009).

11. Nowell PC. The clonal evolution of tumor cell populations. *Science (80-.).* **194,** 23–28 (1976).

12. Clevers, H. The cancer stem cell: Premises, promises and challenges. *Nat. Med.* **17,** 313–319 (2011).

13. Pierce, G. B. & Speers, W. C. Tumors as Caricatures of the Process of Tissue Renewal: Prospects for Therapy by Directing Differentiation. *Cancer Res.* **48,** 1996–2004 (1988).

14. Visvader, J. E. & Lindeman, G. J. Cancer stem cells in solid tumours: Accumulating evidence and unresolved questions. *Nat. Rev. Cancer* **8,** 755–768 (2008).

15. Pattabiraman, D. R. & Weinberg, R. A. Tackling the cancer stem cells-what challenges do they pose? *Nat. Rev. Drug Discov.* **13,** 497–512 (2014).

16. Kreso, A. & Dick, J. E. Evolution of the cancer stem cell model. *Cell Stem Cell* **14,** 275–291 (2014).

17. Hurt, E. M. & Farrar, W. L. in *Cancer Stem Cells* (ed. Farrar, W. L.) 11–14 (Cambridge University Press, 2009).

18. Nguyen, L. L. V, Vanner, R., Dirks, P. & Eaves, C. C. J. Cancer stem cells: an evolving concept. *Nat. Rev. Cancer* **12,** 133–43 (2012).

19. Kleinsmith, L. J. & Pierce, G. Multipotentiality of Single Embryonal Carcinoma Cells. *Cancer Res* **24,** 1544–1551 (1964).

20. Pierce, G. B. & Wallace, C. Differentiation of Malignant to Benign Cells Differentiation of Malignant to Benign Cells ’. *Cancer Res* **31,** 127–134 (1971).

21. Huntly, B. J. P. & Gilliland, D. G. Leukaemia stem cells and the evolution of cancer-stem-cell research. *Nat. Rev. Cancer* **5,** 311–321 (2005).

22. Lapidot, T. *et al.* A cell initiating human acute myeloid leukaemia after transplantation into SCID mice. *Nature* **367,** 645–648 (1994).

23. Bonnet, D. & Dick, J. E. Human acute myeloid leukemia is organized as a hierarchy that originates from a primitive hematopoietic cell. *Nat. Med.* **3,** 730–737 (1997).

24. Al-Hajj, M., Wicha, M. S., Benito-Hernandez, A., Morrison, S. J. & Clarke, M. F. Prospective identification of tumorigenic breast cancer cells. *PNAS* **100,** 3983–8 (2003).

25. Valent, P. *et al.* Cancer stem cell definitions and terminology: The devil is in the details. *Nat. Rev. Cancer* **12,** 767–775 (2012).

26. Clarke, M. F. *et al.* Cancer stem cells - Perspectives on current status and future directions: AACR workshop on cancer stem cells. *Cancer Res.* **66,** 9339–9344 (2006).

27. Visvader, J. E. Cells of origin in cancer. *Nature* **469,** 314–322 (2011).

28. White, A. C. & Lowry, W. E. Refining the role for adult stem cells as cancer cells of origin. *Trends Cell Biol.* **25,** 11–20 (2015).

29. Karamboulas, C. & Ailles, L. Developmental signaling pathways in cancer stem cells of solid tumors. *Biochim. Biophys. Acta* **1830,** 2481–2495 (2013).

30. Pece, S. *et al.* Biological and Molecular Heterogeneity of Breast Cancers Correlates with Their Cancer Stem Cell Content. *Cell* **140,** 62–73 (2010).

31. Reya, T., Morrison, S. J., Clarke, M. F. & Weissman, I. L. Stem Cells, Cancer, and Cancer Stem Cells. *Nature* **414,** 105–111 (2001).

32. Reya, T. & Clevers, H. Wnt signalling in stem cells and cancer. *Nature* **434,** 843–850 (2005).

33. Imbert, A., Eelkema, R., Jordan, S., Feiner, H. & Cowin, P. DeltaN89Beta-Catenin Induces Precocious Development, Differentiationand Neoplasia in Mammary Gland. *J. Cell Biol.* **153,** 555–568 (2001).

34. Howe, L. R. & Brown, A. M. C. Wnt signaling and breast cancer. *Cancer Biol. Ther.* **3,** 36–41 (2004).

35. Zhan, T., Rindtorff, N. & Boutros, M. Wnt signaling in cancer. *Oncogene* **36,** 1461–1473 (2017).

36. Liu, S. *et al.* Hedgehog signaling and Bmi-1 regulate self-renewal of normal and malignant human mammary stem cells. *Cancer Res.* **66,** 6063–6071 (2006).

37. Fiaschi, M., Rozell, B., Bergström, Å. & Toftgård, R. Development of mammary tumors by conditional expression of GLI1. *Cancer Res.* **69,** 4810–4817 (2009).

38. Dontu, G. *et al.* Role of Notch signaling in cell-fate determination of human mammary stem/progenitor cells. *Breast Cancer Res.* **6,** R605 (2004).

39. Mani, S. a *et al.* The epithelial-mesenchymal transition generates cells with properties of stem cells. *Cell* **133,** 704–715 (2008).

40. Sato, R., Semba, T., Saya, H. & Arima, Y. Concise Review: Stem Cells and Epithelial-Mesenchymal Transition in Cancer: Biological Implications and Therapeutic Targets. *Stem Cells* **34,** 1997–2007 (2016).

41. Nassar, D. & Blanpain, C. Cancer Stem Cells: Basic Concepts and Therapeutic Implications. *Annu. Rev. Pathol. Mech. Dis.* **11,** 47–76 (2016).

42. Morel, A.-P. *et al.* Generation of Breast Cancer Stem Cells through Epithelial-Mesenchymal Transition. *PLoS One* **3,** e2888 (2008).

43. Onder, T. T. *et al.* Loss of E-cadherin promotes metastasis via multiple downstream transcriptional pathways. *Cancer Res.* **68,** 3645–3654 (2008).

44. Bartucci, M. *et al.* TAZ is required for metastatic activity and chemoresistance of breast cancer stem cells. *Oncogene* **34,** 681–690 (2015).

45. Cordenonsi, M. *et al.* The hippo transducer TAZ confers cancer stem cell-related traits on breast cancer cells. *Cell* **147,** 759–772 (2011).

46. Abraham, B. K. *et al.* Prevalence of CD44 + / CD24 − / low Cells in Breast Cancer May Not Be Associated with Clinical Outcome but May Favor Distant Metastasis. *Clin. Cancer Res.* **11,** 1154–1159 (2005).

47. Marcato, P. *et al.* Aldehyde Dehydrogenase Activity of Breast Cancer Stem Cells is Primarily Due to Isoform ALDH1A3 and Its Expression is Predictive of Metastasis. *Stem Cells* **29,** 32–45 (2011).

48. Oskarsson, T., Batlle, E. & Massagué, J. Metastatic stem cells: Sources, niches, and vital pathways. *Cell Stem Cell* **14,** 306–321 (2014).

49. Balic, M. *et al.* Most early disseminated cancer cells detected in bone marrow of breast cancer patients have a putative breast cancer stem cell phenotype. *Clin. Cancer Res.* **12,** 5615–5621 (2006).

50. Liu, S. *et al.* Breast cancer stem cells transition between epithelial and mesenchymal states reflective of their normal counterparts. *Stem Cell Reports* **2,** 78–91 (2014).

51. Creighton, C. J. *et al.* Residual breast cancers after conventional therapy display mesenchymal as well as tumor-initiating features. *Proc. Natl. Acad. Sci.* **106,** 13820–13825 (2009).

52. Koren, E. & Fuchs, Y. The bad seed: Cancer stem cells in tumor development and resistance. *Drug Resist. Updat.* **28,** 1–12 (2016).

53. Gasch, C., Ffrench, B., O'Leary, J. J. & Gallagher, M. F. Catching moving targets: cancer stem cell hierarchies, therapy-resistance & considerations for clinical intervention. *Mol. Cancer* **16,** 43 (2017).

54. Cojoc, M., Mäbert, K., Muders, M. H. & Dubrovska, A. A role for cancer stem cells in therapy resistance: Cellular and molecular mechanisms. *Semin. Cancer Biol.* **31,** 16–27 (2015).

55. Chen, W., Dong, J., Haiech, J., Kilhoffer, M. C. & Zeniou, M. Cancer stem cell quiescence and plasticity as major challenges in cancer therapy. *Stem Cells Int.* **2016,** (2016).

56. Singh, S. *et al.* Aldehyde Dehydrogenases in Cellular Responses to Oxidative/electrophilic Stress. *Free Radic Biol Med* **56,** 89–101 (2013).

57. Raha, D. *et al.* The Cancer Stem Cell Marker Aldehyde Dehydrogenase Is Required to Maintain a Drug-Tolerant Tumor Cell Subpopulation. *Cancer Res.* **74,** 3579–3590 (2014).

58. Chen, J. *et al.* A restricted cell population propagates glioblastoma growth following chemotherapy. *Nature* **488,** 522–526 (2012).

59. Vlashi, E. *et al.* In vivo imaging, tracking, and targeting of cancer stem cells. *J. Natl. Cancer Inst.* **101,** 350–359 (2009).

60. Hu, X. *et al.* Induction of cancer cell stemness by chemotherapy. *Cell Cycle* **11,** 2691–2698 (2012).

61. Auffinger, B. *et al.* Conversion of differentiated cancer cells into cancer stem-like cells in a glioblastoma model after primary chemotherapy. *Cell Death Differ.* **21,** 1119–1131 (2014).

62. Wang, Y. *et al.* Blocking the formation of radiation–induced breast cancer stem cells. *Oncotarget* **5,** 3743–3755 (2014).

63. Lagadec, C., Vlashi, E., Della Donna, L., Dekmezian, C. & Pajonk, F. Radiation-induced reprogramming of breast cancer cells. *Stem Cells* **30,** 833–844 (2012).

64. Ghisolfi, L., Keates, A. C., Hu, X., Lee, D. ki & Li, C. J. Ionizing radiation induces stemness in cancer cells. *PLoS One* **7,** 1–11 (2012).

65. Frank, N. Y., Schatton, T. & Frank, M. H. The therapeutic promise of the cancer stem cell concept. *J. Clin. Invest.* **120,** 41–50 (2010).

66. Paula, A. da C. & Lopes, C. Implications of Different Cancer Stem Cell Phenotypes in Breast Cancer. *Anticancer Res.* **37,** 2173–2183 (2017).

67. Doherty, M. R., Smigiel, J. M., Junk, D. J. & Jackson, M. W. Cancer stem cell plasticity drives therapeutic resistance. *Cancers (Basel).* **8,** 1–13 (2016).

68. Goldman, A. *et al.* Temporally sequenced anticancer drugs overcome adaptive resistance by targeting a vulnerable chemotherapy-induced phenotypic transition. *Nat. Commun.* **6,** 1–13 (2015).

69. Jaggupilli, A. & Elkord, E. Significance of CD44 and CD24 as cancer stem cell markers: An enduring ambiguity. *Clin. Dev. Immunol.* **2012,** (2012).

70. Ricardo, S. *et al.* Breast cancer stem cell markers CD44, CD24 and ALDH1: expression distribution within intrinsic molecular subtype. *J. Clin. Pathol.* **64,** 937–946 (2011).

71. Yan, Y., Zuo, X. & Wei, D. Concise Review: Emerging Role of CD44 in Cancer Stem Cells: A Promising Biomarker and Therapeutic Target. *Stem Cells Transl. Med.* **4,** 1033–43 (2015).

72. Grange, C., Lanzardo, S., Cavallo, F., Camussi, G. & Bussolati, B. Sca-1 identifies the tumor-initiating cells in mammary tumors of BALB-neuT transgenic mice. *Neoplasia* **10,** 1433–43 (2008).

73. Ginestier, C. *et al.* ALDH1 is a marker of normal and malignant human mammary stem cells and a predictor of poor clinical outcome. *Cell Stem Cell* **1,** 555–567 (2007).

74. Jones, R. J. *et al.* Assessment of aldehyde dehydrogenase in viable cells. *Blood* **85,** 2742–2746 (1995).

75. Goodell, B. M. A., Brose, K., Paradis, G., Conner, A. S. & Mulligan, R. C. Isolation and Functional Properties of Murine Hematopoietic Stem Cells that are Replicating in Vivo. *J Exp Med* **183,** 1797–1806 (1996).

76. Golebiewska, A., Brons, N. H. C., Bjerkvig, R. & Niclou, S. P. Critical appraisal of the side population assay in stem cell and cancer stem cell research. *Cell Stem Cell* **8,** 136–147 (2011).

77. Reynolds, B. A. & Weiss, S. Nervous System Generation of Neurons and Astrocytes from Isolated Cells of the Adult Mammalian Central Nervous System. *Science (80-.).* **255,** 1707–1710 (1992).

78. Uchida, N. *et al.* Direct isolation of human central nervous system stem cells. *PNAS* **97,** 14720–5 (2000).

79. Ponti, D. *et al.* Isolation and In vitro Propagation of Tumorigenic Breast Cancer Cells with Stem / Progenitor Cell Properties. *Cancer Res.* **65,** 5506–5512 (2005).

80. Singh, S. K. *et al.* Identification of a cancer stem cell in human brain tumors. *Cancer Res.* **63,** 5821–5828 (2003).

81. Dontu, G. *et al.* In vitro propagation and transcriptional profiling of human mammary stem/progenitor cells. *Genes Dev.* **17,** 1253–1270 (2003).

82. Weiswald, L. B., Bellet, D. & Dangles-Marie, V. Spherical cancer models in tumor biology. *Neoplasia* **17,** 1–15 (2015).

83. Charafe-Jauffret, E. *et al.* Cancer Stem Cells in Breast: Current Opinion and Future Challenges. *Pathobiology* **75,** 75–84 (2008).

84. Kenny, P. A. *et al.* The morphologies of breast cancer cell lines in three-dimensional assays correlate with their profiles of gene expression. *Mol. Oncol.* **1,** 84–96 (2007).

85. Smart, C. E. *et al.* In Vitro Analysis of Breast Cancer Cell Line Tumourspheres and Primary Human Breast Epithelia Mammospheres Demonstrates Inter- and Intrasphere Heterogeneity. *PLoS One* **8,** (2013).

86. Kuch, V., Schreiber, C., Thiele, W., Umansky, V. & Sleeman, J. P. Tumor-initiating properties of breast cancer and melanoma cells in vivo are not invariably reflected by spheroid formation in vitro, but can be increased by long-term culturing as adherent monolayers. *Int. J. Cancer* **132,** (2013).

87. Calvet, C. Y., André, F. M. & Mir, L. M. The culture of cancer cell lines as tumorspheres does not systematically result in cancer stem cell enrichment. *PLoS One* **9,** (2014).

88. Iezzi, M. *et al.* in *Translational Animal Models in Drug Discovery and Development* 139–166 (2012).

89. Lollini, P., Cavallo, F., Nanni, P. & Forni, G. Vaccines for tumour prevention. *Nat. Rev. Cancer* **6,** 204–216 (2006).

90. Cavallo, F., Calogero, R. A. & Forni, G. Are oncoantigens suitable targets for anti-tumour therapy? *Nat. Rev. Cancer* **7,** 707–713 (2007).

91. Iezzi, M. *et al.* DNA vaccination against oncoantigens A promise. *Oncoimmunology* **1,** 316–325 (2012).

92. Conti, L. *et al.* The noninflammatory role of high mobility group box 1/Toll-like receptor 2 axis in the self-renewal of mammary cancer stem cells. *FASEB J.* **27,** 4731–44 (2013).

93. Parish, C. R. Cancer immunotherapy : The past , the present and the future. *Immunol. Cell Biol.* 106–113 (2003).

94. Dunn, G. P., Bruce, A. T., Ikeda, H., Old, L. J. & Schreiber, R. D. Cancer immunoediting : from immuno-surveillance to tumor escape. *Nat. Immunol.* **3,** 991–998 (2002).

95. Schumacher, T. N. & Schreiber, R. D. Neoantigens in cancer immunotherapy. *Science (80-.).* **348,** 69–74 (2015).

96. Alexandrov, L. B. *et al.* Signatures of mutational processes in human cancer. *Nature* **500,** 415–421 (2013).

97. McGranahan, N., Furness, A. J. S., Rosenthal, R., Quezada, S. A. & Swanton, C. Clonal neoantigens elicit T cell immunoreactivity and sensitivity to immune checkpoint blockade. *Science (80-.).* **351,** 1463–1470 (2016).

98. Yuan, J. *et al.* Genetic Basis for Clinical Response to CTLA-4 Blockade in Melanoma. *N. Engl. J. Med.* **371,** 2189–2199 (2014).

99. Rizvi, N. A. *et al.* Mutational landscape determines sensitivity to PD-1 blockade in non – small cell lung cancer. *Science (80-.).* **348,** 124–129 (2016).

100. Allen, E. M. Van *et al.* Genomic correlates of response to CTLA-4 blockade in metastatic melanoma. *Science (80-.).* **350,** 207–212 (2015).

101. Oliver, S. E. *et al.* Prevalence of Human Papillomavirus Among Females After Vaccine Introduction—National Health and Nutrition Examination Survey, United States, 2003–2014. *J. Infect. Dis.* **216,** 594–603 (2017).

102. Yang, A., Farmer, E., Wu, T. C. & Hung, C.-F. Perspectives for therapeutic HPV vaccine development. *J. Biomed. Sci.* **23,** 75 (2016).

103. Brichard, B. V. *et al.* The Tyrosinase Gene Codes for an Antigen Recognized by Autologous Cytolytic T Lymphocytes on HLA-A2 Melanomas. *J. Exp. Med.* **178,** 489–495 (1993).

104. Gjerstorff, M. F., Andersen, M. H. & Ditzel, H. J. Oncogenic cancer / testis antigens : prime candidates for immunotherapy. *Oncotarget* **6,** (2015).

105. Yuan, J. *et al.* Immunologic responses to xenogeneic tyrosinase DNA vaccine administered by electroporation in patients with malignant melanoma. *J. Immunother. Cancer* 1–11 (2013).

106. Kimura, T. & Finn, O. J. MUC1 immunotherapy is here to stay. *Expert Opin. Biol. Ther.* **13,** 35–49 (2012).

107. Owens, M. A., Horten, B. C. & Da Silva, M. M. HER2 amplification ratios by fluorescence in situ hybridization and correlation with immunohistochemistry in a cohort of 6556 breast cancer tissues. *Clin. Breast Cancer* **5,** 63–69 (2004).

108. Goodell, V. *et al.* Level of HER-2/neu protein expression in breast cancer may affect the development of endogenous HER-2/neu-specific immunity. *Mol. Cancer Ther.* **7,** 449–454 (2008).

109. Montgomery, R. B., Makary, E., Schiffman, K., Goodell, V. & Disis, M. L. Endogenous anti-HER2 antibodies block HER2 phosphorylation and signaling through extracellular signal-regulated kinase. *Cancer Res.* **65,** 650–656 (2005).

110. Schreiber, R. D. Cancer Immunoediting : Integrating Suppression and Promotion. *Science (80-.).* **1565,** (2011).

111. Dunn, G. P., Old, L. J. & Schreiber, R. D. The Three Es of Cancer Immunoediting. *Annu. Rev. Immunol.* **22,** 329–60 (2004).

112. Zitvogel, L., Tesniere, A. & Kroemer, G. Cancer despite immunosurveillance: immunoselection and immunosubversion. *Nat. Rev. Immunol.* **6,** (2006).

113. Hanahan, D. & Coussens, L. M. Accessories to the Crime : Functions of Cells Recruited to the Tumor Microenvironment. *Cancer Cell* **21,** 309–322 (2012).

114. Khong, H. T. & Restifo, N. P. Natural selection of tumor variants in the generation of ‘ tumor escape ’ phenotypes. *Nat. Immunol.* **3,** 999–1005 (2002).

115. Concha-benavente, F., Srivastava, R., Ferrone, S. & Ferris, R. L. Immunological and clinical significance of HLA class I antigen processing machinery component defects in malignant cells. *Oral Oncol.* **58,** 52–58 (2016).

116. Okazaki, T. & Honjo, T. The PD-1 – PD-L pathway in immunological tolerance. *Trends Immunol.* **27,** (2006).

117. Rabinovich, G. A., Gabrilovich, D. & Sotomayor, E. M. Immunosuppressive Strategies that are Mediated by Tumor Cells. (2007). doi:10.1146/annurev.immunol.25.022106.141609

118. Munn, D. H. & Bronte, V. Immune suppressive mechanisms in the tumor microenvironment. *Curr. Opin. Immunol.* **39,** 1–6 (2016).

119. Zou, W. Regulatory T cells , tumour immunity and immunotherapy. *Nat. Rev. Immunol.* **6,** 295–307 (2006).

120. Mantovani, A. *et al.* Macrophage polarization : tumor-associated macrophages as a paradigm for polarized M2

mononuclear phagocytes. *Trends Immunol.* **23,** 549–555 (2002).

121. Marigo, I., Dolectti, L., Serafini, P., Zanovello, P. & Brinte, V. Tumor-induced tolerance and immune suppression by myeloid derived suppressor cells. *Immunol. Rev.* **222,** 162–179 (2008).

122. Joffre, O. P., Segura, E., Savina, A. & Amigorena, S. Cross-presentation by dendritic cells. *Nat. Rev. Immunol.* **12,** (2012).

123. Gooden, M. J. M., Bock, G. H. De, Leffers, N., Daemen, T. & Nijman, H. W. The prognostic influence of tumour-infiltrating lymphocytes in cancer : a systematic review with meta-analysis. *Br. J. Cancer* **105,** 93–103 (2011).

124. Tsou, P., Katayama, H., Ostrin, E. J. & Hanash, S. M. The Emerging Role of B Cells in Tumor Immunity. *Cancer Res.* 1–6 (2016). doi:10.1158/0008-5472.CAN-16-0431

125. Waldhauer, I. & Steinle, A. NK cells and cancer immunosurveillance. *Oncogene* 5932–5943 (2008). doi:10.1038/onc.2008.267

126. Galluzzi, L. *et al.* Classification of current anticancer immunotherapies. *Oncotarget* **5,** (2014).

127. Weiner, G. J. Building better monoclonal antibody-based therapeutics. *Nat. Rev. Cancer* **15,** 361–370 (2015).

128. Rosenberg, S. A. & Restifo, N. P. Adoptive cell transfer as personalized immunotherapy for human cancer. *Science (80-.).* **348,** (2015).

129. Schmitt, T. M., Ragnarsson, G. B. & Greenberg, P. D. T Cell Receptor Gene Therapy for Cancer. *Hum. Gene Ther.* **1248,** 1240–1248 (2009).

130. Jena, B., Dotti, G. & Cooper, L. J. N. Redirecting T-cell specificity by introducing a tumor-specific chimeric antigen receptor. *Blood* **116,** 1035–1045 (2010).

131. Galluzzi, L., Buqué, A., Kepp, O., Zitvogel, L. & Kroemer, G. Immunogenic cell death in cancer and infectious disease. *Nat. Rev. Immunol.* **17,** 97–111 (2016).

132. Bracci, L., Schiavoni, G., Sistigu, A. & Belardelli, F. Immune-based mechanisms of cytotoxic chemotherapy: implications for the design of novel and rationale-based combined treatments against cancer. *Cell Death Differ.* **21,** 15–25 (2014).

133. Lee, S. & Margolin, K. Cytokines in Cancer Immunotherapy. *Cancers (Basel).* 3856–3893 (2011). doi:10.3390/cancers3043856

134. Pardoll, D. M. The blockade of immune checkpoints in cancer immunotherapy. *Nat. Rev. Cancer* **12,** (2012).

135. Postow, M. A., Callahan, M. K. & Wolchok, J. D. Immune Checkpoint Blockade in Cancer Therapy. *J. Clin. Oncol.* **33,** (2017).

136. Rahner, N. & Steinke, V. Hereditary Cancer Syndromes. *Deuthsches Arzteblatt Int.* **105,** 706–714 (2008).

137. Lohmueller, J. J. *et al.* Antibodies elicited by the first non-viral prophylactic cancer vaccine show tumor-specificity and immunotherapeutic potential. *Sci. Rep.* 1–12 (2016). doi:10.1038/srep31740

138. Kimura, T. *et al.* MUC1 vaccine for individuals with advanced adenoma of the colon: A cancer immunoprevention feasibility study. *Cancer Prev. Res.* **6,** 18–26 (2013).

139. Fracol, M. *et al.* Response to HER-2 Pulsed DC1 vaccines is predicted by both HER-2 and estrogen receptor expression in DCIS. *Ann. Surg. Oncol.* **20,** 3233–3239 (2013).

140. Melief, C. J. M., Hall, T. Van, Arens, R., Ossendorp, F. & Burg, S. H. Van Der. Therapeutic cancer vaccines. *J. Clin. Invest.* **125,** 3401–3412 (2015).

141. Burg, S. H. Van Der, Arens, R., Ossendorp, F., Hall, T. Van & Melief, C. J. M. Vaccines for established cancer : overcoming the challenges posed by immune evasion. *Nat. Rev. Cancer* **16,** 219–233 (2016).

142. Cheever, M. A. & Higano, C. S. PROVENGE (Sipuleucel-T) in Prostate Cancer : The First FDA-Approved Therapeutic Cancer Vaccine. *Clin. Cancer Res.* **17,** 3520–3527 (2011).

143. Dranoff, G. *et al.* Vaccination with irradiated tumor cells engineered to secrete murine granulocyte-macrophage colony-stimulating factor stimulates potent , specific , and long-lasting anti-tumor immunity. *PNAS* **90,** 3539–

3543 (1993).

144. Butterfield, L. H. Cancer vaccines. *BMJ* 1–14 (2015). doi:10.1136/bmj.h988

145. Aranda, F., Vacchelli, E., Eggermont, A., Galon, J. & Sautès-fridman, C. Peptide vaccines in cancer therapy Trial Watch. *Oncoimmunology* 1–11 (2013).

146. Rice, J., Ottensmeier, C. H. & Stevenson, F. K. DNA vaccines : precision tools for activating effective immunity against cancer. *Nat. Rev. Cancer* **8,** (2008).

147. Khan, S., Camps, M., Drijfhout, J. W. & Silva, A. L. Dendritic cells process synthetic long peptides better than whole protein , improving antigen presentation and T-cell activation. *Eur. J. Immunol.* 2554–2565 (2013). doi:10.1002/eji.201343324

148. Bol, K. F., Schreibelt, G., Gerritsen, W. R., Vries, I. J. M. De & Figdor, C. G. Dendritic Cell – Based Immunotherapy : State of the Art and Beyond. *Clin. Cancer Res.* 1897–1907 (2016). doi:10.1158/1078-0432.CCR-15-1399

149. Aurisicchio, L. & Ciliberto, G. Genetic cancer vaccines : current status and perspectives. *Expert Opin Biol Ther* 1043–1058 (2012).

150. Rovero, S. *et al.* DNA Vaccination Against Rat Her-2/Neu p185 More Effectively Inhibits Carcinogenesis Than Transplantable Carcinomas in Transgenic BALB/c Mice. *J. Immunol.* (2000). doi:10.4049/jimmunol.165.9.5133

151. Castle, J. C. *et al.* Exploiting the mutanome for tumor vaccination. *Cancer Res.* **72,** 1081–1091 (2012).

152. Kreiter, S. *et al.* Mutant MHC class II epitopes drive therapeutic immune responses to cancer. *Nature* **520,** 692–696 (2015).

153. Sahin, U. *et al.* Personalized RNA mutanome vaccines mobilize poly-specific therapeutic immunity against cancer. *Nature* (2017). doi:10.1038/nature23003

154. Chiocca, E. & Rabkin, S. Oncolytic Viruses and Their Application to Cancer Immunotherapy. *Cancer Immunol Res* **2,** 295–300 (2014).

155. Jacca, S. *et al.* Bovine herpesvirus 4-based vector delivering a hybrid rat / human HER-2 oncoantigen efficiently protects mice from autochthonous Her-2 mammary cancer. *Oncoimmunology* **5,** 1–14 (2015).

156. Redaelli, M. *et al.* Herpes simplex virus type 1 thymidine kinase – armed bovine herpesvirus type 4-based vector displays enhanced oncolytic properties in immunocompetent orthotopic syngenic mouse and rat glioma models. *Neuro. Oncol.* **14,** 288–301 (2012).

157. Tang, D. C., DeVit, M. & Johnston, S. A. Genetic immunization is a simple method for eliciting an immune response. *Nature* **356,** 152–154 (1992).

158. Ulmer, J. B. *et al.* Heterologous Protection Against Influenza by Injection of DNA Encoding a Viral Protein. *Science (80-.).* **259,** 1745–1749 (1993).

159. Fynan, E. F., Webstert, R. G., Fullert, D. H., Haynes, J. R. & Santoro, J. C. DNA vaccines : Protective immunizations by parenteral , mucosal , and gene-gun inoculations. *PNAS* **90,** 11478–11482 (1993).

160. Wang, B. I. N. *et al.* Gene inoculation generates immune responses against human immunodeficiency virus type 1. *PNAS* **90,** 4156–4160 (1993).

161. Kutzler, M. A. & Weiner, D. B. REVIEWS DNA vaccines : ready for prime time ? *Nat. Rev. Genet.* **9,** 776–788 (2008).

162. Barber, G. N. Cytoplasmic DNA innate immune pathways. *Immunol. Rev.* **243,** 99–108 (2011).

163. Fuller, D. H., Loudon, P. & Schmaljohn, C. Preclinical and clinical progress of particle-mediated DNA vaccines for infectious diseases. *Methods* **40,** 86–97 (2006).

164. Sardesai, N. Y. & Weiner, D. B. Electroporation delivery of DNA vaccines : prospects for success. *Curr. Opin. Immunol.* **23,** 421–429 (2011).

165. Gammaitoni, L. *et al.* Immunotherapy of cancer stem cells in solid tumors: initial findings and future prospective. *Expert Opin Biol Ther* **14,** 1259–1270 (2014).

166. Castriconi, R. *et al.* NK Cells Recognize and Kill Human Glioblastoma Cells with Stem Cell-Like Properties 1. *J. Immunol.* (2009). doi:10.4049/jimmunol.0802845

167. Di Tomaso, T. *et al.* Immunobiological Characterization of Cancer Stem Cells Isolated from Glioblastoma Patients. *Clin. Cancer Res.* **16,** 800–814 (2010).

168. Pietra, G. *et al.* Natural killer cells kill human melanoma cells with characteristics of cancer stem cells. *Int. Immunol.* **21,** 793–801 (2009).

169. Volonté, A. *et al.* Cancer-Initiating Cells from Colorectal Cancer Patients Escape from T Cell − Mediated Immunosurveillance In Vitro through Membrane-Bound IL-4. *J Immunol* (2014). doi:10.4049/jimmunol.1301342

170. Schatton, T. *et al.* Modulation of T-Cell Activation by Malignant Melanoma Initiating Cells. *Cancer Res.* 697–709 (2010). doi:10.1158/0008-5472.CAN-09-1592

171. Pellegatta, S. *et al.* Neurospheres Enriched in Cancer Stem – Like Cells Are Highly Effective in Eliciting a Dendritic Cell – Mediated Immune Response against Malignant Gliomas. *Cancer Res.* 10247–10253 (2006). doi:10.1158/0008-5472.CAN-06-2048

172. Brown, C. E. *et al.* Recognition and Killing of Brain Tumor Stem-Like Initiating Cells by CD8 + Cytolytic T Cells. *Cancer Res.* 8886–8894 (2009). doi:10.1158/0008-5472.CAN-09-2687

173. Xu, Q. *et al.* Antigen-Specific T-Cell Response from Dendritic Cell Vaccination Using Cancer Stem-Like Cell-Associated Antigens. *Stem Cells* (2009). doi:10.1002/stem.102

174. Jachetti, E. *et al.* Prostate cancer stem cells are targets of both innate and adaptive immunity and elicit tumor-specific immune responses. *Oncoimmunology* 1–12 (2013).

175. Wu, D. *et al.* Effect of targeted ovarian cancer immunotherapy using ovarian cancer stem cell vaccine. *J. Ovarian Res.* 1–10 (2015). doi:10.1186/s13048-015-0196-5

176. Yao, X., Dong, Z., Zhang, Q., Wang, Q. & Lai, D. Epithelial ovarian cancer stem-like cells expressing α -gal epitopes increase the immunogenicity of tumor associated antigens. *BMC Cancer* 1–15 (2015). doi:10.1186/s12885-015-1973-7

177. Ning, N. *et al.* Cancer Stem Cell Vaccination Confers Significant Antitumor Immunity. *Cancer Res.* 1853–1865 (2012). doi:10.1158/0008-5472.CAN-11-1400

178. Lu, L. *et al.* Cancer stem cell vaccine inhibits metastases of primary tumors and induces humoral immune responses against cancer stem cells. *Oncoimmunology* (2017). doi:10.4161/2162402X.2014.990767

179. Hu, Y. *et al.* Therapeutic Efficacy of Cancer Stem Cell Vaccines in the Adjuvant Setting. *Cancer Res.* 4661–4673 (2016). doi:10.1158/0008-5472.CAN-15-2664

180. Vik-Mo, E. *et al.* Therapeutic vaccination against autologous cancer stem cells with mRNA-transfected dendritic cells in patients with glioblastoma. *Cancer Immunol. Immunother.* 1499–1509 (2013). doi:10.1007/s00262-013-1453-3

181. Lin, M., Xu, S. L. K., Feng, Z. L. & Yuan, M. Y. Safety and efficacy study of lung cancer stem cell vaccine. *Immunol. Res.* 16–22 (2015). doi:10.1007/s12026-015-8631-7

182. Lin, M. *et al.* Prospective study of the safety and efficacy of a pancreatic cancer stem cell vaccine. *J. Cancer Res. Clin. Oncol.* 1827–1833 (2015). doi:10.1007/s00432-015-1968-4

183. Maccalli, C., Volonte, A., Cimminiello, C. & Parmiani, G. Immunology of cancer stem cells in solid tumours . A review. *Eur. J. Cancer* 649–655 (2014). doi:10.1016/j.ejca.2013.11.014

184. Pan, Q. *et al.* Concise Review : Targeting Cancer Stem Cells Using Immunologic Approaches. *Stem Cells* 2085–2092 (2015).

185. Lewerenz, J. *et al.* The cystine/glutamate antiporter system x(c)(-) in health and disease: from molecular mechanisms to novel therapeutic opportunities. *Antioxid. Redox Signal.* **18,** 522–55 (2013).

186. Bassi, M. T. *et al.* Identification and characterisation of human xCT that co-expresses, with 4F2 heavy chain, the amino acid transport activity system xc-. *Pflugers Arch.* **442,** 286–296 (2001).

187. Galadari, S., Rahman, A., Pallichankandy, S. & Thayyullathil, F. Reactive oxygen species and cancer paradox:

To promote or to suppress? *Free Radic. Biol. Med.* **104,** 144–164 (2017).

188. Kensler, T. W., Wakabayashi, N. & Biswal, S. Cell Survival Responses to Environmental Stresses Via the Keap1-Nrf2-ARE Pathway. *Annu. Rev. Pharmacol. Toxicol.* **47,** 89–116 (2007).

189. Lewerenz, J. & Maher, P. Basal levels of eIF2alpha phosphorylation determine cellular antioxidant status by regulating ATF4 and xCT expression. *J. Biol. Chem.* **284,** 1106–1115 (2009).

190. Daemen, A. *et al.* Article Glutamine Sensitivity Analysis Identifies the xCT Antiporter as a Common Triple-Negative Breast Tumor Therapeutic Target. *Cancer Cell* **24,** 450–465 (2013).

191. Robe, P. A. *et al.* Early termination of ISRCTN45828668, a phase 12 prospective, randomized study of Sulfasalazine for the treatment of progressing malignant gliomas in adults. *BMC Cancer* **9,** 1–8 (2009).

192. Dixon, S. J. *et al.* Ferroptosis : An Iron-Dependent Form of Nonapoptotic Cell Death. *Cell* **149,** 1060–1072 (2012).

193. Yang, W. S. *et al.* Regulation of Ferroptotic Cancer Cell Death by GPX4. *Cell* **156,** 317–331 (2014).

194. Sakakura, Y. *et al.* Expression and function of cystine/glutamate transporter in neutrophils. *J. Leukoc. Biol.* **81,** 974–982 (2007).

195. Srivastava, M. K., Sinha, P., Clements, V. K., Rodriguez, P. & Ostrand-Rosenberg, S. Myeloid-derived suppressor cells inhibit T-cell activation by depleting cystine and cysteine. *Cancer Res.* **70,** 68–77 (2010).

196. Sleire, L. *et al.* Drug repurposing : sulfasalazine sensitizes gliomas to gamma knife radiosurgery by blocking cystine uptake through system Xc − , leading to glutathione depletion. *Oncogene* **34,** 5951–5959 (2015).

197. Satoru, T. *et al.* Increased xCT Expression Correlates With Tumor Invasion and Outcome in Patients with Glioblastomas. *Neurosurgery* **72,** 33–41 (2013).

198. Robert, S. M. *et al.* SLC7A11 expression is associated with seizures and predicts poor survival in patients with malignant glioma. *Sci. Transl. Med.* **7,** (2015).

199. Savaskan, N. E. *et al.* Small interfering RNA – mediated neurodegeneration and alleviates brain edema. *Nat. Med.* **14,** 629–632 (2008).

200. Ye, Z., Rothstein, J. D. & Sontheimer, H. Compromised Glutamate Transport in Human Glioma Cells : Reduction – Mislocalization of Sodium-Dependent Glutamate Transporters and Enhanced Activity of Cystine – Glutamate Exchange. *J. Neurosci.* **19,** 10767–10777 (1999).

201. Yang, Y. & Yee, D. IGF-I Regulates Redox Status in Breast Cancer Cells by Activating the Amino Acid Transport Molecule xC-. *Cancer Res* **74,** 2295–2306 (2014).

202. Wang, S. *et al.* Mitochondrial dysfunction enhances cisplatin resistance in human gastric cancer cells via the ROS-activated GCN2-eIF2α- ATF4-xCT pathway. *Oncotarget* **7,** (2016).

203. Ma, M. *et al.* Xc − inhibitor sulfasalazine sensitizes colorectal cancer to cisplatin by a GSH-dependent mechanism. *Cancer Lett.* **368,** 88–96 (2015).

204. Guo, W. *et al.* Disruption of xCT inhibits cell growth via the ROS / autophagy pathway in hepatocellular carcinoma. *Cancer Lett.* **312,** 55–61 (2011).

205. Kinoshita, H. *et al.* Cystine / glutamic acid transporter is a novel marker for predicting poor survival in patients with hepatocellular carcinoma. *Oncol. Rep.* **29,** 685–689 (2013).

206. Wang, J. *et al.* Collecting duct carcinoma of the kidney is associated with CDKN2A deletion and SLC family gene up-regulation. *Oncotarget* **7,** (2016).

207. Lo, M., Ling, V., Wang, Y. Z. & Gout, P. W. The xc cystine / glutamate antiporter : a mediator of pancreatic cancer growth with a role in drug resistance. *Br. J. Cancer* **99,** 464–472 (2008).

208. Shiozaki, A., Iitaka, D., Ichikawa, D., Nakashima, S. & Fujiwara, H. xCT , component of cysteine / glutamate transporter , as an independent prognostic factor in human esophageal squamous cell carcinoma. *J Gastroenterol* **49,** 853–863 (2014).

209. Koglin, N. *et al.* Specific PET imaging of x C- transporter activity using a 18F-labeled glutamate derivative reveals a dominant pathway in tumor metabolism. *Clin. Cancer Res.* **17,** 6000–6011 (2011).

210. Mittra, E. S. *et al.* Pilot preclinical and clinical evaluation of (4S)-4-(3-[18F]Fluoropropyl)-L-Glutamate (18F-FSPG) for PET/CT imaging of intracranial malignancies. *PLoS One* **11,** 1–17 (2016).

211. Nagano, O., Okazaki, S. & Saya, H. Redox regulation in stem-like cancer cells by CD44 variant isoforms. *Oncogene* **32,** 5191–5198 (2013).

212. Ishimoto, T. *et al.* Article CD44 Variant Regulates Redox Status in Cancer Cells by Stabilizing the xCT Subunit of System xc – and Thereby Promotes Tumor Growth. *Cancer Cell* **19,** 387–400 (2011).

213. Yae, T. *et al.* Alternative splicing of CD44 mRNA by ESRP1 enhances lung colonization of metastatic cancer cell. *Nat. Commun.* **3,** 883–889 (2012).

214. Yoshikawa, M., Tsuchihashi, K., Ishimoto, T., Yae, T. & Motohara, T. xCT Inhibition Depletes CD44v-Expressing Tumor Cells That Are Resistant to EGFR-Targeted Therapy in Head and Neck Squamous Cell Carcinoma. *Cancer Res* **73,** 1855–1867 (2013).

215. Wada, T. *et al.* Functional role of CD44v-xCT system in the development of spasmolytic polypeptide-expressing metaplasia. *Cancer Sci.* **104,** 1323–1329 (2013).

216. Siroy, A. *et al.* MUC1 is expressed at high frequency in early-stage basal-like triple negative breast cancer. *Hum Pathol* **44,** 2159–2166 (2013).

217. Hasegawa, M., Takahashi, H., Rajabi, H. & Alam, M. Functional interactions of the cystine / glutamate antiporter , CD44v and MUC1-C oncoprotein in triple-negative breast cancer cells. **7,** (2016).

218. Tsuchihashi, K. *et al.* The EGF Receptor Promotes the Malignant Potential of Glioma by Regulating Amino Acid Transport System xc (—). *Cancer Res* **76,** 2954–2964 (2016).

219. Xie, Y. *et al.* Ferroptosis : process and function. *Cell Death Differ.* **23,** 369–379 (2016).

220. Jiang, L. *et al.* Ferroptosis as a p53-mediated activity during tumour suppression. *Nature* **520,** 57–62 (2015).

221. Jiang, L., Hickman, J. H., Wang, S. & Gu, W. Dynamic roles of p53-mediated metabolic activities in ROS-induced stress responses. *Cell Cycle* **4101,** 2881–5 (2015).

222. Li, T., Liu, X., Jiang, L., Manfredi, J. & Zha, S. Loss of p53-mediated cell-cycle arrest , senescence and apoptosis promotes genomic instability and premature aging. *Oncotarget* **7,** 11838–49 (2016).

223. Liu, D. S. *et al.* Inhibiting the system xC-glutathione axis selectively targets cancers with mutant-p53 accumulation. *Nat. Commun.* **8,** 1–14 (2017).

224. Chen, R. *et al.* Disruption of xCT inhibits cancer cell metastasis via the caveolin-1 /beta-catenin pathway. *Oncogene* **28,** 599–609 (2009).

225. Linher-melville, K. & Singh, G. The complex roles of STAT3 and STAT5 in maintaining redox balance : Lessons from STAT-mediated xCT expression in cancer cells. *Mol. Cell. Endocrinol.* (2017). doi:10.1016/j.mce.2017.02.014

226. Sina, K. L., Patrick, H. & Gurmit, G. Signal transducer and activator of transcription 3 and 5 regulate system Xc- and redox balance in human breast cancer cells. *Mol. Cell. Biochem.* 205–221 (2015). doi:10.1007/s11010-015-2412-4

227. Linher-melville, K., Nashed, M. G., Ungard, R. G. & Haftchenary, S. Chronic Inhibition of STAT3 / STAT5 in Treatment-Resistant Human Breast Cancer Cell Subtypes : Convergence on the ROS / SUMO Pathway and Its Effects on xCT Expression and System xc- Activity. *PLoS One* 1–31 (2016). doi:10.1371/journal.pone.0161202

228. Toyin Adeyemi Ogunrinu; Harald Sontheimer. Hypoxia Increases the Dependence of Glioma Cells on. *J. Biol. Chem.* **285,** 37716–37724 (2010).

229. Lu, H. *et al.* Chemotherapy triggers HIF-1 – dependent glutathione synthesis and copper chelation that induces the breast cancer stem cell phenotype. *PNAS* **112,** (2015).

230. Parks, S. K., Cormerais, Y., Marchiq, I. & Pouyssegur, J. Molecular Aspects of Medicine Hypoxia optimises tumour growth by controlling nutrient import and acidic metabolite export. *Mol. Aspects Med.* **47–48,** 3–14 (2016).

231. Liu, X. *et al.* MicroRNA-26b is underexpressed in human breast cancer and induces cell apoptosis by targeting SLC7A11. *FEBS Lett.* **585,** 1363–1367 (2011).

232. Drayton, R. M. *et al.* Reduced Expression of miRNA-27a Modulates Cisplatin Resistance in Bladder Cancer by Targeting the Cystine / Glutamate Exchanger SLC7A11. *Clin Cancer Res* **2,** (2014).

233. Ye, Z. & Sontheimer, H. Glioma Cells Release Excitotoxic Concentrations of Glutamate Glioma Cells Release Excitotoxic Concentrations of Glutamate 1. *Cancer Res* **59,** 4383–4391 (1999).

234. Dai, L., Noverr, M. C., Parsons, C., Kaleeba, J. A. R. & Qin, Z. xCT , not just an amino-acid transporter : a multi-functional regulator of microbial infection and associated diseases. *Front Microbiol.* **6,** 1–5 (2015).

235. Gottesman, M. M. Mechanisms of cancer drug resistance. *Annu. Rev. Med.* **53,** 615–27 (2002).

236. Trachootham, D., Alexandre, J. & Huang, P. Targeting cancer cells by ROS-mediated mechanisms : a radical therapeutic approach ? *Nat. Rev. Drug Discov.* **8,** 579–591 (2009).

237. Traverso, N. *et al.* Role of Glutathione in Cancer Progression and Chemoresistance. *Oxid. Med. Cell. Longev.* **Article ID,** (2013).

238. Huang, Y., Dai, Z., Barbacioru, C. & Sade, W. Cystine-Glutamate Transporter SLC7A11 in Cancer Chemosensitivity and Chemoresistance. *Cancer Res* **65,** 7446–7455 (2005).

239. Dai, Z., Huang, Y., Sadee, W. & Blower, P. Chemoinformatics Analysis Identifies Cytotoxic Compounds Susceptible to Chemoresistance Mediated by Glutathione and Cystine/Glutamate Transport System x c -. *J Med Chem* **50,** 1896–1906 (2007).

240. Huang, Y., Bpharm, S. P., Bs, A. P. & Wang, J. Genetic variations and gene expression of transporters in drug disposition and response. *Expert Opin. Drug Metab. Toxicol.* **4,** 237–54 (2008).

241. Liu, R. *et al.* Cystine-Glutamate Transporter SLC7A11 Mediates Resistance to Geldanamycin but Not to 17-(Allylamino)-17-demethoxygeldanamycin. *Mol Pharmacol* **72,** 1637–46 (2007).

242. Pham, A., Blower, P. E., Alvarado, O., Ravula, R. & Gout, P. W. Pharmacogenomic Approach Reveals a Role for the x ͨ Cystine / Glutamate Antiporter in Growth and Celastrol Resistance of Glioma Cell Lines. *J Pharmacol Exp Theor* **332,** 949–958 (2010).

243. Okuno, S. *et al.* Role of cystine transport in intracellular glutathione level and cisplatin resistance in human ovarian cancer cell lines. *Br. J. Cancer* **88,** 951–956 (2003).

244. Zhang, P. *et al.* xCT expression modulates cisplatin resistance in Tca8113 tongue carcinoma cells. *Oncol Lett* **12,** 307–314 (2016).

245. Roh, J., Kim, E. H., Jang, H. & Shin, D. Aspirin plus sorafenib potentiates cisplatin cytotoxicity in resistant head and neck cancer cells through xCT inhibition. *Free Radic. Biol. Med.* **104,** 1–9 (2017).

246. Sehm, T. *et al.* Temozolomide toxicity operates in a xCT / SLC7a11 dependent manner and is fostered by ferroptosis. *Oncotarget* **7,** (2016).

247. Chen, L. *et al.* Erastin sensitizes glioblastoma cells to temozolomide by restraining xCT and cystathionine- γ - lyase function. *Oncol. Rep.* **33,** 1465–1474 (2015).

248. Narang, V. S., Pauletti, G. M., Gout, P. W., Buckley, D. J. & Buckley, A. . Sulfasalazine-Induced Reduction of Glutathione Levels in Breast Cancer Cells : Enhancement of Growth-Inhibitory Activity of Doxorubicin. *Chemotherapy* **4,** 210–217 (2007).

249. Starheim, K. K. *et al.* Intracellular glutathione determines bortezomib cytotoxicity in multiple myeloma cells. *Blood Cancer J.* **6,** (2016).

250. Geninatti, S. *et al.* Mn-loaded apoferritin : a highly sensitive MRI imaging probe for the detection and characterization of hepatocarcinoma lesions in a transgenic mouse model. *Contrast Media Mol. Imaging* **7,** 281–288 (2012).

251. Cutrin, J. C., Crich, S. G., Burghelea, D., Dastru, W. & Aime, S. Curcumin/Gd Loaded Apoferritin: A Novel ‘ Theranostic ’ Agent To Prevent Hepatocellular Damage in Toxic Induced Acute Hepatitis. (2013).

252. Ravindran, J., Prasad, S. & Aggarwal, B. B. Curcumin and Cancer Cells : How Many Ways Can Curry Kill Tumor Cells Selectively ? *AAPS J.* **11,** (2009).

253. Choi, K. Y., Liu, G., Lee, S. & Chen, X. Theranostic nanoplatforms for simultaneous cancer imaging and therapy : current approaches and future perspectives. *Nanoscale* **4,** (2012).

254. Lammers, T., Kiessling, F., Hennink, W. E. & Storm, G. Drug targeting to tumors : Principles , pitfalls and (pre-) clinical progress. *J. Control. Release* **161,** 175–187 (2012).

255. Lammers, T., Aime, S., Hennink, W. I. M. E., Storm, G. & Kiessling, F. Theranostic Nanomedicine. *Acc. Chem. Res.* **44,** 1029–1038 (2011).

256. Sun, D. Nanotheranostics : Integration of Imaging and Targeted. *Mol. Pharm.* **7,** 1003652 (2010).

257. Stanley, S. Biological nanoparticles and their influence on organisms. *Curr. Opin. Biotechnol.* **28,** 69–74 (2014).

258. Truffi, M. *et al.* Ferritin nanocages : A biological platform for drug delivery , imaging and theranostics in cancer. *Pharmacol. Res.* **107,** 57–65 (2016).

259. Li, J. Y. *et al.* Scara5 Is a Ferritin Receptor Mediating Non-Transferrin Iron Delivery. *Dev. Cell* **16,** 35–46 (2009).

260. Jiang, Y., Oliver, P., Davies, K. E. & Platt, N. Identification and Characterization of Murine SCARA5 , a Novel Class A Scavenger Receptor That Is Expressed by Populations of Epithelial Cells *. *J. Biol. Chem.* **281,** 11834–11845 (2006).

261. Sarraj, M. A., Mcclive, P. J., Wilmore, H. P., Loveland, K. L. & Sinclair, A. H. Novel Scavenger Receptor Gene Is Differentially Expressed in the Embryonic and Adult Mouse Testis. *Dev Dyn* 1026–1033 (2005). doi:10.1002/dvdy.20594

262. Risto, J., Ojala, M., Pikkarainen, T., Elmberger, G. & Tryggvason, K. Progressive Reactive Lymphoid Connective Tissue Disease and Development of Autoantibodies in Scavenger Receptor A5 e De fi cient Mice. *Am. J. Pathol.* **182,** 1681–1695 (2013).

263. Huang, J. *et al.* Genetic and epigenetic silencing of SCARA5 may contribute to human hepatocellular carcinoma by activating FAK signaling. *J. Clin. Invest.* **120,** 223–241 (2010).

264. Khamas, A. *et al.* Screening for Epigenetically Masked Genes in Colorectal Cancer Using 5-Aza-2 ' - deoxycytidine , Microarray and Gene Expression Profile. *Cancer Genomics Proteomics* **76,** 67–75 (2012).

265. Xu, Z. *et al.* Rock2 promotes RCC proliferation by decreasing SCARA5 expression through b -catenin / TCF4 signaling. *Biochem. Biophys. Res. Commun.* **480,** 586–593 (2016).

266. Liu, J. *et al.* Suppression of SCARA5 by Snail1 is essential for EMT-associated cell migration of A549 cells. *Oncogenesis* 1–10 (2013). doi:10.1038/oncsis.2013.37

267. Wen, X., Wang, N. A. N., Zhang, F. & Dong, C. Overexpression of SCARA5 inhibits tumor proliferation and invasion in osteosarcoma via suppression of the FAK signaling pathway. *Mol. Med. Rep.* **13,** 2885–2891 (2016).

268. Yan, N. *et al.* Therapeutic upregulation of Class A scavenger receptor member 5 inhibits tumor growth and metastasis. *Cancer Sci* **103,** 1631–1639 (2012).

269. You, K., Su, F., Liu, L., Lv, X. & Zhang, J. SCARA5 plays a critical role in the progression and metastasis of breast cancer by inactivating the ERK1 / 2 , STAT3 , and AKT signaling pathways. *Mol. Cell. Biochem.* (2017). doi:10.1007/s11010-017-3055-4

270. Zhao, J. *et al.* Knockdown of SCARA5 inhibits PDGF-BB-induced vascular smooth muscle cell proliferation and migration through suppression of the PDGF signaling pathway. *Mol. Med. Rep.* **13,** 4455–4460 (2016).

271. Finazzi, D. & Arosio, P. Biology of ferritin in mammals : an update on iron storage , oxidative damage and neurodegeneration. *Arch Toxicol* **88,** 1787–1802 (2014).

272. Arosio, P. & Levi, S. Cytosolic and mitochondrial ferritins in the regulation of cellular iron homeostasis and oxidative damage. *Biochim. Biophys. Acta* **1800,** 783–792 (2010).

273. Wang, Z. *et al.* Functional ferritin nanoparticles for biomedical applications. *Front. Chem. Sci. Eng.* 1–14 (2017). doi:10.1007/s11705-017-1620-8

274. Wang, W., Ann, M., Coffman, L. G., Torti, F. M. & Torti, S. V. Serum ferritin : Past , present and future. *Biochim. Biophys. Acta* **1800,** 760–769 (2010).

275. Alkhateeb, A. A. & Connor, J. R. The significance of ferritin in cancer : Anti-oxidation , inflammation and

tumorigenesis. *Biochim. Biophys. Acta* **1836,** 245–254 (2013).

276. Alkhateeb, A. A. *et al.* Elevation in Inflammatory Serum Biomarkers Predicts Response to Trastuzumab-Containing Therapy. *PLoS One* **7,** 1–6 (2012).

277. Jézéquel, P. *et al.* Validation of tumor-associated macrophage ferritin light chain as a prognostic biomarker in node-negative breast cancer tumors : a multicentric 2004 national PHRC study. *Int. J. Cancer* **131,** 426–437 (2011).

278. Pinnix, Z. K. *et al.* Ferroportin and Iron Regulation in Breast Cancer Progression and Prognosis. *Sci. Transl. Med.* **2,** (2010).

279. Geninatti Crich, S. *et al.* Targeting ferritin receptors for the selective delivery of imaging and therapeutic agents to breast cancer cells. *Nanoscale* **7,** 6527–6533 (2015).

280. Xing, R. *et al.* Characterization and cellular uptake of platinum anticancer drugs encapsulated in apoferritin. *J. Inorg. Biochem.* **103,** 1039–1044 (2009).

281. Bellini, M. *et al.* Protein nanocages for self-triggered nuclear delivery of DNA-targeted chemotherapeutics in Cancer Cells. *J. Control. Release* **196,** 184–196 (2014).

282. Liang, M. *et al.* H-ferritin-nanocaged doxorubicin nanoparticles specifically target and kill tumors with a single-dose injection. *PNAS* **111,** 14900–14905 (2014).

283. Falvo, E. *et al.* Antibody-drug conjugates: targeting melanoma with cisplatin encapsulated in protein-cage nanoparticles. *Nanoscale* **5,** 12278–12285 (2013).

284. He, D. & Marles-Wright, J. Ferritin family proteins and their use in bionanotechnology. *N. Biotechnol.* **32,** 651–657 (2015).

285. Li, Y. & Zhang, T. Targeting cancer stem cells by curcumin and clinical applications. *Cancer Lett.* **346,** 197–205 (2014).

286. Gupta, S. C., Patchva, S. & Aggarwal, B. B. Therapeutic Roles of Curcumin : Lessons Learned from Clinical Trials. *AAPS J.* **15,** (2013).

287. Kakarala, M. *et al.* Targeting breast stem cells with the cancer preventive compounds curcumin and piperine. *Breast Cancer Res Treat* **122,** 777–785 (2010).

288. Mukherjee, S. *et al.* Curcumin inhibits breast cancer stem cell migration by amplifying the E-cadherin / β - catenin negative feedback loop. *Stem Cell Res. Ther.* **5,** 1–19 (2014).

289. Charpentier, M. S. *et al.* Curcumin Targets Breast Cancer Stem – like Cells with Microtentacles That Persist in Mammospheres and Promote Reattachment. *Cancer Res* **74,** 1250–1261 (2014).

290. Zhou, Q. *et al.* Curcumin Improves the Tumoricidal Effect of Mitomycin C by Suppressing ABCG2 Expression in Stem Cell-Like Breast Cancer. *PLoS One* **10,** 1–12 (2015).

291. Sordillo, P. P., Helson, L. & Pharma, S. Curcumin and Cancer Stem Cells : Curcumin Has Asymmetrical Effects on Cancer and Normal Stem Cells. *Anticancer Res.* **614,** 599–614 (2015).

292. Cheng, A. *et al.* Phase I clinical trial of curcumin, a chemopreventive agent, in patients with high-risk or pre-malignant lesions. *Anticancer Res.* 2895–2900 (2001).

293. Esatbeyoglu, T. *et al.* Curcumin — From Molecule to Biological Function. *Angew. Rev.* 5308–5332 (2012). doi:10.1002/anie.201107724

294. Anand, P., Kunnumakkara, A. B., Newman, R. A. & Aggarwal, B. B. Bioavailability of Curcumin : Problems and Promises. *Mol. Pharm.* **4,** 807–818 (2007).

295. Chen, L., Bai, G., Yang, S., Yang, R. & Zhao, G. Encapsulation of curcumin in recombinant human H-chain ferritin increases its water-solubility and stability. *FRIN* **62,** 1147–1153 (2014).

296. Cai, W. & Chen, X. Nanoplatforms for Targeted Molecular Imaging in Living Subjects. *Nanomedicine* 1840–1854 (2007). doi:10.1002/smll.200700351

297. Pathak, A. P. *et al.* Molecular and Functional Imaging of Cancer : Advances in MRI and MRS. *Methods Enzymol.* **386,** (2004).

298. Geraldes, C. F. G. C. & Laurent, S. Classification and basic properties of contrast agents for magnetic resonance imaging. *Contrast Media Mol. Imaging* **4,** 1–23 (2009).

299. Koboldt, D. C. *et al.* Comprehensive molecular portraits of human breast tumours. *Nature* **490,** 61–70 (2012).

300. Bianchini, G., Balko, J. M., Mayer, I. A., Sanders, M. E. & Gianni, L. Triple-negative breast cancer: challenges and opportunities of a heterogeneous disease. *Nat. Rev. Clin. Oncol.* **13,** 674–690 (2016).

301. Schmadeka, R., Harmon, B. E. & Singh, M. Triple-negative breast carcinoma: Current and emerging concepts. *Am. J. Clin. Pathol.* **141,** 462–477 (2014).

302. Dent, R. *et al.* Triple-negative breast cancer: Clinical features and patterns of recurrence. *Clin. Cancer Res.* **13,** 4429–4434 (2007).

303. Liedtke, C. *et al.* Response to neoadjuvant therapy and long-term survival in patients with triple-negative breast cancer. *J. Clin. Oncol.* **26,** 1275–1281 (2008).

304. Carey, L. A. *et al.* The triple negative paradox: Primary tumor chemosensitivity of breast cancer subtypes. *Clin. Cancer Res.* **13,** 2329–2334 (2007).

305. Foulkes, W. D., Smith, I. E. & Reis-Filho, J. S. Triple-Negative Breast Cancer. *N. Engl. J. Med.* **363,** 1938–1948 (2010).

306. Lehmann, B. D. B. *et al.* Identification of human triple-negative breast cancer subtypes and preclinical models for selection of targeted therapies. *J. Clin. Invest.* **121,** 2750–2767 (2011).

307. Lehmann, B. D. & Pietenpol, J. A. Identification and use of biomarkers in treatment strategies for triple-negative breast cancer subtypes. *J. Pathol.* **232,** 142–150 (2014).

308. Masuda, H. *et al.* Differential response to neoadjuvant chemotherapy among 7 triple-negative breast cancer molecular subtypes. *Clin. Cancer Res.* **19,** 5533–5540 (2013).

309. Neve, R. M. *et al.* A collection of breast cancer cell lines for the study of functionally distinct cancer subtypes. *Cancer Cell* **10,** 515–527 (2006).

310. Guler, G. *et al.* Stem cell-related markers in primary breast cancers and associated metastatic lesions Gulnur. *Mod Pathol* **25,** 949–955 (2012).

311. Honeth, G. *et al.* The CD44+/CD24-phenotype is enriched in basal-like breast tumors. *Breast Cancer Res.* **10,** R53 (2008).

312. Park, S. Y. *et al.* Heterogeneity for stem cell-related markers according to tumor subtype and histologic stage in breast cancer. *Clin. Cancer Res.* **16,** 876–887 (2010).

313. Park, S. Y. *et al.* Distinct patterns of promoter CpG island methylation of breast cancer subtypes are associated with stem cell phenotypes. *Mod. Pathol.* **25,** 185–196 (2012).

ACKNOWLEDGEMENTS

Firstly, I would like to express my sincere gratitude to my tutor Prof. Federica Cavallo for the continuous support of my Ph.D study and related research, for giving me the opportunity of joining her research group and growing as a scientist, for always keeping in consideration my opinions, and for believing in me. Her guidance helped me in all the time of research and writing of this thesis. She was an excellent mentor for my Ph.D study.

Besides my tutor, I would like to thank the reviewers of my thesis: Prof. Pier Giuseppe Pelicci and Prof. Pier Luigi Lollini for their insightful comments and questions that incented me to improve the accuracy of my work.

My sincere thanks also go to Dr. Laura Conti and Dr. Stefania Lanzardo, who made me really feel part of their team and provided continuous guidance throughout these 4 years of doctoral research. I thank them for involving me in their research project and sharing it with me. I thank them for having treated me on a par, despite their much greater expertise in the field. I thank them for their patience, because I know my temperament has been unbearable sometimes. Without their priceless and unconditional support, it would not have been possible for me to conduct this research and to be where I am now.

I thank my lab mates Dr. Elisabetta Bolli, Dr. Valeria Rolih, Dr. Irene Merighi, Dr. Federica Riccardo and Dr. Giuseppina Barutello for their help in my research, but also for making the laboratory environment less formal and more pleasant.

I thank Dr. Maddalena Arigoni for the very stimulating discussions and for being beside me in the odyssey that finally brought to our co-first-authored paper.

I thank Prof. Elena Quaglino for supervising my work during the aforementioned odyssey.

I thank Prof. Raffaele Calogero for his support in the bioinformatics analysis.

I thank Prof. Simonetta Geninatti-Crich and the other staff members from the Molecular Imaging Center for their precious collaboration in the Ferritin paper.

I thank Prof. Natalia Savelyeva and Prof. Christian Ottensmeier for hosting me in the Cancer Sciences Unit, University of Southampton, and for giving me the opportunity to work with their team and for providing me a very different perspective on what doing research means.

I thank all those who contributed in any way to my research, which are many people.

I also thank all those that made me understand what I want to become, and what I do not want to become.

Last but not least, I want to thank those who supported me in the life outside the laboratory. These 4 years of doctoral studies have been a bumpy ride, with many ups and downs, and I have often felt myself wandering in the dark forest of Dante's Inferno. If it were not for them, I would have already given up long time ago. These are my family, my mother, father and sister, which gave me the strength to get up when I was down. These are my friends, with whom I have the opportunity to really be myself. This is my girlfriend, which is the most wonderful girl in the world and which makes me a better person.

Thanks to all who took part in this path.

ATTACHMENT A

Papers included in the thesis

PAPER I

Cancer Research

Immunotargeting of Antigen xCT Attenuates Stem-like Cell Behavior and Metastatic Progression in Breast Cancer

Stefania Lanzardo[1], Laura Conti[1], Ronald Rooke[2], Roberto Ruiu[1], Nathalie Accart[3], Elisabetta Bolli[1], Maddalena Arigoni[1], Marco Macagno[1], Giuseppina Barrera[4], Stefania Pizzimenti[4], Luigi Aurisicchio[5], Raffaele Adolfo Calogero[1], and Federica Cavallo[1]

Abstract

Resistance to therapy and lack of curative treatments for metastatic breast cancer suggest that current therapies may be missing the subpopulation of chemoresistant and radioresistant cancer stem cells (CSC). The ultimate success of any treatment may well rest on CSC eradication, but specific anti-CSC therapies are still limited. A comparison of the transcriptional profiles of murine Her2$^+$ breast tumor TUBO cells and their derived CSC-enriched tumorspheres has identified xCT, the functional subunit of the cystine/glutamate antiporter system x_c^-, as a surface protein that is upregulated specifically in tumorspheres. We validated this finding by cytofluorimetric analysis and immunofluorescence in TUBO-derived tumorspheres and in a panel of mouse and human triple negative breast cancer cell-derived tumorspheres. We further show that downregulation of xCT impaired tumorsphere generation and altered CSC intracellular redox balance *in vitro*, suggesting that xCT plays a functional role in CSC biology. DNA vaccination based immunotargeting of xCT in mice challenged with syngeneic tumorsphere-derived cells delayed established subcutaneous tumor growth and strongly impaired pulmonary metastasis formation by generating anti-xCT antibodies able to alter CSC self-renewal and redox balance. Finally, anti-xCT vaccination increased CSC chemosensitivity to doxorubicin *in vivo*, indicating that xCT immunotargeting may be an effective adjuvant to chemotherapy. *Cancer Res; 76(1); 62–72. ©2015 AACR.*

Introduction

Despite recent advances in breast cancer management resulting in a decrease in overall mortality (1), minimal residual disease and local and distant posttreatment recurrences are still major obstacles to complete remission. According to the cancer stem cell (CSC) model, these residual elements are caused by a stem-like subpopulation of tumor cells that are endowed with self-renewal and multilineage differentiation capabilities, chemo- and radio-resistance and the ability to give metastases (2). The therapeutic implication of the CSC model is that a tumor needs to be deprived of its CSC population to be completely eradicated. Novel anticancer strategies must therefore be developed to face this new challenge.

Active immunotherapy, i.e., vaccination, is an attractive approach to target CSC. Preclinical studies have shown that CSC are immunogenic and a more effective antigen source for inducing protective antitumor immunity in mice than unselected tumor cells (3). Several clinical trials in which CSC lysate or mRNA are used to pulse or transfect autologous dendritic cells (DC), that are then injected back into the patients, are currently underway in various tumor settings (4). However, this technique presents the difficulty of setting up standardized functional DC production procedures (5). A promising alternative can be found in powerful and versatile DNA-based vaccines, which combines lower manufacturing costs and more standardized production processes while also inducing strong immunologic responses against tumor antigens. Nevertheless, one must identify a suitable target to develop a DNA-based vaccine; as no consensus on the expression of specific vaccination targets by CSC currently exists, preclinical screening by high-throughput technologies can be of use in uncovering antigens for CSC-targeted genetic vaccines.

We have compared the transcription profile of the murine Her2$^+$ breast cancer TUBO cell line (6) with that of its CSC-enriched tumorspheres in order to identify antigens expressed by mammary CSC. Among the genes upregulated in tumorspheres and associated with poor prognosis in several data sets of human mammary cancer, we focused on xCT. It is the light chain of the antiporter system x_c^-, which imports the aminoacid cystine into cells in exchange with glutamate. Cystine is the rate-limiting substrate for the synthesis of the antioxidant glutathione (GSH), which is known to be involved in the detoxification of reactive oxygen species (ROS; ref. 7). xCT is highly expressed by a variety of malignant tumors (7–12) and plays an important role in

[1]Department of Molecular Biotechnology and Health Sciences, Molecular Biotechnology Center, University of Turin, Turin, Italy. [2]Elsalys Biotech, Illkirch Graffenstaden, France. [3]Novartis Institute for Medical Research, Basel, Switzerland. [4]Department of Clinical and Biological Sciences, University of Turin, Turin, Italy. [5]Takis, Via di Castel Romano, Rome, Italy.

Note: Supplementary data for this article are available at Cancer Research Online (http://cancerres.aacrjournals.org/).

S. Lanzardo and L. Conti contributed equally to this article.

Corresponding Author: Federica Cavallo, University of Torin, Molecular Biotechnology Center, Via Nizza 52, 10126 Turin, Italy. Phone: 39-011-6706457; Fax: 39-011-2365417; E-mail: federica.cavallo@unito.it

doi: 10.1158/0008-5472.CAN-15-1208

cancer growth, progression, metastatic dissemination (13–15), and drug resistance (16). Moreover, its membrane expression is stabilized via direct interaction with a CD44 variant (CD44v; ref. 13), although targeting xCT has been found to deplete undifferentiated CD44v-expressing cancer cells in a xenografted model of head and neck squamous cell carcinoma, sensitizing the tumor to other therapies (17).

We herein report that xCT upregulation is a general feature of breast CSC and that plays a functional role in CSC biology and intracellular redox balance. We demonstrate that anti-xCT DNA vaccination slows established subcutaneous tumor growth, efficiently impairs lung metastasis formation, and increases CSC chemosensitivity, thus making it a novel therapeutic approach for breast cancer treatment.

Materials and Methods

Cell and tumorsphere cultures

MDA-MB-231, HCC-1806, and 4T1 cells were purchased from the ATCC (LGC Standards) and cultured as in ref. 18. NIH/3T3 cells were cultured as in ref. 19. Cells were passaged in our laboratory for fewer than 6 months after their resuscitation. TUBO cells and tumorspheres were generated as in ref. 18. Human cell lines were tested utilizing short tandem repeat profiling.

FACS analysis

Cells and tumorspheres were stained with AlexaFluor647-anti-Sca-1, PE-anti-CD44, and PE/Cy7-anti-CD24 (Biolegend), and with goat anti-xCT (Santa Cruz Biotechnology) antibodies followed by rabbit FITC-anti-goat Ig (Dako), or with Aldefluor kit (StemCell Technologies), as in ref. 18. To quantify anti-xCT antibody titers, tumorsphere-derived and NIH/3T3 cells were incubated with sera of vaccinated mice and subsequently with rabbit FITC-anti-mouse Ig (Dako). Cells were stained with 2′,7′-dihydrochlorofluorescein diacetate (DHCF-DA, Sigma-Aldrich) as in ref. 20. All samples were analyzed on a CyAnADP Flow Cytometer, using the Summit 4.3 software (Beckman Coulter).

Fluorescent microscopy

Tumor microarrays (TMA; Biochain # T8234700-2, lot # B406087, and Biochain # T6235086-5, lot # B112136) of normal or tumor human tissues were blocked in 3% H_2O_2 (Sigma-Aldrich), followed by 1% BSA, and then incubated with anti-xCT or isotype-matched control antibodies (Abcam). The signal was amplified as in ref. 21 and sections were fixed in 1% formaldehyde (Sigma-Aldrich), counterstained with DAPI (Sigma-Aldrich), and mounted in Mowiol (Calbiochem). Images were acquired using a confocal microscope LSM700 and Zen software 7.0.0.285 (Zeiss). Slides were scanned on a slide scanner (Hamamatsu Nanozoomer 2.0RS) using the Calopix software. xCT^+ cell percentage was defined by quantifying blue (nuclei) and red (xCT) surface areas and calculated as the ratio of xCT expression (i.e., xCT stained surface/xCT + nuclei surface).

Tumorspheres were cytospinned to glass slides, fixed in 4% formaldehyde and then incubated with rabbit anti-OCT4 (Abcam), rat PE-anti-Sca-1 (Santa Cruz Biotechnology), mouse APC/eFluor780-anti-Thy1.1 (eBioscience), or the matched isotype control antibodies. Cytospinned tumorspheres or NIH/3T3 cultured on glass coverslips were stained with IgG purified from immunized mice sera and then with rabbit AlexaFluor488-anti-mouse or goat Texas red-anti-rabbit secondary antibodies (Life Technologies). Images were acquired on the ApoTome system and AxioVision Release4.8 software (Zeiss).

In vitro cytotoxicity

Twenty-four hours after TUBO cells and tumorspheres seeding in 96-well plates, scalar doses of doxorubicin or sulfasalazine (SASP; Sigma-Aldrich) were added and incubated at 37°C for 72 hours. Cytotoxicity was evaluated with MTT using the Cell Proliferation Kit I (Roche Diagnostics).

RNA interference

xCT downregulation in tumorspheres was performed using a pool of specific siRNAs, or scrambled siRNAs (Invitrogen Corp.), as in ref. 18.

SASP effects on tumorsphere formation

Dissociated tumorspheres were cultured with scalar doses of SASP or its diluent DMSO (Sigma-Aldrich), and the total number of tumorspheres/well was counted 5 days later.

Measurement of ROS and GSH

ROS amount was analyzed as 2′,7′-dichlorofluorescin (DCF) formation in cells incubated with 5 μmol/L DHCF-DA for 20 minutes at 37°C using the Luminescence Spectrometer LS 55 (Perkin–Elmer), quantified using a DCF standard curve, and expressed as pmol DCF formed/min/mg protein (22). GSH content was assessed by determining nonprotein sulphydryl content, as in ref. 23, and calculated using a GSH standard curve. Results are expressed as μg GSH/mg of cellular proteins.

Plasmids

The cDNA sequence for mouse xCT (NM_011990.2), in the pDream2.1 plasmid (GenScript), was cloned in a pVAX1 (Invitrogen) plasmid (pVAX1-xCT), sequenced (BMR Genomics), and produced with EndoFree Plasmid Giga Kits (Qiagen Inc.).

Immune sera effect on tumorsphere formation

Serum IgG from vaccinated mice were purified using the Melon Gel Purification Kit (Thermo Scientific) and incubated with tumorsphere-derived cells. After 5 days, spheres were counted and analyzed for CSC markers expression and ROS production by FACS.

In vivo treatments

Female 6- to 8-week-old wild-type (Charles River Laboratories) and Ig μ-chain gene knocked out (BALB-μIgKO; ref. 24) BALB/c mice were maintained at the Molecular Biotechnology Center, University of Torin, and treated in accordance with the University Ethical Committee and European guidelines under Directive 2010/63. Vaccination, performed either before or after tumor challenge, consisted of two intramuscular electroporations at 2 weeks interval, of pVAX1 or pVAX1-xCT plasmids as previously described (25).

Primary s.c. tumors were induced by injecting 1×10^4 TUBO or 4T1 tumorsphere-derived cells. Some tumors were explanted and tumorspheres generated as in ref. 26. Lung metastases were induced either by injecting i.v. 5×10^4 TUBO tumorsphere-derived cells or by injecting s.c. 1×10^4 4T1 tumorsphere-derived cells. In the latter case, lungs were removed when s.c. tumors reached 10 mm mean diameter. Micrometastases were counted on a Nikon SMZ1000 stereomicroscope (Mager Scientific).

Doxorubicin treatment consisted of the i.v. administration of a total dose of 10 mg/Kg either in a single injection or in two administration at a week interval.

Statistical analysis

Differences in latency, sphere formation, protein expression, GSH, and ROS levels and metastasis number were evaluated using a Student *t* test. Data are shown as the mean ± SEM unless otherwise stated. Values of $P < 0.05$ were considered statistically significant.

Results

xCT is upregulated in breast CSC

To identify the transcripts associated with mouse and human mammary CSC, we compared the transcription profile of $Her2^+$ murine TUBO cells, which had been cultured as an epithelial monolayer, with the profiles of the first three *in vitro* passages of their derived tumorspheres (P1, P2, and P3) using MouseWG-6 v2.0 Illumina beadchips (GSE21451; Supplementary Fig. S1A). This analysis uncovered a cluster of transcripts whose expression rose, as well as three clusters whose expression decreased from TUBO through P1 to P3 cells (Supplementary Fig. S1B).

We devised a ranking procedure according to the clinical outcome of tumors expressing the transcripts that we found increased in tumorspheres (27), using data from six public human breast cancer data sets (see Supplementary Methods). One of the genes with the best clinical outcome score was *xCT* (*Slc7a11*, Supplementary Fig. S1C; ref. 7), whose expression increased progressively from TUBO to P3 tumorspheres, as confirmed by FACS (Fig. 1A) and qPCR (Supplementary Fig. S2) analyses. Interestingly, most P3-derived cells that express the stem cell marker Sca-1 (26) are also xCT^+ (Fig. 1B). The immunofluorescence analysis revealed widespread xCT positivity in tumorspheres that are essentially composed of CSC, as confirmed by Sca-1, OCT4, and Thy1.1 marker expression patterns (Fig. 1C). xCT upregulation is a feature of breast CSC and is not due to tumorsphere culture conditions, because it was also observed on the small $CD44^{high}/CD24^{low}$ CSC population present in TUBO cells (Fig. 1D). Moreover, xCT upregulation is not restricted to TUBO-derived CSC as it was also observed in tumorspheres derived from mouse (4T1) and human (HCC-1806 and MDA-MB-231) triple negative breast cancer (TNBC) cell lines (Fig. 1E), suggesting that xCT may be a hallmark of breast cancer CSC.

xCT expression in the TMA of normal and neoplastic samples was evaluated to address its distribution in human cancers. xCT expression was low in normal mammary glands (Fig. 1F, left) as it was in the other normal tissues tested (Supplementary Fig. S3A). By contrast, xCT was expressed at high levels in many neoplastic tissues (Supplementary Fig. S3B), including hyperplastic mammary lesions and invasive ductal breast carcinomas (IDC; Fig. 1F, middle and right) displaying a pattern in which it is confined to neoplastic cells. In particular, we found xCT expression in 62% of $Her2^+$, 57% of estrogen/progesterone $receptor^+$ $Her2^-$ (ER/PR^+Her2^-), and 35% of TNBC samples (Fig. 1G), suggesting that xCT may well be a commonly upregulated target in breast cancers.

xCT downregulation impairs tumorsphere generation and alters intracellular redox balance

A MTT test was performed on TUBO cells and tumorspheres that had either been treated or not with scalar doses of xCT inhibitor SASP (28). Although SASP did not decrease TUBO cell viability, except for the highest dose (100 μmol/L; IC_{50}, 126.1 ± 25.7 μmol/L; Fig. 2A), tumorsphere viability was inhibited in a dose-dependent manner (IC_{50}, 51.6 ± 3.5 μmol/L; Fig. 2B), suggesting that CSC are sensitive to xCT inhibition. Similarly, xCT silencing through a pool of specific siRNAs impaired tumorspheres but not TUBO cell viability (Fig. 2A and B). Moreover, SASP treatment and xCT silencing impaired tumorsphere generation (Fig. 2C and D). FACS analyses performed 24 hours after siRNA transfection showed that the reduction in xCT^+ cells (Fig. 2E and F) is accompanied by a reduction in CSC, i.e., $Sca1^+$ and $CD44^{high}/CD24^{low}$ cells (Fig. 2F). On the contrary, xCT overexpression increases colony generating ability, as confirmed by the higher number of colonies generated in soft agar by NIH/3T3 and HEK-293 cells transfected with xCT when compared with the corresponding cells transfected with empty plasmids (Supplementary Fig. S4). Taken together, these data suggest that xCT plays an important role in CSC maintenance and sphere generation.

As xCT is an important determinant of redox balance (13), we evaluated GSH and ROS levels in TUBO cells and tumorspheres. GSH amount was significantly greater in tumorspheres than in TUBO cells (Fig. 2G), whereas ROS levels were lower (Fig. 2H). xCT downregulation caused a significant decrease in GSH and an increase in ROS levels (Fig. 2G and H) as compared with controls, suggesting that CSC have a higher ROS defense capability than epithelial tumor cells.

Anti-xCT vaccination induces antibodies that inhibit CSC

BALB/c mice were vaccinated with either pVAX1-xCT or pVAX1 to evaluate whether xCT is a potential target for cancer immunotherapy. No T-cell response was observed against the $H\text{-}2K^d$ dominant mouse xCT peptide (Supplementary Fig. S5A and S5B). Tumorsphere-derived cells were stained with the sera of vaccinated mice to evaluate their humoral response, and specific antibody binding was analyzed by FACS. pVAX1-xCT vaccination induced the production of CSC-binding antibodies, which were not detectable in empty pVAX1-vaccinated mouse sera (Fig. 3A–C). These results were confirmed by the ability of purified IgG, from pVAX1-xCT-vaccinated mouse sera, to stain tumorspheres (Fig. 3D). These antibodies are specific for xCT, as no binding was observed in NIH/3T3 cells negative for xCT expression (Fig. 3E–H).

Of note, TUBO cells incubated with IgG purified from pVAX1-xCT-vaccinated mice displayed reduced sphere-generation ability (Fig. 3I), a lower percentage of stem cell marker positive cells (Fig. 3J), but increased ROS content as compared with control IgG (Fig. 3K).

These results suggest that anti-xCT vaccination induces antibodies targeting xCT, thus affecting self-renewal and ROS production in CSC.

Anti-xCT vaccination slows *in vivo* breast tumor growth

TUBO-derived tumorspheres were s.c. implanted into BALB/c mice that were vaccinated when tumors reached 2 or 4 mm mean diameter to evaluate whether xCT immune-targeting hinders breast cancer growth (Fig. 4A–D). Tumors grew progressively in the pVAX1 group of 2 mm vaccinated mice (Fig. 4A), although tumors regressed in 23.8% of pVAX1-xCT-vaccinated mice (Fig. 4B). Tumor growth kinetics were slower in the latter group than in the pVAX1 group, as proven

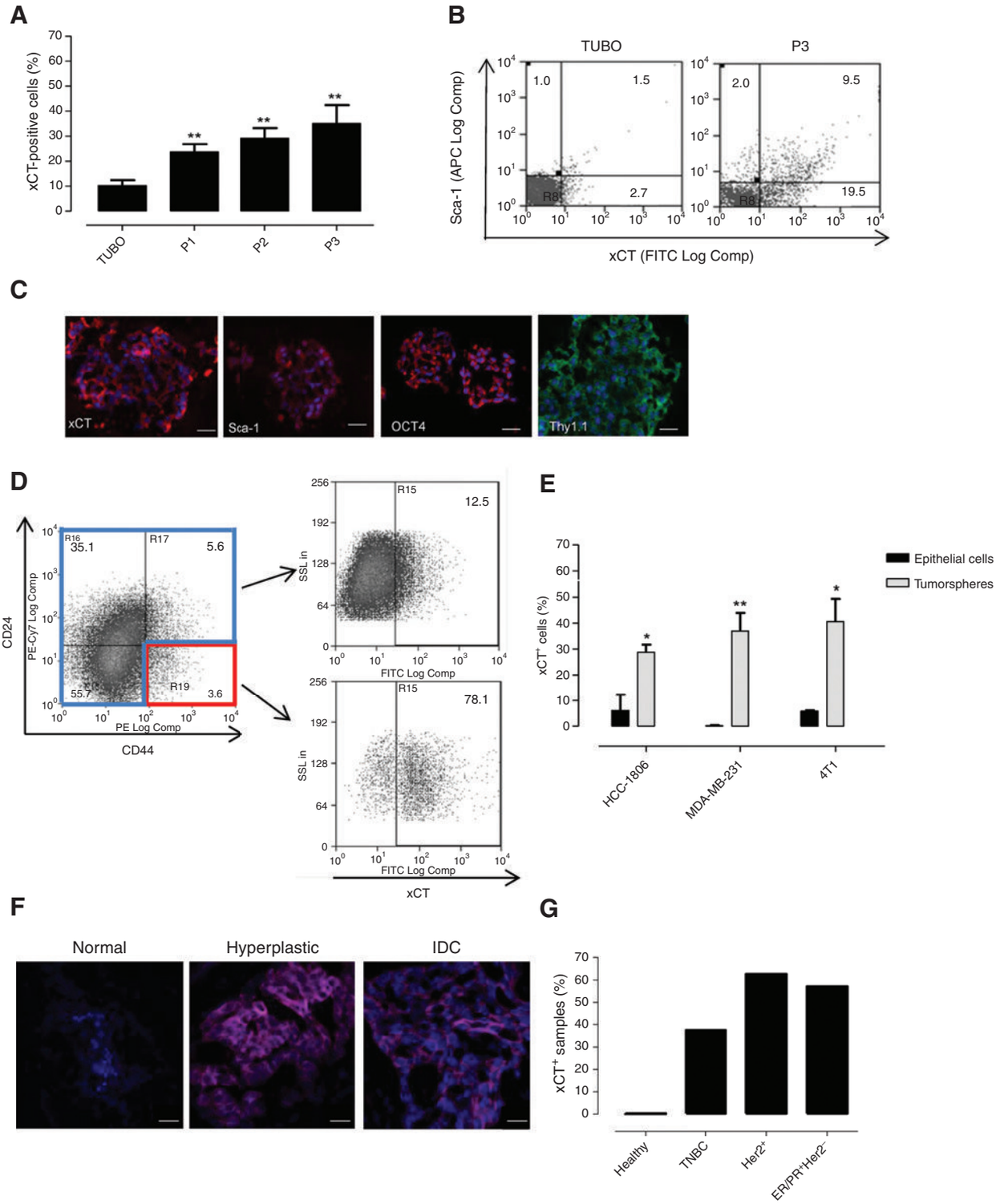

Figure 1.
xCT expression in breast CSC and tumors. A, FACS analysis of xCT expression in TUBO cells and P1 to P3 tumorsphere passages over six independent experiments. B, representative density plots of xCT and Sca-1 expression on TUBO and tumorspheres. Numbers show the percentage of cells in each quadrant. C, representative immunofluorescence staining of xCT, Sca-1, OCT4, and Thy1.1 on tumorspheres. DAPI stains the nucleus. Scale bar, 20 μm. D, representative density plots of xCT expression in TUBO cells stained with CD44 and CD24. E, FACS analysis of xCT expression in HCC-1806, MDA-MB-231, and 4T1 cells and their derived tumorspheres over three independent experiments. *, $P < 0.05$; **, $P < 0.01$; ***, $P < 0.001$, Student t test. F, immunofluorescence of xCT expression (red) in normal breast, hyperplastic, and IDC breast carcinoma. Scale bar, 20 μm. G, percentage of xCT^+ samples in normal mammary gland and in TNBC, $Her2^+$, or ER/PR^+Her2^- breast cancer subtypes.

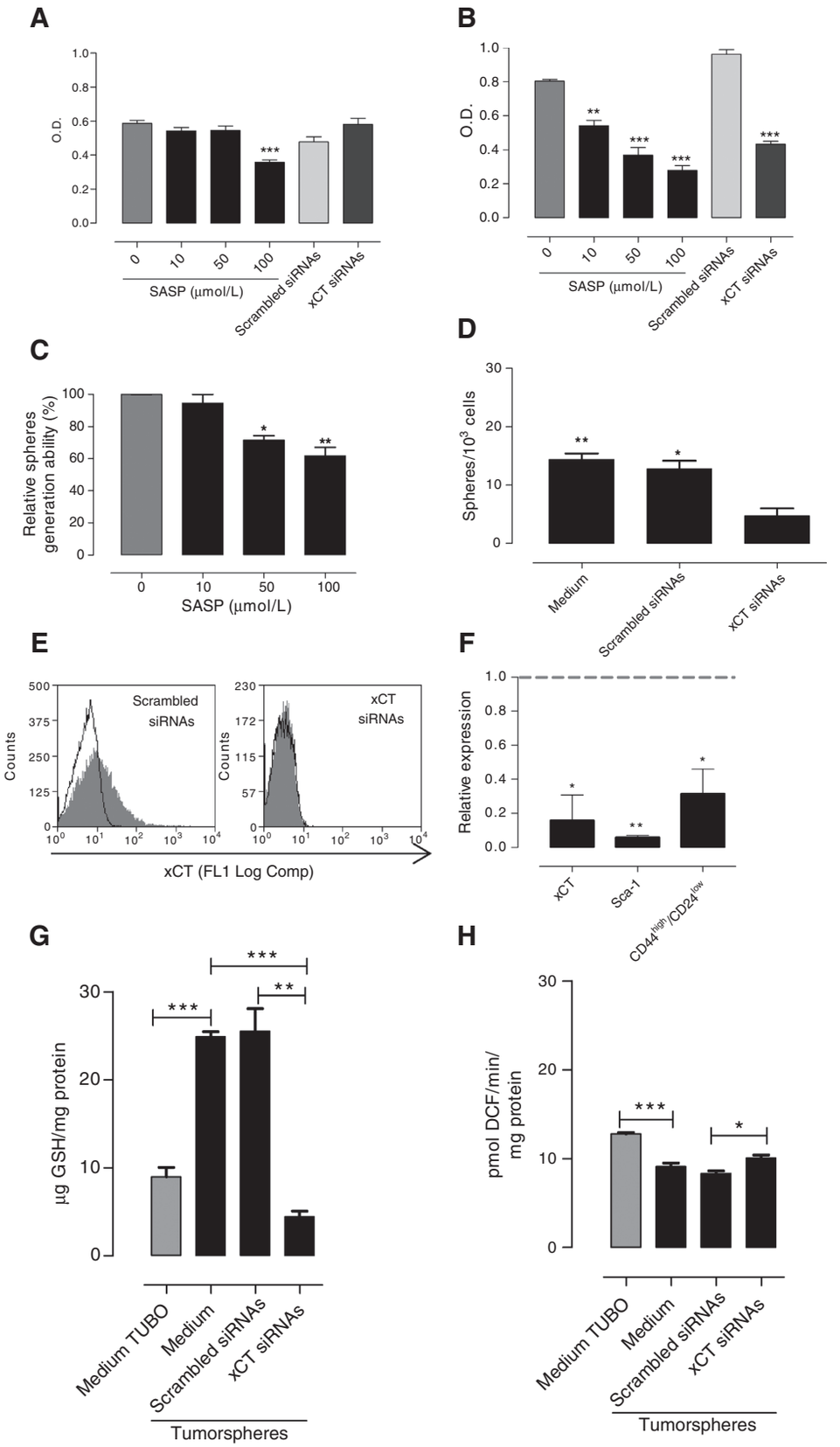

Figure 2.
xCT regulates CSC self-renewal and the intracellular redox balance. A and B, MTT assay of the cytotoxic effect exerted by scalar doses of SASP or by anti-xCT siRNAs on TUBO (A) and tumorspheres (B). C, sphere generation ability relative to untreated cells of tumorspheres incubated with SASP. D, sphere generation ability of tumorspheres incubated with siRNAs to xCT, scrambled siRNAs, or not at all shown as tumorsphere number/10^3 plated cells. E and F, FACS analysis of xCT and CSC marker expression in spheres 24 hours after transfection with siRNAs to xCT or scrambled siRNAs. E, gray histograms show xCT expression; open histograms show the background of negative control IgG stained cells from one representative experiment. F, relative expression (%) of xCT^+, $Sca\text{-}1^+$, and $CD44^{high}/CD24^{low}$ cells in tumorsphere-derived cells transfected with siRNAs to xCT (black bars) compared with cells transfected with scrambled siRNAs (dashed line). G and H, GSH (G) and ROS (H) levels in TUBO cells and their derived tumorspheres after either seeding in normal conditions, transfection with siRNAs to xCT, or scrambled siRNAs over three independent experiments. *, $P<0.05$; **, $P<0.01$; ***, $P<0.001$, Student t test.

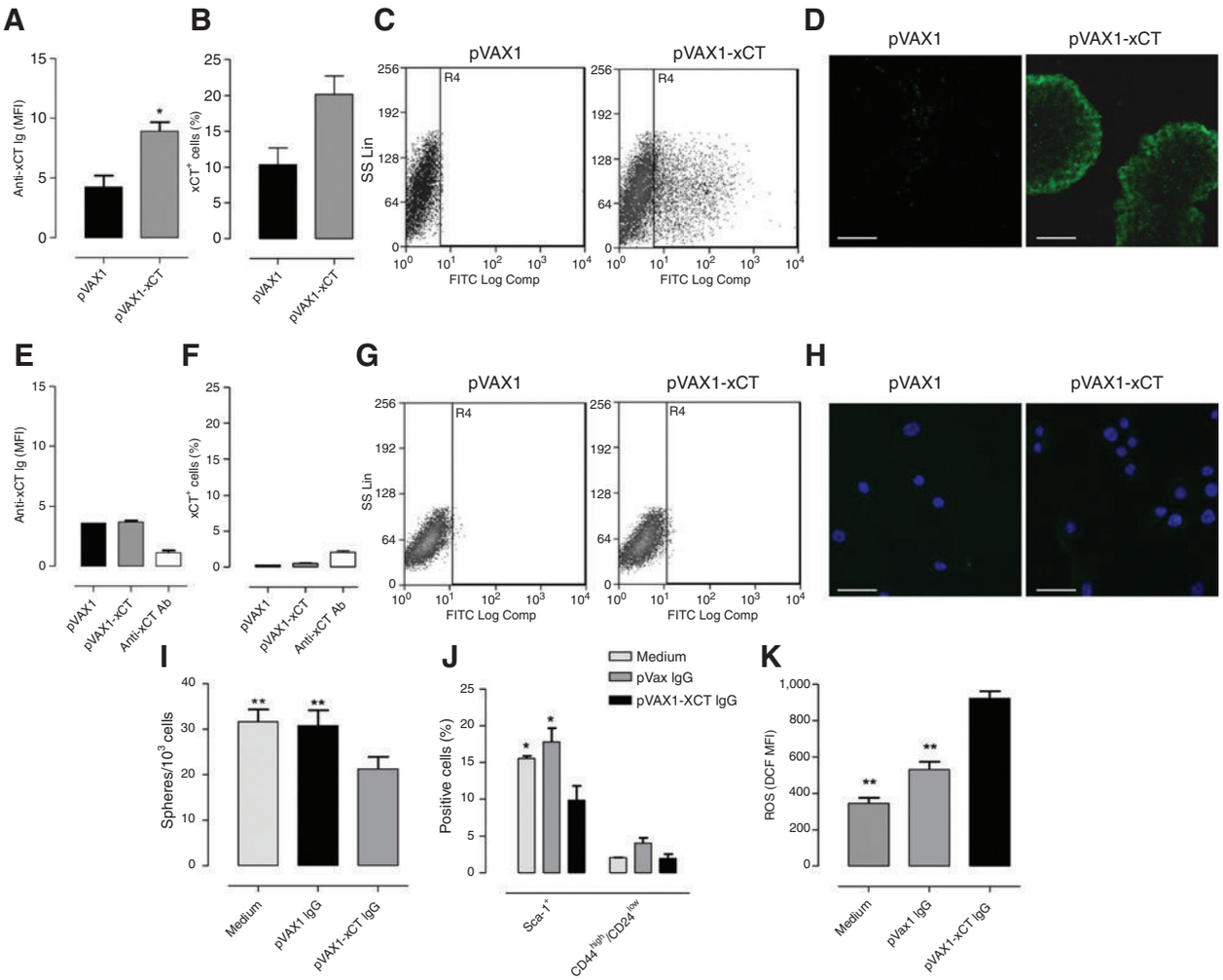

Figure 3.
Vaccine-induced antibodies target CSC and affect their self-renewal and ROS flux. A–G, TUBO-derived tumorsphere (A–C) or NIH/3T3 cell staining by antibodies present in the sera of BALB/c mice vaccinated with pVAX1 or pVAX1-xCT (E–G), analyzed by FACS. Results are reported as the mean fluorescence intensity (MFI; A and E) from 7 mice per group, the percentage of positive cells (B and F), and two representative dot plots (C and G). D and H, representative images of TUBO-tumorspheres (D) or NIH/3T3 cells stained with IgG purified from sera of mice vaccinated with pVAX1 or pVAX1-xCT (H). Scale bar, 20 μm. I, sphere generating ability of tumorspheres incubated for 5 days with IgG purified from the sera of mice vaccinated with pVAX1, pVAX1-xCT, or not at all. Graph shows tumorsphere number/10^3 plated cells. FACS analysis of CSC marker expression (J) or ROS production (K) in tumorspheres incubated for 5 days with IgG purified from the sera of vaccinated mice or not at all, reported as percentage of positive cells (D) or DCF MFI (E) from four independent experiments. *, $P < 0.05$; **, $P < 0.01$, Student t test.

by the significantly shorter time required for tumors to reach 4 or 6 mm mean diameter (20.7 ± 2.7 and 30.7 ± 3.6 days in pVAX1-xCT-vaccinated mice vs. 12.9 ± 2 and 20.8 ± 2.5 days in control mice). Anti-xCT vaccination also induced tumor regression in 16% of mice that were treated when their tumors measured 4 mm mean diameter (Fig. 4D), while all tumors in the pVAX1 group reached 10 mm mean diameter in less than 60 days (Fig. 4C). The efficacy of anti-xCT vaccination was then evaluated against 2 or 4 mm mean diameter tumors obtained when 4T1 tumorsphere-derived cells were injected s.c. (Fig. 4E–H). In 2 mm tumor-vaccinated mice, tumors grew rapidly in pVAX1 group (Fig. 4E), while tumor growth kinetics were generally slower and the time required for the tumors to reach 4, 6, 8, or 10 mm mean diameter was significantly longer in the pVAX1-xCT-vaccinated group (10.4 ± 1.3; 15.6 ± 1.6; 20.4 ± 1.3; 23.4 ± 1.2 days in pVAX1-xCT-vaccinated mice vs. 4.9 ± 0.5; 10 ± 1.1; 14.6 ± 1.0; 17.4 ± 0.8 days in control mice). Similarly, the 4 mm tumor-vaccinated group displayed slower tumor growth in pVAX1-xCT-vaccinated mice (Fig. 4E and H), and the time required for the tumors to reach 6, 8, or 10 mm mean diameter was significantly longer (9.2 ± 0.9; 13.1 ± 0.9; 17.0 ± 0.5 days in pVAX1-xCT-vaccinated mice vs. 5.2 ± 0.9; 8.8 ± 1.0; 13.0 ± 1.6 days in control mice), indicating that xCT immunotherapy may be beneficial in various breast cancer subtypes.

Tumor remission in vaccinated mice might be due to a reduction of CSC frequency as a consequence of the treatment, as suggested by the decrease in the percentage of Aldefluor$^+$ cells

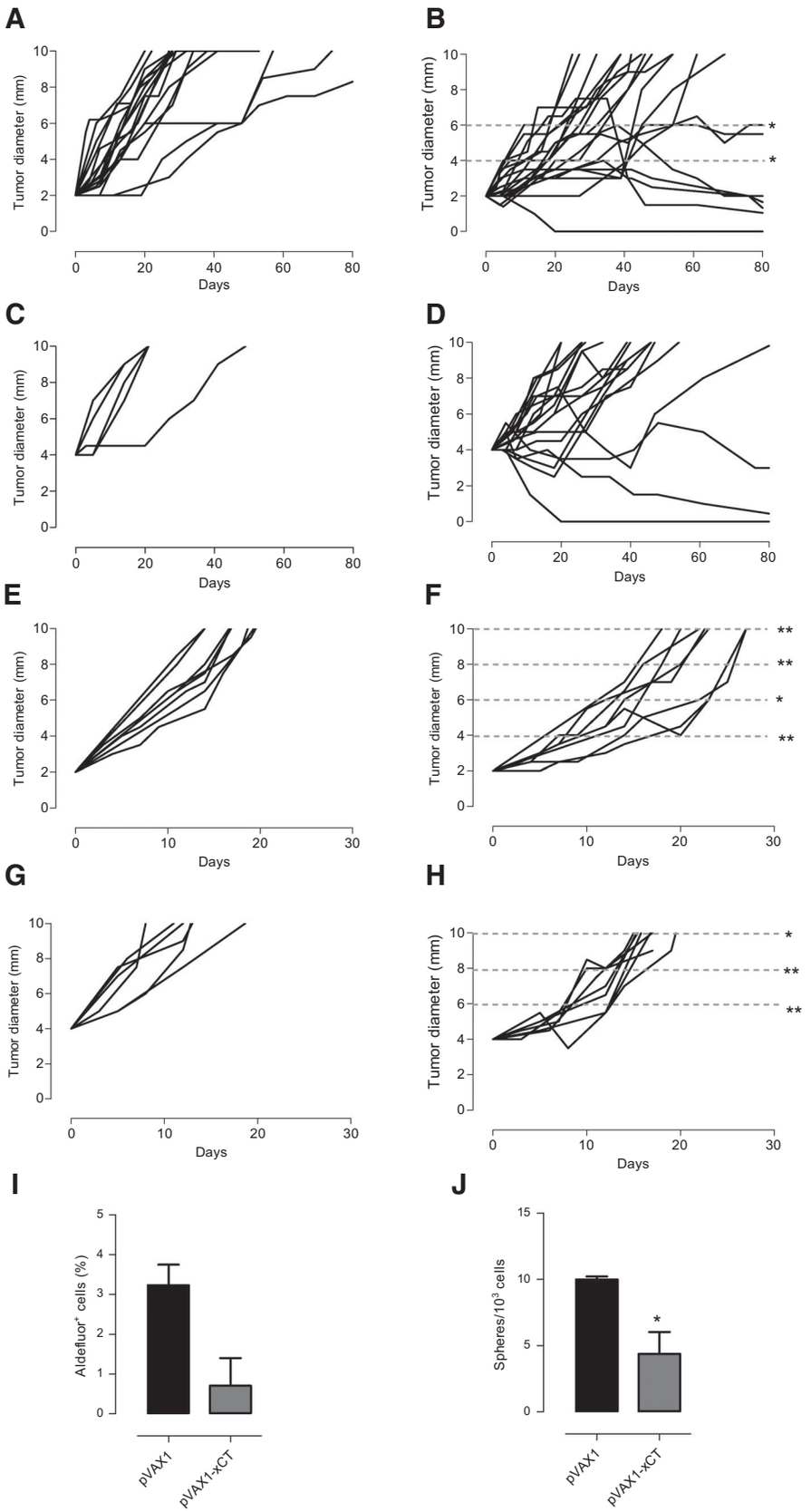

Figure 4.
Anti-xCT vaccination delays CSC-induced tumor growth *in vivo*. BALB/c mice were s.c. challenged with tumorspheres derived from either TUBO (A–D) or 4T1 (E–H) cells and electroporated with pVAX1 (A, C, E, and G) or pVAX1-xCT (B, D, F, and H) plasmids when their tumor reached 2 (A, B, E, and F) or 4 mm (C, D, G, and H) mean diameter. Each black line depicts the growth of a single tumor. Data were cumulated from three independent and concordant experiments. Statistically significant differences in mean time required for pVAX1-xCT group and pVAX1 group tumors to reach 4, 6, 8, or 10 mm mean diameter are indicated by dashed gray lines. I and J, analysis of the percentage of Aldefluor$^+$ cells in tumors explanted from vaccinated mice challenged s.c. with TUBO-derived tumorspheres (I) and the number of tumorspheres generated *in vitro* by cells from the same tumors (J). *, $P < 0.05$; **, $P < 0.01$, Student *t* test.

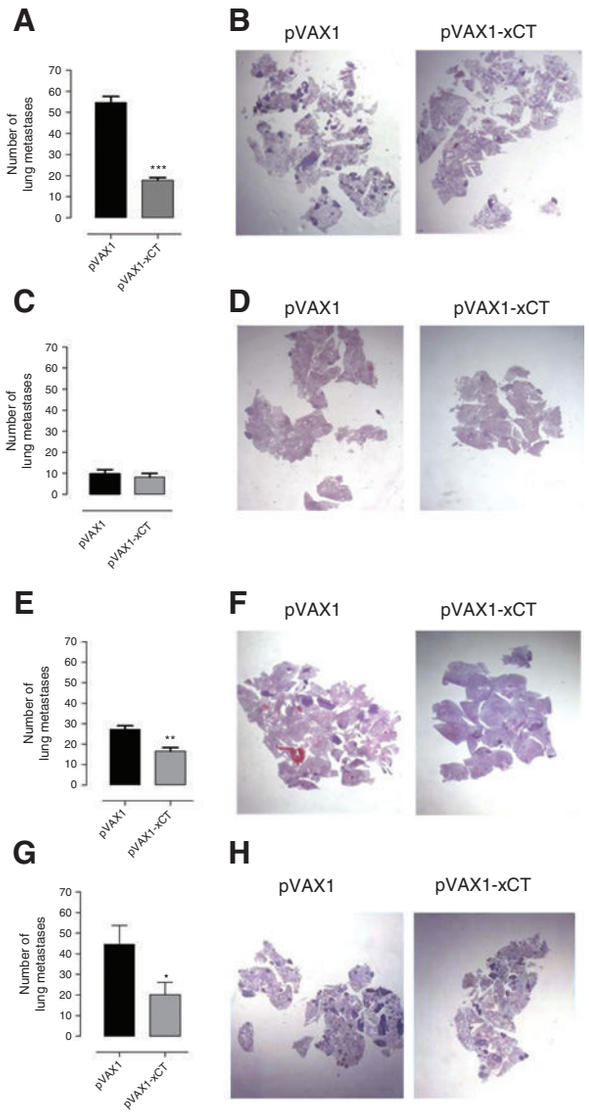

Figure 5.
Anti-xCT vaccination reduces CSC-generated lung metastasis formation. BALB/c (A, B, E, and H) and BALB-μIgKO (C and D) mice were vaccinated with either pVAX1 or pVAX1-xCT plasmids before tumorspheres injection (A, C, and E) or when mice had 2 mm mean diameter tumor (G). Number of lung metastases in mice challenged i.v. with TUBO- (A and C) or s.c. with 4T1-derived tumorspheres (E and G) and enumerated 20 days later (A and C) or when the primary tumor reached 10 mm mean diameter (E and G). B, D, F, and H, representative images of lung metastases after H&E staining. **, $P < 0.01$; ***, $P < 0.001$, Student t test.

in regressing tumors from mice vaccinated with pVAX1-xCT plasmid (Fig. 4I). Moreover, the cells composing the tumor mass had a significantly decreased tumorsphere forming ability (Fig. 4J) when compared with cells derived from tumors grown in pVAX1-vaccinated mice.

Anti-xCT vaccination prevents lung metastasis formation

BALB/c mice were vaccinated with pVAX1 or pVAX1-xCT plasmids and i.v. injected with TUBO-derived tumorspheres to evaluate the effects of anti-xCT vaccination on lung metastasis formation. Metastasis number was significantly reduced after pVAX1-xCT vaccination, as reported in Fig. 5A and B. This antimetastatic effect is dependent on the specific antibodies elicited by anti-xCT vaccination, because no effect was observed vaccinating BALB-μIgKO mice i.v. injected with TUBO-derived tumorspheres (Fig. 5C and D).

Anti-xCT vaccination was also able to reduce the number of spontaneous metastases generated from the s.c. injection of 4T1-derived tumorspheres, either when vaccination was performed before tumorsphere injection (Fig. 5E and F) or when mice already had a 2-mm mean diameter tumor (Fig. 5G and H).

Altogether, these findings suggest that anti-xCT vaccination interferes with CSC metastatic properties both in a preventive and therapeutic setting. This antimetastatic activity is due to CSC immunotargeting, because no effect was observed in xCT-vaccinated mice injected with differentiated tumor cells (Supplementary Fig. S6A and S6B) or in mice vaccinated against Her3 (29) and injected with TUBO-derived tumorspheres (Supplementary Fig. S7A–S7F). In this model Her3 is not a CSC-specific antigen, because it is equally expressed on TUBO cells and tumorspheres.

Anti-xCT vaccination enhances the effect of doxorubicin

In accordance with CSC resistance to chemotherapy (2), TUBO cells display a higher sensitivity to doxorubicin than tumorspheres (Fig. 6A and B). Because xCT is involved in maintaining the intracellular redox balance, thus counteracting the effects of ROS-generating cytotoxic drugs (13), it is likely that targeting xCT could increase CSC chemosensitivity. In order to explore this hypothesis *in vivo*, unvaccinated, pVAX1-xCT, and pVAX1-vaccinated mice were i.v. injected with TUBO-derived tumorspheres and either treated with doxorubicin or not. As shown in Fig. 6C, pVAX1-xCT determined a decrease in the number of lung metastases compared with the control and doxorubicin-treated mice and the combination of vaccination and doxorubicin significantly improved the activity of individual treatments.

Similar results were observed in mice challenged with s.c. injection of TUBO-derived tumorspheres and subjected to vaccination and chemotherapy when tumors reached 2 mm mean diameter. The tumor regressed in 25% of mice treated with doxorubicin alone (Fig. 6D) or in combination with pVAX1 plasmid (Fig. 6E), although the combination of doxorubicin and anti-xCT vaccination stopped tumor progression in 60% of mice (Fig. 6F).

All together, these data suggest that anti-xCT vaccination may well be an efficient adjuvant treatment for chemotherapy both in a preventive and in a therapeutic setting.

Discussion

A key challenge in anticancer therapy is the development of treatments able to both shrink a tumor and kill CSC, which are resistant to current chemo- and radiotherapies, and are considered the source of tumor recurrence and metastatic spread. However, the identification of ideal CSC-associated targets is a particularly tough task because CSC appear to be "moving targets" that switch between different cell states during cancer progression (30). Hence, antigens that are upregulated in CSC but also present in

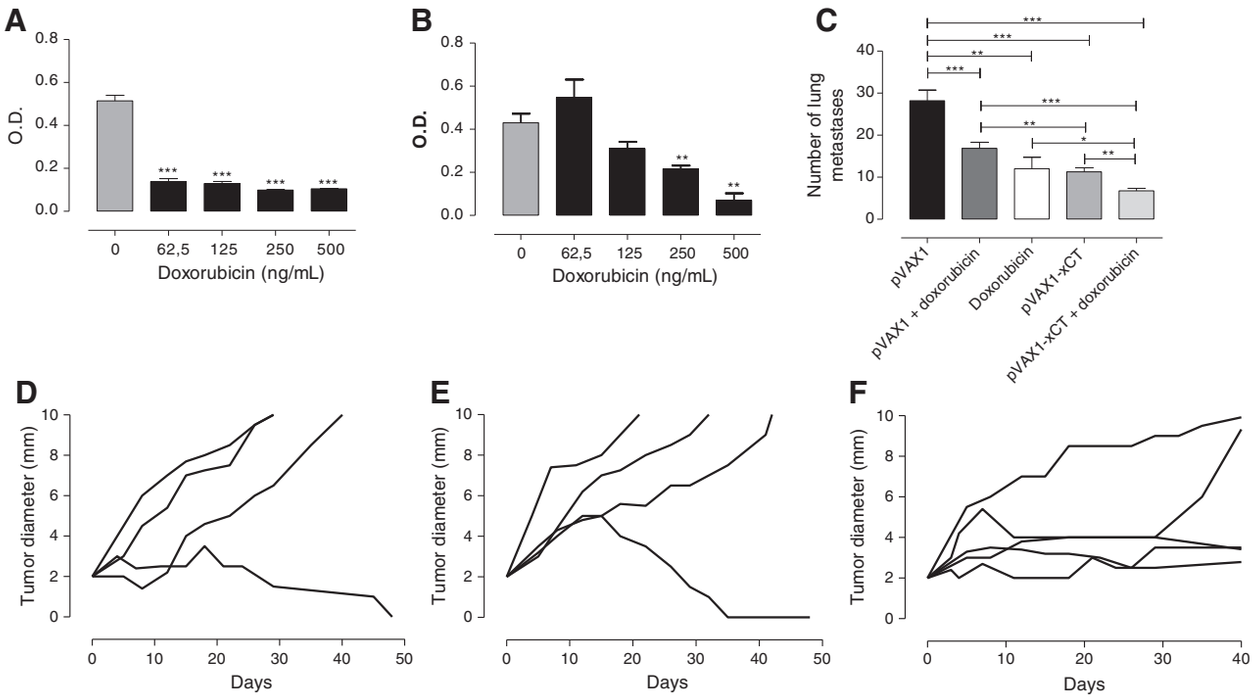

Figure 6.

Anti-xCT vaccination enhances the effect of doxorubicin *in vivo*. A and B, MTT assay of the cytotoxic effect exerted by incubation with scalar doses of doxorubicin in TUBO (A) and tumorspheres (B). C, number of lung metastases in mice challenged i.v. with TUBO-derived tumorspheres and either vaccinated or not with pVAX1 and pVAX1-xCT plasmids alone or in combination with doxorubicin administration. D–F, tumor growth curves of BALB/c mice s.c. injected with TUBO-derived tumorspheres and treated with doxorubicin in combination with pVAX1 (E) or pVAX1-xCT (F) vaccination when their tumors reached 2 mm mean diameter. Treatments were repeated the week later. Each black line depicts the growth of a single tumor. *, $P < 0.05$; **, $P < 0.01$; ***, $P < 0.001$, Student t test.

more differentiated cancer cells would appear to be outstanding candidates.

A possible candidate with these features is xCT, which we have identified as upregulated in breast Her2$^+$ and TNBC CSC. Importantly, its expression is not confined to CSC, because we were able to detect its presence on cancer cells in human hyperplastic mammary glands as well as in IDC, independently from their histologic subtype. xCT possesses all the features of an ideal target for immunotherapy against undifferentiated and more differentiated cancer cells. This speculation is strengthened by our meta-analyses, performed on human breast cancer data sets, which link high xCT expression to poor prognosis.

Moreover, xCT expression is not limited to breast cancer. Our analyses, performed on a plethora of healthy and neoplastic tissues, and data obtained elsewhere in other tumors (7, 31, 32) have identified xCT as a distinctive cancer marker and suggested that its targeting may be of benefit in the treatment of a wide range of neoplastic diseases.

Another important feature of xCT as immunotherapy target is its functional role, which becomes essential in CSC. Indeed, the impairment of sphere generation following the pharmacologic or genetic downregulation of xCT reflects the role of this protein in the regulation of CSC self-renewal, indicating that xCT is not a simple bystander of the stem-like phenotype in breast cancer, but that it also plays a role in CSC biology.

xCT function in CSC self-renewal might be mediated by the regulation of the mechanisms that govern CSC intracellular redox balance. Although further studies are needed to better define this mechanism in our model, it has been shown that intracellular ROS concentration can affect CSC viability and self-renewal (33–35). CSC upregulate the key regulator of the antioxidant response nuclear factor erythroid 2-related factor 2 (36) and many antioxidant enzymes, such as superoxide dismutase 2, GSH peroxidases, and heme oxygenase 1, which attempt to maintain intracellular ROS at levels lower than those observed in differentiated cancer cells (37). In accordance with this, a basal increase in GSH and decrease in ROS levels were observed in tumorspheres as compared with TUBO cells, which can be explained by xCT upregulation in tumorspheres and proven by the fact that xCT downregulation reverts this phenotype.

Several authors have advocated the use of xCT as a therapeutic target for pharmacologic inhibition using the administration of SASP, a FDA-approved, anti-inflammatory drug for the treatment of inflammatory bowel disease, ulcerative colitis, and Crohn's disease (38). However, SASP exerts many effects in addition to its ability to interfere with xCT function, so it cannot be considered a specific xCT inhibitor (39). Although recent preclinical models demonstrated that SASP impairs cancer growth and metastatic spread via xCT inhibition (15, 17, 40), its use in cancer patients is hampered by its low specificity, short bio-availability, and numerous side effects (41).

We have chosen DNA-based antitumor vaccination as our xCT targeting option on the basis of our consolidated expertise in the field and the considerations stated above. In fact, DNA

vaccination is a cost-effective technology able to induce a significant immune activation against tumor antigens in a specific and well tolerated way, thus reducing off-target effects (42). This paper sees the first report of xCT being targeted with a DNA-based vaccination strategy that efficiently slows mammary tumor growth and prevents lung metastasis formation. Our data show that, despite xCT being a self-antigen, DNA vaccination is able to induce an antibody-based immune response against the tumor; a lack of T-cell response against xCT may be caused by a thymic depletion of high-avidity T-cell clones, as we have previously reported for the Her2 antigen in the BALB-neuT model (43). Notably, the antitumor effects were lost in B cell–deficient mice, confirming the central role of vaccine-induced antibodies. The antitumor effects observed *in vivo* may result from the CSC self-renewal and redox balance impairment induced by anti-xCT antibodies, as indicated by our *in vitro* observations. This is particularly evident in the inhibition of lung metastasis formation, most likely because CSC self-renewal is essential for re-initiating growth at the metastatic site (44).

Interestingly, we were not able to detect any vaccine side effect as xCT expression in normal tissues is almost completely limited to the brain, which can barely be reached by circulating antibodies by virtue of the blood–brain barrier (45). However, it has been reported that xCT may also regulate immune cell functions. In fact, xCT mediates cystine uptake in macrophages and DC, which are the only source of free cysteine release, which, in turn, is essential for the antigen-driven activation of T lymphocytes (46). However, by vaccinating mice against both xCT and Her2, we observed that xCT targeting does not impair the Her2-specific T-cell response (Supplementary Fig. S5C and S5D). The safety of xCT immune targeting is further sustained by the fact that its genetic ablation in mice does not alter vital biologic functions (47).

xCT participate in cancer cells' resistance to a variety of antitumor drugs (16). Its action here is thought to be linked to its role in intracellular redox balance, as many chemotherapeutic drugs exert their function, at least in part, by increasing oxidative stress (48). It is worth noting that tumorspheres display significantly increased resistance to doxorubicin, a drug largely used in breast cancer therapy, as compared with epithelial TUBO cells. This fits with the observation that CSC are chemo-resistant (2), and may reflect the increased expression of xCT in tumorspheres. In this regard, it has been demonstrated that xCT inhibition promotes the sensitization of tumor cells to doxorubicin (49, 50). In accordance with these findings, we have observed that a combination of anti-xCT vaccination and doxorubicin strongly enhanced the antimetastatic potential of the individual treatments. This observation strengthens the translatability of this immunotherapeutic approach to clinical trials, where new experimental protocols are routinely tested in combination with standard treatments.

In conclusion, we have shown for the first time that xCT immunotargeting is effective in impairing tumor growth and metastasis formation *in vivo*. We propose a mechanism by which anti-xCT vaccination exerts its antineoplastic function across two separate, but complementary, fronts: (i) a direct effect on CSC through immune-mediated eradication and (ii) inhibition of xCT function on CSC, leading to impairment of tumorigenic and stem-like properties and their sensitizing to chemotherapy. Moreover, a possible additional anticancer mechanism may occur, by which the anti-xCT antibodies induced by vaccination may suppress the myeloid-derived suppressor cells that exploit xCT for their inhibitory activity (46). However, this hypothesis is still to be verified.

Further studies will thoroughly investigate the interactions between chemotherapy and anti-xCT vaccination and all possible side effects in order to accelerate translation to the clinic, as a safe tool to combat CSC in patients is sorely needed.

Disclosure of Potential Conflicts of Interest

No potential conflicts of interest were disclosed.

Authors' Contributions

Conception and design: S. Lanzardo, L. Conti, R. Rooke, F. Cavallo
Development of methodology: S. Lanzardo, L. Conti, R. Ruiu, N. Accart, E. Bolli, M. Arigoni, M. Macagno, F. Cavallo
Acquisition of data (provided animals, acquired and managed patients, provided facilities, etc.): S. Lanzardo, L. Conti, R. Rooke, R. Ruiu, N. Accart, E. Bolli, M. Arigoni, M. Macagno, S. Pizzimenti, L. Aurisicchio, F. Cavallo
Analysis and interpretation of data (e.g., statistical analysis, biostatistics, computational analysis): S. Lanzardo, L. Conti, R. Rooke, R. Ruiu, N. Accart, M. Arigoni, M. Macagno, R.A. Calogero, F. Cavallo
Writing, review, and/or revision of the manuscript: S. Lanzardo, L. Conti, R. Rooke, R. Ruiu, N. Accart, M. Arigoni, M. Macagno, G. Barrera, F. Cavallo
Administrative, technical, or material support (i.e., reporting or organizing data, constructing databases): F. Cavallo
Study supervision: F. Cavallo

Grant Support

This work has been supported with grants from the Italian Association for Cancer Research (IG 11675), Fondazione Ricerca Molinette Onlus, the University of Turin, and the Compagnia di San Paolo (Progetti di Ricerca Ateneo/CSP). L. Conti has been supported with a fellowships from the Fondazione Umberto Veronesi, "Pink is Good" project.

The costs of publication of this article were defrayed in part by the payment of page charges. This article must therefore be hereby marked *advertisement* in accordance with 18 U.S.C. Section 1734 solely to indicate this fact.

Received May 11, 2015; revised September 9, 2015; accepted September 30, 2015; published OnlineFirst November 13, 2015.

References

1. Siegel R, DeSantis C, Virgo K, Stein K, Mariotto A, Smith T, et al. Cancer treatment and survivorship statistics, 2012. CA Cancer J Clin 2012;62:220–41.
2. Frank NY, Schatton T, Frank MH. The therapeutic promise of the cancer stem cell concept. J Clin Invest 2010;120:41–50.
3. Ning N, Pan Q, Zheng F, Teitz-Tennenbaum S, Egenti M, Yet J, et al. Cancer stem cell vaccination confers significant antitumor immunity. Cancer Res 2012;72:1853–64.
4. Kwiatkowska-Borowczyk EP, Gabka-Buszek A, Jankowski J, Mackiewicz A. Immunotargeting of cancer stem cells. Contemp Oncol 2015;19:A52–9.
5. Aurisicchio L, Ciliberto G. Genetic cancer vaccines: current status and perspectives. Expert Opin Biol Ther 2012;12:1043–58.
6. Rovero S, Amici A, Di Carlo E, Bei R, Nanni P, Quaglino E, et al. DNA vaccination against rat her-2/Neu p185 more effectively inhibits carcinogenesis than transplantable carcinomas in transgenic BALB/c mice. J Immunol 2000;165:5133–42.
7. Lewerenz J, Hewett SJ, Huang Y, Lambros M, Gout PW, Kalivas PW, et al. The cystine/glutamate antiporter system x(c)(-) in health and disease: from molecular mechanisms to novel therapeutic opportunities. Antioxid Redox Signal 2013;18:522–55.

8. Gout PW, Buckley AR, Simms CR, Bruchovsky N. Sulfasalazine, a potent suppressor of lymphoma growth by inhibition of the x(c)- cystine transporter: a new action for an old drug. Leukemia 2001;15:1633–40.
9. Chung WJ, Lyons SA, Nelson GM, Hamza H, Gladson CL, Gillespie GY, et al. Inhibition of cystine uptake disrupts the growth of primary brain tumors. J Neurosci 2005;25:7101–10.
10. Narang VS, Pauletti GM, Gout PW, Buckley DJ, Buckley AR. Suppression of cystine uptake by sulfasalazine inhibits proliferation of human mammary carcinoma cells. Anticancer Res 2003;23:4571–9.
11. Doxsee DW, Gout PW, Kurita T, Lo M, Buckley AR, Wang Y, et al. Sulfasalazine-induced cystine starvation: potential use for prostate cancer therapy. Prostate 2007;67:162–71.
12. Jiang L, Kon N, Li T, Wang SJ, Su T, Hibshoosh H, et al. Ferroptosis as a p53-mediated activity during tumour suppression. Nature 2015;520: 57–62.
13. Ishimoto T, Nagano O, Yae T, Tamada M, Motohara T, Oshima H, et al. CD44 variant regulates redox status in cancer cells by stabilizing the xCT subunit of system xc(-) and thereby promotes tumor growth. Cancer Cell 2011;19:387–400.
14. Timmerman LA, Holton T, Yuneva M, Louie RJ, Padro M, Daemen A, et al. Glutamine sensitivity analysis identifies the xCT antiporter as a common triple-negative breast tumor therapeutic target. Cancer Cell 2013;24:450–65.
15. Chen RS, Song YM, Zhou ZY, Tong T, Li Y, Fu M, et al. Disruption of xCT inhibits cancer cell metastasis via the caveolin-1/beta-catenin pathway. Oncogene 2009;28:599–609.
16. Huang Y, Dai Z, Barbacioru C, Sadee W. Cystine-glutamate transporter SLC7A11 in cancer chemosensitivity and chemoresistance. Cancer Res 2005;65:7446–54.
17. Yoshikawa M, Tsuchihashi K, Ishimoto T, Yae T, Motohara T, Sugihara E, et al. xCT inhibition depletes CD44v-expressing tumor cells that are resistant to EGFR-targeted therapy in head and neck squamous cell carcinoma. Cancer Res 2013;73:1855–66.
18. Conti L, Lanzardo S, Arigoni M, Antonazzo R, Radaelli E, Cantarella D, et al. The noninflammatory role of high mobility group box 1/Toll-like receptor 2 axis in the self-renewal of mammary cancer stem cells. FASEB J 2013;27:4731–44.
19. Quaglino E, Mastini C, Amici A, Marchini C, Iezzi M, Lanzardo S, et al. A better immune reaction to Erbb-2 tumors is elicited in mice by DNA vaccines encoding rat/human chimeric proteins. Cancer Res 2010;70: 2604–12.
20. Donato MT, Martinez-Romero A, Jimenez N, Negro A, Herrera G, Castell JV, et al. Cytometric analysis for drug-induced steatosis in HepG2 cells. Chem Biol Interact 2009;181:417–23.
21. Fend L, Accart N, Kintz J, Cochin S, Reymann C, Le Pogam F, et al. Therapeutic effects of anti-CD115 monoclonal antibody in mouse cancer models through dual inhibition of tumor-associated macrophages and osteoclasts. PLoS One 2013;8:e73310.
22. Ravindranath V. Animal models and molecular markers for cerebral ischemia-reperfusion injury in brain. Methods Enzymol 1994;233:610–9.
23. Sedlak J, Lindsay RH. Estimation of total, protein-bound, and nonprotein sulfhydryl groups in tissue with Ellman's reagent. Anal Biochem 1968; 25:192–205.
24. Nanni P, Landuzzi L, Nicoletti G, De Giovanni C, Rossi I, Croci S, et al. Immunoprevention of mammary carcinoma in HER-2/neu transgenic mice is IFN-gamma and B cell dependent. J Immunol 2004;173: 2288–96.
25. Arigoni M, Barutello G, Lanzardo S, Longo D, Aime S, Curcio C, et al. A vaccine targeting angiomotin induces an antibody response which alters tumor vessel permeability and hampers the growth of established tumors. Angiogenesis 2012;15:305–16.
26. Grange C, Lanzardo S, Cavallo F, Camussi G, Bussolati B. Sca-1 identifies the tumor-initiating cells in mammary tumors of BALB-neuT transgenic mice. Neoplasia 2008;10:1433–43.
27. Riccardo F, Arigoni M, Buson G, Zago E, Iezzi M, Longo D, et al. Characterization of a genetic mouse model of lung cancer: a promise to identify non-small cell lung cancer therapeutic targets and biomarkers. BMC Genomics 2014;15 Suppl 3:S1.
28. Lo M, Wang YZ, Gout PW. The x(c)- cystine/glutamate antiporter: a potential target for therapy of cancer and other diseases. J Cell Physiol 2008;215:593–602.
29. Sithanandam G, Anderson LM. The ERBB3 receptor in cancer and cancer gene therapy. Cancer Gene Ther 2008;15:413–48.
30. Schwitalla S. Tumor cell plasticity: the challenge to catch a moving target. J Gastroenterol 2014;49:618–27.
31. Kinoshita H, Okabe H, Beppu T, Chikamoto A, Hayashi H, Imai K, et al. Cystine/glutamic acid transporter is a novel marker for predicting poor survival in patients with hepatocellular carcinoma. Oncol Rep 2013; 29:685–9.
32. Sugano K, Maeda K, Ohtani H, Nagahara H, Shibutani M, Hirakawa K. Expression of xCT as a predictor of disease recurrence in patients with colorectal cancer. Anticancer Res 2015;35:677–82.
33. Singer E, Judkins J, Salomonis N, Matlaf L, Soteropoulos P, McAllister S, et al. Reactive oxygen species-mediated therapeutic response and resistance in glioblastoma. Cell Death Dis 2015;6:e1601.
34. Sato A, Okada M, Shibuya K, Watanabe E, Seino S, Narita Y, et al. Pivotal role for ROS activation of p38 MAPK in the control of differentiation and tumor-initiating capacity of glioma-initiating cells. Stem Cell Res 2014; 12:119–31.
35. Shi X, Zhang Y, Zheng J, Pan J. Reactive oxygen species in cancer stem cells. Antioxid Redox Signal 2012;16:1215–28.
36. Ryoo IG, Choi BH, Kwak MK. Activation of NRF2 by p62 and proteasome reduction in sphere-forming breast carcinoma cells. Oncotarget 2015;6: 8167–84.
37. Mizuno T, Suzuki N, Makino H, Furui T, Morii E, Aoki H, et al. Cancer stem-like cells of ovarian clear cell carcinoma are enriched in the ALDH-high population associated with an accelerated scavenging system in reactive oxygen species. Gynecol Oncol 2015;137:299–305.
38. Linares V, Alonso V, Domingo JL. Oxidative stress as a mechanism underlying sulfasalazine-induced toxicity. Expert Opin Drug Saf 2011;10: 253–63.
39. de la Fuente V, Federman N, Fustinana MS, Zalcman G, Romano A. Calcineurin phosphatase as a negative regulator of fear memory in hippocampus: control on nuclear factor-kappaB signaling in consolidation and reconsolidation. Hippocampus 2014;24:1549–61.
40. Dai L, Cao Y, Chen Y, Parsons C, Qin Z. Targeting xCT, a cystine-glutamate transporter induces apoptosis and tumor regression for KSHV/HIV-associated lymphoma. J Hematol Oncol 2014;7:30.
41. Robe PA, Martin DH, Nguyen-Khac MT, Artesi M, Deprez M, Albert A, et al. Early termination of ISRCTN45828668, a phase 1/2 prospective, randomized study of sulfasalazine for the treatment of progressing malignant gliomas in adults. BMC Cancer 2009;9:372.
42. Aurisicchio L, Mancini R, Ciliberto G. Cancer vaccination by electro-gene-transfer. Expert Rev Vaccines 2013;12:1127–37.
43. Rolla S, Nicolo C, Malinarich S, Orsini M, Forni G, Cavallo F, et al. Distinct and non-overlapping T cell receptor repertoires expanded by DNA vaccination in wild-type and HER-2 transgenic BALB/c mice. J Immunol 2006;177:7626–33.
44. Liao WT, Ye YP, Deng YJ, Bian XW, Ding YQ. Metastatic cancer stem cells: from the concept to therapeutics. Am J Stem Cells 2014;3:46–62.
45. Pardridge WM. The blood-brain barrier: bottleneck in brain drug development. NeuroRx 2005;2:3–14.
46. Srivastava MK, Sinha P, Clements VK, Rodriguez P, Ostrand-Rosenberg S. Myeloid-derived suppressor cells inhibit T-cell activation by depleting cystine and cysteine. Cancer Res 2010;70:68–77.
47. McCullagh EA, Featherstone DE. Behavioral characterization of system xc- mutant mice. Behav Brain Res 2014;265:1–11.
48. Conklin KA. Chemotherapy-associated oxidative stress: impact on chemotherapeutic effectiveness. Integr Cancer Ther 2004;3:294–300.
49. Narang VS, Pauletti GM, Gout PW, Buckley DJ, Buckley AR. Sulfasalazine-induced reduction of glutathione levels in breast cancer cells: enhancement of growth-inhibitory activity of Doxorubicin. Chemotherapy 2007;53: 210–7.
50. Wang F, Yang Y. Suppression of the xCT-CD44v antiporter system sensitizes triple-negative breast cancer cells to doxorubicin. Breast Cancer Res Treat 2014;147:203–10.

Lanzardo et al., Supplementary Figure 1

A

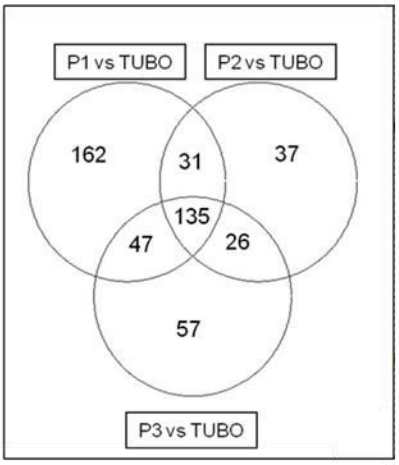

B

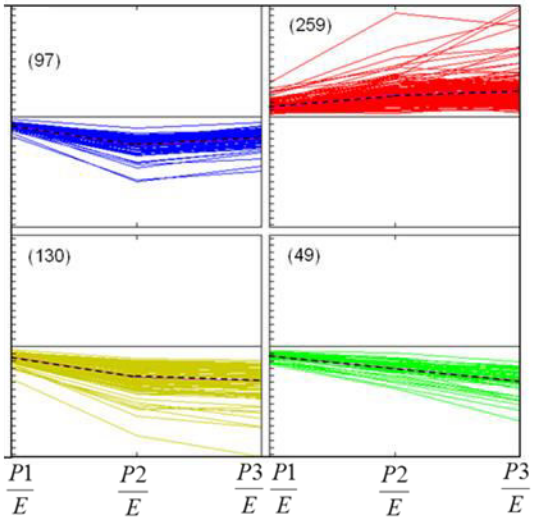

C

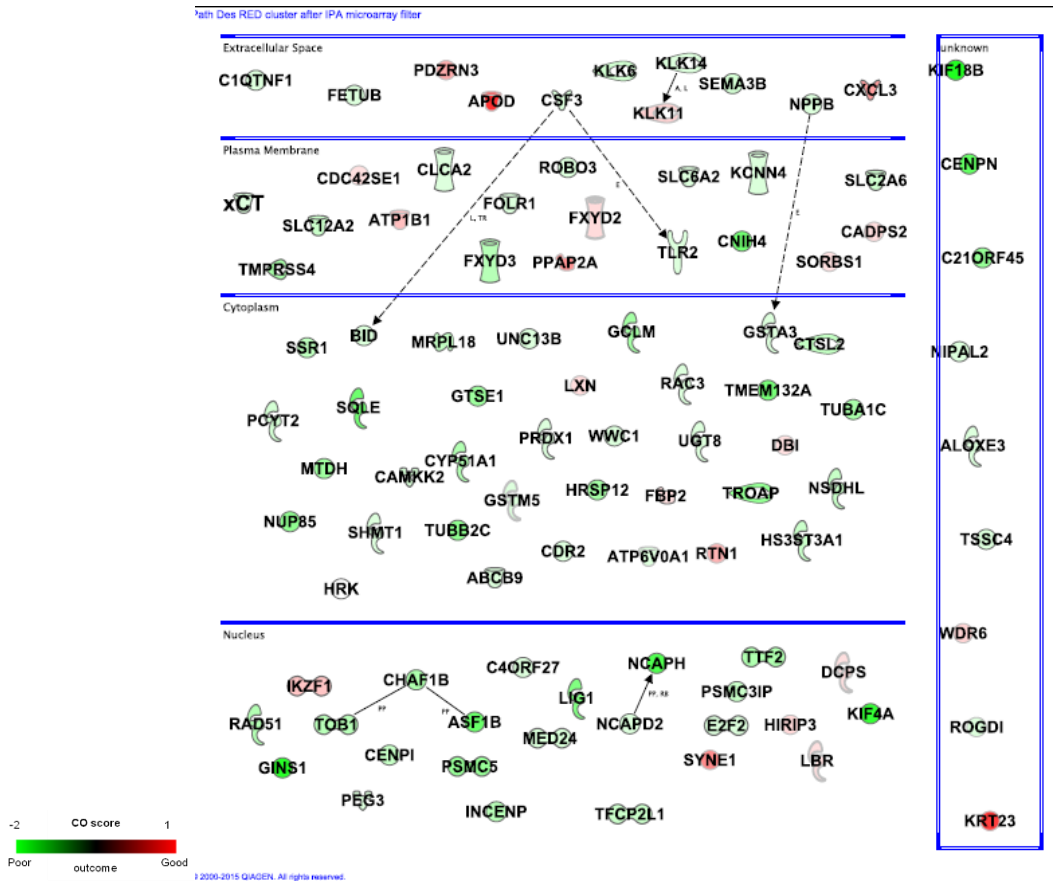

Supplementary Figure 1. Cellular localization and correlation with breast cancer patient clinical outcome (CO) of genes differentially expressed in TUBO cells and tumorspheres. A)

Venn diagrams showing 495 differentially expressed genes in TUBO cells versus P1, P2 and P3 tumorspheres. B) K-mean clustering performed on differentially expressed transcripts whose expression rose (red cluster) or decreased (blue, yellow and green clusters) in tumorspheres, as compared to TUBO cells. C) Ingenuity Knowledge base generated graph showing the cellular localization of red cluster genes colored according to the CO score of breast cancer patients expressing them. Non-colored genes were added to show connections. Arrows indicate direct (continuous) or indirect (dashed) relationships between genes.

Lanzardo et al., Supplementary Figure 2

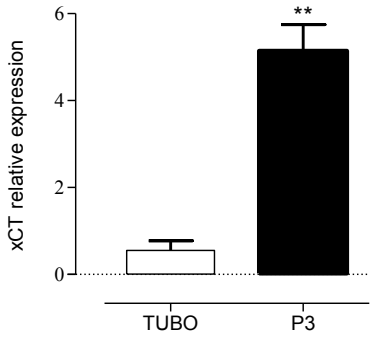

Supplementary Figure 2. xCT is overexpressed in tumorspheres. xCT expression levels in P3 tumorspheres relative to epithelial TUBO cells, analyzed with qPCR, normalized on β-actin and reported as fold changes (means ± SEM). **, $P < 0.01$, Student's *t*-test.

Lanzardo et al., Supplementary Figure 3

A

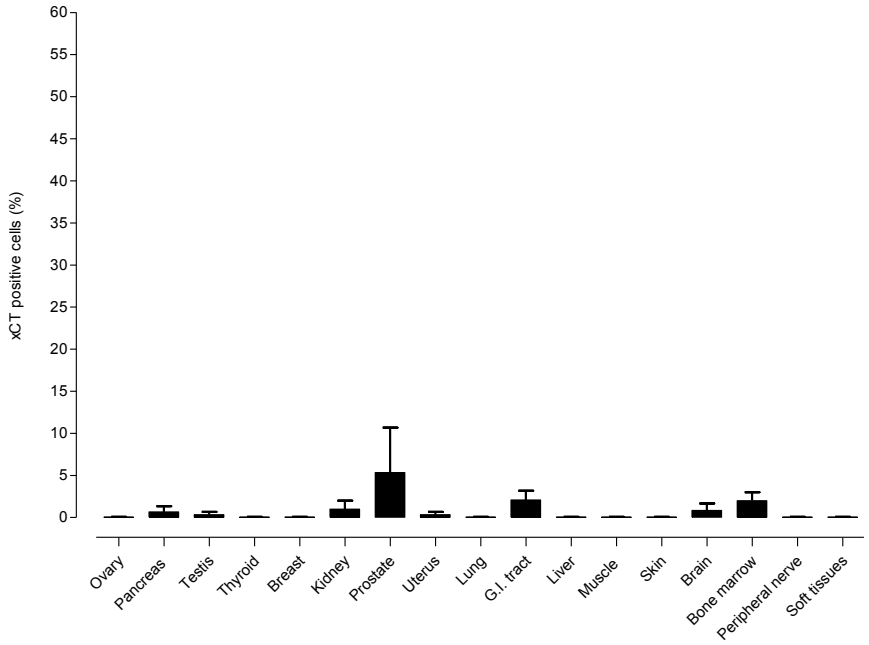

B

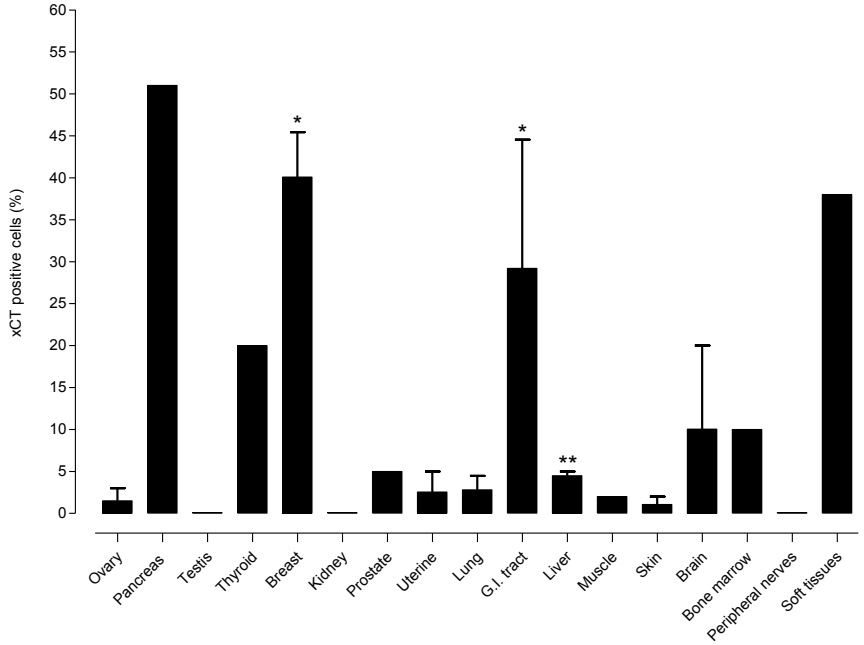

Supplementary Figure 3. Analysis of xCT expression in human tissues. Percentage of xCT^+ cells observed by immunofluorescence analysis in (A) normal and (B) neoplastic human tissues from a TMA collection. Differences between neoplastic and healthy tissues were calculated with the Student's *t*-test, * $P < 0.05$, ** $P < 0.01$.

Lanzardo et al., Supplementary Figure 4

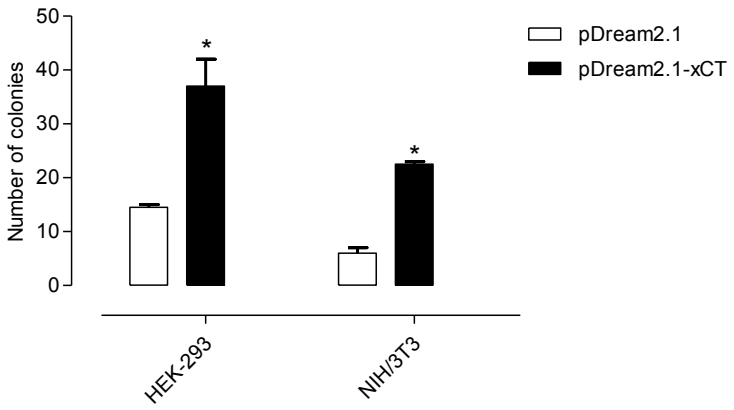

Supplementary Figure 4. xCT expression confers colony generating ability to cells. Soft agar colony formation assay of HEK-293 and NIH/3T3 cells transfected with empty pDream2.1 or pDream2.1-xCT. The graph shows the means ± SEM of the number of colonies every 10^3 cells. *, $P < 0.05$, Student's *t*-test.

Lanzardo et al., Supplementary Figure 5

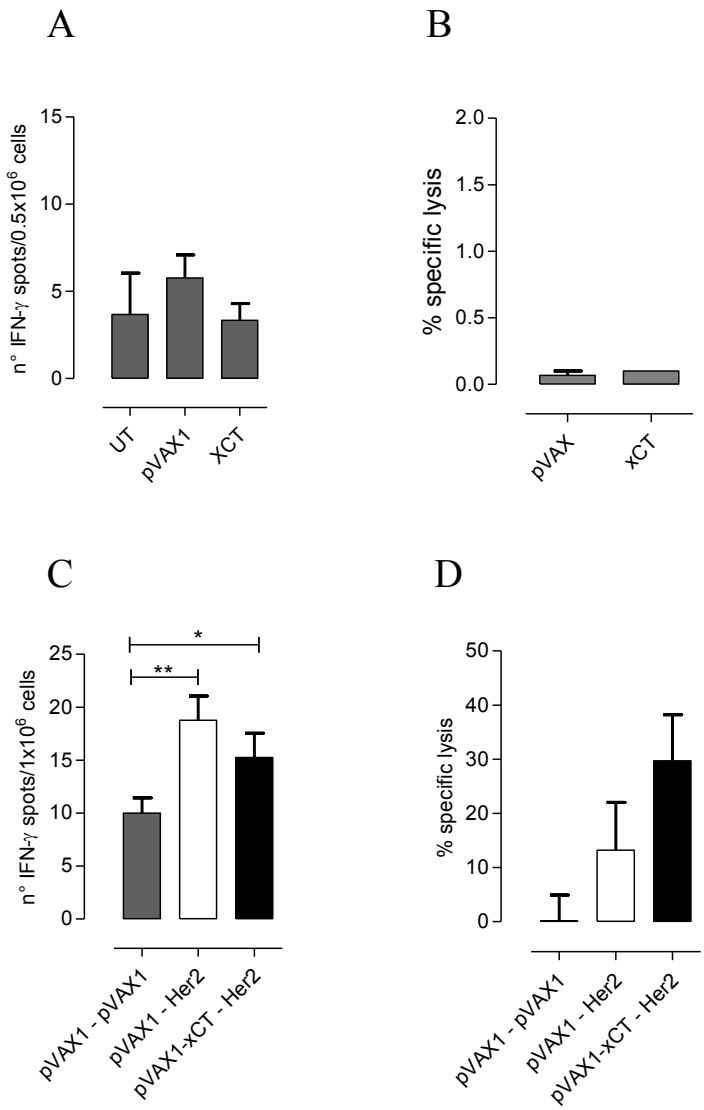

Supplementary Figure 5. Analysis of the cellular response induced by anti-xCT vaccination. (A) ELISpot analysis of IFN-γ production by splenocytes from mice vaccinated with pVAX1 or pVAX1-xCT, that had been re-stimulated for 48 h with 15 μg/mL of H-2K^d dominant mouse xCT peptide. IFN-γ secretion was evaluated as number of spots and means ± SEM of triplicates from 7 mice per group were plotted. (B) *In vivo* cytotoxicity against cells pulsed with 15 μg/mL of H-2K^d dominant xCT peptide, injected i.v. in pVAX1 or pVAX1-xCT vaccinated mice. A representative experiment of three independently performed is shown. (C, D) BALB/c mice were vaccinated twice with pVAX1 or pVAX1-xCT and then vaccinated or not once against rat Her2. (C) ELISpot analysis of IFN-γ production by splenocytes re-stimulated for 24 h with 15 μg/mL of rat Her2

dominant peptide. IFN-γ secretion was evaluated as number of spots and means ± SEM of triplicates from 3 mice per group were plotted. (D) *In vivo* cytotoxicity against cells pulsed with 15 μg/mL of Her2 dominant xCT peptide, injected i.v. in vaccinated mice. A representative experiment of three independently performed is shown. * P <0.05, ** P <0.01, Student's *t*-test.

Lanzardo et al., Supplementary Figure 6

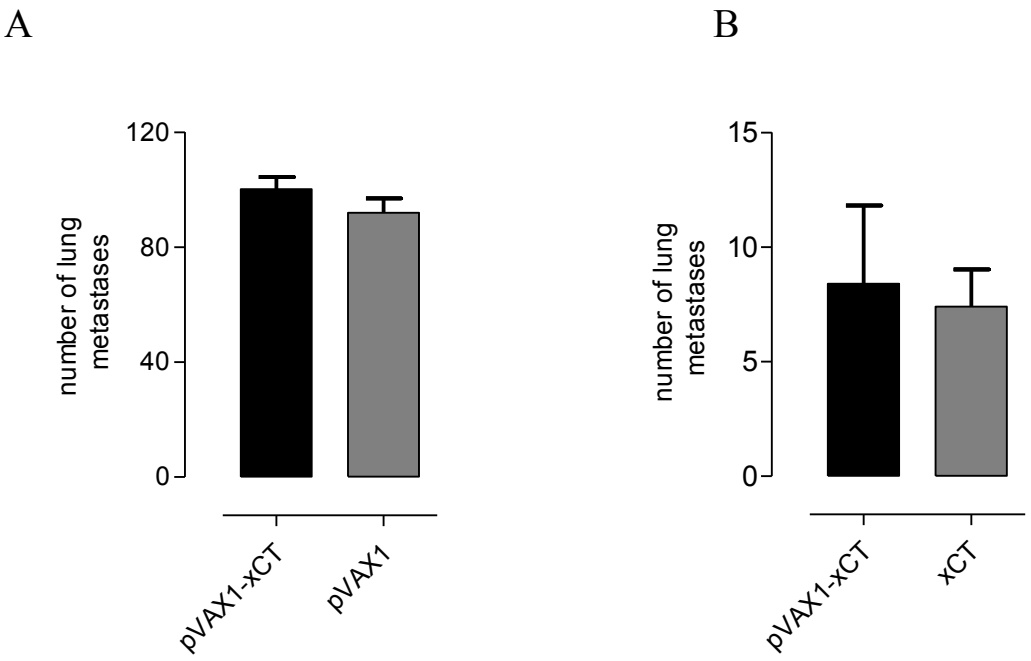

Supplementary Figure 6. Anti-xCT vaccination is not effective on TUBO or 4T1 derived lung metastases. BALB/c mice were electroporated twice with either pVAX1 or pVAX1-xCT plasmids and challenged 7 days after (A) i.v. with TUBO or (B) s.c. with 4T1 cells. The number of lung metastases was calculated after H&E staining and shown as means ± SEM 20 days after cell injection (A) or when the primary tumor reached 10 mm mean diameter (B).

Lanzardo et al., Supplementary Figure 7

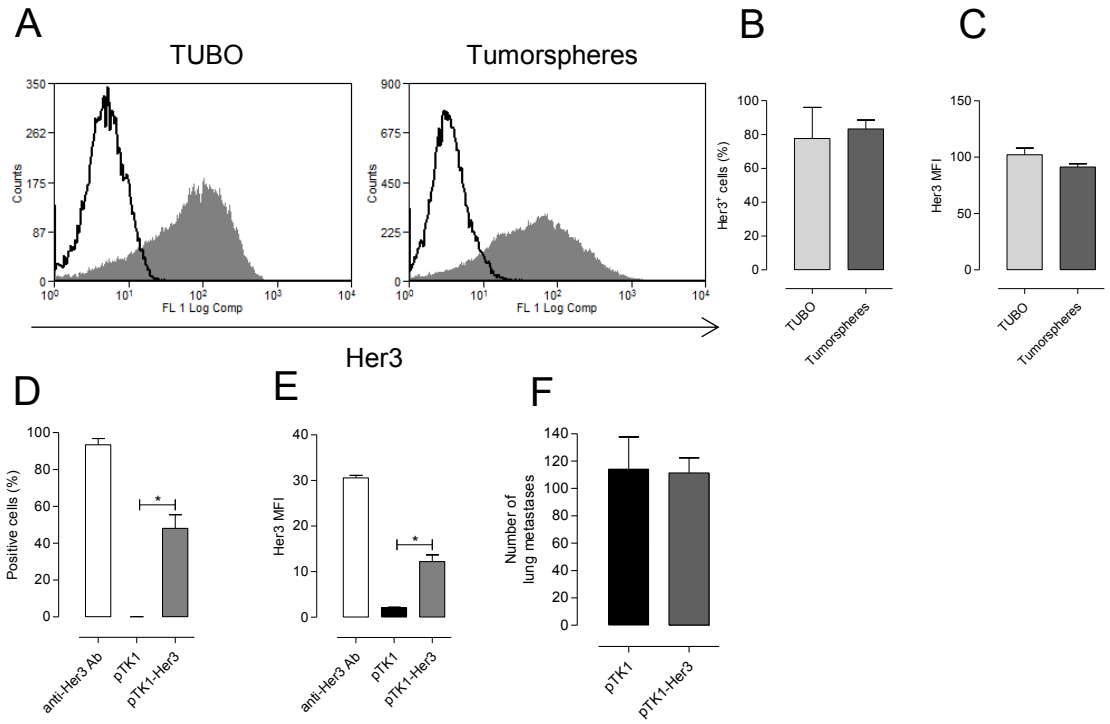

Supplementary Figure 7. Effect of immunotherapy with non CSC-specific targets. (A-C) FACS analysis of Her3 expression on TUBO and tumorspheres. (A) Gray histograms show Her3 expression, open histograms show the background of negative control stained cells from one representative experiment. Graphs show mean ± SEM of (A) $Her3^{+}$ cell percentage and (B) Her3 MFI over four independent experiments. (D-F) BALB/c mice were electroporated twice with either pTK1 or pTK1-Her3 plasmids. 7 days after, sera were collected and mice were challenged i.v. with TUBO-derived tumorspheres. (D, E) TSA cell staining by anti-Her3 commercial antibody or Her3 specific antibodies present in the sera of vaccinated mice, analyzed by FACS. Results are reported as the percentage of positive cells (D) and the MFI (E) from 4 mice per group. (F) Number of lung metastases analyzed 20 days later. * $P < 0.05$, Student's *t*-test.

Lanzardo et al., Supplementary methods

Microarray analysis

The quality and quantity of total RNA extracted as reported in (1) from tumorspheres and TUBO cells cultured in tumorsphere medium was determined using an Agilent 2100 Bioanalyzer and a Nanodrop spectrophotometer. cRNA was synthesized using an Illumina RNA amplification kit (Ambion), starting from 500 ng of total RNA according to the procedure suggested by the manufacturer. MouseWG-6 v2.0 Expression BeadChip hybridization, washing and staining were also carried out as suggested by the manufacturer. Arrays were scanned on an Illumina BeadStation 500. All array data were deposited into the GEO database (2) and the superserie GSE21486 embeds MouseWG-6 v2.0 Illumina beadchips (GSE21451). BeadChip array data quality control was carried out using Illumina BeadStudio software version 3. Average probe intensity signal was calculated using BeadStudio without background correction.

Raw data were analyzed with Bioconductor (3) using the oneChannelGUI package (4). Average probe intensities were $\log_2$ transformed and normalized using the lowess method (5). To remove the non-significant probes, i.e. the non-expressed probes, all experimental groups were filtered to inter-quartile range ≥ 0.25 for each probe (6). Differential expression between TUBO cells and P1, P2 or P3 tumorspheres was assessed using an empirical Bayes method, (7) together with a false discovery rate correction of the P value (8). Putative oncoantigens within red cluster genes were selected using the CO score ranking (9), with a procedure that was applied independently to six public human breast cancer datasets (GSE1456; GSE2034; GSE2990; GSE3494; GSE6532; GSE7390).

Mice vaccination

To analyze the effect of vaccination on T cell function, BALB/c mice (Charles River Laboratories) were vaccinated twice with either 50 μg of pVAX1 or pVAX1-xCT plasmids and 7 days after vaccinated again with pVAX1 or with a pVAX plasmid coding for a chimeric rat/human Her2 protein (RHuT) (10). In other experiments, mice were vaccinated twice with a pTK1 plasmid coding for mouse Her3 under the control of CMV promoter or with empty pTK1 plasmid and 14

days after the second vaccination were injected i.v. with $5x10^4$ TUBO tumorsphere-derived cells, and lung metastases enumerated 20 days later.

To evaluate the efficacy of anti-xCT vaccination in tumors not-enriched in CSC, BALB/c mice were electroporated twice with either pVAX1 or pVAX1-xCT plasmids and challenged 7 days after i.v. with TUBO or s.c. with 4T1 cells. 20 days after cell injection or when the primary tumor reached 10 mm mean diameter, mice were sacrificed and lung metastases enumerated.

In vivo T lymphocyte specific cytotoxicity

The percentage of specific cytotoxicity *in vivo* was evaluated by labeling spleen cells (SPCs) collected from BALB/c mice with two different concentrations of carboxyfluorescein diacetate succinimidyl ester (CFSE; Molecular Probes) as described (11). SPCs labeled with 5 μM CFSE ($CFSE^{high}$) were pulsed for 1 hour at 37°C with 15 μg/mL of H-$2K^d$ dominant mouse xCT (S Y A E L G T S I) peptide, identified using the Syfpeithi Epitope Prediction website and synthesized by InBios, or with H-$2K^d$ dominant rat Her2 TYVPANASL peptide (12). The control SPCs were left without peptide and labeled with 0.5 μM CFSE ($CFSE^{low}$ cells). $CFSE^{high}$ and $CFSE^{low}$ SPCs were then mixed in equal proportion and injected i.v. into BALB/c mice, which had been vaccinated twice with either pVAX1 or pVAX1-xCT plasmids, two weeks after the second vaccination. Two days after cell injection, mice were killed and SPCs analyzed by FACS. Specific cytolytic activity was calculated as follows: 100 (% CFSE low cells - % CFSE high cells) / % CFSE low cells (13).

IFN-γ enzyme-linked immunospot assay (ELISPOT)

Two weeks after vaccination, $1x10^6$ SPCs were added to the wells of 96-well HTS IP plates (Millipore) that had been pre-coated with 5 μg/ml of rat anti-mouse IFN-γ antibody (clone R4-6A2, BD Biosciences). SPCs were stimulated with 15 μg/ml of H-$2K^d$ dominant mouse xCT peptide for 48 hours, or with 15 μg/mL of rat Her2 peptide for 24 hours, then IFN-γ spots were enumerated as previously described (12).

qRT-PCR (qPCR) for xCT detection.

Total RNA was isolated from cells and tumorspheres as described in Materials and Methods. For xCT mRNA detection, 1 μg of DNase-treated RNA (DNA-free™ kit, Ambion) was retrotranscribed with RETROscript™ reagents (Ambion) and qPCRs were carried out using gene-specific primers (QuantiTect Primer Assay, Qiagen), SYBR green (Applied Biosystems) and 7900HT RT-PCR System (Applied Biosystems). Quantitative normalization was performed on the expression of β-actin. The relative expression levels between samples were calculated using the comparative ΔCt method (13). Results were calculated as fold changes (mean ± SEM) relative to TUBO cells. Two-tailed Student's *t*-test was used for comparisons.

Soft agar colony formation assay

NIH/3T3 mouse fibroblasts and HEK-293 human embryonic kidney cells were transfected with empty pDream2.1 plasmid or with pDream2.1 containing the cDNA for mouse and human xCT (GenScript), respectively. Transfected cells were selected with G418 (Sigma-Aldrich) and xCT expression was confirmed by FACS (not shown). Cells were counted and diluted to get 1000 cells per 1,5 ml complete DMEM containing 0.4 % low melting point agar. Cell suspensions was layered on top of 1,5 ml complete DMEM containing 2% low melting point agar in 6 well plates in duplicate. Fresh medium supplemented with G418 was added every 3 days. After 25 days of culture, colonies were counted using the stereomicroscope Nikon SMZ-10.

FACS analysis

TUBO, tumorspheres and BALB/c adenocarcinoma TSA (14) cells were fixed and permeabilized with Cytofix/Cytoperm Fixation/Permeabilization Kit (BD Biosciences) and stained with rabbit anti-Her3 antibody (Santa Cruz Biotechnology) followed by FITC anti-rabbit Ig (Dako). TSA cells were incubated with vaccinated mice sera and subsequently with FITC-rabbit anti-mouse Ig (Dako) in order to quantify anti-Her3 antibody titers. All samples were analyzed on a CyAnADP Flow Cytometer, using Summit 4.3 software (Beckman Coulter).

References

1. Conti L, Lanzardo S, Arigoni M, Antonazzo R, Radaelli E, Cantarella D, et al. The noninflammatory role of high mobility group box 1/Toll-like receptor 2 axis in the self-renewal of mammary cancer stem cells. FASEB J 2013;27(12):4731-44.
2. Barrett T, Troup DB, Wilhite SE, Ledoux P, Rudnev D, Evangelista C, et al. NCBI GEO: archive for high-throughput functional genomic data. Nucleic Acids Res 2009;37(Database issue):D885-90.
3. Huber W, Gentleman R. matchprobes: a Bioconductor package for the sequence-matching of microarray probe elements. Bioinformatics 2004;20(10):1651-2.
4. Sanges R, Cordero F, Calogero RA. oneChannelGUI: a graphical interface to Bioconductor tools, designed for life scientists who are not familiar with R language. Bioinformatics 2007;23(24):3406-8.
5. Bolstad BM, Irizarry RA, Astrand M, Speed TP. A comparison of normalization methods for high density oligonucleotide array data based on variance and bias. Bioinformatics 2003;19(2):185-93.
6. Bourgon R, Gentleman R, Huber W. Independent filtering increases detection power for high-throughput experiments. Proceedings of the National Academy of Sciences of the United States of America 2010;107(21):9546-51.
7. Smyth GK. Linear models and empirical bayes methods for assessing differential expression in microarray experiments. Stat Appl Genet Mol Biol 2004;3:Article3.
8. Reiner A, Yekutieli D, Benjamini Y. Identifying differentially expressed genes using false discovery rate controlling procedures. Bioinformatics 2003;19(3):368-75.
9. Riccardo F, Arigoni M, Buson G, Zago E, Iezzi M, Longo D, et al. Characterization of a genetic mouse model of lung cancer: a promise to identify Non-Small Cell Lung Cancer therapeutic targets and biomarkers. BMC genomics 2014;15 Suppl 3:S1.
10. Quaglino E, Mastini C, Amici A, Marchini C, Iezzi M, Lanzardo S, et al. A better immune reaction to Erbb-2 tumors is elicited in mice by DNA vaccines encoding rat/human chimeric proteins. Cancer Res 2010;70(7):2604-12.
11. Schimpff RM, Bozzola M, Lhiaubet AM, Spadaro B, Tettoni K, Rostene W. Effects of growth hormone administration on neurotensin release in children with growth delay. Horm Res 1994;42(3):95-9.
12. Mastini C, Becker PD, Iezzi M, Curcio C, Musiani P, Forni G, et al. Intramammary application of non-methylated-CpG oligodeoxynucleotides (CpG) inhibits both local and systemic mammary carcinogenesis in female BALB/c Her-2/neu transgenic mice. Curr Cancer Drug Targets 2008;8(3):230-42.
13. Ambrosino E, Spadaro M, Iezzi M, Curcio C, Forni G, Musiani P, et al. Immunosurveillance of Erbb2 carcinogenesis in transgenic mice is concealed by a dominant regulatory T-cell self-tolerance. Cancer Res 2006;66(15):7734-40.
14. Olgasi C, Dentelli P, Rosso A, Iavello A, Togliatto G, Toto V, et al. DNA vaccination against membrane-bound Kit ligand: a new approach to inhibiting tumour growth and angiogenesis. Eur J Cancer 2014;50(1):234-46.

PAPER II

Research Paper

L-Ferritin targets breast cancer stem cells and delivers therapeutic and imaging agents

Laura Conti[1,*], Stefania Lanzardo[1,*], Roberto Ruiu[1], Marta Cadenazzi[1], Federica Cavallo[1], Silvio Aime[1], Simonetta Geninatti Crich[1]

[1]Department of Molecular Biotechnology and Health Sciences, Molecular Biotechnology Center, University of Turin, Turin, Italy

[*]These authors have contributed equally to this work

Correspondence to: *Stefania Lanzardo,* ***email:*** *stefania.lanzardo@unito.it*
Simonetta Geninatti Crich, ***email:*** *simonetta.geninatti@unito.it*

Keywords: *ferritin, cancer stem cells, theranostic agents, magnetic resonance imaging, mammary tumors*

Received: *February 23, 2016* ***Accepted:*** *July 18, 2016* ***Published:*** *July 29, 2016*

ABSTRACT

A growing body of evidence suggests that cancer stem cells (CSC) have the unique biological properties necessary for tumor maintenance and spreading, and function as a reservoir for the relapse and metastatic evolution of the disease by virtue of their resistance to radio- and chemo-therapies. Thus, the efficacy of a therapeutic approach relies on its ability to effectively target and deplete CSC. In this study, we show that CSC-enriched tumorspheres from breast cancer cell lines display an increased L-Ferritin uptake capability compared to their monolayer counterparts as a consequence of the upregulation of the L-Ferritin receptor SCARA5. L-Ferritin internalization was exploited for the simultaneous delivery of Curcumin, a natural therapeutic molecule endowed with antineoplastic action, and the MRI contrast agent Gd-HPDO3A, both entrapped in the L-Ferritin cavity. This theranostic system was able to impair viability and self-renewal of tumorspheres *in vitro* and to induce the regression of established tumors in mice. In conclusion, here we show that Curcumin-loaded L-Ferritin has a strong therapeutic potential due to the specific targeting of CSC and the improved Curcumin bioavailability, opening up the possibility of its use in a clinical setting.

INTRODUCTION

The occurrence of resistance to chemotherapeutic drugs, tumor recurrences and metastases formation show the difficulties in finding effective cancer treatments and raise the question whether current anti-cancer therapies target the right cancer cell population. There is a growing concern that the commonly used treatments might indeed miss a small population of tumor cells called "tumor-initiating cells" or "cancer stem cells" (CSC), composed of stem-like cells that play a critical role in cancer progression. Like normal stem cells, CSC have the capacity to self-renew and to give rise to a more differentiated progeny, and share common signalling pathways. According to the CSC theory, CSC can be: i) the source of all the tumor cells present in a malignant tumor and ii) responsible for tumor relapse and dissemination, being associated to the resistance to radiotherapy and to the conventional chemotherapeutic agents [1]. CSC have been identified in several human solid tumors and prospectively isolated through specific markers [2], although there is no general consensus on the best markers to identify these cells [3]. In human breast carcinoma, CSC have been identified for the first time by Al Hajj et al. [4] as a rare population of $CD44^{+}/CD24^{-/low}$ cells. Furthermore, CSC have the ability to survive and proliferate in anchorage-independent conditions giving rise to non-adherent spheres called tumorspheres that can be selectively cultured and expanded. This property was first described for neuronal progenitors [5] and then extended to progenitor cells of the mammary gland [6], to breast cell lines [7-9], and to human and murine breast carcinomas [10]. Given the central role of CSC in tumor progression, spreading and relapse, the cure for cancer might rely on CSC eradication. On the light of this therapeutic implication, several CSC-targeted approaches

are being studied. These approaches range from indirect strategies, such as antiangiogenic therapies [1], to direct targeting, pursued through differentiation therapies, reversal of resistance mechanisms [1], and immunotherapy [11-13]. Another promising strategy consists in the identification of new and more specific biomarkers related to CSC status, which could serve as new targets, as we previously described [8, 9]. Moreover, these targets could be used for the development of new diagnostic tools able to provide an insight into the frequency of CSC within the tumor. Based on evidences obtained from both epidemiological and molecular studies, new insights are emerging linking the presence of excess iron and altered iron metabolism to cancer [14, 15]. Recently, Schonberg et al. [16] have demonstrated an enhanced iron scavenging ability in CSC of glioblastoma multiforme, due to a significant overexpression of the transferrin receptor (TfR) and a consequent increase in transferrin uptake, which is indicative of increased tumorigenicity. Therefore, targeting iron regulation within tumor-specific pathways could represent a potential approach for the development of new effective anti-cancer treatments.

In this study, we exploited the sphere-forming ability of CSC to selectively enrich the stem-like cell population present in a human (MDA-MB-231) and murine (TUBO) breast cancer cell lines, as described in [8], and for the first time we demonstrated that the uptake of L-Ferritin increased in CSC-enriched tumorspheres generated from both cell lines compared to their more differentiated counterparts. We surmise that this behaviour may be associated to their enhanced expression of the L-Ferritin receptor Scavenger Receptor Class A member 5 (SCARA5) that mediates Ferritin endocytosis [17]. Ferritin is the main iron storage protein and is composed of 24 subunits of heavy (H)- or light (L)-chain polypeptides that are present at different ratios in various organs to form a cage architecture of 12 nm in external diameter, with an inner cavity of 8 nm [18]. Once deprived of iron, this cavity can be used for the selective delivery of imaging and therapeutic agents to cells expressing Ferritin receptors [19]. The use of these nanotheranostic agents permits the non-invasive analysis of the pharmacokinetics and biodistribution of the nanomedicine formulation. Consequently, it is possible to monitor the efficacy of the therapy in real time and thereby to adapt the treatment regimens [20-22]. Several papers have explored the use of H-Ferritin to deliver selectively doxorubicin to cancer cells [23, 24]. In this contest, we have previously reported that the selective uptake of native horse spleen Ferritin and Apoferritin (composed by 85% and 15% L and H chains, respectively) loaded with MRI contrast agents and the anticancer drug Curcumin in the human breast cancer cell line MCF7 causes a significant reduction in cell proliferation *in vitro* [25]. Curcumin has been selected as therapeutic agent since it has been reported to exhibit anticancer activity *in vitro* and to be highly tolerated when administered to patients [26]. However, its poor water solubility and low bioavailability hampers its use as anti-cancer drug [27]. Therefore, loading Curcumin into Apoferritin can represent a solution for its delivery to cancer cells *in vivo*. Herein, we show that Apoferritin can be exploited for the simultaneous delivery of Gd-based MRI contrast agents and Curcumin for breast CSC targeting. Moreover, we show that administration of Curcumin-loaded Apoferritin leads to the regression of breast tumors *in vivo*. This approach could potentially enhance the responsiveness to current anticancer treatment regimens and might reduce the risk of relapse and dissemination of the disease.

RESULTS AND DISCUSSION

SCARA5 is upregulated in breast CSC

A transcriptional analysis comparing the transcription profile of $Her2^+$ murine TUBO cells cultured as monolayer with those of the first three *in vitro* passages of their derived CSC-enriched tumorspheres using MouseWG-6 v2.0 Illumina beadchips (GSE21451) [28] proved that SCARA5 is upregulated in tumorspheres (Figure 1A). SCARA5 protein expression increased from TUBO to tumorsphere-derived cells, as demonstrated by the representative images (panel B, C) and by the quantification of fluorescence intensity (panel D) reported in Figure 1. This enhanced expression is not restricted to TUBO-derived CSC, as it was also observed in tumorspheres derived from human triple negative breast cancer (TNBC) cell line MDA-MB-231 (Figure 1E-1G), further suggesting that SCARA5 may be a promising target of breast CSC.

Breast CSC internalize more Ferritin than differentiated cancer cells

Since SCARA5 mediates L-Ferritin uptake [29], the first step of this study was the evaluation of the ability of MDA-MB-231 and TUBO tumorspheres to take up Ferritin from the medium compared to their corresponding more differentiated cells. For this purpose, horse spleen Ferritin, composed mostly of L-Ferritin chains and containing ca. 1000 iron atoms per protein, was used without any further modification. The experimental protocol consisted in the measurement of the amount of iron internalized by cells upon 24 hours of incubation in Ferritin-containing medium. The amount of internalized Ferritin was assessed by the ICP-MS determination of the intracellular iron content. The amount of internalized iron was significantly higher in tumorspheres than in differentiated cells, and increased with Ferritin concentration in both TUBO (Figure 2A) and MDA-MB-231 (Figure 2B) cell lines.

Ferritin contains a superparamagnetic ferrihydrite ($5Fe_2O_3 \cdot 9H_2O$) crystal that increases the transverse NMR

relaxation rate (R_2) of solvent water protons, causing a negative contrast in the corresponding MR images [30]. In order to assess whether native Ferritin can be exploited as a natural MRI probe for CSC detection, T_2-weighted MR images were acquired following Ferritin incubation on both MDA-MB-231 and TUBO cells and their derived tumorspheres. Figure 2C shows that tumorspheres incubated with Ferritin displayed a markedly lower signal intensity when compared to untreated tumorspheres, while only small changes in signal intensity (SI) were observed in differentiated cells incubated in the absence or in the presence of Ferritin, respectively (Supplementary Material, Supplementary Table S1). Since spheroid diameter range is between 80 and 120 μm, TUBO-derived tumorspheres incubated 24 hours with 0.52 μM Ferritin were detectable as isolated spots after their dispersion in agar (Figure 2D). Altogether, these data show that Ferritin-based contrast agents may be exploited for the MRI detection of CSC. The specificity of the uptake was assessed by carrying out a competition study by incubating cells for 24 hours in the presence of an excess of native Apoferritin. In both MDA-MB-231- and TUBO-derived tumorspheres, the iron uptake measured by ICP-MS decreased of about 60% and 66%, respectively, confirming that iron uptake was mediated by Ferritin specific receptors. To ensure that the uptake of Ferritin by CSC is specifically mediated by SCARA5, we assessed the effect of SCARA5 silencing on the ability of cells to internalize Ferritin. TUBO-derived

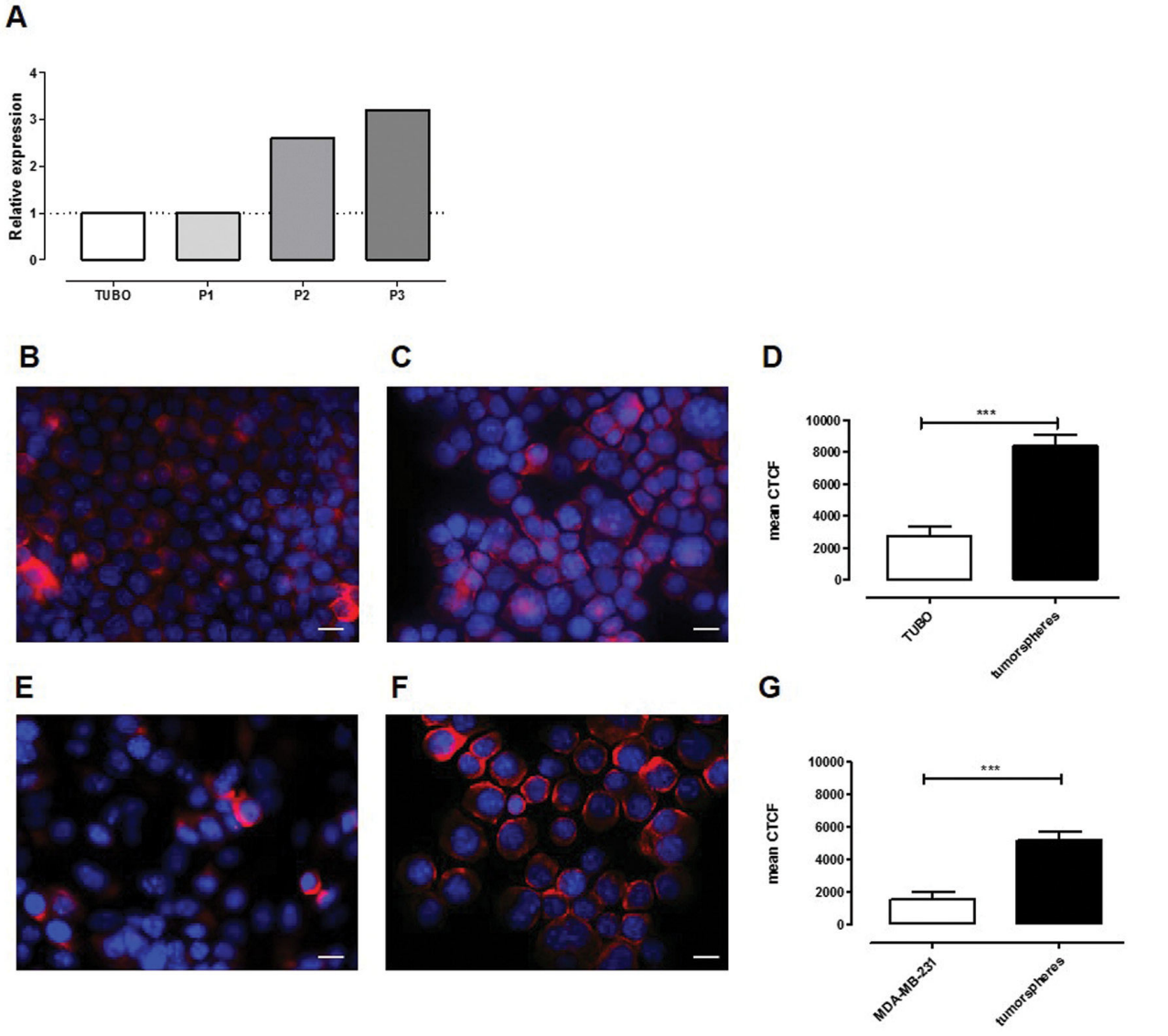

Figure 1: SCARA5 expression is upregulated in tumorspheres. A. Relative transcript expression level of SCARA5 in TUBO cells and in three different tumorsphere passages. **B, E.** Representative images of TUBO and MDA-MB-231 cells or of **C, F.** their derived tumorspheres stained with an anti-SCARA5 mAb (red). Nuclei were counterstained with DAPI (blue). Scale bar, 20 μM. **D, G.** Graphs represent the mean ± SEM of the corrected total cell fluorescence (CTCF), calculated on at least 100 cells per sample as a quantification of SCARA5 expression in TUBO and MDA-MB-231 cells or in their derived tumorspheres.

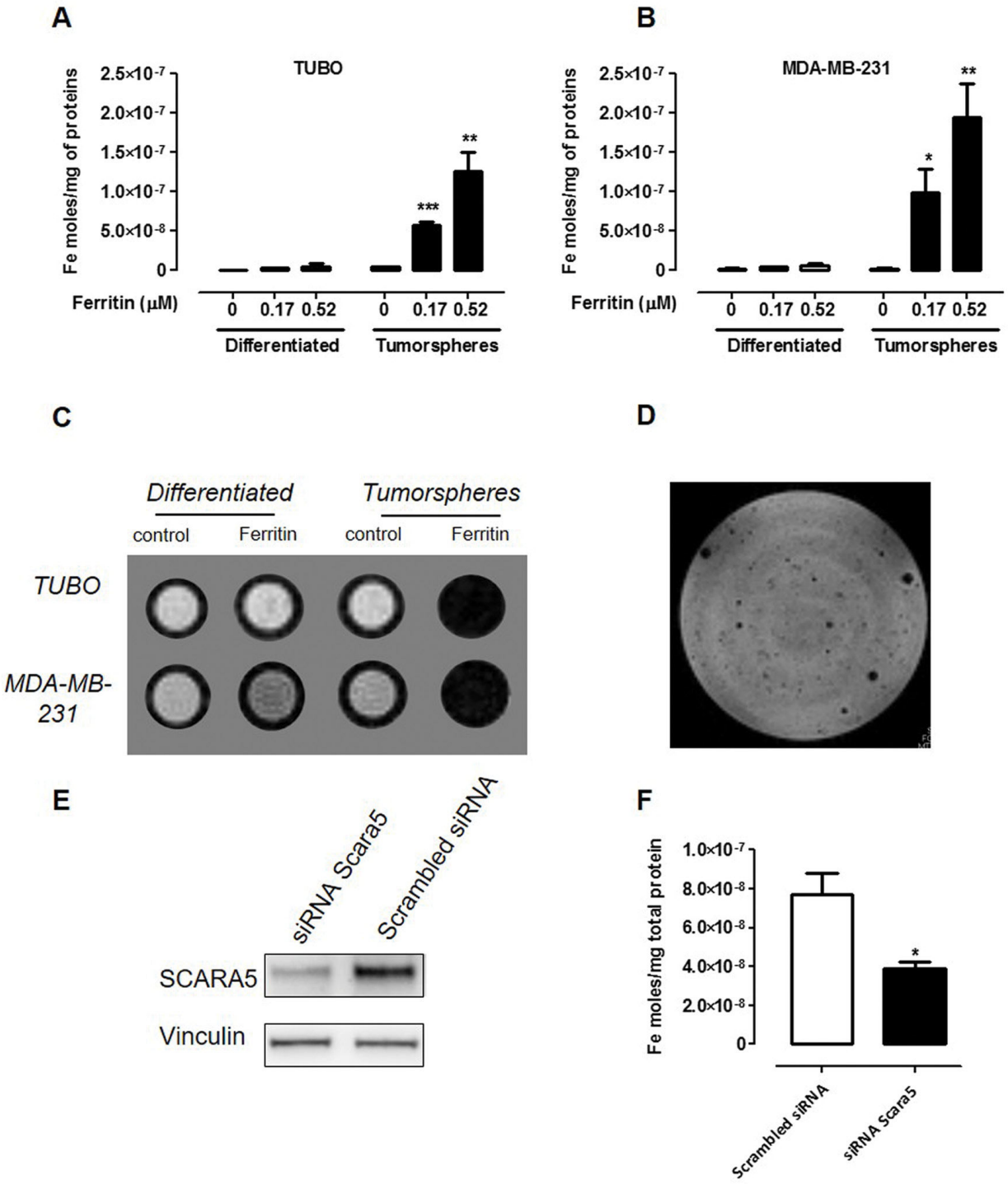

Figure 2: CSC display a higher Ferritin uptake than differentiated cells. A, B. ICP-MS determination of the intracellular iron content of TUBO (A) and MDA-MB-231 (B) cells and their derived tumorspheres cultured for 24 hours with or without Ferritin 0.17 and 0.52 μM. Graphs show the mean ± SEM of internalized iron moles every mg of cell proteins from 3 independent experiments. **C.** A representative T_2-weighted RARE MR image of an agar phantom containing TUBO and MDA-MB-231 cells (both differentiated and tumorspheres) incubated or not for 24 hours with L-Ferritin 0.52 μM. **D.** MRI of TUBO tumorspheres dispersed in agar. Each hypo-intense spot corresponds to the signal arising from one tumorsphere. **E, F.** TUBO derived tumorspheres were transfected with a siRNA to SCARA5 or a scrambled siRNA, and 48 hours after incubated with L-Ferritin for additional 24 hours. (E) Representative immunoblot of SCARA5 expression 48 hours after cell transfection. Vinculin expression was used as internal control. (F) Graph showing mean ± SEM of iron moles every mg of cell proteins, evaluated by ICP-MS, from 3 independent experiments. *p<0.05, Student's *t* test.

tumorspheres were incubated with a siRNA specific to SCARA5 or with a negative control scrambled siRNA, and the levels of SCARA5 protein were analyzed 24, 48 and 72 hours after transfection. SCARA5 transcript silencing (Supplementary Material, Supplementary Figure S1), led to a threefold decrease in SCARA5 protein level 48 hours after transfection, and this was maintained for the subsequent 24 hours (Figure 2E, Supplementary Figure S1). Hence, 48 hours after transfection, cells were incubated with 0.52 μM Ferritin for 24 hours. As shown in Figure 2F, the amount of iron internalized by cells treated with siRNA to SCARA5 was significantly lower than that internalized by control cells, thus confirming that SCARA5 mediates Ferritin uptake in breast CSC.

In order to further confirm that breast tumorspheres take up more Ferritin than their differentiated counterpart, Apoferritin was labelled with FITC on its external surface (hereafter referred to as APO-FITC), and TUBO cells and their derived tumorspheres were incubated for 24 hours in the presence of APO-FITC. Flow cytometric analysis revealed that APO-FITC was internalized by both TUBO and tumorspheres, but its intake in tumorspheres was significantly higher, as demonstrated by their enhanced mean fluorescence intensity (MFI, Figure 3A) when compared to TUBO cells. Of note, all cells expressing the stem cell marker Sca-1 [8], only present in tumorspheres, displayed a higher APO-FITC uptake than the remaining cells (Figure 3B, $Sca1^{+}$ $APO\text{-}FITC^{high}$ cells in the red boxes), suggesting that Ferritin uptake is higher in CSC than in more differentiated cells. Similarly, a small amount of APO-FITC was internalized in MDA-MB-231 differentiated cells, while its internalization in their derived tumorspheres was significantly higher (Figure 3C).

Uptake and intracellular distribution of rhodamine isothiocyanate labelled apoferritin (Apo-Rhod)

In order to perform a dose-response study using low Apoferritin concentrations, thus evaluating its affinity to SCARA5 receptors, Apoferritin was conjugated on its external surface with Rhodamine isothiocyanate (hereafter referred to as APO-Rhod), and incubated 24 hours with TUBO, MDA-MB-231 and their derived tumorspheres. Figure 4A shows the amount of APO-Rhod taken up by cells, determined using a calibration curve performed with a Rhodamine standard solution. These results confirm that the amount of internalized APO-Rhod was significantly higher in tumorspheres than in differentiated cells even at nanomolar concentrations, which is an indication of the high affinity of Apoferritin for SCARA5 receptor.

In order to assess whether the presence of 15% of H-chains in the horse spleen Ferritin used in this study can mediate its uptake through H-Ferritin receptors, a further competition study was carried out by incubating both MDA-MB-231 and TUBO tumorspheres for 24 hours with APO-Rhod in the presence of a 10-fold excess of recombinant H-Ferritin [31, 32]. The H-Ferritin excess did not affect the amount of APO-Rhod internalized in both MDA-MB-231 and TUBO tumorspheres (Figure 4B) thus excluding the involvement of H-Ferritin receptors in the internalization of Horse spleen Apoferritin.

To explore the underlying internalization mechanism, APO-Rhod was incubated with TUBO-derived tumorspheres for fluorescence microscopy observation (Figure 4). Cells were then stained either for the early endosomal marker EEA-1 (panels C-F) or for the lysosomal marker LAMP-1 (panels G-L) to observe the process of APO-Rhod cellular trafficking. Two hours after incubation, APO-Rhod was located in the cytoplasm of most cells where it colocalized with early endosomes, as shown in panel F. LAMP-1 was distributed throughout the cytoplasm and the codistribution of APO-Rhod with LAMP-1 signal was circumscribed to the granular regions in the cytoplasm of some cells (Figure 4, panel L). These observations indicate that APO-Rhod was delivered to early endosomes after internalization. In the canonical receptor-mediated endocytosis pathway, early endosomes gradually mature to became late endosomes that then converge in lysosomes [33]. Most probably, APO-Rhod partly follows this path after internalization, since it colocalizes with the lysosomal marker LAMP-1.

Uptake of apoferritin loaded with Gd-HPDO3A MRI contrast agent and Curcumin (Gd-APO-curcumin)

Despite its structural stability under physiological conditions, Ferritin displays a pH-dependent de-assembly, which can be exploited to load it with both therapeutic agents and imaging probes. Indeed, there are many examples where Ferritin nanoarchitecture was broken down in acidic environment and restored by retuning the pH to 7.4, after the entrapment of the desired solutes in its inner cavity [22, 34]. Using this procedure, Curcumin and the commercially available MRI contrast agent Gd-HPDO3A, neutral and safe even at high concentrations [35], were entrapped in the Apoferritin cavity (Figure 5A). Curcumin was selected as therapeutic agent since it has been reported to exhibit anti-oxidant, anti-inflammatory, anti-microbial and anti-cancer activity *in vitro* and in animal models of several diseases, such as acute hepatitis, acute ileitis, neuroinflammation, ischaemia and cancer [36]. Its anti-cancer activity is operated through modulation or inhibition of multiple molecular pathways [37]. Furthermore, during the past few years, a number of studies have suggested that Curcumin may have direct or indirect influence on CSC self-renewal pathways, including Wnt/b-catenin, sonic hedgehog, and Notch [38-40]. Another important property is that, unlike other known chemotherapeutic compounds, Curcumin does not

cause any damage to normal cells [41]. Since SCARA5 is also expressed in the liver, the observation that Curcumin had no effect on normal rat hepatocytes [41] is essential to promote its use as a valid chemopreventive and chemotherapeutic agent for CSC using Apoferritin as a delivery platform. Furthermore, loading Curcumin into its protein cavity improves Curcumin bioavailability and stability under physiological conditions, maintaining its peculiar pharmacological properties [22]. Curcumin-loaded Apoferritin (APO-Curcumin) stability was assessed spectrophotometrically by measuring absorbance decrease at 430 nm. In the first 2 hours the absorbance showed a small decrease (15%), then it remained essentially constant during the entire experimental time (48 hours). Without Apoferritin, more than 90% of Curcumin decomposed rapidly (30 minutes) in buffer at neutral pH as already reported by Zebib et al. [42].

Using the protocol described above, the number of molecules that remained in Apoferritin inner cavity after the dissociation/reassociation procedure was 228 ± 48 and 9.6 ± 2 for Curcumin and Gd-HPDO3A, respectively. Gd-APO-Curcumin is stable for at least 48h as assessed by

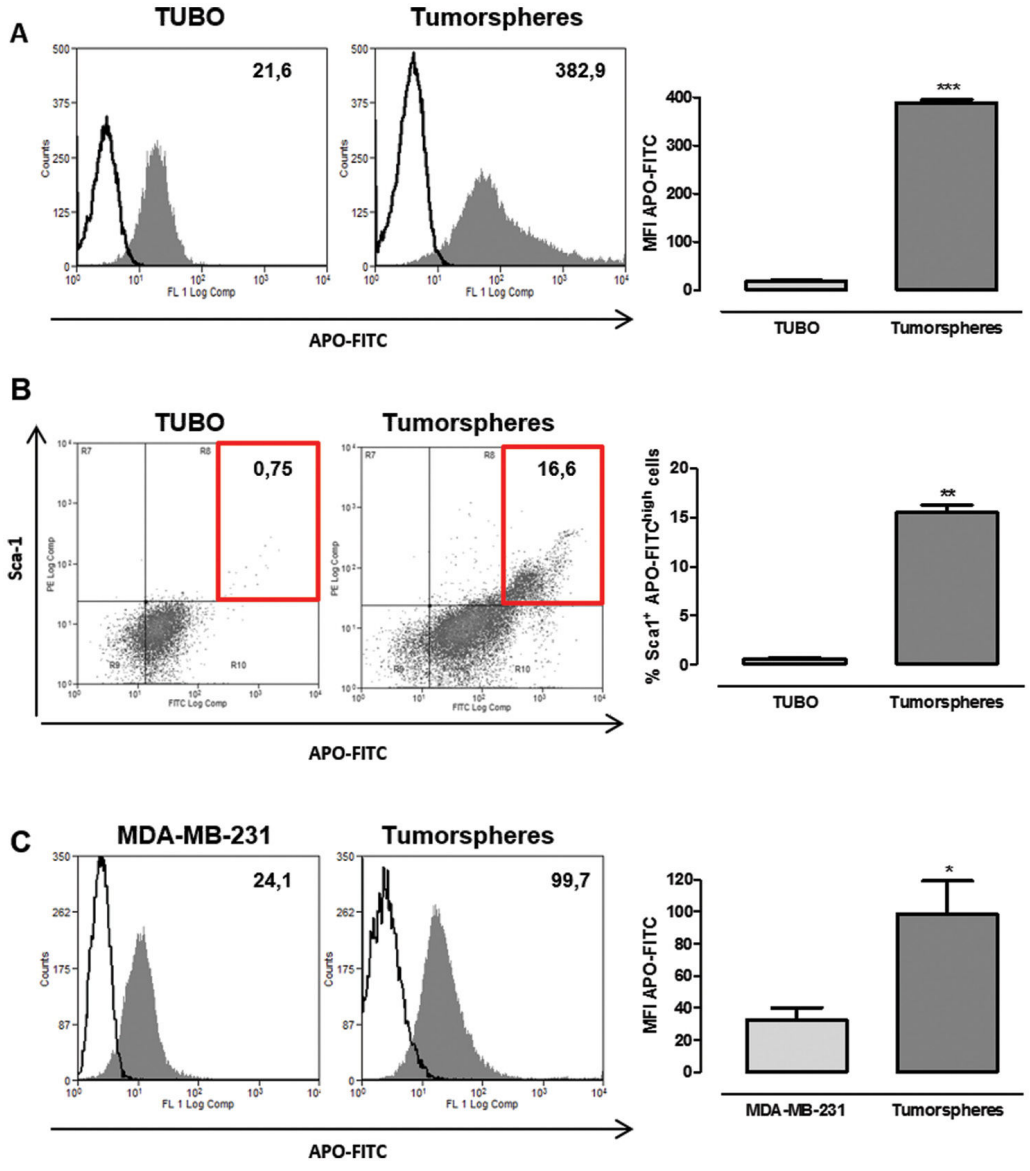

Figure 3: CSC display a higher APO-FITC uptake than differentiated cells. FACS analysis of TUBO and MDA-MB-231 cells and their derived tumorspheres cultured with or without APO-FITC for 24 hours. **A, C.** Representative histograms of untreated (open histograms) or APO-FITC treated (gray histograms) TUBO (A) and MDA-MB-231 (C) cells and tumorspheres. Numbers show mean fluorescent intensity (MFI), the graphs show the mean ± SEM of APO-FITC MFI observed in cells and tumorspheres from 4 independent experiments. **B.** Representative dot plots of APO-FITC and Sca-1 expression in TUBO and tumorspheres. Numbers in quadrants show the percentage of APO-FITC^{high} Sca1^{+} cells (evidenced by the red boxes), the graph shows the mean ± SEM of the percentage of APO-FITC^{high} Sca-1^{+} cells in TUBO and tumorspheres from 4 independent experiments. *$P < 0.05$, **$P < 0.01$, ***$P < 0.001$; Student's t test.

measuring absorbance at 430 nm [17]. The T_1-weighted MRI image, recorded after 24 hours incubation in the presence of Gd-APO-Curcumin (2.7 μM), showed that the signal arising from labelled tumorspheres was clearly hyperintense compared to the untreated control tumorspheres for both cell lines (Figure 5B and Supplementary Materials, Supplementary Table S2). On the contrary, no significant signal enhancement was observed in Gd-APO-Curcumin-treated differentiated cells when compared to untreated cells. These observations were confirmed by the significantly higher amount of Gd taken-up by tumorspheres, measured by ICP-MS (Figure 5C). On the basis of the ICP-MS Gd measurements, it was possible to calculate the intracellular Gd, and consequently Curcumin, concentrations. In fact, since the Curcumin/Gd ratio in the Apoferritin preparation was 16, estimated intracellular Curcumin concentrations of 1400 and 460 μg/g were obtained for MDA-MB-231 and TUBO derived tumorspheres, respectively.

APO-Curcumin induces cell death and reduces self-renewal of CSC

In order to seek whether APO-Curcumin is able to induce inhibitory effects on CSC survival and self-renewal, TUBO cells and their derived tumorspheres where incubated in the presence or absence of APO-Curcumin for different time intervals, and cell death was evaluated by citofluorimetric analysis with Annexin V and propidium iodide staining. As shown in Figure 6A, APO-Curcumin did not induce cell death in TUBO cells, while progressively caused cell death in tumorspheres when compared to untreated cells. Of note, APO-Curcumin was more efficient than free Curcumin in inducing cell

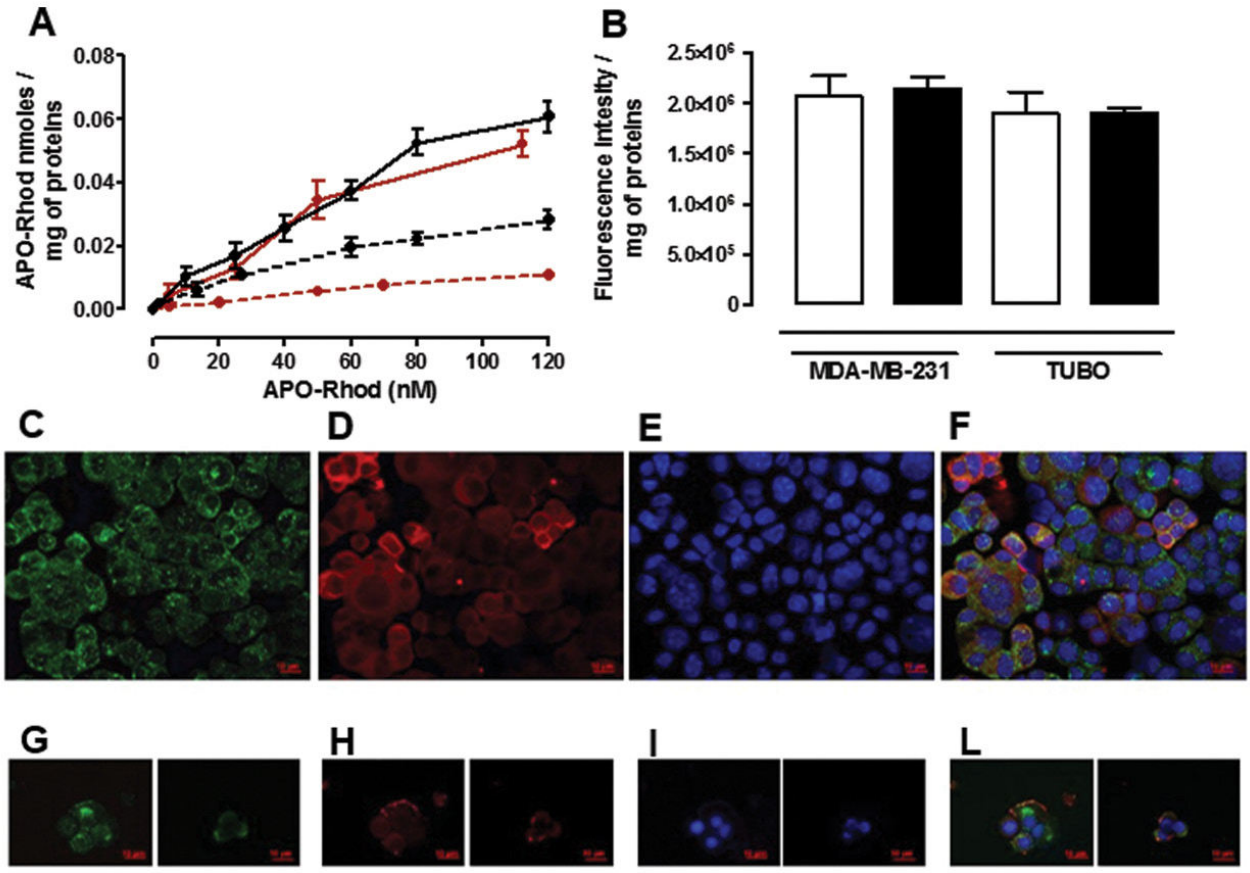

Figure 4: Uptake and intracellular distribution of Apo-Rhod. A. Dose-response curve obtained by incubating different concentrations of APO-Rhod 24 hours with TUBO (red dotted line), MDA-MB-231 (black dotted line) and their derived tumorspheres (red and black continuous lines respectively). **B.** Apo-Rhod concentrations were determined by measuring fluorescence (ex/em 555/575 nm) on cytosolic extracts and were normalized to the cell proteins. Fluorescence intensity (au) of cytosolic extracts of TUBO and MDA-MB-231 derived tumorspheres, incubated in the absence (white bars) or in the presence of a 10 fold excess of H-Apoferritin. **C-L.** Representative images of TUBO derived tumorspheres incubated for 2 hours at 37°C with APO-Rhod (red, D and H) and stained with an anti-EEA1 antibody (green, C) or an anti-LAMP-1 antibody (green, G). Nuclei were counterstained with DAPI (blue, E and I). The co-localization between APO-Rhod and EEA1 or LAMP-1 is shown in the merged images of panels F and L, respectively. Scale bar, 10 μM.

death in tumorspheres (Figure 6B). This enhanced effect was not due to any toxicity of the protein itself, since treatment with Apoferritin did not induce cell death in either TUBO or tumorspheres (Figure 6B), but likely to the ability of APO-Curcumin to enhance Curcumin uptake by CSC. APO-Curcumin and Curcumin affected

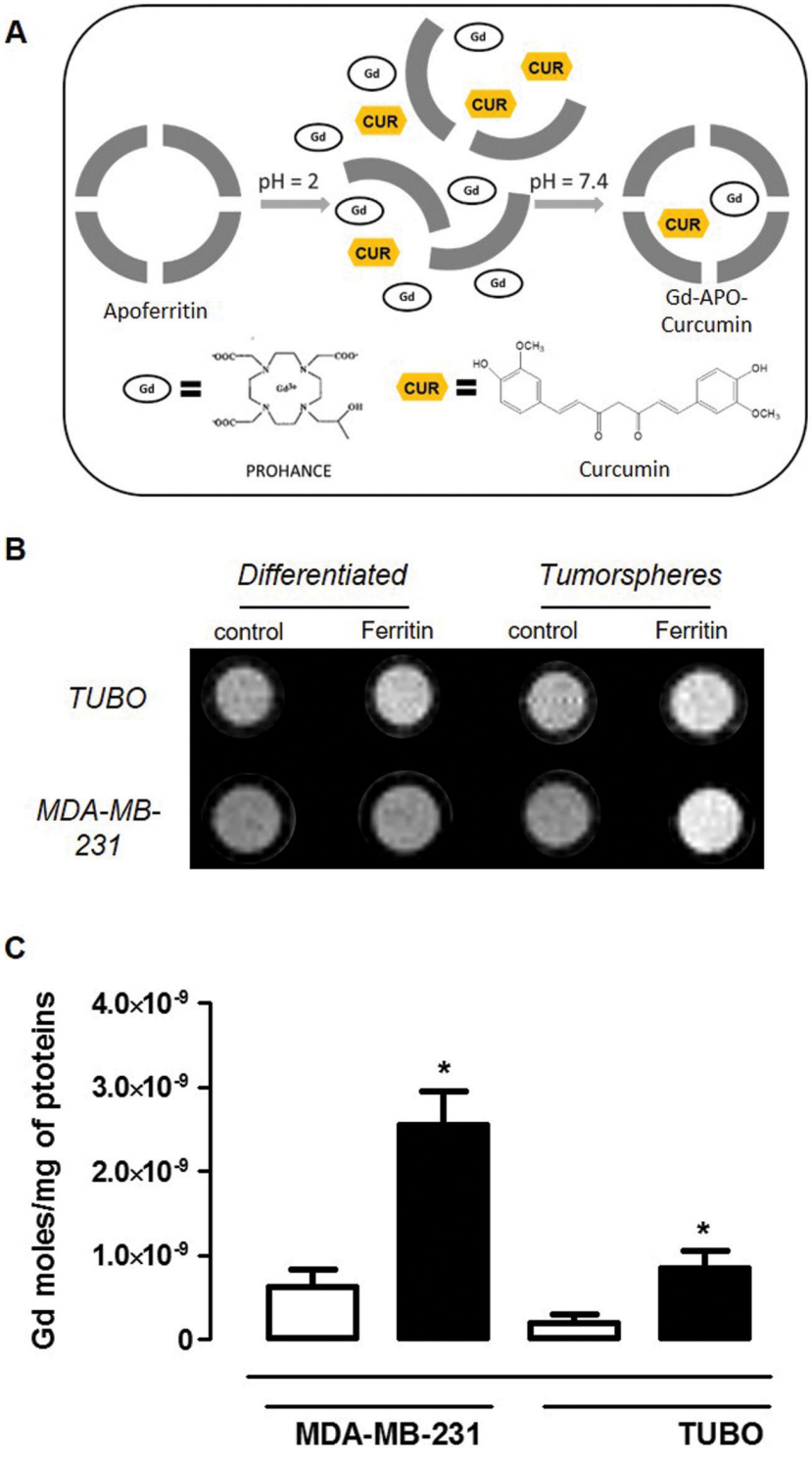

Figure 5: Gd-APO-Curcumin uptake is higher in CSC than in differentiated cells. A. Schematic representation of Gd-APO-Curcumin preparation. **B.** A representative T_1-weighted spin echo image of an agar phantom containing TUBO and MDA-MB-231 (both differentiated and tumorspheres) cells incubated or not for 24 hours with Gd-APO-Curcumin (2.7 μM in protein). **C.** Mean ± SEM of internalized Gd moles every mg of cell proteins from 3 independent experiments, measured by ICP-MS as in (B). *$P < 0.05$; Student's *t* test.

not only tumorsphere viability, but also CSC self-renewal capacity as shown by a decreased ability of treated cells to re-generate tumorspheres, which on the contrary was not hindered by treatment with Apoferritin alone (Figure 6C). None of these compounds altered TUBO cell morphology (Figure 6D, upper panels), while tumorspheres cultured in presence of Curcumin and APO-Curcumin were smaller than those cultured in medium alone or with Apoferritin

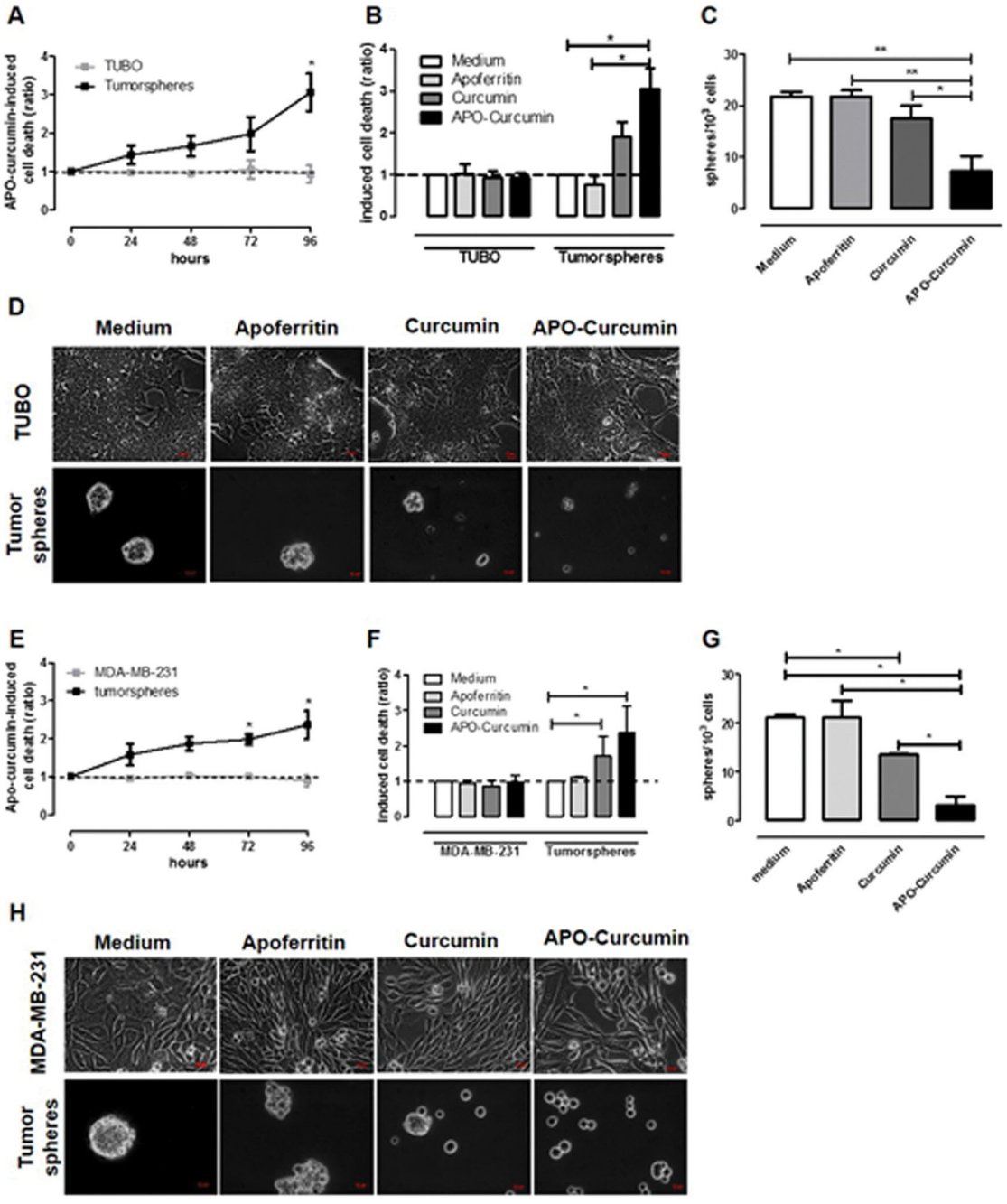

Figure 6: APO-Curcumin induces cell death and reduces self-renewal in tumorspheres. TUBO **A-D.** and MDA-MB-231 **E-H.** cells were cultured as monolayer or tumorpsheres in presence of Apoferritin, APO-Curcumin or Curcumin. (A, E) After 24, 48, 72 or 96 hours, cells were stained with Annexin-V and PI and analyzed by FACS. The graphs show means ± SEM of the ratio of dead cells between APO-Curcumin-treated and untreated cells, calculated as described in M&M. (B, F) Graphs showing means ± SEM of the ratio of the percentage of dead cells present in samples treated for 96 hours with Apoferritin, APO-Curcumin or Curcumin in comparison to untreated samples. (C, G) The graphs show means ± SEM of the number of spheres generated every 10^3 cells plated in the absence or presence of Apoferritin, APO-Curcumin or Curcumin. (D, H) Representative images of differentiated (upper panels) or tumorspheres (lower panels) cultured for 96 hours with the different treatments. Magnification 40X, scale bars 100 μm. All experiments were repeated at least 4 times. *$P < 0.05$; **$P < 0.01$; Student's t test.

(Figure 6D, lower panels). The ability of APO-Curcumin to target CSC and decrease their survival and self-renewal is not restricted to the TUBO model, since similar results were obtained with MDA-MB-231 cells (Figure 6E-6H). While the increased effect of APO-Curcumin on tumorspheres compared to differentiated cells can be explained by tumorspheres' increased expression of SCARA5 receptor, the reason why even free Curcumin (50 μM) affects tumorspheres but not differentiated cells is more speculative. It has been shown by others [38, 43] that Curcumin acts primarily on undifferentiated stem and progenitor cells rather than on more differentiated cells from mammary tissue and breast cancer cell lines. This effect appears to be mediated, at least in part, by the inhibition of intracellular signalling pathways that are upregulated in CSC [38]. It is therefore highly likely that a similar mechanism of action occurs also in our model.

APO-Curcumin inhibits breast cancer growth *in vivo*

To explore the efficacy of APO-Curcumin on established tumors *in vivo*, we set up a model that consists in the subcutaneous (s.c.) implantation of TUBO-derived tumorspheres into syngeneic BALB/c mice. After implantation, these cells maintain a prevalent CSC phenotype, as demonstrated by the presence of an higher level of both $CD44^{+}/CD24^{-}$ and $Aldefluor^{+}$ expressing cells when compared to tumors generated by TUBO cells (Supplementary Material, Supplementary Figure S2). When tumors reached 2 mm mean diameter, mice were treated with APO-Curcumin or Apoferritin (10 mg/Kg of Curcumin and 53 mg/Kg of protein) intravenously (i.v.) every 3 days, or left untreated (Figure 7). The extremely low Curcumin water solubility prevents its direct i.v.

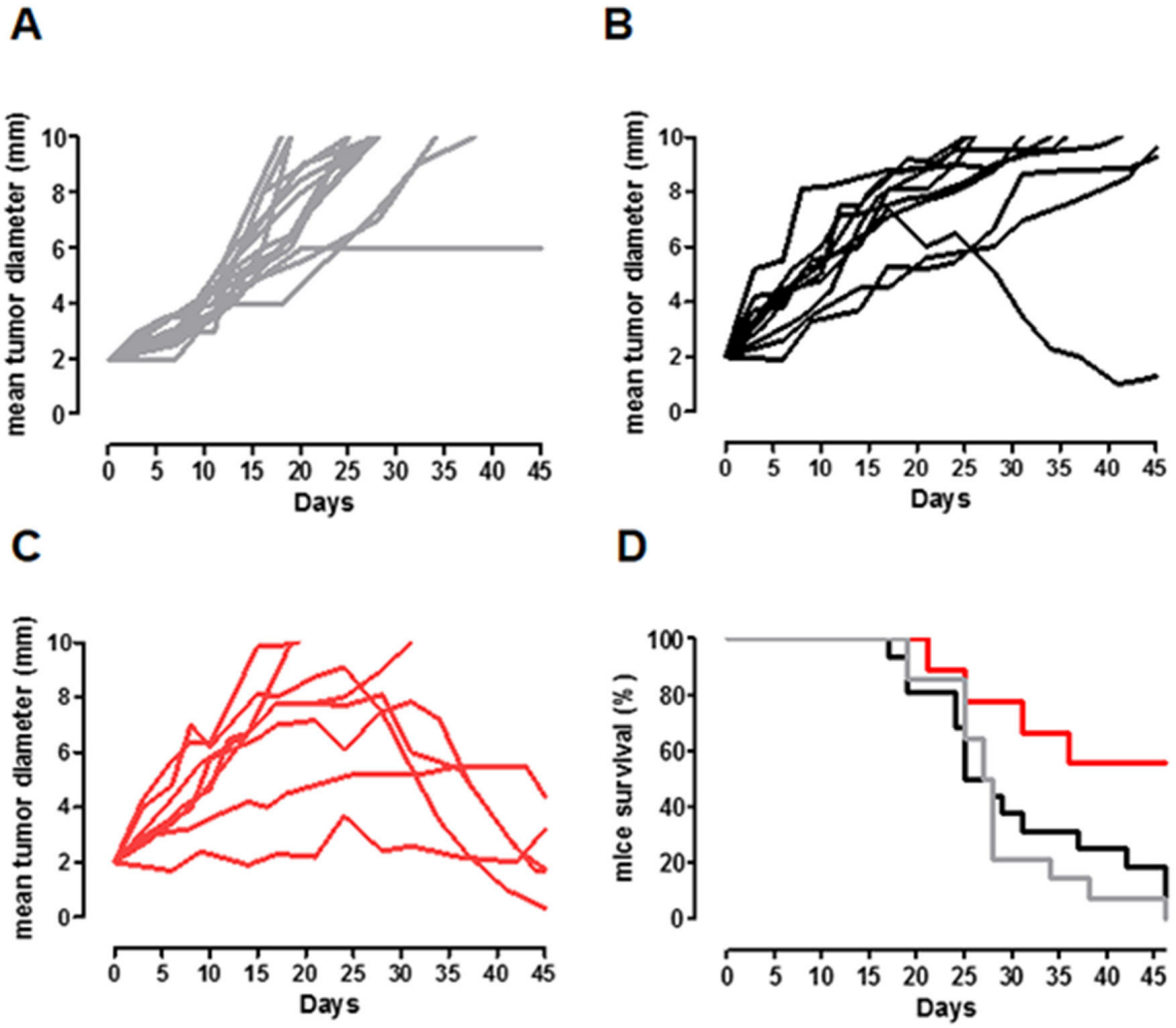

Figure 7: APO-Curcumin treatment delays CSC-induced tumor growth *in vivo*. A-C. BALB/c mice were challenged s.c. with TUBO-derived tumorspheres and left untreated (**A**, gray lines) or treated i.v. with Apoferritin (**B**, 53 mg/Kg; black lines) or APO-Curcumin (**C**, 10 mg/Kg of Curcumin and 53 mg/Kg of protein; red lines) every 3 days, starting when their tumor reached 2 mm mean diameter. Each line depicts the growth of a single tumor. **D.** Kaplan-Meier survival curves. APO-Curcumin vs Apoferritin treated mice: P=0.0189; Apoferritin treated mice vs Untreated mice: P = 0.5; APO-Curcumin treated mice vs Untreated mice: P= 0.0054, Log-rank (Mantel-Cox) Test. Data were cumulated from two independent and concordant experiments.

Table 1: Percentage of mice whose tumor regressed (responders) or grew (non responders) in the three groups

	APO-Curcumin	Apoferritin	Untreated
Responders	5/8 (62.5%)	1/10 (10%)	0/11 (0%)
Non Responders	3/8 (37.5%)	9/10 (90%)	11/11 (100%)

Data were cumulated from two independent and concordant experiments. APO-Curcumin vs Apoferritin treated mice: $P = 0{,}043$; Apoferritin treated mice vs Untreated mice: $P = 0.47$; APO-Curcumin treated mice vs Untreated mice: $P = 0.0048$, Chi square test.

administration without exploiting a nanoformulation/emulsion, therefore it was not possible to insert a Curcumin-treated group. Whereas virtually all tumors grew progressively in untreated or Apoferritin-treated mice (Figure 7A, 7B and Table 1), they did not progress or eventually regressed in about 60% of APO-Curcumin treated mice (Figure 7C and Table 1).

Considering the animal survival, whereas all untreated mice died at the end of the experiment, about 60% of APO-Curcumin treated mice were still alive, compared to only 10% in the Apoferritin treated group (Figure 7D; P=0.018, Chi square test), suggesting that Curcumin-loaded Apoferritin may represent a promising tool for breast cancer treatment.

In order to verify that APO-Curcumin is not toxic to the liver, being SCARA 5 also expressed on hepatocytes, histological assessment of liver damage was carried out at the end point of the treatment. Periportal hepatocytes from both Apoferritin and APO-Curcumin treated animals did not show any injury but only a moderate degree of vacuolar degeneration, which is compatible with lysosomal compartment enlargement due to the endocytic uptake of the nanodevice (Supplementary Material, Supplementary Figure S3).

In conclusion, in this work it was shown that both human and mice breast CSC display an increased L-Ferritin uptake capability compared to their more differentiated counterparts. This is mediated at least in part by the upregulation of the L-Ferritin receptor SCARA5. These results open new horizons in the design of targeting strategies for the eradication of CSC, which are usually highly resistant to conventional chemo- and radiotherapy. Indeed, the increased L-Ferritin uptake can be exploited for the delivery of Curcumin to CSC, as the loading of Curcumin into L-Apoferritin does not cause any reduction of its affinity for the SCARA5 receptor. Of note, loading Curcumin into Apoferritin not only enables specific targeting to SCARA5-expressing cells, and thus to breast CSC, but also improves Curcumin bioavailability, opening up the possibility of *in vivo* treatments. Our *in vivo* results highlight the therapeutic potential of APO-Curcumin. However, to improve the clinical translatability of this approach, further experiments are needed in order to explore the synergistic effect of APO-Curcumin and classical chemotherapy. In this way, the elimination of CSC, exerted by APO-Curcumin, could be accompanied by the eradication of more differentiated tumor cells, leading to overcome tumor resistance and reduce recurrence. The relatively low sensitivity of MRI hampers the use of Gd-APO-Curcumin for the *in vivo* detection of CSC that represent a very low proportion of the tumor mass. However, this important objective might be achieved by developing more sensitive Apoferritin based PET or optical probes, which could provide new theranostic tools to improve breast patient stratification and monitoring of their response to therapy.

MATERIALS AND METHODS

Preparation of Gd-HPDO3A and Curcumin loaded Apoferritin (Gd-APO-Curcumin)

Gd-HPDO3A (ProHance) was kindly provided by Bracco Imaging S.p.A. Apoferritin, Ferritin (from horse spleen), Curcumin and all other chemicals were purchased from Sigma-Aldrich. H-Ferritin was kindly provided by Paola Turano (Center for Magnetic Resonance, University of Florence Italy) and prepared as described in [31, 32]. The loading of Curcumin and Gd-HPDO3A in the iron free Apoferritin cavity was carried out as described previously [22]. Briefly, the dissociation of Apoferritin into its subunits was done by lowering the pH of the 4.1×10^{-6} M protein solution (8 mL) to pH 2 using 1 M HCl and maintaining this low pH for about 15 minutes. Afterwards, 50 µL of a Curcumin solution in DMSO (200 mg/mL) and 2 mL 0.5 M Gd-HPDO3A were added to the Apoferritin solution. Then the pH was adjusted to 7.4 using 1 M NaOH. The resulting solution was stirred at room temperature for 2 hours, centrifuged, purified by gel filtration (Superdex G25 Column, Amersham) and dialysis. The solution was then concentrated using Vivaspin centrifugal concentrators (50 000 MWCO, Sigma-Aldrich). At the end of this process the concentrations of the protein and of Curcumin were measured by Bradford assay (using bovine serum albumin as a standard) and spectrophotometrically at 430 nm in ethanol, respectively. The final Gd concentration was determined by inductively

coupled plasma mass spectrometry (ICP-MS) (Element-2; Thermo-Finnigan). Sample digestion was performed with 2 mL of concentrated HNO_3 (70%) under microwave heating (Milestone MicroSYNTH Microwave Labstation).

Cell lines

MDA-MB-231 were purchased from LGC Standards and grown in DMEM (Invitrogen Corp.) supplemented with 10% FBS (Sigma-Aldrich). TUBO cells [44] were generated from a spontaneous tumor of Her2/neu transgenic (BALB-neuT) mice [45] and were cultured in DMEM supplemented with 20% FBS. All cells were tested negative for mycoplasma by PCR assay and passaged in our laboratory for fewer than six months after their resuscitation. For tumorsphere generation, cells were detached and plated in ultra-low attachment flasks (Sigma-Aldrich) at 6×10^4 viable cells/mL in mammosphere medium, as previously reported [8].

Ferritin uptake experiments

MDA-MB-231, TUBO cells and their derived tumorspheres were incubated with increasing concentrations of Ferritin, Gd-APO-Curcumin and Apoferritin 24 hours post seeding. After 24 hours of incubation, cells were washed three times with ice-cold PBS and detached with trypsin/EDTA (Sigma-Aldrich). Then cells were lysed by sonication using an ultrasonic probe device (30% power). The Fe or Gd content in each cell line was determined by ICP-MS as described above. For MRI analysis (see below) cells were transferred into glass capillaries. The protein concentration was determined from cell lysates by the Bradford assay. The amounts of iron (measured by ICP-MS) internalized by cells were normalized to cell proteins concentration. 1 mg of proteins measured on cell lysate correspond to $3.1\pm0.3\times10^6$ and $2.8\pm0.3\times10^6$ MDA-MB-231 differentiated cells and tumorspheres, respectively, and to $2.9\pm0.4\times10^6$ and $3.8\pm0.35\times10^6$ TUBO differentiated cells and tumorspheres, respectively.

MRI

All the MR images were acquired on a Bruker Avance 300 spectrometer (7 T) equipped with a Micro 2.5 microimaging probe (Bruker BioSpin). For *in vitro* determinations, glass capillaries containing 2×10^6 cells were placed in an agar phantom and MRI was performed using a standard T_1-weighted multislice spin-echo sequence (TR/TE/NEX = 250/3.3/8, FOV = 1.2 cm, NEX = number of excitations; FOV = field of view). T_2-Weighted MRI images were obtained using a RARE sequence protocol (TR/TE/NEX = 5000/53/4; FOV= 1.2cm; MTX 128x128). The T_1/T_2 relaxation times were calculated using a standard saturation recovery spin echo. The image of tumorspheres dispersed in agar were obtained using a 3D FLASH gradient echo (TR/TE/NEX = 3500/18/2; FOV=1.14 cm; MTX 128x128x128).

APO-FITC and APO-rhodamine preparation

2 mg/mL Apoferritin solution in 0.1 M sodium carbonate buffer at pH 9 was prepared. Fluorescein isothiocyanate (FITC, Sigma-Aldrich) or Rhodamine isothiocyanate (Rhod) were dissolved in anhydrous DMSO at 1 mg/mL. For each mg of protein, 50 µL of dye (FITC or Rhod) solution were added slowly (in 5 µL aliquots) while stirring the protein solution. When all the required amount of dye solution had been added, the reaction mixture was incubated in the dark for 16 hours at 4°C. Then NH_4Cl was added to the solution to a final concentration of 50 mM, and it was incubated for other 2 hours at 4°C. The obtained Apoferritin solution was purified from non-entrapped dye with gel filtration using a G25 sephadex column, followed by dialysis. After purification, the solution was characterized in terms of protein concentration using the Bradford assay. The dye concentration was determined by measuring fluorescence (Horiba FluoroMax-4 spectrofluorometer), in Triton 0.1%, at 492/517 nm and 555/575 nm excitation/emission for FITC and Rhod, respectively.

APO-Rhodamine uptake experiments

MDA-MB-231, TUBO cells and their derived tumorspheres were incubated with increasing concentrations of APO-Rhod 24 hours post seeding. After 24 hours of incubation, cells were washed three times with ice-cold PBS and detached with trypsin/EDTA. Then cells were lysed by sonication using an ultrasonic probe device (30% power) and rhodamine concentration in the cytosolic extracts was determined by measuring fluorescence as described in the previous paragraph. Competition study has been performed by comparing fluorescence intensity of TUBO and MDA-MB-231 tumorspheres incubated with APO-Rhod 25 nM (protein concentration) in the presence and in the absence of H-Ferritin 250 nM for 24 hours. Fluorescence intensity (expressed as arbitrary units) was normalized to the total protein cell content.

Fluorescent microscopy

For SCARA5 detection, 3×10^5 TUBO and MDA-MB-231 cells were plated on glass coverslips and left to adhere overnight at 37°C in a 5% CO_2 incubator. 1×10^5 tumorsphere-derived cells were cytospinned (Cytospin 4, ThermoScientific) to glass slides. Then, cells were fixed with 4% formaldehyde solution in PBS (Sigma-Aldrich) and stained with an anti-SCARA5 antibody (Thermo Scientific), as previously described [25]. To visualize the internalization of Apoferritin, 6×10^5 disaggregated

TUBO-derived tumorspheres were incubated for 2 hours at 37°C with APO-Rhod (0,47 μM in Rhod and 0,073 μM in Apoferritin). Cells were then washed twice with ice-cold PBS, cytospinned to glass slides, fixed in cooled methanol for 10 min and permeabilized in cooled acetone for 1 min. Slides were then stained with anti-EEA1 (Cell Signaling Technology) or with anti-LAMP-1 (Santa Cruz Biotechnology) antibodies and visualized with AlexaFluor488 goat anti-rabbit or goat anti-mouse AlexaFluor488 secondary antibodies (Invitrogen), respectively. Cells were visualized with an ApoTome fluorescence microscope (Zeiss). Photographs were taken by using a digital CCD camera and images were processed using the AxioVision 4.8 software. The mean corrected total cell fluorescence (CTCF) was calculated on at least 100 cells per sample, using the following equation: CTCF = Integrated Density of selected cell - (Area of selected cell x Mean fluorescence of background readings). All measurements were performed using the ImageJ software.

Flow cytometric (FACS) analysis

Cells cultured as monolayers and their derived tumorspheres were incubated for different time intervals in the presence or absence of APO-Curcumin, free Curcumin, at a final Curcumin concentration of 50 μM, or Apoferritin (0.22 μM). Cells were then harvested and subsequently disaggregated using enzymatic and mechanical dissociation and washed in PBS supplemented with 0.2% BSA and 0.01% sodium azide (Sigma-Aldrich). Cells were then stained with the Annexin V apoptosis detection kit (eBioscience) according to the manufacturer's instructions. The amount of cell death induced by the treatments was calculated as ratio among the percentage of Annexin V^+ and propidium iodide $(PI)^+$ cells in treated samples compared to control cells.

To quantify APO-FITC uptake, cells were cultured with APO-FITC (1μM in FITC and 0.3 μM in APO) for 24 hours, then dissociated and stained with Alexa-Fluor647-conjugated anti-Sca-1 monoclonal antibody (Biolegend) as previously described [8]. All samples were analyzed using a CyAn ADP Flow Cytometer and the Summit 4.3 software (Beckman Coulter).

CSC self-renewal assay

Tumorspheres generated from MDA-MB-231 and TUBO cells were dissociated after 5 days of culture and plated at the density of 6×10^4 cells/mL in ultra low attachment six-well dishes in presence or not of APO-Curcumin, free Curcumin, at a final Curcumin concentration of 50 μM, or Apoferritin 0.22 μM. The total number of tumorspheres in each well was counted after 96 hours of culture and reported as number of tumorspheres generated per 10^3 cells plated [8].

Cell transfection

200 pmol of siRNA specific for SCARA5 (MSS291462) or negative control scrambled siRNA (Stealth RNAi Negative Control Hi-GC) were incubated with 10 μL Lipofectamin 2000 and diluted in Opti-MEM Reduced Serum Media (all from Thermo Fisher Scientific) according to the manifacturer's instructions. 1×10^6 TUBO tumorsphere-derived cells suspended in 2 mL tumorsphere growth medium were incubated with the transfection mix and harvested after 24, 48 or 72 hours and used for further experiments.

Western blotting

Cells were lysed with cell lysis buffer (0,5% NP-40, 150 mM NaCl, 50 mM Tris-HCl, 0,25 mM EDTA, 1 mM DTT, 1 mM Na_3VO_4 and 1:2000 protease inhibitor cocktail (all from Sigma-Aldrich)) as in [46]. 40 μg total proteins were resolved by SDS-PAGE and electroblotted onto PVDF membranes. After blocking with non-fat dry milk diluted in Tris-Buffered Saline – Tween (TTBS) 0,05%, membranes were probed with rabbit anti-SCARA5 (Santa Cruz Biotechnology) or mouse anti-vinculin (Santa Cruz Biotechnology) antibodies followed by HRP-conjugated anti-rabbit IgG or anti-mouse IgG (all from Sigma-Aldrich) and visualized with the ECL Western blotting substrate (Thermo Fisher Scientific), using a ChemiDoc Touch Imaging System (Biorad).

In vivo experiments

BALB/c mice (Charles River Laboratories) were maintained at the Molecular Biotechnology Center, University of Turin, and treated in accordance with University Ethical Committee and European guidelines under Directive 2010/63. Mice were subcutaneously (s.c.) challenged with 1×10^4 tumorsphere-derived cells (TUBO) and treated intravenously (i.v.) with APO-Curcumin (10 mg/Kg of Curcumin dose, corresponding to a protein dose of 53 mg/Kg) or Apoferritin (at the same protein dose) every three days, starting when they have developed a 2 mm mean diameter tumor, or left untreated. Tumor growth was monitored twice a week with a caliper and reported as the mean of two perpendicular diameters. When tumors reached 10 mm mean diameter, mice were euthanized for ethical reasons.

ACKNOWLEDGMENTS

Prof. Paola Turano, Dr. Caterina Bernacchioni, Dr. Silvia Ciambellotti are acknowledged for the preparation and purification of H-Ferritin and Prof. Juan Carlos Cutrin for histological analysis of mouse livers.

CONFLICTS OF INTEREST

All authors declare no conflicts of interest.

GRANT SUPPORT

This research was funded by MIUR (PRIN 2012 code 2012SK7ASN) and by the AIRC investigator Grant IG2013. This research was performed in the framework of the EU COST Action TD1004. L.C. was supported by a fellowship from Fondazione Umberto Veronesi.

REFERENCES

1. Frank NY, Schatton T, Frank MH. The therapeutic promise of the cancer stem cell concept. J Clin Invest. 2010; 120:41-50.
2. Maccalli C, De Maria R. Cancer stem cells: perspectives for therapeutic targeting. Cancer Immunol Immunother. 2015; 64:91-97.
3. La Porta CA, Zapperi S. Human breast and melanoma cancer stem cells biomarkers. Cancer Lett. 2013; 338:69-73.
4. Al-Hajj M, Wicha MS, Benito-Hernandez A, Morrison SJ, Clarke MF. Prospective identification of tumorigenic breast cancer cells. Proc Natl Acad Sci U S A. 2003; 100:3983-3988.
5. Nicolis SK. Cancer stem cells and "stemness" genes in neuro-oncology. Neurobiol Dis. 2007; 25:217-229.
6. Dontu G, Abdallah WM, Foley JM, Jackson KW, Clarke MF, Kawamura MJ, Wicha MS. In vitro propagation and transcriptional profiling of human mammary stem/progenitor cells. Genes Dev. 2003; 17:1253-1270.
7. Charafe-Jauffret E, Ginestier C, Birnbaum D. Breast cancer stem cells: tools and models to rely on. BMC Cancer. 2009; 9:202.
8. Conti L, Lanzardo S, Arigoni M, Antonazzo R, Radaelli E, Cantarella D, Calogero RA, Cavallo F. The noninflammatory role of high mobility group box 1/Toll-like receptor 2 axis in the self-renewal of mammary cancer stem cells. FASEB J. 2013; 27:4731-4744.
9. Lanzardo S, Conti L, Rooke R, Ruiu R, Accart N, Bolli E, Arigoni M, Macagno M, Barrera G, Pizzimenti S, Aurisicchio L, Calogero RA, Cavallo F. Immunotargeting of Antigen xCT Attenuates Stem-like Cell Behavior and Metastatic Progression in Breast Cancer. Cancer Res. 2016; 76:62-72.
10. Farnie G, Clarke RB, Spence K, Pinnock N, Brennan K, Anderson NG, Bundred NJ. Novel cell culture technique for primary ductal carcinoma in situ: role of Notch and epidermal growth factor receptor signaling pathways. J Natl Cancer Inst. 2007; 99:616-627.
11. Tallerico R, Todaro M, Di Franco S, Maccalli C, Garofalo C, Sottile R, Palmieri C, Tirinato L, Pangigadde PN, La Rocca R, Mandelboim O, Stassi G, Di Fabrizio E, et al. Human NK cells selective targeting of colon cancer-initiating cells: a role for natural cytotoxicity receptors and MHC class I molecules. J Immunol. 2013; 190:2381-2390.
12. Todaro M, D'Asaro M, Caccamo N, Iovino F, Francipane MG, Meraviglia S, Orlando V, La Mendola C, Gulotta G, Salerno A, Dieli F, Stassi G. Efficient killing of human colon cancer stem cells by gammadelta T lymphocytes. J Immunol. 2009; 182:7287-7296.
13. Sangiolo D, Mesiano G, Gammaitoni L, Leuci V, Todorovic M, Giraudo L, Cammarata C, Dell'Aglio C, D'Ambrosio L, Pisacane A, Sarotto I, Miano S, Ferrero I, Carnevale-Schianca F, Pignochino Y, Sassi F, et al. Cytokine-induced killer cells eradicate bone and soft-tissue sarcomas. Cancer Res. 2014; 74:119-129.
14. Lui GY, Kovacevic Z, Richardson V, Merlot AM, Kalinowski DS, Richardson DR. Targeting cancer by binding iron: Dissecting cellular signaling pathways. Oncotarget. 2015; 6:18748-18779. doi: 10.18632/oncotarget.4349.
15. Raza M, Chakraborty S, Choudhury M, Ghosh PC, Nag A. Cellular iron homeostasis and therapeutic implications of iron chelators in cancer. Curr Pharm Biotechnol. 2014; 15:1125-1140.
16. Schonberg DL, Miller TE, Wu Q, Flavahan WA, Das NK, Hale JS, Hubert CG, Mack SC, Jarrar AM, Karl RT, Rosager AM, Nixon AM, Tesar PJ, et al. Preferential Iron Trafficking Characterizes Glioblastoma Stem-like Cells. Cancer Cell. 2015; 28:441-455.
17. Geninatti Crich S, Cutrin JC, Lanzardo S, Conti L, Kalman FK, Szabo I, Lago NR, Iolascon A, Aime S. Mn-loaded apoferritin: a highly sensitive MRI imaging probe for the detection and characterization of hepatocarcinoma lesions in a transgenic mouse model. Contrast Media Mol Imaging. 2012; 7:281-288.
18. Finazzi D, Arosio P. Biology of ferritin in mammals: an update on iron storage, oxidative damage and neurodegeneration. Arch Toxicol. 2014; 88:1787-1802.
19. Tosha T, Behera RK, Ng HL, Bhattasali O, Alber T, Theil EC. Ferritin protein nanocage ion channels: gating by N-terminal extensions. J Biol Chem. 2012; 287:13016-13025.
20. Sun C, Yuan Y, Xu Z, Ji T, Tian Y, Wu S, Lei J, Li J, Gao N, Nie G. Fine-tuned h-ferritin nanocage with multiple gold clusters as near-infrared kidney specific targeting nanoprobe. Bioconjug Chem. 2015; 26:193-196.
21. Fantechi E, Innocenti C, Zanardelli M, Fittipaldi M, Falvo E, Carbo M, Shullani V, Di Cesare Mannelli L, Ghelardini C, Ferretti AM, Ponti A, Sangregorio C, Ceci P. A smart platform for hyperthermia application in cancer treatment: cobalt-doped ferrite nanoparticles mineralized in human ferritin cages. ACS Nano. 2014; 8:4705-4719.
22. Cutrin JC, Crich SG, Burghelea D, Dastru W, Aime S. Curcumin/Gd loaded apoferritin: a novel "theranostic" agent to prevent hepatocellular damage in toxic induced acute hepatitis. Mol Pharm. 2013; 10:2079-2085.

23. Gumulec J, Fojtu M, Raudenska M, Sztalmachova M, Skotakova A, Vlachova J, Skalickova S, Nejdl L, Kopel P, Knopfova L, Adam V, Kizek R, Stiborova M, Babula P, Masarik M. Modulation of induced cytotoxicity of doxorubicin by using apoferritin and liposomal cages. Int J Mol Sci. 2014; 15:22960-22977.

24. Liang M, Fan K, Zhou M, Duan D, Zheng J, Yang D, Feng J, Yan X. H-ferritin-nanocaged doxorubicin nanoparticles specifically target and kill tumors with a single-dose injection. Proc Natl Acad Sci U S A. 2014; 111:14900-14905.

25. Geninatti Crich S, Cadenazzi M, Lanzardo S, Conti L, Ruiu R, Alberti D, Cavallo F, Cutrin JC, Aime S. Targeting ferritin receptors for the selective delivery of imaging and therapeutic agents to breast cancer cells. Nanoscale. 2015; 7:6527-6533.

26. Gupta SC, Patchva S, Aggarwal BB. Therapeutic roles of curcumin: lessons learned from clinical trials. AAPS J. 2013; 15:195-218.

27. Anand P, Kunnumakkara AB, Newman RA, Aggarwal BB. Bioavailability of curcumin: problems and promises. Mol Pharm. 2007; 4:807-818.

28. Lanzardo S, Conti L, Rooke R, Ruiu R, Accart N, Bolli E, Arigoni M, Macagno M, Barrera G, Pizzimenti S, Aurisicchio L, Calogero RA, Cavallo F. Immunotargeting of antigen xCT attenuates stem-like cell behavior and metastatic progression in breast cancer. Cancer Res. 2016; 76:62-72.

29. Li JY, Paragas N, Ned RM, Qiu A, Viltard M, Leete T, Drexler IR, Chen X, Sanna-Cherchi S, Mohammed F, Williams D, Lin CS, Schmidt-Ott KM, Andrews NC, Barasch J. Scara5 is a ferritin receptor mediating non-transferrin iron delivery. Dev Cell. 2009; 16:35-46.

30. Gossuin Y, Muller RN, Gillis P. Relaxation induced by ferritin: a better understanding for an improved MRI iron quantification. NMR Biomed. 2004; 17:27-432.

31. Pozzi C, Di Pisa F, Bernacchioni C, Ciambellotti S, Turano P, Mangani S. Iron binding to human heavy-chain ferritin. Acta Crystallogr D Biol Crystallogr. 2015; 71:1909-1920.

32. Ravera E, Ciambellotti S, Cerofolini L, Martelli T, Kozyreva T, Bernacchioni C, Giuntini S, Fragai M, Turano P, Luchinat C. Solid-State NMR of PEGylated Proteins. Angew Chem Int Ed Engl. 2016; 55:2446-2449.

33. Sigismund S, Confalonieri S, Ciliberto A, Polo S, Scita G, Di Fiore PP. Endocytosis and signaling: cell logistics shape the eukaryotic cell plan. Physiol Rev. 2012; 92:273-366.

34. Aime S, Frullano L, Geninatti Crich S. Compartmentalization of a gadolinium complex in the apoferritin cavity: a route to obtain high relaxivity contrast agents for magnetic resonance imaging. Angew Chem Int Ed Engl. 2002; 41:1017-1019.

35. Runge VM, Parker JR. Worldwide clinical safety assessment of gadoteridol injection: an update. Eur Radiol. 1997; 7 Suppl 5:243-245.

36. Esatbeyoglu T, Huebbe P, Ernst IM, Chin D, Wagner AE, Rimbach G. Curcumin-from molecule to biological function. Angew Chem Int Ed Engl. 2012; 51:5308-5332.

37. Ravindran J, Prasad S, Aggarwal BB. Curcumin and cancer cells: how many ways can curry kill tumor cells selectively? AAPS J. 2009; 11:495-510.

38. Kakarala M, Brenner DE, Korkaya H, Cheng C, Tazi K, Ginestier C, Liu S, Dontu G, Wicha MS. Targeting breast stem cells with the cancer preventive compounds curcumin and piperine. Breast Cancer Res Treat. 2010; 122:777-785.

39. Li Y, Zhang T. Targeting cancer stem cells by curcumin and clinical applications. Cancer Lett. 2014; 346:197-205.

40. Kesharwani P, Banerjee S, Padhye S, Sarkar FH, Iyer AK. Hyaluronic Acid Engineered Nanomicelles Loaded with 3,4-Difluorobenzylidene Curcumin for Targeted Killing of CD44+ Stem-Like Pancreatic Cancer Cells. Biomacromolecules. 2015; 16:3042-3053.

41. Syng-Ai C, Kumari AL, Khar A. Effect of curcumin on normal and tumor cells: role of glutathione and bcl-2. Mol Cancer Ther. 2004; 3:1101-1108.

42. Zebib B, Mouloungui Z, Noirot V. Stabilization of curcumin by complexation with divalent cations in glycerol/water system. Bioinorg Chem Appl. 2010:292760.

43. Charpentier MS, Whipple RA, Vitolo MI, Boggs AE, Slovic J, Thompson KN, Bhandary L, Martin SS. Curcumin targets breast cancer stem-like cells with microtentacles that persist in mammospheres and promote reattachment. Cancer Res. 2014; 74:1250-1260.

44. Cavallo F, Quaglino E, Cifaldi L, Di Carlo E, Andre A, Bernabei P, Musiani P, Forni G, Calogero RA. Interleukin 12-activated lymphocytes influence tumor genetic programs. Cancer Res. 2001; 61:3518-3523.

45. Astolfi A, Landuzzi L, Nicoletti G, De Giovanni C, Croci S, Palladini A, Ferrini S, Iezzi M, Musiani P, Cavallo F, Forni G, Nanni P, Lollini PL. Gene expression analysis of immune-mediated arrest of tumorigenesis in a transgenic mouse model of HER-2/neu-positive basal-like mammary carcinoma. Am J Pathol. 2005; 166:1205-1216.

46. Conti L, De Palma R, Rolla S, Boselli D, Rodolico G, Kaur S, Silvennoinen O, Niccolai E, Amedei A, Ivaldi F, Clerico M, Contessa G, Uccelli A, Durelli L, Novelli F. Th17 cells in multiple sclerosis express higher levels of JAK2, which increases their surface expression of IFN-gammaR2. J Immunol. 2012; 188:1011-1018.

L-Ferritin targets breast cancer stem cells and delivers therapeutic and imaging agents

SUPPLEMENTARY MATERIALS AND METHODS

FACS analysis of CSC in tumors

Female BALB/c mice (Charles River Laboratories) were s.c. challenged with 1×10^4 tumorsphere-derived cells (TUBO) or with 1×10^5 TUBO cells, and tumor growth was monitored twice a week with a caliper. When tumors reached 10 mm mean diameter, mice were euthanized and tumors were explanted, finely minced with scissors and then digested by incubation with 1 mg/ml collagenase IV (Sigma Aldrich) in RPMI-1640 (Life Technologies) at 37°C for 1 hour in an orbital shaker. After washing in PBS supplemented with 2% FBS (Sigma-Aldrich), the cell suspension was incubated in an erylise buffer (155mM NH_4Cl, 15.8mM Na_2CO_3, 1mM EDTA, pH 7.3) for 10 minutes at room temerature. After washing in RPMI-1640 supplemented with 10% FBS, the cell suspension was passed through a 40 μm pore cell strainer, centrifuged at 1400 rpm for 10 minutes, treated with Fc receptor blocker (anti-CD16/CD32, BD Bioscences) and stained with PE-conjugated anti-CD44 and PE-Cy7-conjugated anti-CD24 antibodies (Biolegend) or with the Aldefluor kit (Stem Cell Technologies) according to the manufacturer's instructions. All samples were analyzed using a CyAn ADP Flow Cytometer and the Summit 4.3 software (Beckman Coulter).

Histopathological assesment

Liver fragments of 0.5 × 0.3 × 0.2 cm were fixed overnight in 4 % buffered formaldehyde solution at 4°C and processed by standard methods. Some 5 μm dewaxed sections stained with hematoxylin and eosin were used to evaluate the degree of damage.

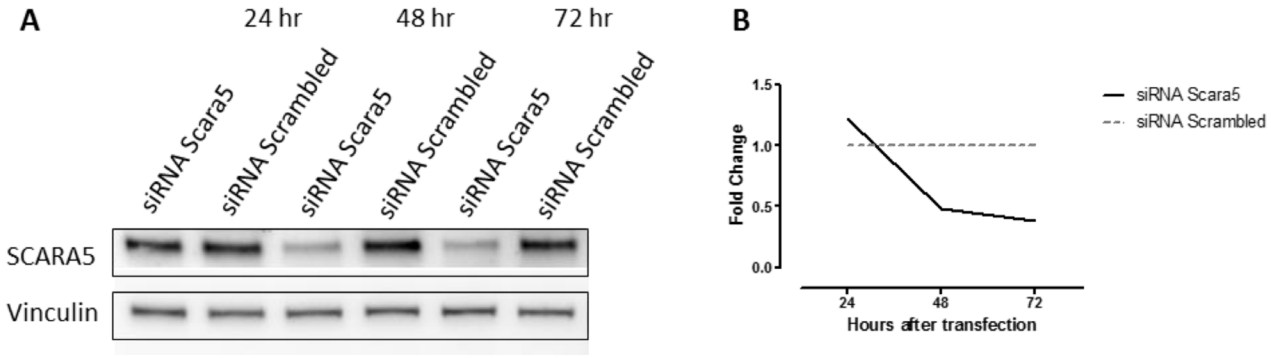

Supplementary Figure S1: Kinetics of SCARA5 silencing in tumorspheres. A. Immunoblot showing SCARA5 expression in TUBO-derived tumorspheres harvested 24, 48 or 72 hours after transfection with a siRNA specific for SCARA5 or with a negative control Scrambled siRNA. Vinculin expression was used as internal control. **B.** Graph showing fold-change values of SCARA5 protein expression in cells transfected with siRNA to SCARA5 versus cells transfected with Scrambled siRNA, normalized on vinculin levels.

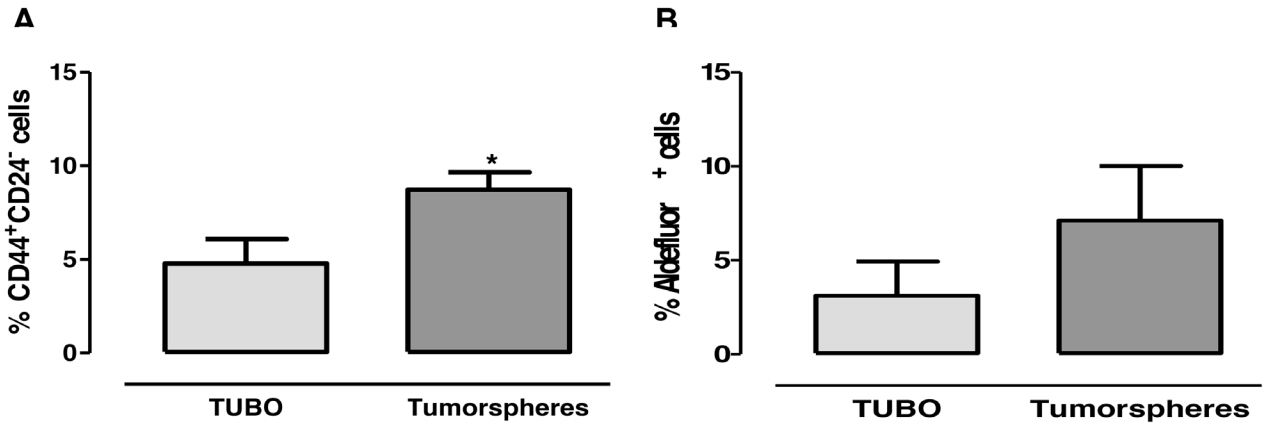

Supplementary Figure S2: Tumorsphere-induced tumors maintan a higher CSC percentage than TUBO tumors *in vivo*. FACS analysis of **A.** $CD44^+CD24^-$ and **B.** $Aldefluor^+$ CSC in 10 mm mean diameter tumors generated by s.c. injection of 10^5 TUBO or 10^4 tumosphere-derived cells in BALB/c mice. The graphs show the mean ± SEM of $CD44^+CD24^-$ or $Aldefluor^+$ cells from 7 tumors per group.*, $P<0.05$, Student's t test.

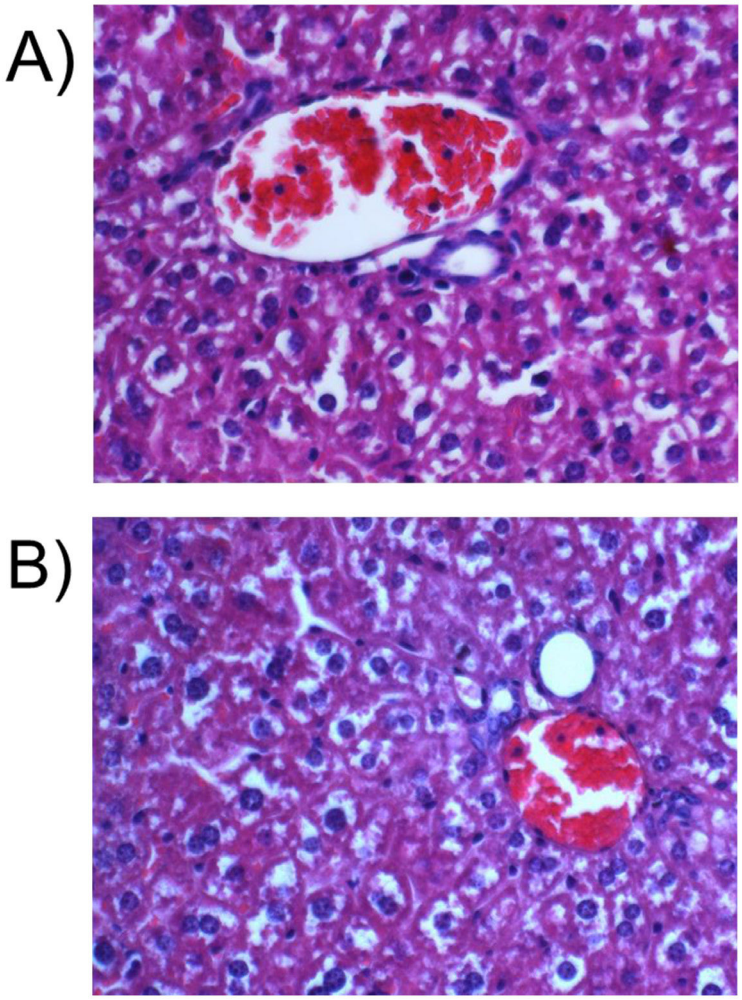

Supplementary Figure S3: APO-Curcumin treatment does not cause liver damage. Representative histological liver pictures from APO-curcumin **A.** and Apoferritin **B.** treated mice. 5µm tissue slices were stained with hematoxylin and eosin.

Supplementary Table S1: T_2 weighted MRI image Signal Intensities (S.I.)

	S.I. TUBO differentiated	*S.I.* TUBO tumorspheres	*S.I.* MDA-MB-231 differentiated	*S.I.* MDA-MB-231 tumorspheres
CTRL	$2.38x10^5$±0.20	$2.39x10^5$±0.25	$2.27x10^5$±0.19	$2.21x10^5$±0.063
Ferritin	$2.38x10^5$±0.17	$0.186x10^5$±0.051	$1.72x10^5$±0.059	$0.21x10^5$±0.070

Signal Intensity (S.I.) measured on T_2-weighted MRI images of TUBO and MDA-MB-231 cells (differentiated and tumorspheres) reported in Figure 2C.

Supplementary Table S2: Longitudinal Relaxation Rates (R_{1obs}, s^{-1}) measured at 7T

	$R_{1obs}(s^{-1})$ TUBO differentiated	$R_{1obs}(s^{-1})$ TUBO tumorspheres	$R_{1obs}(s^{-1})$ MDA-MB-231 differentiated	$R_{1obs}(s^{-1})$ MDA-MB-231 tumorspheres
CTRL	0.436±0.015	0.449±0.006	0.384±0.017	0.429±0.030
Apo-Gd	0.52±0.0068	0.597±0.008	0.483±0.015	0.717±0.020

Longitudinal Relaxation Rates (s^{-1}) measured on T_1-weighted MRI images of TUBO and MDA-MB-231 cells (differentiated and tumorspheres) reported in Figure 2C.

Addendum

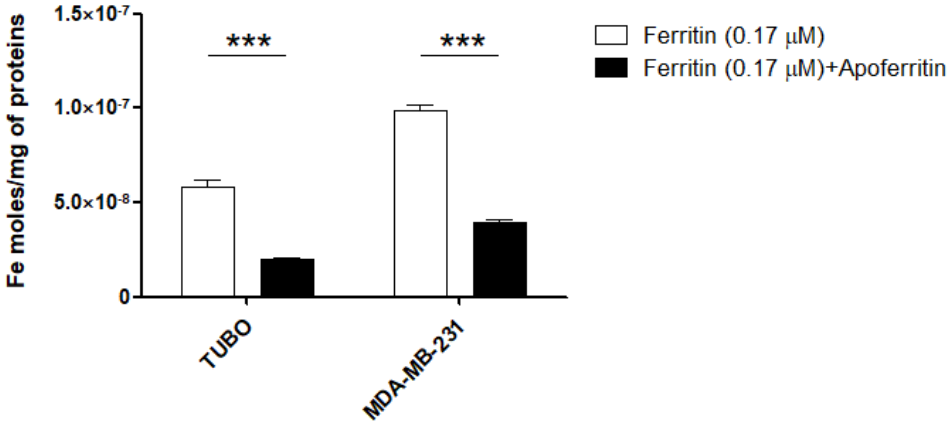

Competition study. ICP-MS determination of the intracellular iron content of tumorspheres from TUBO or MDA-MB-231 cultured for 24 hours with Ferritin 0.17 μM with or without excess Apoferritin. Graph shows the mean ± SEM of internalized iron moles every mg of cell proteins from three independent experiments. *** $p < 0.001$, unpaired Student's t test.

PAPER III

Comparative Transcriptomics of Triple Negative Breast Cancer Stem Cells and Differentiated Tumor Cells Identifies Teneurin-4 as a Potential Therapeutic Target

Roberto Ruiu[1], Maddalena Arigoni[1], Federica Riccardo, Laura Conti, Stefania Lanzardo, Raffaele Adolfo Calogero, Federica Cavallo and Elena Quaglino

Department of Molecular Biotechnology and Health Sciences, Molecular Biotechnology Center, University of Turin, Turin, Italy.

[1]These authors equally contributed to this work.

Abstract

Triple-negative breast cancer (TNBC) is insensitive to the most effective therapies for other breast cancers, thus the lack of specific treatments prompted us to search for new TNBC-associated molecules to be used as targets for cancer therapy. As patients with TNBC usually experience a quicker relapse and metastatic progression compared to other breast cancer subtypes, we hypothesized that cancer stem cells (CSC) could play a central role in TNBC. We thus directed our focus on genes differentially expressed between CSC and non-CSC of TNBC cell lines.

We established tumorsphere cultures from mouse and human mammary cancer cell lines to enrich the CSC population. RNA-Seq was used to identify differences in gene expression between tumorspheres and their monolayer counterparts.

Seventy-four transcripts were found upregulated in the tumorspheres, while forty-two genes were downregulated. Enrichment analysis of biological processes showed an up-regulation in genes involved in regulation of apoptosis in tumorspheres, and a down-regulation in genes involved in lipid metabolism and cell cycle regulation.

By focusing on up-regulated genes coding for cell membrane-associated proteins, we selected Teneurin-4 (TENM4) as a candidate for further studies. 4T1 tumorspheres treated with a siRNA specific to TENM4 showed a decrease in TENM4 mRNA and protein levels, which was reflected by a significant impairment of tumorsphere-forming ability. TENM4 silencing also led to a decrease in Focal Adhesion Kinase (FAK) phosphorylation, which has been previously linked to CSC biology, thus strengthening the possible link between TENM4 and a CSC-like phenotype.

Overall, our results indicate that the stem-like status of TNBC cells is accompanied by altered regulation of apoptosis, cell cycle and lipid metabolism pathways. Furthermore, we identified TENM4 as a potential novel player in CSC biology, and its targeting could help to improve the outcome of TNBC patients in the future.

Introduction

Triple negative breast cancer (TNBC) is one of the most aggressive types of human breast cancer, affecting 15-20% of breast cancer patients [1]. It is characterized by the lack of expression of estrogen receptor (ER), progesterone receptor (PR), and Her2. Compared with other subgroups of breast cancer patients, those with TNBC have a significantly higher risk of distant recurrence and death within 5 years from diagnosis [2]. Being negative for the expression of ER, PR and Her2, TNBC is insensitive to both endocrine and Her2-targeted therapies. The current lack of targeted therapies for TNBC leaves cytotoxic chemotherapy the main therapeutic approach. Despite an overall poor prognosis, TNBC patients have a higher response rate to chemotherapy compared to non-TNBC, with patients reaching a pathologic complete response having good prognosis. However, TNBC patients with residual disease (which represent 60-70% of chemotherapy treated patients [3]) usually have a shorter overall survival driven by higher relapse rate compared to non-TNBC-patients, a phenomenon described as "TNBC paradox" [4].

In recent years, cancer stem cells (CSC) have gained intense interest as they are thought to play a pivotal role in recurrence following chemotherapy [5]. CSC are a small population of tumor-initiating cells in the tumor that are endowed with the ability to self-renew and differentiate into non-tumorigenic daughter cells that constitute the bulk of the tumor. Conventional treatments - i.e. chemo- and radiotherapy - designed to shrink the bulk of a tumor may fail to eliminate the small fraction of CSC, or even drive the evolution of differentiated tumor cells towards the CSC phenotype [6]. Therefore, the final success of a treatment may rest on complete or functional CSC suppression [7]. The identification of appropriate molecular targets expressed by CSC thus may be critical in the development of more effective anticancer therapies.

Stem cell culture as floating monoclonal spheres was first described for normal neural stem cells [8,9], and was subsequently adopted for normal stem cells from other tissues, including breast [10]. Growth medium for stem cell expansion as spheres is commonly deprived of serum and enriched with growth factors such as epidermal growth factor (EGF) and basic fibroblast growth factor (bFGF), as well

insulin and other stimuli that favor stem cell proliferation [11]. Moreover, the growth in low-attachment flasks leads to death by *anoikis* of differentiated cells, while stem cells proliferate as spherical clones [11]. The need to expand the small population of CSC and to study its properties *in vitro* prompted researchers to adopt the tumorsphere methodology as a strategy to propagate and maintain long-term culture of CSC [12]. Moreover, the assessment of the ability of cells to generate tumorspheres (tumorsphere-forming assay) has been frequently adopted as an *in vitro* surrogate of tumor initiating potential evaluation [11].

Our experience with tumorspheres and CSC started in 2008, when tumorspheres were used to enrich a subpopulation of Sca-1$^+$ breast cancer cells deriving from mammary tumors of the rat Her2-transgenic mouse model BALB-neuT. These Sca-1$^+$ cancer cells were found to be responsible for tumor-initiation *in vivo* [13]. Since then, we have exploited the tumorsphere model as a means to discover potential targets for cancer therapy, by comparing the gene expression profile of tumorspheres derived from a BALB-neuT derived mammary tumor cell line with that of the same cell line grown as monolayer [14]. This approach allowed us to identify novel therapeutic targets for breast cancer, including TLR2 [15], xCT [16] and SCARA5 [17].

In the current study, taking advantage of our workflow developed for the identification of antigens expressed by Her2$^+$ breast CSC [15], we performed a transcriptome analysis of epithelial-like cells grown as a monolayer (hereafter named parental cells and abbreviated as P in the graphs) and CSC-enriched tumorspheres derived from human and mouse TNBC cell lines. This analysis led us to the identification of different biological processes differentially regulated between parental cells and tumorspheres, as well as a novel candidate TNBC-associated target - teneurin transmembrane protein 4 (TENM4) - whose expression increases from parental cells to tumorspheres.

TENM4 is a ~300 kDa member of the tenascin family of transmembrane glycoproteins, which plays fundamental roles in embryogenesis and central nervous system (CNS) development. Little is known about the function of teneurins in adult organisms. Several studies suggest that they may be

implicated in tumorigenesis in various but not defined ways [18]. This is the first study that reports a TENM4 role in the triple negative breast CSC biology.

Materials and Methods

Cell cultures and Tumorsphere formation

4T1 (cod. CRL-2539), HCC1806 (cod. CRL-2335), MDA-MB-231 (cod. HTB-26), MCF-7 (cod. HTB-22) and SK-BR-3 (cod. HTB-30) cell lines were purchased from American Type Culture Collection (ATCC, Manassas, VA, USA). 4T1, HCC1806 and MCF-7 cells were grown in RPMI-1640 growth medium (Sigma-Aldrich, St. Louis, MO, USA) while MDA-MB-231 and SK-BR-3 were grown in Dulbecco's Modified Eagle Medium (DMEM, Thermo-Fisher Scientific, Waltham, MA, USA). Both growth media were supplemented with 10% fetal bovine serum (FBS, Sigma-Aldrich) and Penicillin/Streptomycin solution at 1x dilution (Sigma-Aldrich). When sub-confluency was reached - approximatively every second day - cells were dissociated using trypsin-EDTA 0.5% at 1x dilution in PBS (Sigma-Aldrich) and seeded into new flasks. To generate first-passage tumorspheres (referred to as T1), trypsin-dissociated cells were resuspended in tumorsphere growth medium at a concentration of 1.5 x 10^5 cells/mL in Corning® ultra-low attachment flasks (Sigma-Aldrich). Tumorsphere growth medium was composed of DMEM/Nutrient Mixture F-12 Ham (Sigma-Aldrich) supplemented with 0.4% bovine serum albumin (BSA, Sigma-Aldrich), 20 ng/mL bFGF (PeproTech EC Ltd., London, UK), 20 ng/mL EGF (Sigma-Aldrich) and 5 µg/mL insulin (Sigma-Aldrich). Tumorsphere growth medium was added fresh every second day. After 5 days in culture, T1 tumorspheres were enzymatically dissociated and a single-cell suspension was plated as for T1 to generate second-passage tumorspheres (referred to as T2). The same protocol was performed to generate third-passage tumorspheres (referred to as T3) from dissociated T2. All the cells were periodically tested for mycoplasma contamination with the MycoAlert™ Mycoplasma Detection Kit (Lonza, Basel, Switzerland). All cells used resulted to be free of mycoplasma.

Immuno-staining and flow cytometry analysis

Following enzymatic dissociation, cells were stained within flow cytometry tubes with AlexaFluor®647 anti-mouse Sca-1, PE anti-human/mouse CD44, AlexaFluor®488 anti-human CD24 or PE/Cy7 anti-mouse CD24, and AlexaFluor®647 anti-human/mouse CD49f antibodies (all from BioLegend, San Diego, CA, USA) at a 1:100 dilution. Following 30 min incubation at 4°C, cells were washed in PBS supplemented with 0.2% BSA and 0.01% sodium azide. For the evaluation of ALDH activity, Aldefluor™ kit (STEMCELL Technologies, Vancouver, Canada) was used. Briefly, ALDH substrate was administered to cells treated or not with the ALDH inhibitor DEAB within flow cytometry tubes. Following 45 minutes incubation at 37°C, 5% CO_2, cells were rinsed in Aldefluor buffer. Cell viability was assessed by evaluating propidium iodide (PI) incorporation. Data were acquired through CyAn ADP flow cytometer (DakoCytomation, Beckman Coulter, Brea, CA, USA) and data were analyzed using Summit 4.3.02 Build software (Beckman Coulter).

Total RNA extraction and RNA sequencing.

Total RNA was isolated from 2 x 10^6 parental cells and T2-derived cells from HCC1806 and 4T1 cell lines using the TriZol reagent (Thermo-Fisher Scientific) and following manufacturer's instructions. Genomic DNA contaminations were removed from RNA samples with the Ambion® DNA-free kit (Thermo-Fisher Scientific). RNA concentration and quality were estimated with NanoVuePlus Spectrophotometer (GE Healthcare, Little Chalfont, UK) and Agilent 2100 Bioanalyzer (Agilent Technologies, Santa Clara, CA, USA), respectively. Libraries for RNA sequencing were generated using TruSeq RNA sample preparation kit v2 (Illumina Inc., San Diego, CA, USA) following manufacturer's instructions, using 1 µg of total RNA as input material and 15 PCR cycles for DNA amplification. Libraries were quantified by Qubit 2.0 Fluorometer using ds DNA High Sensitivity Qubit Assay (Thermo-Fisher Scientific) and pooled together in equimolar amounts.

Cluster generation was performed using a cBot System (Illumina Inc.). Libraries were sequenced with an Illumina HiSeq 1000 sequencer (Illumina Inc.) generating 100-bp paired-end sequences.

RNAseq data analysis

The quality of RNAseq data was evaluated with FASTQC tool (http://www.bioinformatics.babraham.ac.uk/projects/fastqc/). Coding RNAs were quantified mapping reads against UCSC database. Differential expression analysis was performed with limma [19] using voom normalization and BH procedure for p value correction [20]. The genes with a $Log_2FC \geq 1$ or $Log_2FC \leq -1$ and adjusted p-value ≤ 0.1 were considered as differentially expressed between bulk cell line and the corresponding tumorspheres. The resulting datasets were then loaded on Ingenuity Pathway Analysis (IPA, www.ingenuity.com) and only annotated transcripts were considered for further analysis. As ultimate filter, only annotated transcripts that resulted to be up- or down-regulated in the tumorspheres of both mouse 4T1 and human HCC1806 cell lines were considered. This allowed the generation of down-regulated and up-regulated genesets.

Gene ontology analysis

Down-regulated and up-regulated genesets were separately entered into the Gene Ontology (GO) enrichment analysis tool available at the Gene Ontology Consortium website (http://www.geneontology.org/page/go-enrichment-analysis) and analyzed through the PANTHER Overrepresentation Test (release version 2016/07/15) using the *Homo sapiens* reference list (all genes in the GO database released on 2017/02/28). Gene ontology option "GO biological process complete" was selected and a functional annotation chart was generated. A maximum *p*-value of 0.05 was chosen to select only significant categories.

Meta-analysis on patient databases

For prognostic analyses, the Kaplan-Meier Plotter free software (http://kmplot.com/analysis/) [21] was used. Relapse-free survival (RFS) data were presented as Kaplan – Meier plots and tested for significance using log-rank tests. Patients were stratified by expression of the gene of interest. To define the cutoff between high and low expression, all percentiles between the lower and upper quartiles were computed, and the best performing threshold was used as a cutoff through "auto select best cutoff" function.

In case the gene of interest had more than one microarray reporter available (Affymetrix ID), the mean expression of all available probes for a given gene was used. Analysis was restricted to samples displaying negative ER, PR and Her2 status.

The relative mRNA expression of TENM4 in human breast tumor samples was determined by querying the Oncomine database (https://www.oncomine.org/ version 4.5). TENM4 mRNA expression was queried in The Cancer Genome Atlas (TCGA) breast cancer dataset (released 2011/09/02) investigating the Agilent IDs A_23_P47746, A_24_P342309 and A_24_P342312. Oncomine output data were sorted to isolate specified associations as indicated and reported as the log2 median-centered ratio using box-and-whiskers plots (dots: maximum and minimum values; whiskers, 90/10 percentiles; box, 75/25 percentiles; line, median of all samples).

Real-Time PCR

DNA-free RNA was prepared as reported above in the RNA extraction section. cDNA was obtained by 1 µg of RNA retro-transcribed with Ambion® RETROscript reagents (Thermo-Fisher Scientific). Target mRNA was amplified through real-time PCR using gene-specific primers (QuantiTect Primer Assay; Qiagen, Chatsworth, CA, USA) and SYBR green PCR Master Mix (Applied Biosystems). A 7300 RT-PCR system (Applied Biosystems) was used to perform the real-time PCR and the Applied Biosystems SDS Software Version 1.3.1 was used to analyze data. Quantitative normalization was performed on the expression of GAPDH. The expression levels relative to parental cells were calculated using the comparative ΔCt method [22].

Immunoblotting

Frozen or fresh cells, not previously treated with trypsin, were incubated in RIPA buffer (150 mM NaCl; 50 mM Tris-HCl pH 8.00; Sodium dodecyl sulphate (SDS) 0.1%; Sodium Deoxycholate 0.5%; Nonidet P-40 1%) supplemented with $NaVO_4$, NaF, PMSF and protease inhibitors cocktail (Sigma-Aldrich) for 40 min on ice. Cell lysates were centrifuged 5 min at 14.000 *g* and the protein-containing supernatant was harvested for use. Total protein concentration was quantified using the Pierce™ BCA Protein Assay Kit (Thermo-Fisher Scientific). Following 5' denaturation at 95°C in 2-Mercaptoethanol-containing Laemmli Sample Buffer (Bio-Rad, Hercules, CA, USA), equal amounts of protein (ranging between 30 and 70 µg) were separated through electrophoresis in an Any kDa Mini-Protean TGX precast gel (Bio-Rad) and then transferred onto an Immobilion-P PVDF membrane (Merck Millipore, Billerica, MA, USA). Following blocking with 5% nonfat dry milk (Santa Cruz Biotechnology, Dallas, TX, USA) or 5% BSA (Sigma-Aldrich) in wash buffer (Tris Buffered Saline (TBS) supplemented with 0.05% Tween-20 from Sigma-Aldrich), the membrane was incubated overnight at 4°C with sheep anti-TENM4 (R&D Systems, Minneapolis, MN, USA), mouse anti-total FAK (Thermo-Fisher Scientific), rabbit anti-pY397 FAK (Cell Signaling Technology, Danvers, MA, USA), rabbit anti-pY925 FAK (Cell Signaling Technology), mouse anti-Vinculin (produced in house) or mouse anti-β-Actin (Santa Cruz Biotechnology) antibodies in blocking buffer. Membrane was then rinsed and incubated 1 hr at room temperature with HRP-conjugated anti-rabbit (Sigma-Aldrich), anti-mouse (Sigma-Aldrich) or anti-sheep (R&D Systems) antibody in blocking buffer. Vinculin or β-actin were used as loading control. Membranes were incubated with Pierce® ECL Western Blotting Substrate (Thermo Fisher Scientific) and images were acquired using a ChemiDoc™ Touch Imagin System (Bio-Rad). Peak area was computed using ImageJ software (imagej.nih.gov/ij/index.html). Relative density of the signal of the protein of interest or of the loading control was calculated using the sample with the most intense signal as a reference. Relative density of the protein of interest was further normalized on the relative density of the loading control.

RNAi

A mixture of four TENM4-specific siRNA provided as a single reagent (ON-TARGETplus siRNA Pool; Dharmacon Inc, Lafayette, CO, USA) was used to downregulate the expression of murine TENM4 mRNA. A mixture of four non-specific siRNAs provided as a single reagent (ON-TARGETplus Non-targeting Control Pool; Dharmacon) was used as negative control. 4T1 T2-derived single cell suspension was seeded in 2 mL antibiotic-free tumorsphere growth medium per well in a Corning® Ultra-Low attachment 6-well plate (Thermo-Fisher Scientific). The following day, 500 pmoles of TENM4-specific or negative control siRNA were incubated with Lipofectamine® 2000 (Thermo-Fisher Scientific) in a final volume of 0.5 mL Gibco® Opti-MEM I Reduced Serum Medium (Thermo-Fisher Scientific) and administered to the cells. 48 hrs after transfection, tumorspheres were harvested and frozen for downstream application or counted to assess the tumorsphere-generation ability of treated cells.

Tumorsphere-generation assay

To assess the clonogenic potential of cells in low-attachment conditions, a 4T1 T2-derived single cell suspension was seeded in antibiotic-free tumorsphere growth medium at a concentration of 6 x 10^4 cells/mL in a Corning® Ultra-Low attachment 6-well plate (Thermo Fisher Scientific) and treated as reported above in the "RNAi" section. Forty-eight hrs after treatment, tumorspheres were harvested and 400 µL of tumorsphere suspension were distributed dropwise in a 96-well plate. The number of tumorspheres per well were counted though an optical microscope in a 400x magnification and summed, then the total number of tumorspheres was calculated and the ratio of tumorspheres generated per 1 x 10^3 cells seeded was inferred with the following formula:

$$X = \frac{(Total\ number\ of\ tumorsphere\ ) \times 10^3}{Total\ number\ of\ cells\ initially\ plated}$$

Cell proliferation assay

The tumorspheres were harvested, washed with PBS, centrifuged and resuspended in PBS. The tumosphere suspension was then distributed in a 96-well plate, 50 µL/well, and incubated with 0.83 µg/µL of 3-(4,5-dimetiltiazol-2-il)-2,5-difeniltetrazol (MTT; Merck Millipore). Following overnight incubation at 37°C, formazan crystals were dissolved by adding 100µL isopropanol with HCl 0.04 N to each well. Optical density was measured on an ELISA plate reader with a test wavelength of 570 nm and a reference wavelength of 630 nm. Difference between 570 nm and 630 nm readings represents the output value.

Statistical analysis

Differences of gene expression assessed by real-time PCR or western blot, tumorsphere generation potential and proliferation were evaluated using an unpaired *Student's t test*. RFS of patients was assessed through a log rank test. Data are generally shown as means ± SEM unless otherwise stated. Values of $P < 0.05$ were considered significant unless otherwise stated.

Results

Tumorspheres formation and characterization.

We selected the 4T1 and HCC1806 cell lines as model for Triple Negative Breast Cancer in mouse and human, respectively. Based on culture conditions previously established for these and other breast cancer cell lines[15–17], we successfully generated tumorspheres from the parental cells **(Fig. 1A)**. Since breast CSC are generally isolated through mammary stem cell marker expression, we assessed CSC enrichment in tumorspheres by analyzing the expression of different stem cell markers by flow cytometry. As shown in **Fig. 1B and C**, parental cells and tumorpheres of both 4T1 and HCC1806 cell lines displayed high variability in the expression of such markers in a cell line-dependent manner. In general, almost 100% of 4T1 cells grown either as monolayer or tumorspheres were positive for both CD44 and CD24 expression, with $CD44^+/CD24^-$ phenotype being represented only by a small minority of cells (**Fig. 1B, C**). Conversely, less than 1% of HCC1806 cells grown as monolayer or tumorspheres displayed positivity either for CD44 or CD24, with the majority of the cells being double negative. Regarding the marker CD49f, both parental cells and tumorspheres from 4T1 were all positive, but 4T1 tumorspheres displayed a mean fluorescence intensity (MFI) that was significantly higher compared to parental cells (**Fig. 1C**). Regarding the murine CSC marker Sca-1, 4T1 tumorspheres displayed a trend of increase in the percentage of $Sca\text{-}1^+$ cells and a significant increase in the MFI compared to parental cells. These data indicate that $Sca1^+$ or $CD49f^+$ parental cells and cell composing tumorspheres in 4T1 are similar in percentage, but the latter have a significantly higher expression of such markers. In HCC1806, CD49f was expressed to a similar extent in parental cells and tumorspheres. Another CSC property frequently investigated is the positivity for ALDH activity, performed through an enzymatic assay (Aldefluor assay) that allows assessment of $ALDH^+$ through flow cytometry. 4T1 and HCC1806 displayed a different behavior in this context, with tumorspheres from HCC1806 having a trend of increase in ALDH activity compared to cells grown as monolayers (**Fig. 1B, C**), while a completely opposite situation was

observed for 4T1 cells (**Fig. 1B**). Hence, markers commonly used for the characterization of breast CSC display a high degree of heterogeneity in the two cell lines.

Identification of downregulated and upregulated gene sets and their related biological processes

RNA from parental cells and tumorspheres was extracted and sequenced, and RNA sequencing data were analyzed as reported in the "materials and methods" section. We considered as differentially expressed only genes whose $\log_2$ fold change in expression was either $\leq$-1 (down-regulated in tumorspheres) or $\geq$1 (up-regulated in tumorspheres) with a p-value $\leq$0.1. Results are summarized in **Fig. 2A**, which shows the proportion of transcripts up-regulated, down-regulated or non-changing for each cell line. Among the differentially expressed transcripts, a minor proportion was shared between 4T1 and HCC1806 cell lines, thus allowing us to narrow the field of analysis to find CSC-associated transcripts in common between murine and human TNBC (**Fig. 2A**, right panels). In summary, 74 transcripts were up-regulated in the tumorspheres of both HCC1806 and 4T1, while 42 transcripts were down-regulated.

The two sets of genes detected as differentially expressed between parental cell lines and the corresponding tumorspheres were analyzed through the Gene Ontology (GO) enrichment analysis tool. This analysis helped to put data into a biological context and quickly focus on the most relevant genes, thus allowing to better understand the biological implications of the molecular events characterizing the enrichment of CSC within tumorspheres. Results are summarized in **Fig. 2B**. Enrichment analysis of GO biological processes showed an enrichment in genes involved in lipid and cholesterol biosynthesis and cell cycle regulation in the gene set down-regulated in tumorspheres (**Fig. 2C**). It is worth noting that many of the genes in the up-regulated set code for proteins with pleiotropic functions, which are thus involved in different biological processes. Therefore, many of the genes we found to be up-regulated take part to many of the enriched biological processes. For instance, NR4A2 is not only related to negative regulation of apoptosis, but also to positive regulation of biosynthetic process, neurogenesis, response to stress, cell communication and many others (for a

complete list of biological functions enriched in the genesets, and their related genes belonging to the genesets, see **Supplementary Table 1**).

Therefore, since key genes required for the progression of the cell cycle through the G2/M phase and for the biosynthesis of cholesterol and of lipids are significantly down-regulated in tumorspheres, these results suggest that CSC likely are in a relatively quiescent state accompanied by a reduced biosynthesis of cholesterol and lipids. On the contrary, genes that are involved in the negative regulation of apoptosis are upregulated in tumorspheres, suggesting that CSC are more resistant to apoptosis compared to parental cells.

TENM4 emerges as a potential target for TNBC treatment

When looking for candidate targets among the up-regulated genes, we narrowed our search only to genes whose protein products are predicted to be expressed on the cell surface. This approach was chosen in order to find molecules easily targetable by antibody-mediated trategies. The selected genes are listed in **Table 1**. To further select only genes of interest for TNBC patients, we ran a meta-analysis on a set of publicly available microarray data from breast cancer patients (http://kmplot.com/analysis/). High expression of 5 out of the 17 candidate genes were related to good prognosis in terms of relapse-free survival (RFS) in TNBC patients (3 significantly and 2 non-significantly) and were therefore excluded. Among the remaining 12 candidates, 3 significantly related to shorter RFS (ACVR2B, COMTD1 and F11R, p-value < 0.05) and 6 displayed a trend of association to shorter RFS (IGF1R, ITGA10, PIP5K1C, PMP, SSC5D, TENM4, p-value ≤ 0.1) (**Fig. 3** and **Supplementary Fig. 1**). While reviewing the literature, we found TENM4 of particular interest, since it had no reported direct link to cancer but had a role in development, making it an unexplored CSC-associated target. TENM4 was one of the top ranking differentially expressed genes between tumorspheres and parental cells (>5-fold increase in HCC1806, >7-fold increase in 4T1, **Table 1**). Querying for its expression in the TCGA database, TENM4 mRNA resulted to be expressed at higher levels in both Invasive Ductal Carcinoma (IDC) and Invasive Lobular Carcinoma (ILC) of the breast

compared to normal breast (**Fig. 3**). Given these premises, we decided to further investigate the role of TENM4 in our TNBC model.

Teneurin-4 may be functionally related to the CSC phenotype through FAK

TENM4 gene codes for Teneurin transmembrane protein 4 (Teneurin-4, TENM4), a type II transmembrane protein of ~300 kDa, whose expression in healthy tissues is restricted to CNS and developing limbs. Its misregulated expression has been linked to neurological and behavioral disorders, but its link to cancer has not been clarified yet. We observed TENM4 mRNA upregulation in tumorspheres of different breast cancer cell lines compared to parental cells through RT-PCR (**Fig. 4A**, left panel). The upregulation was not restricted only to 4T1 and HCC1806, but was significant also in MDA-MB-231 (human TNBC cell line) and MCF-7 (human ER^+ breast cancer cell line), and with a positive trend in SK-BR-3 (human $Her2^+$ breast cancer cell line). Furthermore, we validated TENM4 upregulation at the protein level in 4T1 and HCC1806 (**Fig. 4A**, right panel, and **Supplementary Fig. 2A**). 4T1 tumorspheres treated with a pool of siRNAs specific to TENM4 showed a significant decrease in TENM4 mRNA and protein levels compared to unspecific siRNA-treated cells (**Fig. 4B** and **Supplementary Fig. 2B**), which was reflected by a partial but significant impairment of tumorsphere-forming ability (**Fig. 4C**). This suggests a role of TENM4 in the maintenance of self-renewal. Since TENM4 has been shown to be functionally linked to FAK in non-transformed cells [23], we investigated whether TENM4 and FAK interact in a cancer cell setting. 4T1 tumorspheres displayed an increase in FAK protein and its phosphorylation level (**Fig. 4A**, right panel), which has been reported in literature to be an important feature of stem-like phenotype [24]. TENM4 silencing through siRNA led to a small but significant decrease in FAK phosphorylation (**Fig. 4B**), thus strengthening the possible link between TENM4 and a CSC-like phenotype.

Discussion

In the present study, we have used a transcriptomic approach to identify genes differentially expressed between TNBC cells grown as monolayer and their derived tumorspheres. We have selected the genes that were differentially expressed in both the TNBC cell lines employed in this study, the murine 4T1 and the human HCC1806. 4T1 cell line is generally described as being triple negative based on the lack of expression of ER, PR and Her2 on its cell membrane. We were interested in studying a murine breast cancer cell line since it would allow a better recapitulation of the disease *in vivo* compared to xenotrasplantation models. Injection of tumor cells in syngeneic mice will allow a proper interaction between the cancer cells and the host microenvironment cells, including those belonging to the immune system. Therefore, selecting molecules of interest in a murine model will allow the development of immune-based targeted approaches, such as anti-tumor vaccination. We included a human TNBC cell line in our analysis to narrow our selection to genes of potential translational relevance in humans.

Despite their ability to form floating tumorspheres in low attachment conditions, 4T1 and HCC1806 cell lines greatly differed one from the other for what concerns CSC marker expression. Despite the $CD44^+/CD24^-$ population being basically absent in tumorspheres of both cell lines, the totality of 4T1 cells (both tumorspheres and parental cells) were strongly positive for both CD44 and CD24 expression, while almost the totality of HCC1806 were negative for both. We are not surprised of this discrepancy. Despite the $CD44^+/CD24^-$ immunophenotype being suggested as identifying breast CSC [25], several authors expressed concerns about their significance as CSC markers [26–28]. Furthermore, in the highly cited paper by Ginestier and colleagues [29], the overlap between $Aldefluor^+$ and $CD44^+/CD24^-$ populations was less than 1%, despite both populations having highly enriched tumorigenic potential. It has been proposed that these two populations reflect distinct epithelial-like and mesenchymal-like CSC, with different phenotypes and different distributions within the same tumor [30], and different distributions between these two populations have been observed for distinct intrinsic subtypes of breast cancer [31]. Given the reported lack of overlap between these populations,

414 it is not surprising that the opposite immunophenotype observed between 4T1 and HCC1806 is
415 reflected by an equally opposite trend in terms of Aldefluor activity, with HCC1806 tumorspheres
416 displaying a higher positivity for Aldefluor compared to parental cells. Regarding another marker,
417 CD49f (Integrin alpha 6), both tumorspheres and parental cells of HCC1806 line were moderately
418 positive, while 4T1 cells were strongly positive, with tumorspheres displaying a significantly higher
419 expression compared to parental cells. Furthermore, tumorspheres from 4T1 cell line had a
420 significantly stronger expression of the murine breast cancer stem cell marker Sca-1 compared to
421 their parental counterpart. This is consistent with what we previously observed for tumorspheres from
422 primary tumor- and cell line-derived $Her2^+$ tumorspheres [13,15], which displayed an increased tumor-
423 initiating potential compared to their monolayer, or $Sca\text{-}1^-$, counterpart.
424 Tumorspheres currently represent a widely used model in cancer stem cell studies, thus a deep
425 understanding of the processes involved in their biology is of relevance for those involved in the field.
426 Comparison of the transcripts differentially expressed in tumorspheres of 4T1 and HCC1806 cell
427 lines allowed us to identify biological processes of interest for both murine and human breast cancer
428 stem cells.
429 The enrichment of genes involved in cell cycle progression in the down-regulated gene set suggests
430 that tumorspheres could be enriched in quiescent or slow cycling cells. The idea that CSC may indeed
431 be quiescent is not new, and a certain number of studies demonstrated that different cancer types
432 contain a subset of quiescent or slow cycling CSC (reviewed in ref [32] and ref [33]), thus recapitulating
433 the features seen in normal adult tissues, where quiescent stem cells give rise to fast proliferating
434 transiently amplifying cells that lack self-renewing potential but contribute to tissue regeneration.
435 Pece and colleagues showed that label-retaining quiescent cells from mammary glands are able to
436 support generation of mammospheres *in vitro* and to completely regenerate mammary glands *in vivo*
437 [34]. Interestingly, the transcriptional signature of these label-retaining cells was shown to be enriched
438 in grade 3 compared to grade 1 tumors, and could separate basal-like breast cancer from other
439 subtypes. Notably, cells from grade 3 tumors display higher content of label-retaining cells, as well

as tumor-initiating potential, compared to grade 1 tumors. This increase in number of CSC could be due to a shift towards symmetrical stem cell division in more undifferentiated tumors [34]. Similar to primary tissue, also breast cancer cell lines seem to retain a subpopulation of cells with stem-like properties that cycle at a slower rate compared to the bulk of the cell line [35]. Importantly, quiescence has been described as one of the several mechanisms actuated by CSC to survive chemotherapy, which preferentially targets actively proliferating cells. Using *in vivo* tracing of a tumor cell subpopulation in a genetically engineered mouse model of glioblastoma, Chen and colleagues showed that not all tumor cells but a restricted and relatively quiescent cell population with CSC features is responsible for the tumor re-growth following treatment of the mice with Temozolomide [36]. Re-growth from these surviving cells was shown to occur through the production of highly proliferative transiently amplifying tumor cells derived from quiescent CSC [36]. Similarly, experiments based on tracing with a fluorescent marker a subpopulation of human breast cancer cells with CSC features in xenograft models showed that fluorescent CSC are not proliferating. However, the pool of fluorescent CSC expanded through increased proliferation following radiotherapy, thus repopulating the tumor [37]. Going back to the tumorsphere model, our findings that genes involved in cell cycle progression are downregulated in tumorspheres is consistent to what reported by others in *in vitro* studies, which showed that the majority of cells composing tumorspheres from primary breast cancer [38] or breast cancer cell lines [39] have a higher proportion of non-proliferating cells compared to cells grown as monolayer. This could be the result of either an artifact due to the culture system, with the cells caged in the inner part of the tumorsphere being forced to cell cycle arrest due to nutrient deprivation, or of a *bona fide* enrichment of intrinsically slow-cycling CSC. The latter option is supported by a study showing that cells in the G_0/G_1 phase sorted from different breast cancer cell lines grown as monolayer or human primary samples have increased tumorsphere-forming ability compared to cells in S and G_2/M phase [40].

Concerning the down-regulation of transcripts coding for proteins involved in the mevalonate pathway, cholesterol metabolism and lipid biosynthesis, this observation is in contrast to what

observed in a similar study by Ginestier and colleagues [41]. In that study, basal/mesenchymal-like tumorspheres, but not luminal tumorspheres, overexpressed enzymes of the mevalonate pathway compared to their monolayer counterpart. In general, a large body of studies supports a pro-tumorigenic role for increased cholesterol and lipid biosynthesis, with cells facing a lipid metabolic reprogramming upon transformation [42]. The mechanisms through which cholesterol and lipids promote cancer have been shown to be multiple, ranging from structural function to cell signaling, passing through post-translational modification of proteins (reviewed in ref. [43] and ref. [44]). On the light of the fundamental lack of literature supporting a pro-tumorigenic role for decreased lipid biosynthesis, we speculate that the down-regulation of key genes involved in mevalonate pathway and lipid/cholesterol biosynthesis in our tumorspheres may be cause or consequence of the cell cycle slowing. Amongst all their functions, cholesterol and lipids are used as building blocks of cell membranes. Slowly proliferating cells, as is the case for cells composing tumorspheres, would then require less cholesterol and lipids to support their duplication. Furthermore, cholesterol has been shown to have a direct causal role in the cell cycle progression, with inhibition of cholesterol biosynthesis resulting in the blocking of cells in G_1 [45]. Of course, this is pure speculation, and further *in vitro* experiment will confirm or reject this hypothesis in our model.

Transcripts found to be upregulated in the tumorspheres of both cell lines show to have pleiotropic functions, being the same genes involved in different biological processes. Among these, we highlight the negative regulation of apoptosis, cytokine production, response to external stimuli, regulation of signal transduction and regulation of developmental processes. This finding is in accordance with the current understanding of the CSC model, in which increased resistance to apoptosis and activation of developmental pathways are considered as hallmarks [46,47].

Looking for a possible therapeutic target in CSC of TNBC, we directed our interest to TENM4. TENM4 is a large type II transmembrane glycoprotein which belongs to a family of four (TENM1 through TENM4) pair-rule proteins, showing high conservation among species and significant homology between the different family members [48]. Animal studies have demonstrated that teneurins

492 are expressed in a highly regulated manner during embryogenesis and with differential spatial and
493 temporal patterns in the adult CNS [49,50]. Besides their predominant neural distribution, teneurins
494 mRNA have been detected in few adult organs such as the testis and thymus although at significant
495 lower levels [51]. Few recent studies have demonstrated elevated TENM4 mRNA levels in brain tumors
496 [18], suggesting an oncogenic potential role for this protein. However, little is known about the role of
497 TENM4 in cancer growth and dissemination. By investigating publicly available breast cancer patient
498 databases, we showed that TENM4 mRNA expression increases in both ductal and lobular invasive
499 carcinoma compared to healthy breast tissue, and higher expression of TENM4 mRNA in TNBC
500 patients is associated with a poorer RFS. This suggests that TENM4 represents a potentially useful
501 target for TNBC. This also prompted us to further investigate how TENM4 affects stem-like
502 properties in the 4T1 model.
503 We validated TENM4 upregulation in tumorspheres from both 4T1 and HCC1806 by Real-Time
504 PCR. For this analysis, we included also other human breast cancer cell lines, including MDA-MB-
505 231 (TNBC), MCF7 (ER^+/$Her2^-$) and SK-BR-3 (ER^-/$Her2^+$) cells, thus confirming the upregulation
506 of TENM4 also in the tumorspheres of these cell lines. This suggests that TENM4 upregulation could
507 be a common feature of breast tumorspheres. To evaluate if TENM4 is only a byproduct of low-
508 attachment growth condition or it has a causal role in the generation of tumorspheres, we silenced
509 TENM4 through RNAi, observing a decrease in the number of tumorspheres, as well as in the total
510 number of cells thereof. This suggests that TENM4 is involved in the self-renewal of CSC, as the
511 tumorsphere-forming assay is an *in vitro* surrogate of tumor-initiating potential [11]. We then sought to
512 explore a possible mechanistic link between TENM4 expression and the observed phenotype.
513 Nowadays, little is known about the mechanisms involved in TENM4 function at cellular and
514 molecular levels. However, evidence suggest that TENM4 may act in cytoskeleton reorganization.
515 Disruption of the *Tenm4* gene in the *furue* mutant mice causes inhibition of cellular process formation
516 in oligodendrocytes, leading to small-diameter axon demyelination and subsequently causing tremors
517 in this mutant mouse model [23]. In that study, it was shown that TENM4 expression positively regulates

518 FAK signaling, which is required for proper oligodendrocyte process formation and myelination of
519 small diameter axons. FAK signaling pathway is also recognized to have an important role in
520 controlling cell movement, invasion, survival, gene expression, and stem cell self-renewal in cancer
521 cells [24]. It has been shown that TENM4 promotes filopodia-like protrusion formation in a
522 neuroblastoma cell line [52] through FAK signaling pathway, and *in vitro*, *in vivo* and clinical evidence
523 suggest that filopodia drive cancer cell invasion [53]. Moreover, disruption of FAK in the mammary
524 epithelium has been shown to suppress tumorigenesis in a MMTV-PyMT mouse model by depleting
525 the pool of cancer stem/progenitor cells in primary tumors, with subsequent impairment of self-
526 renewal, migration and tumor initiating ability [54]. According to these findings, we observed an
527 increase in total FAK protein in 4T1 tumorspheres compared to cells grown as monolayer, suggesting
528 augmented stem-like features in cells composing tumorspheres.

529 When we silenced TENM4 in 4T1 tumorspheres, we observed a small but significant decrease in
530 FAK phosphorylation. Importantly, it has been shown that pharmacological inhibition of FAK
531 significantly impairs syngeneic murine 4T1 orthotopic breast carcinoma tumor growth and
532 spontaneous metastasis to lungs in BALB/c mice, as well as MDA-MB-231 breast carcinoma tumor
533 growth and metastasis in BALB/c SCID mice [55]. These elements all led us to speculate that TENM4
534 could regulate migration and invasion ability of cancer cells, as well as CSC properties, through
535 activation of FAK. Obviously, due to the tridimensional structure and the anchorage-independent
536 growth of tumorspheres, we could not assess the role of TENM4 and FAK in the migratory properties
537 of CSC, neither we could perform silencing assays on cells growing as monolayers due to the
538 extremely low expression of TENM4 and FAK in these cells. However, it has been reported that FAK
539 inhibition or silencing impairs the tumorsphere-forming ability of different breast cancer models,
540 including TNBC cell lines MDA-MB-231 and SUM159 [56,57], SUM149 and HCC1954 [58], as well as
541 in cells from breast cancer patients [59], which could explain the decreased number of tumorspheres
542 following TENM4 silencing.

543 Targeting of TENM4 by siRNA did not lead to a decrease in total FAK protein in our model, but
544 affected FAK phosphorylation at Y925 site, leaving Y397 phosphorylation unaffected. While most
545 studies on the role of FAK in CSC biology focus on Y397 phosphorylation [60], the phosphorylation of
546 Y925 is usually not investigated [55,57,61]. Nonetheless, phosphorylation at Y925 has been proposed to
547 link FAK to the Ras pathway and to epithelial-to-mesenchymal transition (EMT), behaving as binding
548 site for Src [62] and GRB2 [63]. Others reported a role for Y925 phosphorylation in promoting a pro-
549 angiogenic switch in 4T1-derived tumors [64].
550 These findings, together with our observation that FAK phosphorylation at Y925 site is partially
551 dependent on TENM4 expression, let us speculate that TENM4 could be linked to CSC features and
552 metastatic progression of tumors.
553
554 **Conclusions**
555 TNBC are identified by immunohistochemical analysis and in situ hybridization for Her2 locus
556 amplification. From this point of view, TNBC is considered as a single clinical entity and uniformly
557 treated with chemotherapy, but high-throughput approaches revealed a high degree of heterogeneity
558 from the molecular point of view [3]. In the current work, a major limitation is the use of only two cell
559 lines, which cannot obviously recapitulate the diversity of this disease. Nonetheless, this work
560 highlighted a restricted number of potential targets that can be further investigated in the large
561 plethora of existing human breast cancer cell lines belonging to the different molecular subtypes that
562 collectively represent the TNBC complexity [65]. Furthermore, the use of the murine cell line 4T1 will
563 allow the development of preclinical strategies that include immunotherapy, this last approach not
564 being possible in xenotransplantation models. Our work also poses some doubts on the univocal
565 meaning of commonly used CSC markers, evidencing a cell line-dependent heterogeneity that has
566 already been reported by others [28]. Among the genes upregulated in tumorspheres and coding for
567 transmembrane proteins, we focused on TENM-4, showing that its upregulation could be a common
568 feature of tumorspheres of multiple cell lines and that its role in the CSC-phenotype could be mediated

by FAK. *In vivo* experiments, which in this study are lacking, will help us to better define the role of TENM4 on tumor initiation and progression.

Despite the aforementioned limitations, this study highlights the potential relevance of apoptosis resistance, CSC dormancy and cholesterol biosynthesis as pathways to be addressed to find novel approaches to fight CSC in TNBC.

Acknowledgements and funding

This work was supported by a grant from the Compagnia di San Paolo (Progetti di Ricerca Ateneo/CSP, TO_call02_2012_0026) to FC and by a grant from the Italian Association for Cancer Research (IG XXXXX) to EQ. LC was supported by a fellowship from Fondazione Umberto Veronesi.

Conflicts of interest

The authors declare no competing financial interests.

Bibliography

1. Schmadeka, R., Harmon, B. E. & Singh, M. Triple-negative breast carcinoma: Current and emerging concepts. *Am. J. Clin. Pathol.* **141,** 462–477 (2014).
2. Dent, R. *et al.* Triple-negative breast cancer: Clinical features and patterns of recurrence. *Clin. Cancer Res.* **13,** 4429–4434 (2007).
3. Bianchini, G., Balko, J. M., Mayer, I. A., Sanders, M. E. & Gianni, L. Triple-negative breast cancer: challenges and opportunities of a heterogeneous disease. *Nat. Rev. Clin. Oncol.* **13,** 674–690 (2016).
4. Carey, L. A. *et al.* The triple negative paradox: Primary tumor chemosensitivity of breast cancer subtypes. *Clin. Cancer Res.* **13,** 2329–2334 (2007).

595 5. Abdullah, L. N. & Chow, E. K.-H. Mechanisms of chemoresistance in cancer stem cells.
596 *Clin. Transl. Med.* **2,** (2013).
597 6. Noh, K. H. *et al.* Cancer vaccination drives nanog-dependent evolution of tumor cells toward
598 an immune-resistant and stem-like phenotype. *Cancer Res.* **72,** 1717–1727 (2012).
599 7. Frank, N. Y., Schatton, T. & Frank, M. H. The therapeutic promise of the cancer stem cell
600 concept. *J. Clin. Invest.* **120,** 41–50 (2010).
601 8. Reynolds, B. A. & Weiss, S. Generation of Neurons and Astrocytes from Isolated Cells of
602 the Adult Mammalian Central Nervous System. *Science (80-.).* **255,** 1707–1710 (1992).
603 9. Uchida, N. *et al.* Direct isolation of human central nervous system stem cells. *PNAS* **97,**
604 14720–5 (2000).
605 10. Dontu, G. *et al.* In vitro propagation and transcriptional profiling of human mammary
606 stem/progenitor cells. *Genes Dev.* **17,** 1253–1270 (2003).
607 11. Weiswald, L. B., Bellet, D. & Dangles-Marie, V. Spherical cancer models in tumor biology.
608 *Neoplasia* **17,** 1–15 (2015).
609 12. Ponti, D. *et al.* Isolation and In vitro Propagation of Tumorigenic Breast Cancer Cells with
610 Stem / Progenitor Cell Properties. *Cancer Res.* **65,** 5506–5512 (2005).
611 13. Grange, C., Lanzardo, S., Cavallo, F., Camussi, G. & Bussolati, B. Sca-1 identifies the
612 tumor-initiating cells in mammary tumors of BALB-neuT transgenic mice. *Neoplasia* **10,**
613 1433–43 (2008).
614 14. Iezzi, M. *et al.* DNA vaccination against oncoantigens. *Oncoimmunology* **1,** 316–325 (2012).
615 15. Conti, L. *et al.* The noninflammatory role of high mobility group box 1/Toll-like receptor 2
616 axis in the self-renewal of mammary cancer stem cells. *FASEB J.* **27,** 4731–44 (2013).
617 16. Lanzardo, S. *et al.* Immunotargeting of antigen xCT attenuates stem-like cell behavior and
618 metastatic progression in breast cancer. *Cancer Res.* **76,** 62–72 (2016).
619 17. Conti, L. *et al.* L-Ferritin targets breast cancer stem cells and delivers therapeutic and
620 imaging agents. *Oncotarget* **7,** 66713–66727 (2016).

621 18. Ziegler, A., Corval??n, A., Roa, I., Bra??es, J. A. & Wollscheid, B. Teneurin protein family:
622 An emerging role in human tumorigenesis and drug resistance. *Cancer Lett.* **326,** 1–7 (2012).
623 19. Ritchie, M. E. *et al.* limma powers differential expression analyses for RNA-sequencing and
624 microarray studies. *Nucleic Acids Res.* **43,** e47 (2015).
625 20. Law, C. W., Chen, Y., Shi, W. & Smyth, G. K. voom: precision weights unlock linear model
626 analysis tools for RNA-seq read counts. *Genome Biol.* **15,** R29 (2014).
627 21. Győrffy, B. *et al.* An online survival analysis tool to rapidly assess the effect of 22,277 genes
628 on breast cancer prognosis using microarray data of 1,809 patients. *Breast Cancer Res. Treat.*
629 **123,** 725–731 (2010).
630 22. Bookout, A. & Mangelsdorf, D. Quantitative Real-Time PCR Protocol for Analysis of
631 Nuclear Receptor Signaling Pathways. *Nucl. Recept. Signal.* **1,** (2003).
632 23. Suzuki, N. *et al.* Teneurin-4 Is a Novel Regulator of Oligodendrocyte Differentiation and
633 Myelination of Small-Diameter Axons in the CNS. *J. Neurosci.* **32,** 11586–11599 (2012).
634 24. Sulzmaier, F. J., Jean, C. & Schlaepfer, D. D. FAK in cancer: mechanistic findings and
635 clinical applications. *Nat. Rev. Cancer* **14,** 598–610 (2014).
636 25. Al-Hajj, M., Wicha, M. S., Benito-Hernandez, A., Morrison, S. J. & Clarke, M. F.
637 Prospective identification of tumorigenic breast cancer cells. *PNAS* **100,** 3983–8 (2003).
638 26. Fillmore, C. & Kuperwasser, C. Human breast cancer stem cell markers CD44 and CD24:
639 enriching for cells with functional properties in mice or in man? *Breast Cancer Res.* **9,** 303
640 (2007).
641 27. Jaggupilli, A. & Elkord, E. Significance of CD44 and CD24 as cancer stem cell markers: An
642 enduring ambiguity. *Clin. Dev. Immunol.* **2012,** (2012).
643 28. Liu, Y. *et al.* Lack of correlation of stem cell markers in breast cancer stem cells. *Br. J.*
644 *Cancer* **110,** 2063–2071 (2014).
645 29. Ginestier, C. *et al.* ALDH1 Is a Marker of Normal and Malignant Human Mammary Stem
646 Cells and a Predictor of Poor Clinical Outcome. *Cell Stem Cell* **1,** 555–567 (2007).

30. Liu, S. *et al.* Breast cancer stem cells transition between epithelial and mesenchymal states reflective of their normal counterparts. *Stem Cell Reports* **2,** 78–91 (2014).
31. Ricardo, S. *et al.* Breast cancer stem cell markers CD44, CD24 and ALDH1: expression distribution within intrinsic molecular subtype. *J. Clin. Pathol.* **64,** 937–946 (2011).
32. Moore, N. & Lyle, S. Quiescent, slow-cycling stem cell populations in cancer: A review of the evidence and discussion of significance. *J. Oncol.* **2011,** (2011).
33. Chen, W., Dong, J., Haiech, J., Kilhoffer, M. C. & Zeniou, M. Cancer stem cell quiescence and plasticity as major challenges in cancer therapy. *Stem Cells Int.* **2016,** (2016).
34. Pece, S. *et al.* Biological and Molecular Heterogeneity of Breast Cancers Correlates with Their Cancer Stem Cell Content. *Cell* **140,** 62–73 (2010).
35. Fillmore, C. M. & Kuperwasser, C. Human breast cancer cell lines contain stem-like cells that self-renew, give rise to phenotypically diverse progeny and survive chemotherapy. *Breast Cancer Res.* **10,** R25 (2008).
36. Chen, J. *et al.* A restricted cell population propagates glioblastoma growth following chemotherapy. *Nature* **488,** 522–526 (2012).
37. Vlashi, E. *et al.* In vivo imaging, tracking, and targeting of cancer stem cells. *J. Natl. Cancer Inst.* **101,** 350–359 (2009).
38. Kim, S. & Alexander, C. M. Tumorsphere assay provides more accurate prediction of in vivo responses to chemotherapeutics. *Biotechnol Lett.* **36,** 481–488 (2014).
39. Kwon, Y. S., Chun, S. Y., Nam, K. S. & Kim, S. Lapatinib sensitizes quiescent MDA-MB-231 breast cancer cells to doxorubicin by inhibiting the expression of multidrug resistance-associated protein-1. *Oncol. Rep.* **34,** 884–890 (2015).
40. Lamb, R., Lisanti, M. P., Clarke, R. B. & Landberg, G. Co-ordination of cell cycle, migration and stem cell-like activity in breast cancer. *Oncotarget* **5,** 7833–7842 (2014).
41. Ginestier, C. *et al.* Mevalonate metabolism regulates basal breast cancer stem cells and is a potential therapeutic target. *Stem Cells* **30,** 1327–1337 (2012).

673 42. Beloribi-Djefaflia, S., Vasseur, S. & Guillaumond, F. Lipid metabolic reprogramming in
674 cancer cells. *Oncogenesis* **5,** e189 (2016).
675 43. Baenke, F., Peck, B., Miess, H. & Schulze, A. Hooked on fat: the role of lipid synthesis in
676 cancer metabolism and tumour development. *Dis. Model. Mech.* **6,** 1353–1363 (2013).
677 44. Kuzu, O. F., Noory, M. A. & Robertson, G. P. The role of cholesterol in cancer. *Cancer Res.*
678 **76,** 2063–2070 (2016).
679 45. Singh, P., Saxena, R., Srinivas, G., Pande, G. & Chattopadhyay, A. Cholesterol Biosynthesis
680 and Homeostasis in Regulation of the Cell Cycle. *PLoS One* **8,** (2013).
681 46. Fulda, S. Regulation of apoptosis pathways in cancer stem cells. *Cancer Lett.* **338,** 168–173
682 (2013).
683 47. Karamboulas, C. & Ailles, L. Developmental signaling pathways in cancer stem cells of solid
684 tumors. *Biochim. Biophys. Acta* **1830,** 2481–2495 (2013).
685 48. Tucker, R. P., Kenzelmann, D., Trzebiatowska, A. & Chiquet-Ehrismann, R. Teneurins:
686 Transmembrane proteins with fundamental roles in development. *International Journal of*
687 *Biochemistry and Cell Biology* **39,** 292–297 (2007).
688 49. Rubin, B. P., Tucker, R. P., Martin, D. & Chiquet-Ehrismann, R. Teneurins: a novel family
689 of neuronal cell surface proteins in vertebrates, homologous to the Drosophila pair-rule gene
690 product Ten-m. *Dev. Biol.* **216,** 195–209 (1999).
691 50. Zhou, X. H. *et al.* The murine Ten-m/Odz genes show distinct but overlapping expression
692 patterns during development and in adult brain. *Gene Expr. Patterns* **3,** 397–405 (2003).
693 51. Oohashi, T. *et al.* Mouse ten-m/odz is a new family of dimeric type II transmembrane
694 proteins expressed in many tissues. *J. Cell Biol.* **145,** 563–577 (1999).
695 52. Suzuki, N. *et al.* Teneurin-4 promotes cellular protrusion formation and neurite outgrowth
696 through focal adhesion kinase signaling. *FASEB J.* **28,** 1386–1397 (2014).
697 53. Jacquemet, G., Hamidi, H. & Ivaska, J. Filopodia in cell adhesion, 3D migration and cancer
698 cell invasion. *Curr. Opin. Cell Biol.* **36,** 23–31 (2015).

699 54. Luo, M. *et al.* Mammary epithelial-specific ablation of the focal adhesion kinase suppresses
700 mammary tumorigenesis by affecting mammary cancer stem/progenitor cells. *Cancer Res.*
701 **69,** 466–474 (2009).
702 55. Walsh, C. *et al.* Oral delivery of PND-1186 FAK inhibitor decreases tumor growth and
703 spontaneous breast to lung metastasis in pre-clinical models. **9,** 778–790 (2010).
704 56. Thakur, R., Trivedi, R., Rastogi, N., Singh, M. & Mishra, D. P. Inhibition of STAT3, FAK
705 and Src mediated signaling reduces cancer stem cell load, tumorigenic potential and
706 metastasis in breast cancer. *Sci. Rep.* **5,** 10194 (2015).
707 57. Kolev, V. N. *et al.* Inhibition of FAK kinase activity preferentially targets cancer stem cells.
708 *Oncotarget* **8,** 51733–51747 (2017).
709 58. Luo, M. *et al.* Distinct FAK activities determine progenitor and mammary stem cell
710 characteristics. *Cancer Res.* **73,** 5591–5602 (2013).
711 59. Williams, K., Bundred, N., Landberg, G. & Clarke, R. Focal adhesion kinase and Wnt
712 signaling regulate human ductal carcinoma in situ stem cell activity and response to
713 radiotherapy. *Stem Cells* **33,** 327–341 (2014).
714 60. McLean, G. W. *et al.* The role of focal-adhesion kinase in cancer — a new therapeutic
715 opportunity. *Nat. Rev. Cancer* **5,** 505–515 (2005).
716 61. Mitra, S., Lim, S.-T., Chi, A. & Schlaepfer, D. Intrinsic focal adhesion kinase activity
717 controls orthotopic breast carcinoma metastasis via the regulation of urokinase plasminogen
718 activator expression in a syngeneic. *Oncogene* **25,** 4429–4440 (2006).
719 62. Brunton, V. G. *et al.* Identification of Src-specific phosphorylation site on focal adhesion
720 kinase: Dissection of the role of Src SH2 and catalytic functions and their consequences for
721 tumor cell behavior. *Cancer Res.* **65,** 1335–1342 (2005).
722 63. Schlaepfer, D. D., Hanks, S. K., Hunter, T. & van der Geer, P. Integrin-mediated signal
723 transduction linked to Ras pathway by GRB2 binding to focal adhesion kinase. *Nature* **372,**
724 786–791 (1994).

64. Mitra, S. *et al.* Intrinsic FAK activity and Y925 phosphorylation facilitate an angiogenic switch in tumors. *Oncogene* **25,** 5969–84 (2006).

65. Lehmann, B. D. B. *et al.* Identification of human triple-negative breast cancer subtypes and preclinical models for selection of targeted therapies. *J. Clin. Invest.* **121,** 2750–2767 (2011).

751 **Caption to figures**

752 **Figure 1. Tumorspheres generation and characterization.**

753 **A)** Optical microscope photography of sub-confluent parental cells and 5-day old tumorspheres from
754 4T1 (left) and HCC1806 (right) cell lines. **B)** Table representing mean percentage of cells positive
755 for a given marker or the mean fluorescence intensity (MFI) of a given marker ± SEM, as assessed
756 by flow cytometry. **C)** Graphical representation of flow cytometry data reported in panel B. Plots and
757 histograms on the left refer to 4T1 cell line, plots and histograms on the right refer to HCC1806 cell
758 line. Upper panel: dot plot representation of cell staining for CD44 and CD24. Middle panel:
759 histogram representation of cell staining for CD49f. Lower panel: histogram representation of 4T1
760 cell staining for Sca-1, or dot plot representation of HCC1806 cell staining for Aldefluor (y axis: Side
761 Scatter). In the histogram representation, gray fill with dotted line: unstained control cells; no fill with
762 black line: P cells; dark gray fill with no line: T2 tumorspheres.
763 P: parental cells. T2: second passage tumorspheres. * *p-value* < 0,05
764

765 **Figure 2. Gene expression profiling and gene ontology of parental cells and tumorspheres.**

766 **A)** Summary of the number of total genes analyzed (Total), those differentially expressed between
767 tumorspheres and parental cells (Diff), those non-changing (Non-Diff), those up-regulated (Upreg)
768 or down-regulated (Downreg) in tumorspheres compared to parental cells among those differentially
769 expressed. On the right, Venn-diagram representing up-regulated or down-regulated genes shared
770 between 4T1 and HCC1806 cell lines, and cumulative histograms representing the distribution in
771 different cell compartments of proteins coded by genes shared between 4T1 and HCC1806. **B)**
772 Histograms representing the distribution of the genes according to their biological function. The
773 reported classes are Gene ontology (GO) biological processes. The bar represents the ratio between
774 the number of genes observed for a given biological process versus the number of genes that would
775 be observed by chance (expected) for that same biological process. The alternating background helps
776 to visualize biological processes that are related, and that can be interpretable as a group rather than

individually (obtained by the hierarchic sort function of Gene Ontology). **C)** Localization, within the cell cycle and cholesterol biosynthesis, of proteins encoded by genes found in the downregulated dataset. Cell cycle (**upper panel**). Cell Division Cycle Associated 3 (**CDCA3**) is a protein required for entry into mitosis. It acts by participating in E3 ligase complexes that mediate the ubiquitination and degradation of WEE1 kinase – an inhibitor of Cyclin Dependent Kinase 1 (Cdk1) activity - at G2/M phase. **TTK** encodes for a protein kinase essential for chromosome alignment at the centromere and is required for centrosome duplication. It has been found to be a critical mitotic checkpoint protein for accurate segregation of chromosomes. **FAM83D** is required for proper chromosome congression and alignment during metaphase of mitosis. **CCNB2** encodes for Cyclin B2: Cyclin B are mitotic cyclins that associate with Cdk1 and are necessary for the progression of the cells into and out of M phase of the cell cycle, through stimulation of CDC20. **CDC20** is a key player of the metaphase to anaphase transition of the mitosis, since it activates the Anaphase Promoting Complex (APC/C). CDC20-APC/C is required for anaphase to happen, but is blocked by inhibitor Mad2 during the spindle assembly checkpoint. Spindle checkpoint prevents anaphase onset until all chromosomes are properly attached to the spindle. To achieve proper segregation, the two kinetochores on the sister chromatids must be attached to opposite spindle poles. Kinetochores formation requires the intervention of centromere proteins encoded by **CENPU** and **CENPM**, among others. **ERCC6L** encodes for a DNA helicase that contributes to this checkpoint by monitoring tension on centromeric chromatin and by recruiting Mad2 to kinetochores. Once CDC20-APC/C is no more inhibited by Mad2, it leads to ubiquitination and subsequent degradation of Securin, a binder and inhibitor of Separase (encoded by the gene **ESPL1**). Once released, Separase cuts Scc1, a subunit of the cohesin complex that is required to keep together brother chromatids. Kinesins (such as **KIF23** and **KIF2C**) act as microtubule-dependent molecular motors and are required for the movement of chromatids along the mitotic spindle. In particular KIF2C, in complex with KIF18B, constitutes the major microtubule plus-end depolymerizing activity in mitotic cells. It regulates the turnover of

802 microtubules at the kinetochore and functions in chromosome segregation during mitosis, leading to
803 the final steps of mitosis. Finally, **CEP55** plays a role in mitotic exit and cytokinesis.

804 Cholesterol biosynthesis (**lower panel**). Cholesterol biosynthesis, together with isoprenoids
805 synthesis and other processes starts with the synthesis of Acetoacetyl CoA from Acetyl CoA through
806 thiolase (encoded by **ACAT2**) or from Acetatoacetate through Acetoacetyl-CoA Synthetase (**AACS**).
807 This is the first step of the Mevalonate pathway, in which also Mevalonate Kinase (**MVK**),
808 Phosphomevalonate Kinase (**PMVK**) and Mevalonate Diphosphate Decarboxylase (**MVD**) are
809 included, leading to the production of isopentenyl diphosphate. This product is the substrate for the
810 next steps of cholesterol biosynthesis, through the involvement of Isopentenyl-Diphosphate Delta
811 Isomerase 1 (**IDI1**) and Squalene Epoxidase (**SQLE**) among the others. Cytochrome P450 51A1
812 (**CYP5A1**), Methylsterol Monooxygenase 1 (**MSMO1**) and 7-Dehydrocholesterol Reductase
813 (**DHCR7**) are among the enzymes required for the synthesis of cholesterol starting from Lanosterol.
814

815 **Figure 3. TENM4 relevance in breast cancer patients.**

816 **Left.** Oncomine TENM4 mRNA expression data reported as $\log_2$ median-centered ratio using box-
817 and-whiskers plots (dots: maximum and minimum values; whiskers: 90/10 percentiles; box: 75/25
818 percentiles; line: median of all samples). Expression data from normal breast tissue (61 samples) were
819 compared with those from invasive ductal carcinoma (IDC, 389 samples) and invasive lobular
820 carcinoma (ILC, 36 samples). The analysis was performed for three different Agilent ID probes.
821 **Right.** Relapse-Free Survival of TNBC patients, stratified by high (red) or low (black) expression of
822 TENM4 mRNA.
823 * p-value < 0,05; ** p-value < 0,01; ns: non-significant
824

825 **Figure 4. Evaluation of the role of TENM4 in tumorspheres.**

826 **A) Left panel.** Semi-quantitative Real-Time PCR. Bars represent the negative ΔCt (i.e. the difference
827 between the Ct of the internal control gene GADPH and the Ct of TENM4), comparing parental cells

and tumorspheres of different breast cancer cell lines. **Right panel.** Immunoblot of TENM4, total FAK, FAK phosphorylated at the tyrosine 925 residue (Y925) and loading control protein Vinculin, comparing parental cells and tumorspheres of 4T1 cell line. Histograms show the adjusted relative density of the bands as assessed by immunoblot. **B)** TENM4 silencing. Immunoblot of TENM4, total FAK, FAK phosphorylated at Y397 or Y925 and loading control protein Vinculin, comparing 4T1 tumorspheres treated with a pool of TENM4-specific siRNA or a pool of non-targeting siRNA (mock). Histograms show the adjusted relative density of the bands for TENM4 or the adjusted relative phosphorylation of FAK at Y925 as assessed by immunoblot. **C)** Histograms showing how TENM4 silencing on tumorspheres affects their sphere-generation ability and the number of viable cells at the moment of harvesting, assessed through evaluation of optical density (O.D.) following an MTT assay. The number of tumorspheres counted or the O.D: value in the mock siRNA-treated condition was used as reference and considered to be 100%.

P: parental cells. T2: second passage tumorspheres. T3: third passage tumorspheres.

Statistical analysis: unpaired t test. * p-value < 0,05; ** p-value < 0,01; *** p-value < 0,001

ns: non-significant

Table 1

List of genes and corresponding proteins upregulated in both 4T1 and HCC1806 tumorspheres and coding for transmembrane proteins. Log_2FC of mRNA expression in T2 tumorspheres Vs parental cells for the two cell lines is also reported.

Supplementary Figure 1

Relapse-Free Survival of TNBC patients, stratified by high (red) or low (black) mRNA expression of the indicated gene.

Supplementary Figure 2

854 **A)** Immunoblot of TENM4 and loading control protein Vinculin, comparing parental cells and
855 tumorspheres of HCC1806 cell line. Histograms show the adjusted relative density of the bands as
856 assessed by immunoblot. **B)** Histogram showing the relative fold change of TENM4 mRNA level
857 upon siRNA treatment in 4T1 T3 tumorspheres.
858
859 **Supplementary Table 1**
860 List of GO biological processes enriched in the upregulated (A) or downregulated (B) datasets, and
861 their respective genes present in the dataset.

A

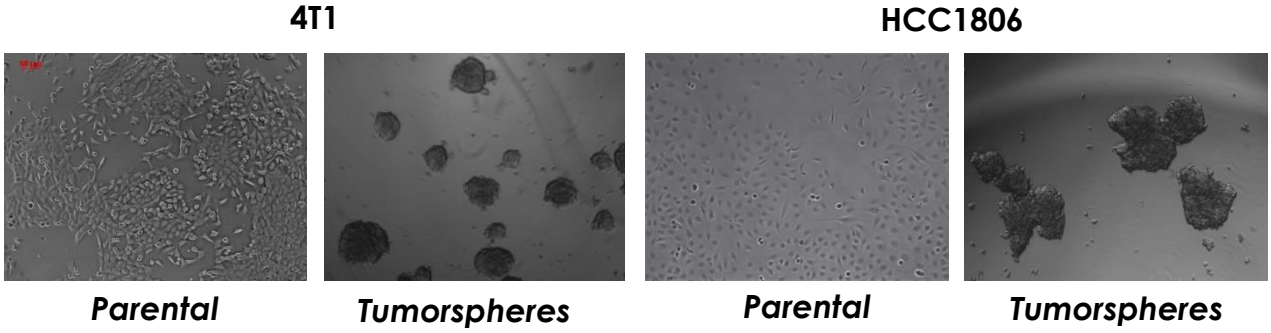

B

cell line	cancer stem cell markers							
4T1	**Sca-1+%**	**Sca-1 MFI**	**CD49f+%**	**CD49f MFI**	**CD24+%**	**CD44+%**	**CD44+/CD24- %**	**ALDH+ %**
P	15,27 ± 2,73	30,63 ± 4,84	99,31 ± 0,39	527,81 ± 104,1	99,4 ± 0,24	99,5 ± 0,18	0,17 ± 0,15	43,34 ± 9,61
T2	29,44 ± 6,53	141,83 ± 39,6	99,39 ± 0,33	941,58 ± 133,5	97,64 ± 0,93	93,3 ± 3,18	1,67 ± 0,95	20,92 ± 1,61
HCC1806			**CD49f+%**	**CD49f MFI**	**CD24+%**	**CD44+%**	**CD44+/CD24- %**	**ALDH+ %**
P			16,35 ± 4,63	6,99 ± 1	0,22 ± 0,08	0,27 ± 0,1	0,17 ± 0,07	35,74 ± 10,72
T2			11,39 ± 2,75	7,12 ± 0,35	0,88 ± 0,42	1,03 ± 0,31	0,41 ± 0,07	58,29 ± 18,13

C

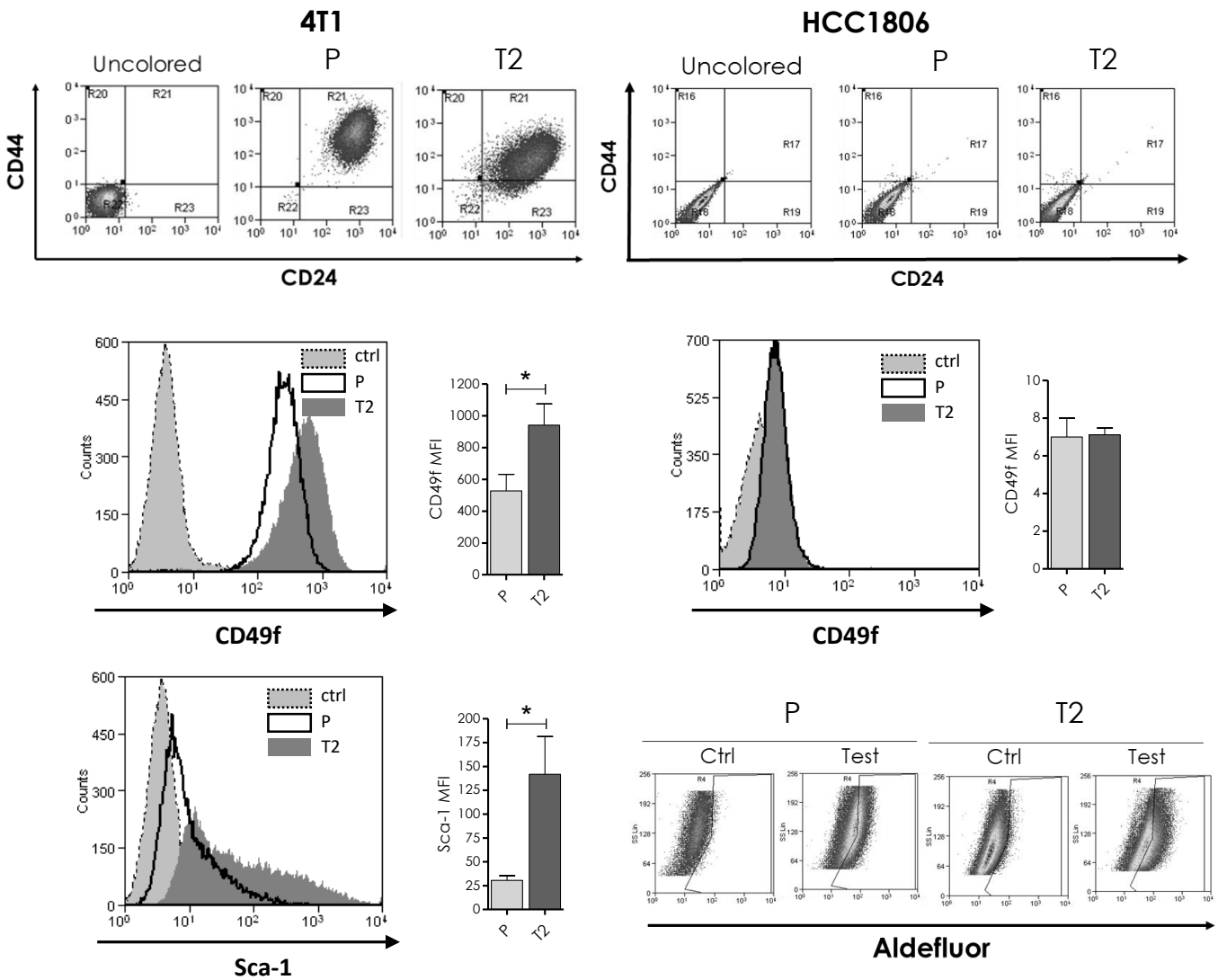

Fig.2

A

4T1

Total	Diff	Non-Diff	Upreg	Downreg
9659	1316	8343	766	550

HCC1806

Total	Diff	Non-Diff	Upreg	Downreg
10198	874	9324	577	297

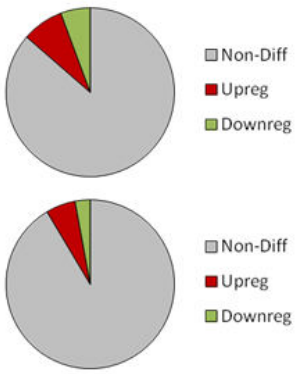

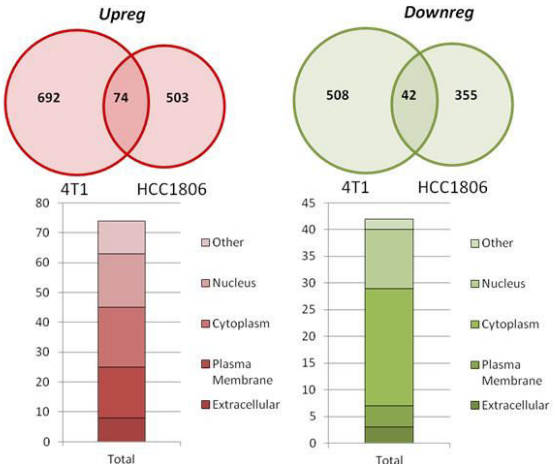

B

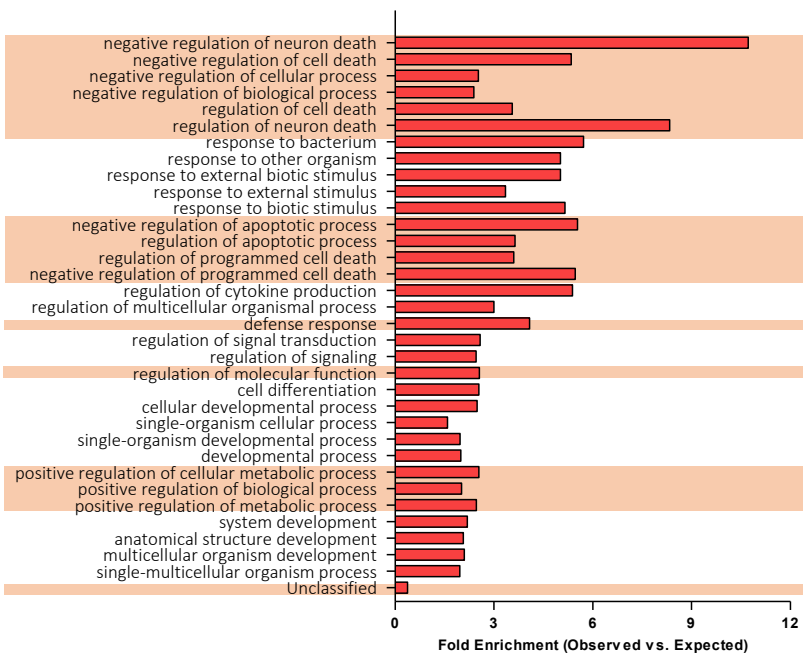

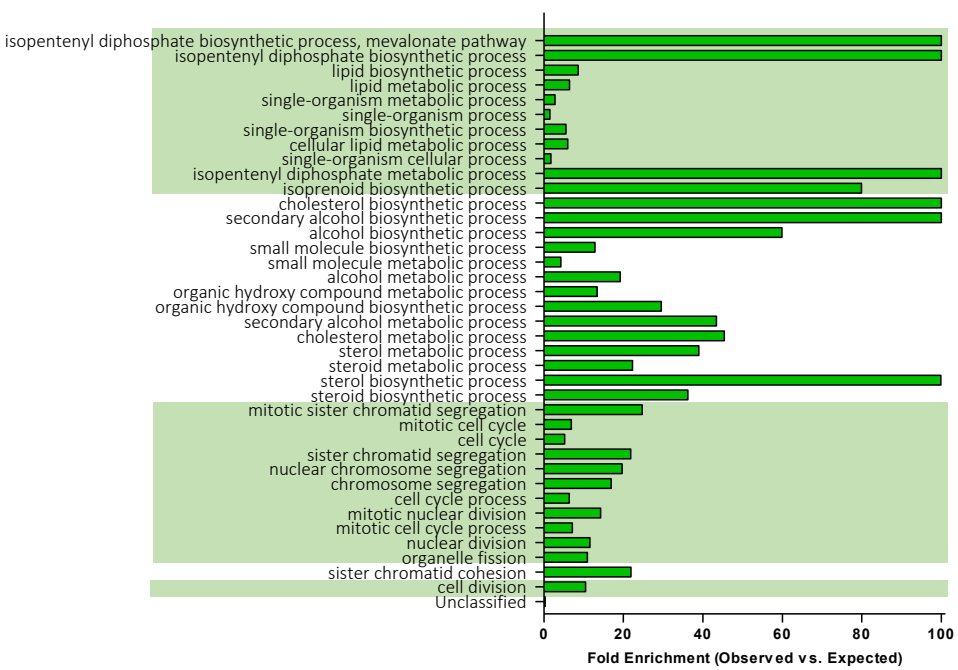

C

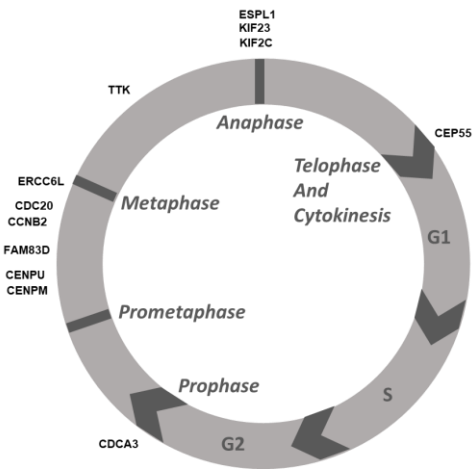

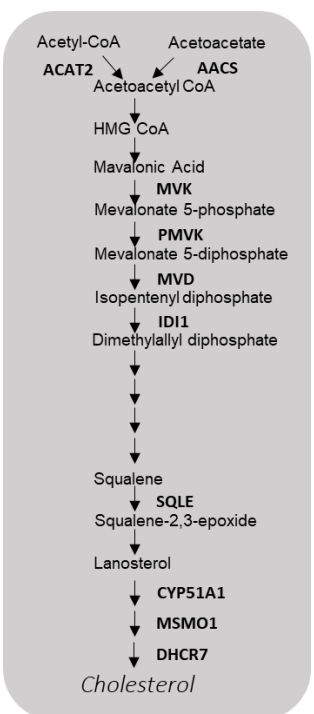

Fig.3

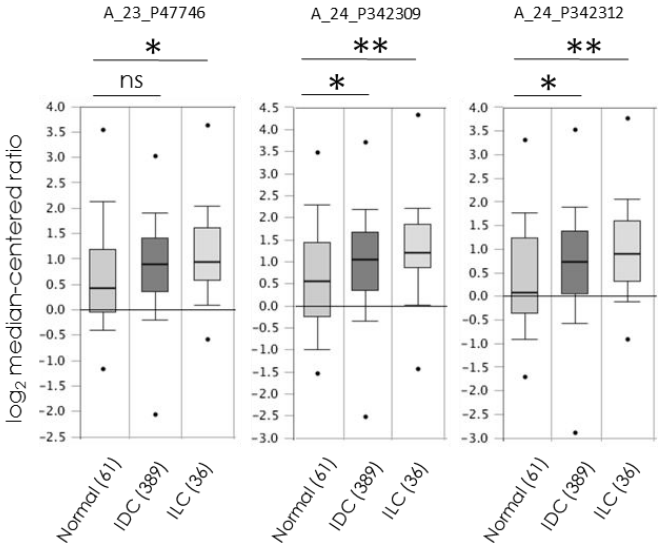
A_23_P47746
A_24_P342309
A_24_P342312
*
ns
**
*
**
*
log2 median-centered ratio
Normal (61)
IDC (389)
ILC (36)

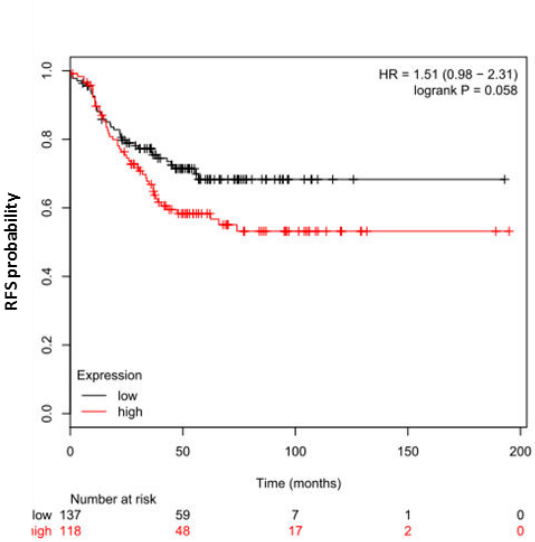
HR = 1.51 (0.98 − 2.31)
logrank P = 0.058
RFS probability
Expression
low
high
Time (months)
Number at risk
low 137 59 7 1 0
high 118 48 17 2 0

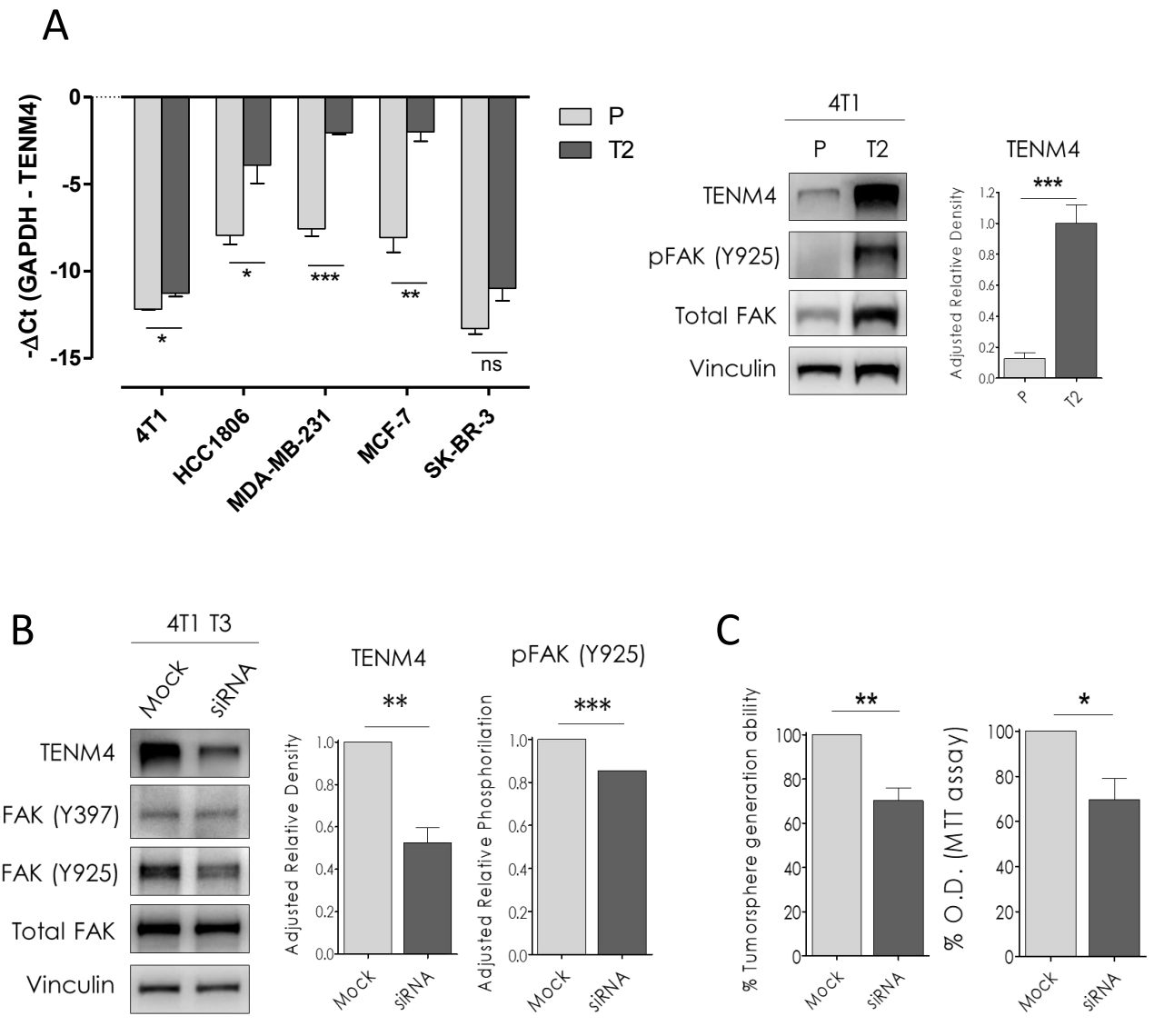
A
-ΔCt (GAPDH - TENM4)
0
-5
-10
-15
P
T2
*
*
***
**
ns
4T1
HCC1806
MDA-MB-231
MCF-7
SK-BR-3
4T1
P
T2
TENM4
pFAK (Y925)
Total FAK
Vinculin
TENM4
***
Adjusted Relative Density
1.2
1.0
0.8
0.6
0.4
0.2
0.0
P
T2
B
4T1 T3
Mock
siRNA
TENM4
pFAK (Y397)
pFAK (Y925)
Total FAK
Vinculin
TENM4
**
Adjusted Relative Density
1.0
0.8
0.6
0.4
0.2
0.0
Mock
siRNA
pFAK (Y925)
***
Adjusted Relative Phosphorilation
1.0
0.8
0.6
0.4
0.2
0.0
Mock
siRNA
C
**
% Tumorsphere generation ability
100
80
60
40
20
0
Mock
siRNA
*
% O.D. (MTT assay)
100
80
60
40
20
0
Mock
siRNA

Supplemetary Fig.1

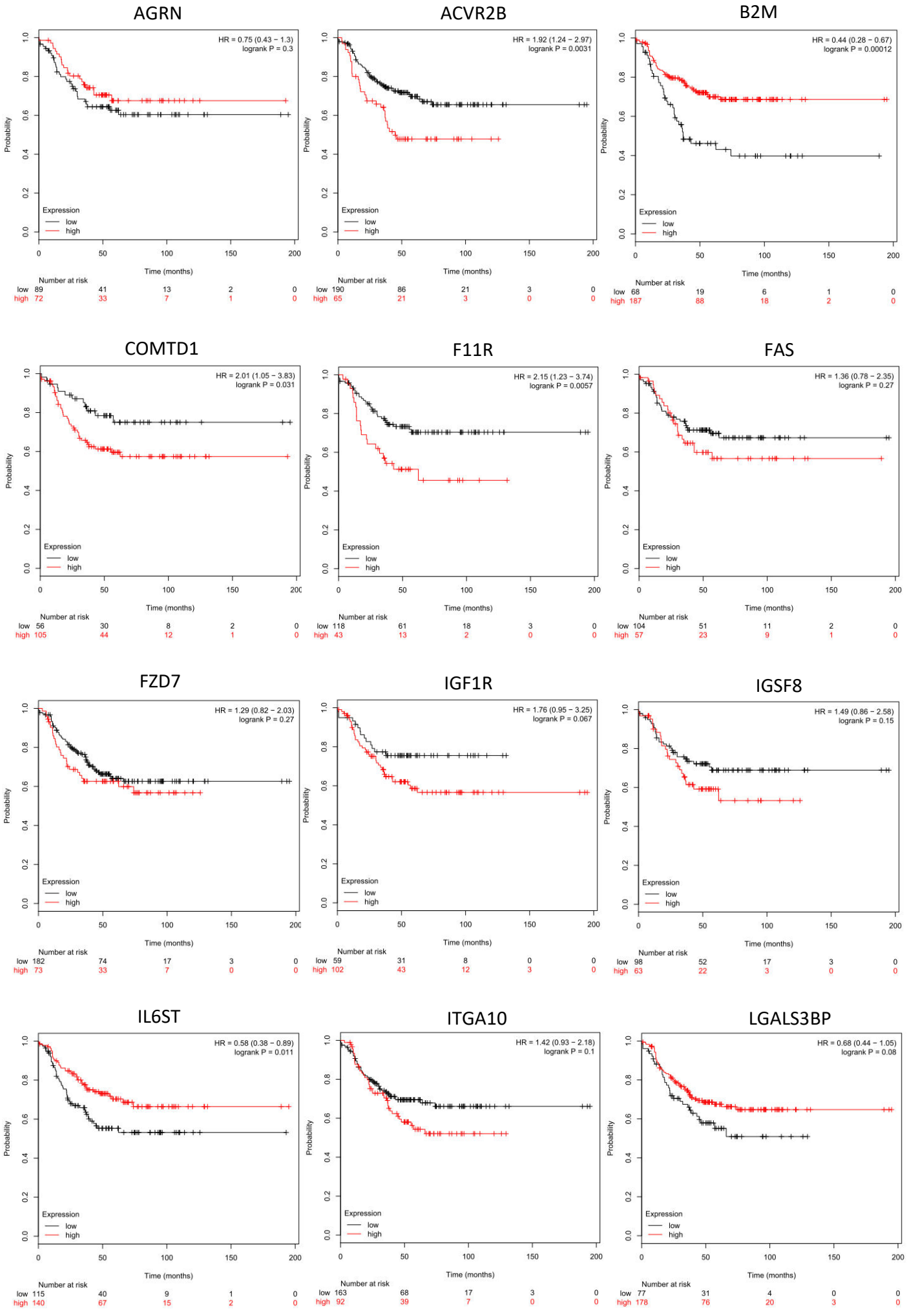

PIP5K1C

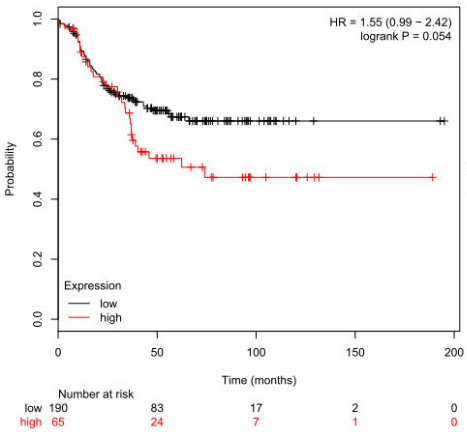

PMP22

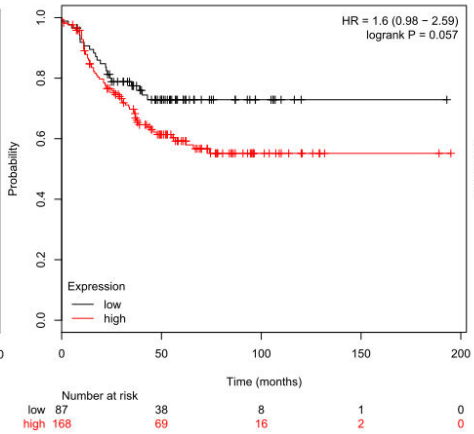

SCARA5

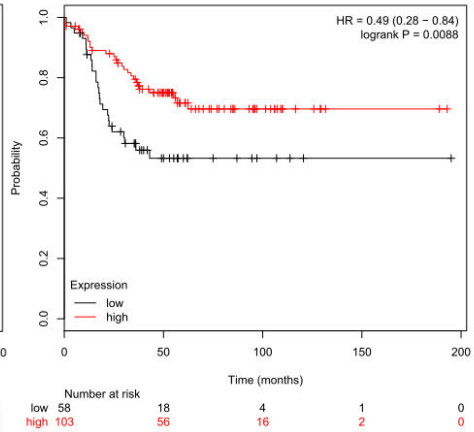

SSC5D

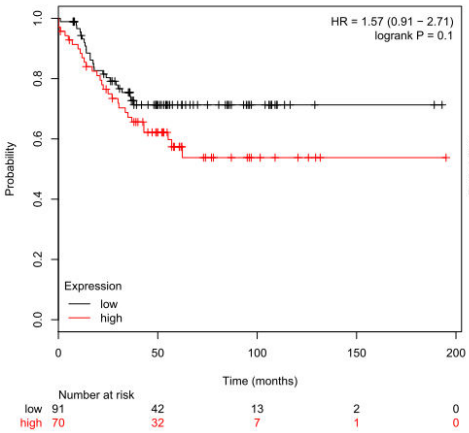

TENM4

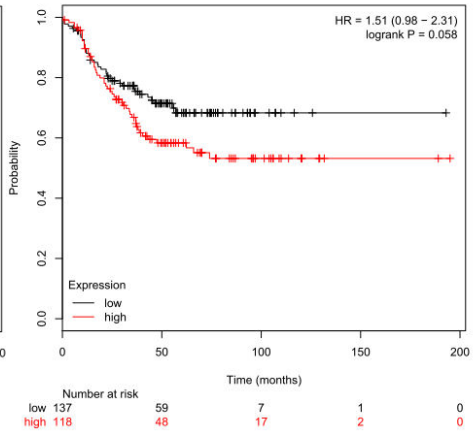

A

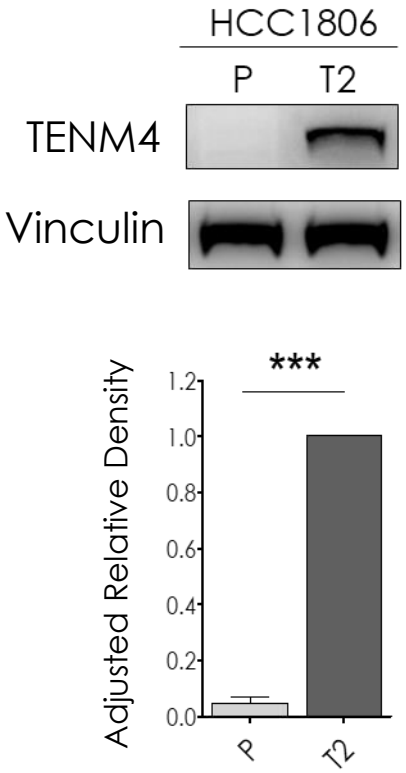
HCC1806
P
T2
TENM4
Vinculin
***
Adjusted Relative Density
1.2
1.0
0.8
0.6
0.4
0.2
0.0
P
T2

B

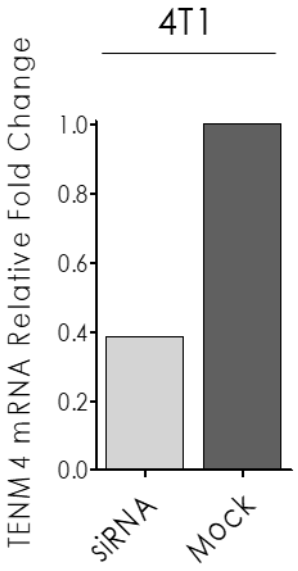
4T1
TENM 4 mRNA Relative Fold Change
1.0
0.8
0.6
0.4
0.2
0.0
siRNA
Mock

Table 1

GENE NAME	**Protein Full Name**	**Log_2FC 4T1**	**Log_2FC HCC1806**
ACVR2B	*Activin receptor type-2B*	1,748951	1,098227
AGRN	*Agrin*	1,871666	1,405154
B2M	*Beta-2 Microglobulin*	1,942163	1,50054
COMTD1	*Catechol-O-Methyltransferase Domain Containing 1*	1,514779	1,281886
F11R	*Junctional adhesion molecule A*	2,138065	2,006326
FAS	*Fas Cell Surface Death Receptor*	2,016033	1,945283
FZD7	*Frizzled-7*	1,672478	1,705518
IGF1R	*Insulin-like growth factor 1 receptor*	1,090656	1,087368
IGSF8	*Immunoglobulin Superfamily, Member 8*	1,429017	1,159
IL6ST	*Interleukin 6 Signal Transducer*	1,518154	1,642875
ITGA10	*Integrin Alpha 10*	2,02747	1,552955
LGALS3BP	*Lectin, Galactoside-binding, Soluble, 3 Binding Protein*	2,217845	1,546496
PIP5K1C	*Phosphatidylinositol 4-phosphate 5-kinase type-1 gamma*	1,301736	1,066668
PMP22	*Peripheral Myelin Protein 22*	2,157392	1,797665
SCARA5	*Scavenger Receptor Class A, Member 5*	4,096917	1,486333
SSC5D	*Scavenger Receptor Cysteine Rich Family, 5 Domains*	1,662582	2,080388
TENM4	*Teneurin Transmembrane Protein 4*	2,862506	2,421285

Supplementary Table 1

A. Genes upregulated in Tumorspheres	
GO Biological Function	**Gene symbols**
negative regulation of neuron death (GO:1901215)	NR4A2, NRBP2, LGMN, CCL2, BDNF, IKBKG, HIPK2
regulation of neuron death (GO:1901214)	NR4A2, CLU, NRBP2, LGMN, CCL2, BDNF, IKBKG, AGRN, HIPK2
regulation of neuron apoptotic process (GO:0043523)	NR4A2, NRBP2, LGMN, CCL2, BDNF, AGRN, HIPK2
response to bacterium (GO:0009617)	SSC5D, NOS2, B2M, BCL3, PTGS2, CCL2, ASS1, FUCA2, SLPI, HIST1H2BK, MALT1
response to biotic stimulus (GO:0009607)	SSC5D, NOS2, B2M, CLU, BCL3, PTGS2, IFI44, CCL2, ASS1, IKBKG, FUCA2, SLPI, HIST1H2BK, TXNIP, MALT1
regulation of cytokine production (GO:0001817)	SSC5D, B2M, CLU, BCL3, PTGS2, F11R, IL6ST, CCL2, IKBKG, BCL6, MALT1
response to other organism (GO:0051707)	SSC5D, NOS2, B2M, CLU, BCL3, PTGS2, IFI44, CCL2, ASS1, IKBKG, FUCA2, SLPI, HIST1H2BK, MALT1
response to external biotic stimulus (GO:0043207)	SSC5D, NOS2, B2M, CLU, BCL3, PTGS2, IFI44, CCL2, ASS1, IKBKG, FUCA2, SLPI, HIST1H2BK, MALT1
negative regulation of apoptotic process (GO:0043066)	NR4A2, CLU, BCL3, IGF1R, IL6ST, NRBP2, LGMN, DUSP1, CCL2, BDNF, FAS, CYR61, BCL6, NR4A1, HIPK2, MALT1
negative regulation of programmed cell death (GO:0043069)	NR4A2, CLU, BCL3, IGF1R, IL6ST, NRBP2, LGMN, DUSP1, CCL2, BDNF, FAS, CYR61, BCL6, NR4A1, HIPK2, MALT1
negative regulation of cell death (GO:0060548)	NR4A2, CLU, BCL3, IGF1R, IL6ST, NRBP2, LGMN, DUSP1, CCL2, BDNF, FAS, IKBKG, CYR61, BCL6, NR4A1, HIPK2, MALT1
enzyme linked receptor protein signaling pathway (GO:0007167)	MVP, ARID5B, TRPS1, ACVR2B, IGF1R, F11R, IL6ST, CCL2, DNM1, BDNF, DUSP4, NR4A1, CSF1, HIPK2, TXNIP
innate immune response (GO:0045087)	SSC5D, NOS2, B2M, CLU, LGMN, CCL2, ASS1, IKBKG, DUSP4, HIST1H2BK, NR4A1, CSF1, TXNIP, MALT1, MASP1
defense response (GO:0006952)	SSC5D, NOS2, B2M, CLU, BCL3, PTGS2, F11R, LGMN, CCL2, ASS1, BDNF, IKBKG, BCL6, SLPI, DUSP4, HIST1H2BK, NR4A1, LGALS3BP, CSF1, TXNIP, MALT1, MASP1
regulation of apoptotic process (GO:0042981)	NR4A2, CLU, TRPS1, BCL3, PTGS2, IGF1R, IL6ST, NRBP2, LGMN, DUSP1, CCL2, BDNF, FAS, CYR61, BCL6, AGRN, NR4A1, HIPK2, TXNIP, MALT1
regulation of programmed cell death (GO:0043067)	NR4A2, CLU, TRPS1, BCL3, PTGS2, IGF1R, IL6ST, NRBP2, LGMN, DUSP1, CCL2, BDNF, FAS, CYR61, BCL6, AGRN, NR4A1, HIPK2, TXNIP, MALT1
immune response (GO:0006955)	SSC5D, NOS2, B2M, CLU, BCL3, IGF1R, LGMN, CCL2, ASS1, FAS, IKBKG, BCL6, SLPI, DUSP4, HIST1H2BK, NR4A1, CSF1, TXNIP, MALT1, MASP1
regulation of cell death (GO:0010941)	NR4A2, CLU, TRPS1, BCL3, PTGS2, IGF1R, IL6ST, NRBP2, LGMN, DUSP1, CCL2, BDNF, FAS, IKBKG, CYR61, BCL6, AGRN, NR4A1, HIPK2, TXNIP, MALT1
positive regulation of multicellular organismal process (GO:0051240)	NOS2, B2M, CLU, BCL3, PTGS2, ACVR2B, IL6ST, CCL2, BDNF, IKBKG, CYR61, NBL1, BCL6, AGRN, CSF1, HIPK2, MALT1, **TENM4**

response to external stimulus (GO:0009605)	SSC5D, NR4A2, NOS2, B2M, CLU, BCL3, PTGS2, IGF1R, IFI44, ATG14, CCL2, DNM1, ASS1, BDNF, FAS, IKBKG, PIP5K1C, CYR61, FUCA2, AGRN, ITGA10, SLPI, HIST1H2BK, NR4A1, TXNIP, MALT1
positive regulation of biosynthetic process (GO:0009891)	NR4A2, NOS2, FOSL2, ARID5B, CLU, CEBPD, BCL3, PTGS2, IGF1R, AHR, CCL2, ASS1, BDNF, CALCOCO1, IKBKG, CYR61, AGRN, FZD7, NR4A1, HIPK2, MALT1
tissue development (GO:0009888)	BDH2, ARID5B, TRPS1, PTGS2, ACVR2B, IGF1R, F11R, DUSP1, IGSF8, BDNF, CYR61, DUSP4, FZD7, NR4A1, CSF1, HIPK2, FNDC3A, TXNIP, **TENM4**
positive regulation of cellular biosynthetic process (GO:0031328)	NR4A2, NOS2, FOSL2, ARID5B, CLU, CEBPD, BCL3, PTGS2, IGF1R, AHR, ASS1, BDNF, CALCOCO1, IKBKG, CYR61, AGRN, FZD7, NR4A1, HIPK2, MALT1
neurogenesis (GO:0022008)	NR4A2, ZSWIM6, CLU, IGF1R, IL6ST, NRBP2, CCL2, DNM1, BDNF, PIP5K1C, NBL1, BCL6, AGRN, ITGA10, FZD7, CSF1, GAS7, HIPK2, **TENM4**
positive regulation of nitrogen compound metabolic process (GO:0051173)	NR4A2, NOS2, FOSL2, ARID5B, CLU, CEBPD, BCL3, PTGS2, IGF1R, AHR, ASS1, BDNF, CALCOCO1, IKBKG, CYR61, AGRN, FZD7, NR4A1, HIPK2, MALT1
regulation of multicellular organismal process (GO:0051239)	SSC5D, NR4A2, NOS2, B2M, ZSWIM6, CLU, TRPS1, BCL3, PTGS2, ACVR2B, F11R, IL6ST, LGMN, CCL2, BDNF, FAS, IKBKG, CYR61, NBL1, BCL6, **SCARA5**, AGRN, FZD7, CSF1, HIPK2, MALT1, **TENM4**
anatomical structure morphogenesis (GO:0009653)	NR4A2, ZSWIM6, CLU, ARID5B, PMP22, BCL3, PTGS2, ACVR2B, IGF1R, DUSP1, CCL2, DNM1, BDNF, PIP5K1C, CYR61, NBL1, BCL6, AGRN, ITGA10, DUSP4, FZD7, NR4A1, CSF1, GAS7, HIPK2, **TENM4**
immune system process (GO:0002376)	SSC5D, NOS2, B2M, CLU, BCL3, IGF1R, LGMN, CCL2, ASS1, FAS, IKBKG, PIPK1C, BCL6, SLPI, DUSP4, FZD7, HIST1H2BK, NR4A1, CSF1, HIPK2, TXNIP, MALT1, MASP1
positive regulation of response to stimulus (GO:0048584)	CREBRF, B2M, CLU, TRPS1, PTGS2, ACVR2B, IGF1R, IL6ST, LGMN, ATG14, CCL2, BDNF, FAS, IKBKG, CYR61, DUSP4, FZD7, CSF1, HIPK2, MALT1, MASP1
cell surface receptor signaling pathway (GO:0007166)	MVP, B2M, ARID5B, TRPS1, ACVR2B, IGF1R, F11R, IL6ST, CCL2, DNM1, BDNF, FAS, CALCOCO1, IKBKG, ITGA10, DUSP4, FZD7, NR4A1, CSF1, HIPK2, TXNIP, MALT1
regulation of molecular function (GO:0065009)	MVP, NR4A2, NOS2, B2M, CLU, ARID5B, BCL3, ACVR2B, IGF1R, F11R, DUSP1, ATG14, CCL2, BDNF, FAS, IKBKG, CYR61, BCL6, AGRN, SLPI, DUSP4, NR4A1, CSF1, HIPK2, KLHL24, TXNIP, MALT1,
regulation of protein metabolic process (GO:0051246)	MVP, NOS2, CREBRF, CLU, TRPS1, BCL3, ACVR2B, IGF1R, IL6ST, DUSP1, ATG14, CCL2, BDNF, FAS, IKBKG, CYR61, BCL6, SLPI, DUSP4, FZD7, NR4A1, CSF1, HIPK2, MALT1, MASP1
cell differentiation (GO:0030154)	BDH2, NR4A2, B2M, ZSWIM6, CLU, ARID5B, TRPS1, BCL3, PTGS2, ACVR2B, IGF1R, F11R, IL6ST, NRBP2, CCL2, DNM1, BDNF, FAS, PIP5K1C, CYR61, NBL1, BCL6, AGRN, ITGA10, FZD7, NR4A1, CSF1, GAS7
regulation of cellular protein metabolic process (GO:0032268)	MVP, CLU, TRPS1, BCL3, ACVR2B, IGF1R, IL6ST, DUSP1, ATG14, CCL2, BDNF, FAS, IKBKG, CYR61, BCL6, SLPI, DUSP4, FZD7, NR4A1, CSF1, HIPK2, MALT1, MASP1
cellular developmental process (GO:0048869)	BDH2, NR4A2, B2M, ZSWIM6, CLU, ARID5B, PMP22, TRPS1, BCL3, PTGS2, ACVR2B, IGF1R, F11R, IL6ST, NRBP2, CCL2, DNM1, BDNF, FAS, PIP5K1C, CYR61, NBL1, BCL6, AGRN, ITGA10, FZD7, NR4A1, CSF1
regulation of signal transduction (GO:0009966)	CREBRF, CLU, TRPS1, BCL3, PTGS2, ACVR2B, IGF1R, IL6ST, LGMN, DUSP1, CCL2, BDNF, FAS, IKBKG, CYR61, CLU, NBL1, BCL6, AGRN, DUSP4, FZD7, CSF1, HIPK2, KLHL24, MALT1

response to stress (GO:0006950)	SSC5D, NR4A2, NOS2, CREBRF, B2M, CLU, BCL3, PTGS2, F11R, LGMN, DUSP1, ATG14, CCL2, ASS1, BDNF, FAS, IKBKG, PIP5K1C, CYR61, PLA2G4A, BCL6, **SCARA5**, ITGA10, SLPI, DUSP4, FZD7, HIST1H2BK, NR4A1, LGALS3BP
positive regulation of cellular metabolic process (GO:0031325)	NR4A2, NOS2, FOSL2, CLU, ARID5B, CEBPD, BCL3, PTGS2, ACVR2B, IGF1R, AHR, IL6ST, ATG14, CCL2, ASS1, BDNF, FAS, CALCOCO1, IKBKG, CYR61, BCL6, AGRN, FZD7, NR4A1, CSF1, HIPK2, MALT1
positive regulation of macromolecule metabolic process (GO:0010604)	NR4A2, CREBRF, FOSL2, CLU, ARID5B, CREBPD, BCL3, ACVR2B, IGF1R, AHR, IL6ST, ATG14, CCL2, BDNF, FAS, CALCOCO1, IKBKG, CYR61, BCL6, AGRN, FZD7, NR4A1, CSF1, HIPK2, MALT1
regulation of signaling (GO:0023051)	MVP, NOS2, CREBRF, CLU, TRPS1, BCL3, PTGS2, ACVR2B, IGF1R, IL6ST, LGMN, DUSP1, CCL2, BDNF, FAS, IKBKG, CYR61, NBL1, BCL6, AGRN, DUSP4, FZD7, CSF1, HIPK2, KLHL24, MALT1
regulation of cell communication (GO:0010646)	NOS2, CREBRF, CLU, TRPS1, BCL3, PTGS2, ACVR2B, IGF1R, IL6ST, NRBP2, LGMN, DUSP1, ATG14, CCL2, BDNF, FAS, IKBKG, CYR61, NBL1, BCL6, AGRN, DUSP4, FZD7, CSF1, HIPK2, KLHL24, MALT1
system development (GO:0048731)	NR4A2, B2M, ZSWIM6, CLU, ARID5B, PMP22, TRPS1, BCL3, PTGS2, ACVR2B, IGF1R, AHR, IL6ST, NRBP2, CCL2, IGSF8, DNM1, ASS1, BDNF, FAS, PIP5K1C, CYR61, NBL1, BCL6, AGRN, ITGA10, FZD7, NR4A1, CSF1
negative regulation of cellular process (GO:0048523)	MVP, SSC5D, NR4A2, CREBRF, CLU, ARID5B, TRPS1, BCL3, PTGS2, ACVR2B, IGF1R, AHR, IL6ST, NRBP2, LGMN, DUSP1, ATG14, CCL2, ASS1, BDNF, FAS, IKBKG, CYR61, NBL1, BCL6, SLPI, DUSP4, FZD7, NR4A1
regulation of response to stimulus (GO:0048583)	CREBRF, B2M, CLU, TRPS1, BCL3, PTGS2, ACVR2B, IGF1R, IL6ST, NRBP2, LGMN, DUSP1, ATG14, CCL2, BDNF, FAS, IKBKG, CYR61, NBL1, BCL6, **SCARA5**, AGRN, DUSP4, FZD7, NR4A1, CSF1, HIPK2, KLHL24
multicellular organismal development (GO:0007275)	SSC5D, NR4A2, B2M, ZSWIM6, CLU, ARID5B, PMP22, TRPS1, BCL3, PTGS2, ACVR2B, IGF1R, AHR, IL6ST, NRBP2, DUSP1, CCL2, IGSF8, DNM1, ASS1, BDNF, FAS, PIP5K1C, CYR61, NBL1, BCL6, AGRN, ITGA10, DUSP4
anatomical structure development (GO:0048856)	BDH2, NR4A2, B2M, ZSWIM6, CLU, ARID5B, PMP22, TRPS1, BCL3, PTGS2, ACVR2B, IGF1R, AHR, F11R, IL6ST, NRBP2, DUSP1, CCL2, IGSF8, DNM1, ASS1, BDNF, FAS, PIP5K1C, CYR61, NBL1, BCL6, AGRN, ITGA10
negative regulation of biological process (GO:0048519)	MVP, SSC5D, NR4A2, NOS2, CREBRF, CLU, ARID5B, TRPS1, BCL3, PTGS2, ACVR2B, IGF1R, AHR, F11R, IL6ST, NRBP2, LGMN, DUSP1, ATG14, CCL2, ASS1, BDNF, FAS, IKBKG, CYR61, NBL1, BCL6, SLPI, DUSP4
positive regulation of metabolic process (GO:0009893)	NR4A2, NOS2, CREBRF, FOSL2, CLU, ARID5B, CEBPD, BCL3, PTGS2, ACVR2B, IGF1R, AHR, F11R, IL6ST, ATG14, CCL2, ASS1, BDNF, FAS, CALCOCO1, IKBKG, CYR61, BCL6, AGRN, FZD7, NR4A1, CSF1, HIPK2
developmental process (GO:0032502)	BDH2, SSC5D, NR4A2, B2M, ZSWIM6, CLU, ARID5B, PMP22, TRPS1, PNPLA7, BCL3, PTGS2, ACVR2B, IGF1R, AHR, F11R, IL6ST, NRBP2, DUSP1, CCL2, IGSF8, DNM1, ASS1, BDNF, FAS, PIP5K1C, CYR61, NBL1, BCL6
single-organism developmental process (GO:0044767)	BDH2, SSC5D, NR4A2, B2M, ZSWIM6, CLU, ARID5B, PMP22, TRPS1, BCL3, PTGS2, ACVR2B, IGF1R, AHR, F11R, IL6ST, NRBP2, DUSP1, CCL2, IGSF8, DNM1, ASS1, BDNF, FAS, PIP5K1C, CYR61, NBL1, BCL6, AGRN
positive regulation of cellular process	NR4A2, NOS2, CREBRF, B2M, FOSL2, CLU, ARID5B, TRPS1, CEBPD, BCL3, PTGS2, ACVR2B, IGF1R, AHR, IL6ST, ATG14, CCL2,

(GO:0048522)	ASS1, BDNF, FAS, CALCOCO1, IKBKG, CYR61, NBL1, BCL6, AGRN, FZD7, NR4A1
signal transduction (GO:0007165)	MVP,NR4A2, NOS2, B2M, CLU, ARID5B, TRPS1, BCL3, ACVR2B, IGF1R, ARL5B, AHR, F11R, IL6ST, LGMN, DUSP1, PLEKHM3, CCL2, DNM1, BDNF, FAS, CALCOCO1, IKBKG, CYR61, BCL6, AGRN, ITGA10, DUSP4, FZD7
positive regulation of biological process (GO:0048518)	NR4A2, NOS2, CREBRF, B2M, FOSL2, CLU, ARID5B, TRPS1, CEBPD, BCL3, PTGS2, ACVR2B, IGF1R, AHR, F11R, IL6ST, LGMN, DUSP1, ATG14, CCL2, ASS1, BDNF, FAS, CALCOCO1, IKBKG, CYR61, NBL1, BCL6, AGRN
cell communication (GO:0007154)	MVP,NR4A2, NOS2, B2M, CLU, ARID5B, PMP22, TRPS1, BCL3, ACVR2B, IGF1R, ARL5B, AHR, F11R, IL6ST, LGMN, DUSP1, PLEKHM3, ATG14, CCL2, DNM1, BDNF, FAS, CALCOCO1, IKBKG, CYR61, BCL6, AGRN
single organism signaling (GO:0044700)	MVP,NR4A2, NOS2, B2M, CLU, ARID5B, PMP22, TRPS1, BCL3, ACVR2B, IGF1R, ARL5B, AHR, F11R, IL6ST, LGMN, DUSP1, PLEKHM3, CCL2, DNM1, BDNF, FAS, CALCOCO1, IKBKG, CYR61, BCL6, AGRN, ITGA10
signaling (GO:0023052)	MVP,NR4A2, NOS2, B2M, CLU, ARID5B, PMP22, TRPS1, BCL3, ACVR2B, IGF1R, ARL5B, AHR, F11R, IL6ST, LGMN, DUSP1, PLEKHM3, CCL2, DNM1, BDNF, FAS, CALCOCO1, IKBKG, CYR61, BCL6, AGRN, ITGA10
cellular response to stimulus (GO:0051716)	MVP,NR4A2, NOS2, CREBRF, B2M, CLU, ARID5B, TRPS1, BCL3, PTGS2, ACVR2B, IGF1R, ARL5B, AHR, F11R, IL6ST, LGMN, DUSP1, PLEKHM3, ATG14, CCL2, DNM1, BDNF, FAS, CALCOCO1, IKBKG, PIP5K1C, CYR61
single-multicellular organism process (GO:0044707)	SSC5D, NR4A2, NOS2, B2M, ZSWIM6, CLU, ARID5B, PMP22, TRPS1, BCL3, PTGS2, ACVR2B, IGF1R, AHR, IL6ST, NRBP2, LGMN, DUSP1, CCL2, IGSF8, DNM1, ASS1, BDNF, FAS, PIP5K1C, CYR61, NBL1, PLA2G4A
multicellular organismal process (GO:0032501)	SSC5D, NR4A2, NOS2, CREBRF, B2M, ZSWIM6, CLU, ARID5B, PMP22, TRPS1, BCL3, PTGS2, ACVR2B, IGF1R, AHR, F11R, IL6ST, NRBP2, LGMN, DUSP1, CCL2, IGSF8, DNM1, ASS1, BDNF, FAS, PIP5K1C, CYR61, NBL1
response to stimulus (GO:0050896)	MVP, SSC5D, NR4A2, NOS2, CREBRF, B2M, CLU, ARID5B, TRPS1, BCL3, PTGS2, ACVR2B, IGF1R, ARL5B, AHR, F11R, IL6ST, LGMN, DUSP1, IFI44, PLEKHM3, ATG14, CCL2, DNM1, ASS1, BDNF, FAS, CALCOCO1, IKBKG, PIP5K1C
Unclassified (UNCLASSIFIED)	RNF122, MFAP3L, LRRN4CL, TCP11L2

B. Genes downregulated in Tumorspheres	
GO Biological Function	**Gene symbols**
isopentenyl diphosphate biosynthetic process, mevalonate pathway (GO:0019287)	MVK, PMVK, MVD
isopentenyl diphosphate biosynthetic process (GO:0009240)	MVK, PMVK, MVD
isopentenyl diphosphate metabolic process (GO:0046490)	MVK, PMVK, MVD

cholesterol biosynthetic process (GO:0006695)	CYP51A1, MVK, PMVK, SQLE, MSMO1, DHCR7, MVD, IDI1
sterol biosynthetic process (GO:0016126)	CYP51A1, MVK, PMVK, SQLE, MSMO1, DHCR7, MVD, IDI1
isoprenoid biosynthetic process (GO:0008299)	MVK, PMVK, MVD, IDI1
cholesterol metabolic process (GO:0008203)	CYP51A1, MVK, PMVK, SQLE, MSMO1, DHCR7, PCSK9, MVD, IDI1
sterol metabolic process (GO:0016125)	CYP51A1, MVK, PMVK, SQLE, MSMO1, DHCR7, PCSK9, MVD, IDI1
steroid biosynthetic process (GO:0006694)	CYP51A1, MVK, PMVK, SQLE, MSMO1, DHCR7, MVD, IDI1
alcohol biosynthetic process (GO:0046165)	CYP51A1, MVK, PMVK, SQLE, MSMO1, DHCR7, MVD, IDI1
mitotic prometaphase (GO:0000236)	CDC20, CCNB2, KIF2C, CENPM, ERCCL6, CENPU
organic hydroxy compound biosynthetic process (GO:1901617)	CYP51A1, MVK, PMVK, SQLE, MSMO1, DHCR7, MVD, IDI1
steroid metabolic process (GO:0008202)	CYP51A1, MVK, PMVK, SQLE, MSMO1, DHCR7, CYP24A1, PCSK9, MVD, IDI1
anaphase (GO:0051322)	CDC20, KIF2C, ESPL1, CENPM, ERCC6L, CENPU
mitotic anaphase (GO:0000090)	CDC20, KIF2C, ESPL1, CENPM, ERCC6L, CENPU
mitotic M phase (GO:0000087)	CDC20, CCNB2, KIF2C, ESPL1, CENPM, ERCC6L, KIF23, CENPU
M phase (GO:0000279)	CDC20, CCNB2, KIF2C, ESPL1, CENPM, ERCC6L, KIF23, CENPU
alcohol metabolic process (GO:0006066)	CYP51A1, MVK, PMVK, SQLE, MSMO1, DBI, DHCR7, CYP24A1, PCSK9, MVD, IDI1
mitotic nuclear division (GO:0007067)	CDC20, CCNB2, KIF2C, MYBL2, CEP55, ESPL1, ERCC6L, CDCA3, KIF23, FAM83D
mitotic cell cycle phase (GO:0098763)	CDC20, CCNB2, KIF2C, ESPL1, CENPM, ERCC6L, KIF23, CENPU
cell cycle phase (GO:0022403)	CDC20, CCNB2, KIF2C, ESPL1, CENPM, ERCC6L, KIF23, CENPU
biological phase (GO:0044848)	CDC20, CCNB2, KIF2C, ESPL1, CENPM, ERCC6L, KIF23, CENPU
nuclear division (GO:0000280)	CDC20, CCNB2, KIF2C, MYBL2, CEP55, ESPL1, ERCC6L, CDCA3, KIF23, FAM83D
organic hydroxy compound metabolic process (GO:1901615)	CYP51A1, MVK, PMVK, SQLE, MSMO1, DHCR7, CYP24A1, PCSK9, MVD, IDI1
small molecule biosynthetic process (GO:0044283)	CYP51A1, MVK, PMVK, SQLE, MSMO1, FADS2, DHCR7, MVD, IDI1
cell division (GO:0051301)	CDC20, CCNB2, KIF2C, CEP55, TUBA1C, ESPL1, ERCC6L, CDCA3, KIF23, FAM83D
organelle fission (GO:0048285)	CDC20, CCNB2, KIF2C, MYBL2, CEP55, ESPL1, ERCC6L, CDCA3, KIF23, FAM83D
lipid biosynthetic process (GO:0008610)	CYP51A1, MVK, PMVK, SQLE, MSMO1, FADS2, DHCR7, MVD, IDI1
mitotic cell cycle (GO:0000278)	CDC20, CCNB2, KIF2C, MYBL2, CEP55, ESPL1, CENPM, ERCC6L, CDCA3, TTK, KIF23, FAM83D, CENPU

mitotic cell cycle process (GO:1903047)	CDC20, CCNB2, KIF2C, MYBL2, CEP55, ESPL1, ERCC6L, CDCA3, TTK, KIF23, FAM83D
lipid metabolic process (GO:0006629)	CYP51A1, MVK, PMVK, SQLE, MSMO1, AACS, FADS2, DBI, DHCR7, ACAT2, CYP24A1, PCSK9, MVD, IDI1, ARSJ
cell cycle (GO:0007049)	CDC20, CCNB2, KIF2C, MYBL2, CEP55, ESPL1, CENPM, ERCC6L, CDCA3, TTK, MND1, KIF23, FAM83D, CENPU
cell cycle process (GO:0022402)	CDC20, CCNB2, KIF2C, MYBL2, CEP55, ESPL1, ERCC6L, CDCA3, TTK, KIF23, FAM83D
small molecule metabolic process (GO:0044281)	CYP51A1, MVK, PMVK, SQLE, MSMO1, AACS, FADS2, CDA, DBI, DHCR7, CYP24A1, PCSK9, MVD, TK1, IDI1, ARSJ
single-organism process (GO:0044699)	CDC20, CYP51A1, MVK, CCNB2, SGK2, KIF2C, PMBK, SQLE, DEPDC1B, MSMO1, MYBL2, AACS, CEP55, FADS2, CDA, MDM1, ITGA2, TUBA1C, HBEGF, RIPK3, ESPL1, CENPM, ERCC6L, CDCA3, TTK, DBI, DHCR7, ACAT2, MND1, CYP24A1
Unclassified (UNCLASSIFIED)	SAPCD2, CEP128

ATTACHMENT B

List of activities performed during the PhD program

STAYS ABROAD

1st May 2016 to 31 July 2016 (3 months): Visiting PhD Student at Cancer Sciences Unit, Faculty of Medicine, University of Southampton (Southampton, UK) under the supervision of Dott. Natalia Savelyeva and Prof. Christian Ottensmaier.
While hosted by Cancer Sciences Unit at the University of Southampton, I had to manage three different projects:

- Identification and validation of neo-epitopes in a HPV^+ tumor model as target of DNA-based anti-tumor vaccination.
- Setting up a protocol for the generation of stable cell lines established from frozen tumor biopsies.
- Generation of DNA-based vaccines encoding a fusion protein consisting of the murine xCT ORF linked to the nontoxic region Fragment C (FrC) of the Tetanus toxin to be used as immunostimolatory sequence.

ABSTRACTS (from 01/12/2016 to 05/12/2017)

- Ruiu R, Arigoni M, Riccardo F, Conti L, Lanzardo S, Calogero RA, Cavallo F, Quaglino E., *Comparative Transcriptomics of Triple Negative Breast Cancer Stem Cells and Differentiated Tumor Cells Identifies TENM4 as a Potential Therapeutic Target.* 1st European PhD and Postdoc ENABLE symposium *"Breaking Down Complexity: Innovative Models and Techniques in Biomedicine", Barcelona (SPAIN), 15-17/11/2017,* ***Poster presentation by Ruiu R***

- Conti L, Lanzardo S, Ballatore A, Ruiu R, Donofrio G, Cavallo F., *Targeting the xCT cystine/glutamate antiporter through a Bovine Herpesvirus 4-based vaccination to eradicate breast cancer stem cells in the preclinical setting.* "International Retreat of PhD Students in Immunology | SIICA", Verona (ITALY) 6-7/10/2017, **Oral presentation by Ruiu R**

- Ruiu R, Arigoni M, Riccardo F, Conti L, Lanzardo S, Calogero RA, Cavallo F, Quaglino E., *TENM4 emerges as a potential target for Triple Negative Breast Cancer Stem Cells-directed vaccination.* "17th International Congress on Progress in Vaccination Against Cancer (PIVAC-17)". Loutraki, Corinth (GREECE), 27-30/09/2017, **Poster and oral presentation by Quaglino E.**

- Conti L, Lanzardo S, Ruiu R, Bolli E, Donofrio G, O'Rourke JP, Pericle F, Cavallo F. *Cytofluorimetric characterization of immune responses induced by a vaccine targeting the cancer stem cell antigen xCT in breast cancer models*. "ESCCA (European Society for Clinical Cell Analysis) 2017". 24-27/09/2017, Thessaloniki (GREECE). **Poster presentation by Conti L**

- Ruiu R, Arigoni M, Riccardo F, Conti L, Lanzardo S, Calogero RA, Cavallo F, Quaglino E., *Comparative Transcriptomics of Triple Negative Breast Cancer Stem Cells and Differentiated Tumor Cells Identifies TENM4 as a Potential Therapeutic Target.* "D-Day of Doctoral School in Life and Health Sciences", Turin (ITALY) 19/09/2017, **Poster presentation by Ruiu R.**

- Ruiu R, Arigoni M, Riccardo F, Conti L, Lanzardo S, Calogero RA, Cavallo F, Quaglino E., *Comparative Transcriptomics of Triple Negative Breast Cancer Stem Cells and Differentiated Tumor Cells Identifies TENM4 as a Potential Therapeutic Target.* "EACR-AACR-SIC (European Association for Cancer Research - American Association for Cancer Research – Società Italiana di Cancerologia) Special Conference 2017: The Challenges of Optimizing

Immuno- and Targeted Therapies: From Cancer Biology to the Clinic", Florence (ITALY) 24-27/06/2017, **Poster presentation by Ruiu R.**

- Conti L, Lanzardo S, Bolli E, Rolih V, Ballatore A, Ruiu R, Donofrio G, O'Rourke JP, Pericle F, Cavallo F. *Mouse breast tumor growth and metastasis inhibition via immunotargeting of the cancer stem cell antigen xCT***. "**XI National Conference SIICA (Società Italiana di Immunologia Clinica e Allergologia)". 28-31/05/2017, Bari (ITALY). **Poster presentation by Conti L**

- Zottnick S, Ruiu R, Wood O, Bryant D, Harden E, Sahota S, Savelyeva N and Ottensmeier C. *Development of mutanome-based DNA vaccines targeting tumour Neo-epitopes.* "Cancer Sciences Unit Conference 2016", Southampton (UNITED KINGDOM) 21/10/2016. **Poster presentation by Zottnick S.**

- Conti L, Lanzardo S, Ruiu R, Bolli E, Rolih V**,** Donofrio G, O'Rourke JP, Pericle F, Calogero RA, and Cavallo F. *Immunotargeting of Antigen xCT Attenuates Stem-Like Cell Behavior and Metastatic Progression in Breast Cancer.* "XIV NIBIT (Network Italiano per la Bio-Terapia dei Tumori) Meeting", Siena (ITALY) 13-15/10/2016. **Poster presentation by Conti L.**

- Crich SG, Cutrin JC, Conti L, Lanzardo S, Ruiu R, Cadenazzi M, and Aime S. *Cancer Stem Cells targeting for tumour therapy and diagnosis*. "COST Action TD1004 Annual meeting", Istambul (TURKEY), 3-4/10/2016. **Poster presentation by Crich SG.**

- Ruiu R, Arigoni M, Riccardo F, Conti L, Lanzardo S, Musiu C, Calogero RA, and Cavallo F. *Comparative Transcriptomics of Triple Negative Breast Cancer Stem Cells and Differentiated Tumor Cells Identifies Teneurin-4 as a Potential Target for Immunotherapy.* "X National Conference SIICA (Società Italiana di Immunologia Clinica e Allergologia", Abano Terme (ITALY) 25-28/05/2016, **Poster presentation by Riccardo F.**

- Crich SG, Conti L, Lanzardo S, Cutrin JC, Ruiu R, and Aime S. *L- Ferritin targets breast cancer stem cells and delivers therapeutic and imaging agents*. "European Molecular Imaging Meeting (EMIM) 2016", Utrecht (NETHERLANDS) 8-10/03/2016. **Poster presentation by Crich SG.**

- Lanzardo S, Conti L, Rooke R, Ruiu R, Accart N, Bolli E, Arigoni M, Macagno M, Barrera G, Pizzimenti S, Aurisicchio L, Calogero RA, Cavallo F., *Mouse breast tumor growth and metastasis inhibition via immunotargeting of the cancer stem cell antigen xCT.* "Cancer Vaccine Conference Amsterdam", Amsterdam (NETHERLANDS) 24-25/11/2015, **Poster presentation by Ruiu R.**

- Lanzardo S, Conti L, Rooke R, Ruiu R, Accart N, Bolli E, Arigoni M, Macagno M, Barrera G, Pizzimenti S, Calogero RA and Cavallo F. *xCT is a new cancer stem cell immunotherapeutic target for breast cancer*. "15th International Congress on Progress In Vaccination Against Cancer (PIVAC-15)", Tubingen (GERMANY) 6-8/10/2015, **Oral presentation by Ruiu R.**

- Ruiu R, Lanzardo S, Conti L, Calogero RA, Cavallo F. *TMPRSS4 is a breast cancer stem cell-associated antigen and a putative target for DNA-based vaccination*. 13th Association for Cancer Immunotherapy (CIMT) Annual Meeting", Mainz (GERMANY) 11-13/05/2015, **Poster presentation by Ruiu R.**

- Conti L, Lanzardo S, Ruiu R, Macagno M, Quaglino E, Calogero RA and Cavallo F. *xCT is a new immunotherapeutic target for breast cancer.* "Dianzani Meeting", Cagliari (ITALY) 20-21/03/2015**. Oral presentation by Conti L.**

- Conti L, Lanzardo S, Ruiu R, Geninatti Crich S, Cadenazzi M, Cutrin JC, Aime S, Calogero RA, Cavallo F. *Class A Scavenger Receptor Member 5 is a promising target for mammary cancer stem cell eradication.* "14th International Congress on Progress in Vaccination Against Cancer (PIVAC-14)", Rome (ITALY) 24-26/09/2014, **Poster presentation by Conti L.**

- Lanzardo S, Conti L, Ruiu R, Antonazzo R, Calogero RA, and Cavallo F. *Mouse-human microarray data integration reveals xCT as a new oncoantigen of breast cancer stem cells*. "14th International Congress on Progress in Vaccination Against Cancer (PIVAC-14)", Rome (ITALY) 24-26/09/2014, **Poster presentation by Lanzardo S.**

- Ruiu R, Lanzardo S, Conti L, Bandini S, Arigoni M, Calogero RA, and Cavallo F. *TMPRSS4 is a breast cancer stem cell-associated target suitable for anti-tumor immune targeting*. "14th International Congress on Progress in Vaccination Against Cancer (PIVAC-14)", Rome (ITALY) 24-26/09/2014, **Poster presentation by Ruiu R.**

- Ruiu R, Conti L, Arigoni M, Calogero RA, Cavallo F, and Lanzardo S. *The type II transmebrane serine protease TMPRSS4 is a promising cancer stem cell-associated target.* "Dangerous Liaisons: translating cancer biology into better patients management - 56° Congresso Nazionale SIC (Società Italiana di Cancerologia)", Ferrara (ITALY) 11-13/09/2014, **Poster presentation by Ruiu R.**

- Lanzardo S, Conti L, Ruiu R, Antonazzo R, Calogero RA and Cavallo F. *Cancer Stem Cell Oncoantigens Identification: two examples from breast cancer.* "Workshop Società Italiana di Cancerologia (SIC): Targeted Therapy of Cancer: Where we are heading", Turin (ITALY) 27/06/2014. **Oral presentation by Lanzardo S.**

- Ruiu R, Cadenazzi M, Geninatti Crich S, Conti L, Lanzardo S, Cutrin JC, Cavallo F, and Aime S. *Class A Scavenger Receptor Member 5 is a promising target in mammary cancer stem cell-specific MRI imaging and therapy.* "Workshop SIC: Targeted Therapy of Cancer: Where we are heading", Turin (ITALY) 27/06/2014, selected for **abstract book**.

- Lanzardo S, Conti L, Ruiu R, Antonazzo R, Calogero RA, and Cavallo F. *Mouse-human microarray data integration reveals xCT as a new oncoantigen of breast cancer stem cells*. "IX National Conference SIICA (Società Italiana di Immunologia Clinica e Allergologia)", Florence (ITALY) 28-31/05/2014, **Poster presentation by Ruiu R**.

ATTENDED CONGRESSES and CONFERENCES (from 01/01/2014 to 05/12/2017)

- 1st European PhD and Postdoc ENABLE symposium "*Breaking Down Complexity: Innovative Models and Techniques in Biomedicine*", Barcelona (SPAIN), 15-17/11/2017

- *"International Retreat of PhD Students in Immunology | SIICA" ,* Verona (ITALY), 6-7/10/2017

- "*Doctoral Day (D-Day) of the Doctoral School of Life and Health Sciences 2017*", MBC, Turin 19/09/2017

- *"EACR-AACR-SIC Special Conference 2017: The Challenges of Optimizing Immuno- and Targeted Therapies: From Cancer Biology to the Clinic",* Florence (ITALY), 24-27/06/2017

- *"Doctoral Day (D-Day) of the Doctoral School of Life and Health Sciences 2016",* MBC Turin 15/09/2016

- *"16th International Congress on Progress In Vaccination Against Cancer (PIVAC) 16",* European Association for Cancer Research (EACR), Winchester (UNITED KINGDOM), 12-14/09/2016

- *"Faculty of Medicine Research Conference 2016",* Faculty of Medicine - University of Southampton, Southampton (UNITED KINGDOM), 23/06/2016

- *"Cancer Vaccine Conference Amsterdam",* Amsterdam (NETHERLANDS) 24-25/11/2015

- *"15th International Congress on Progress In Vaccination Against Cancer (PIVAC) 15",* European Association for Cancer Research (EACR), Tubingen (GERMANY), 6-8/10/2015

- *"Doctoral Day (D-Day) of the Doctoral School of Life and Health Sciences 2015",* Rettorato dell'Università degli Studi di Torino, Torino 16/09/2015

- *"13th CIMT ANNUAL MEETING",* Association for Cancer Immunotherapy (CIMT), Mainz (GERMANY), 11-13/05/2015

- *"Frontiers in Regenerative Medicine"* Molecular Biotechnology Center, Torino (ITALY) 19-20/02/2015

- *"14th International Congress on Progress in Vaccination Against Cancer (PIVAC) 14",* Rome (ITALY) 24-26/09/2014

- *"Dangerous Liaisons: translating cancer biology into better patients management - 56° Congresso Nazionale Società Italiana di Cancerologia (SIC)",* Ferrara (ITALY) 11-13/09/2014

- *"Targeted Therapy of Cancer: Where we are heading",* Società Italiana di Cancerologia (SIC), Turin (ITALY) 27/06/2014

- *"IX National Conference of the Italian Society of Clinical Immunology and Allergology (SIICA)",* Florence (ITALY) 28-31/05/2014

ATTENDED LECTURES (external speakers only), COURSES and WORKSHOPS (from 01/01/2014 to 05/12/2017)

- Course "*Introduction to ImageJ/Fiji*", held by Marta Gai, MBC Turin 01/12/2017.

- Seminar "*NK cell-mediated immunosurveillance against drug-induced senescent tumor cells*", Angela Santoni, hosted by Francesco Novelli and Federica Cavallo, MBC Turin 26/10/2017.
- Workshop "*Giornata dedicata alla valorizzazione delle competenze dei dottori di ricerca e ai loro sbocchi occupazionali*" organized by Doctoral Schools of University of Turin, Cavallerizza Reale, Turin 06/10/2017.
- Seminar "*Phenoptics: Immuno-profiling and phenotyping of multiple immune cell subsets in situ in FFPE tissue sections*" by Perkin Elmer, hosted by Federica Cavallo, MBC Turin 04/10/2017
- Workshop "*How to Brand Yourself*", organized by University of Turin, Politecnique School of Turin, Université de Lyon and CUSO, Archamps (FRANCE) 20-22/09/2017.
- Seminar "*Pathophysiology of the P2X7 receptor: a mastermind in cancer and inflammation*", Francesco di Virgilio, hosted by Silvia Deaglio, Turin 10/07/2017.
- Seminar "*The NCI PREVENT Cancer Program*", Shizuko Sei, hosted by Francesco Novelli, MBC Turin 21/06/2017.
- Course "*Basics of Management for Scientists*", organized by Doctoral School of Life and Health Sciences, MBC Turin 12-16/06/2017
- Seminar "*SIRT6-dependent Metabolic Reprogramming as a Driver of Stemness and Tumorigenesis in the Intestine*", Carlos Sebastian. hosted by Miriam Martini, MBC Turin 08/06/2017
- Workshop "*Principal techniques for project design*", organized by Doctoral Schools of University of Turin, Rettorato, Turin 08/03/2017
- Workshop "*Building your Career in the EU*", organized by Doctoral Schools of University of Turin, Rettorato, Turin 01/03/2017
- Workshop "*Workshop sul trasferimento di conoscenze per dottorandi*", organized by Doctoral Schools of University of Turin, Cavallerizza Reale, Turin 14/12/2016
- Seminar *"Mechanisms and Predictors of Resistance to Immune Checkpoint Blockade",* Nicolas Jacquelot, hosted by Emilio Hirsch, MBC Turin 08/11/2016
- Seminar *"Chemotherapy Resistance and Reversal of Resistance in the Mammary Carcinoma: An In Vitro Perspective",* Ozlem Darcansoy Iseri, hosted by Valeria Poli, MBC Turin 25/10/2016
- Seminar *"Tricks of the Trade: A Personal Perspective on Maximizing the Impact of Your Research",* David Chamberlain, Hosted by Sara Cabodi, MBC Turin 10/10/2016

- Workshop *"Essential Public Spaeking Skills for postdocs",* Andrew Manasseh, promoted by "Scuole di Dottorato – Direzione Ricerca e Relazioni Internazionali", Cavallerizza Reale, Turin 4/10/2016
- *"Giornata dedicate alla valorizzazione delle competenze dei dottori di ricerca e al postdoc – Sessione Plenaria",* promoted by "Scuole di Dottorato – Direzione Ricerca e Relazioni Internazionali", Aula Magna Cavallerizza Reale, Turin 04/10/2016
- Seminar *"CLIC1 protein activation as a novel determinant of human glioblastoma stem cells proliferation",* Michele Mazzanti, hosted by Federica Cavallo, MBC Turin 15/04/2016
- Seminar *"The transparent editorial process, data reproducibility and research integrity at EMBO Press"* Roberto Buccione, hosted by Emilio Hirsch, MBC Turin 21/03/2016
- Course *"Corso di Citofluorimetria",* Società Italiana di Cancerologia in collaboration with Becton Dickinson, IRCCS Candiolo, 18/03/2016
- Course *"Corso d'Inglese Scientifico Livello B1/B2",* Anna Justina Walus, promoted by Scuola di Dottorato SCIVISA, Turin, November 2015 - March 2016. Final Test: PASSED
- Workshop *"Enabling Technologies in 3D cancer organoids",* MBC Turin 8-9/03/16
- Seminar *"The key role of ERBB2 in cardiac regeneration and cancer",* Gabriele D'Uva, hosted by Emilio Hirsch, MBC Turin 26/02/2016
- Seminar *"In vivo imaging of adaptive immune responses",* Matteo Iannacone, hosted by Emilio Hirsch, MBC Turin 23/02/2016
- Seminar *"Inherited damaging mutations in immune-related genes favour the development of genetically heterogeneous synchronous colorectal cancer",* Matteo Cereda, hosted by Salvatore Oliviero, MBC Turin 22/01/2016
- Seminar *"Electric signals regulated cell migration, division and differentiation",* Bing Song, hosted by Emilio Hirsch, Turin 11/11/2015
- *"Valorizzare le competenze dei dottori di ricerca ed accompagnarli nel mondo del lavoro",* promoted by Scuole di Dottorato dell'Università di Torino, Torino 01/10/2015
- Course *"Corso di Biostatistica",* Scuola di dottorato SCIVISA, Torino 15,23,30/06/2015
- Course *"Flow Cytometry in translational cancer research: Believe in rare!",* Achille Anselmo, Humanitas Research Hospital, Rozzano (MI) 10/06/2015
- Seminar *"Circular and linear Non-Coding RNAs in tumorigenesis",* Pier Paolo Pandolfi, hosted by Fiorella Altruda, Turin 06/05/2015
- *"Il trasferimento di conoscenze in ateneo: dalla ricerca alla valorizzazione dell'innovazione",* Ufficio Brevetti e Trasferimento tecnologico dell'università di torino, promoted by Scuole di dottorato dell'università di Torino, Turin 03/02/2015

- Seminar *"The Biology of shape: from Aristotele to Stem Cells",* Stefano Piccolo, hosted by Valeria Poli, Turin 30/01/2015
- Seminar *"Antitumoral effects of metformin on cancer stem cells: identification of novel molecular targets",* Roberto Wurth, hosted by Valeria Poli, Turin 22/01/2015
- Course *"Miti e leggende nella citometria a Flusso",* Enrico Ghersi (Miltenyi Biotech), hosted by Davide Brusa (HuGeF), Turin 3/12/2014
- Seminar "*Senescence therapy for cancer: the key role of the immune system*", Alberto Toso, hosted by Emilio Hirsch, Turin 25/11/2014
- Workshop "*Sperimentazione Animale e Metodi Alternativi: tra miti, polemiche e realtà scientifica*", Fondazione Fondo Ricerca e Talenti, Turin 27/10/2014
- Course "*Introduzione alla ricerca bibliografica*", Doctoral School in Life and Health Sciences, Turin 16,23/10/2014
- Seminar "*Microenvironmental regulation of breast cancer metastasis*", Antoine E. Karnoub, hosted by Daniela Taverna, Turin 12/06/2014
- Seminar "*Reciprocal metabolic deregulation of tumors and their stroma: a new druggable synergy*", Paola Chiarugi, hosted by Valeria Poli, Turin 22/05/2014
- Seminar "*Cracking the code of Pluripotent Stem Cells*", Graziano Martello, hosted by Salvatore Oliviero, Turin 08/05/2014
- Seminar "*Prominin-1 (CD133) Reveals Novel Insights into the Stem and Progenitor Cell Biology*", Denis Corbeil, hosted by Benedetta Bussolati, Turin 25/02/2014
- Seminar "*Molecular Imaging of Enzymatic Activity in Inflammation and Cancer*", Alexei Bogdanov, hosted by Silvio Aime, Turin 13/02/2014
- Seminar "*Fast-tracking Molecular Diagnostics in Oncology*", William Gallagher, hosted by Paola Defilippi, Turin 03/02/2014

“E quindi uscimmo a riveder le stelle.” *“and thence we came forth to see again the stars.”*

Dante Alighieri (1265-1321)

La Divina Commedia - Inferno: C. XXXIV, v. 139

These are the words Dante used at the end of his journey through hell…and the words that well describe the end of my PhD.

Now purgatory awaits.